

BEACH AND DUNE EROSION DURING SEVERE STORMS

By

STEVEN ALLEN HUGHES

A DISSERTATION PRESENTED TO THE GRADUATE COUNCIL OF  
THE UNIVERSITY OF FLORIDA  
IN PARTIAL FULFILLMENT OF THE REQUIREMENTS FOR THE  
DEGREE OF DOCTOR OF PHILOSOPHY

UNIVERSITY OF FLORIDA

1981

Copyright 1981

by

Steven Allen Hughes

Dedicated to my wife, Patty,  
and my daughter, Kelsey . . .  
friends of mine who make life worth living.

## ACKNOWLEDGEMENTS

Many people have provided inspiration and guidance throughout the course of this research. Above all, the author wishes to express his gratitude to his supervisory committee co-chairmen, Dr. B.A. Christensen and Dr. T.Y. Chiu, and to the other committee members, Dr. A.J. Mehta, Dr. E.R. Lindgren, and Dr. D.P. Spangler. Their valuable advice and suggestions are deeply appreciated.

A special indebtedness is owed to the personnel of the Coastal and Oceanographic Engineering Laboratory at the University of Florida, where the experimental portion of the research was conducted. These people provided cheerful and enthusiastic help at all times. More specifically, the author expresses his gratitude to Messrs. G. Howell, V. Sparkman, S. Schofield, M. Skelton, R. Booze, D. Brown, G. Jones, and especially to Mr. Jim Joiner. Mr. Joiner served as project coordinator and his skill, organization, and ability to overcome problems with the wave facility most certainly were the primary forces behind the successful completion of this project.

Special thanks go to Ms. Rena Herb for typing of the draft, Mrs. Adele Koehler for typing of the final manuscript, and Ms. Lillean Pieter for the fine graphics. In addition, the assistance received from Ms. Lucille Lehmann and Ms. Helen Twedell of the Coastal Engineering Archives is appreciated.

This work was supported by a grant from the University of Florida's Sea Grant Program under the National Oceanic and Atmospheric

Administration, Department of Commerce, entitled "Beach and Dune Erosion Caused by Storm Tides and Waves," and by funds made available by the Florida Department of Natural Resources.

## TABLE OF CONTENTS

	<u>Page</u>
ACKNOWLEDGEMENTS . . . . .	iv
LIST OF TABLES . . . . .	ix
LIST OF FIGURES. . . . .	x
ABSTRACT . . . . .	xii
CHAPTER	
I INTRODUCTION. . . . .	1
Important Factors and Assumptions . . . . .	4
Objectives. . . . .	6
II PREVIOUS RESEARCH AND EXPERIENCE. . . . .	7
Previous Simplified Physical Solutions. . . . .	8
Previous Experimental Research. . . . .	12
Discussion. . . . .	18
Proposed Method of Problem Solution . . . . .	19
III WAVE TANK FACILITY. . . . .	21
Air-Sea Wave Tank . . . . .	21
Computer. . . . .	24
Wave Gauge. . . . .	25
Rail Mounted Movable Carriage . . . . .	26
Profiling Instrument. . . . .	29
IV MODEL LAW . . . . .	34
Previous Scale-Model Relationships. . . . .	36
Proposed Model Law for Dune Erosion . . . . .	38
Discussion of the Model Law . . . . .	49
V MODEL VERIFICATION. . . . .	54
Selection of Prototype Conditions . . . . .	56
Selection of Model Scales . . . . .	66
Requirements for Verification . . . . .	69
Early Attempts at Model Verification. . . . .	70

	<u>Page</u>
Irregular Versus Regular Waves. . . . .	72
Verification Runs . . . . .	74
Discussion. . . . .	81
VI EXPERIMENTAL TEST SERIES. . . . .	82
Profile Selection . . . . .	82
Storm Parameters. . . . .	84
General Observations. . . . .	89
Typical Test Procedures . . . . .	91
VII QUALITATIVE ANALYSIS OF EQUILIBRIUM PROFILES. . . . .	96
Surge Level Rise Duration . . . . .	96
The Effect of Dune Height . . . . .	101
The Effect of Storm Surge . . . . .	105
The Effect of Wave Height . . . . .	105
The Effect of Wave Period . . . . .	108
Nearshore Beach Profile . . . . .	108
Dune Erosion in General . . . . .	111
Summary . . . . .	115
VIII EQUILIBRIUM BARRED STORM PROFILE. . . . .	116
Breaker Depth Versus Breaker Height . . . . .	117
Location of Bar Crest . . . . .	121
Location of Bar Trough. . . . .	129
Plunge Distance Hypothesis. . . . .	133
Nearshore Curve Fit . . . . .	139
Offshore Bar Crest Depth Versus Bar Trough Depth. . . . .	144
Wave Runup. . . . .	147
Offshore Curve Fit. . . . .	154
Summary . . . . .	159
Sample Prototype Calculation. . . . .	160
IX TRANSIENT EROSION EFFECTS . . . . .	164
Theoretical Development . . . . .	165
Experimental Results. . . . .	173
Discussion. . . . .	180
Application . . . . .	181
X SUMMARY AND CONCLUSIONS . . . . .	182
Model Law . . . . .	182
Model Verification. . . . .	183
Experimental Test Series. . . . .	184
Qualitative Profile Analysis. . . . .	184
Equilibrium Barred Storm Profile. . . . .	185
Transient Dune Erosion. . . . .	186
Applications and Assumptions. . . . .	186

	<u>Page</u>
Summary . . . . .	187
Recommendations for the Future. . . . .	188
APPENDIX	
A COMPUTER PROGRAM LISTINGS . . . . .	190
B INSTRUMENT CALIBRATIONS . . . . .	200
C TIME-DEPENDENT EXPERIMENTAL PROFILES. . . . .	203
D PROFILE COMPARISONS . . . . .	246
E DERIVATIONS . . . . .	272
BIBLIOGRAPHY . . . . .	285
BIOGRAPHICAL SKETCH. . . . .	291



## LIST OF TABLES

<u>Table</u>		<u>Page</u>
1	WALTON COUNTY SAND ANALYSES. . . . .	60
2	MODEL SCALE RATIOS . . . . .	67
3	FIRST VERIFICATION RUN . . . . .	75
4	SECOND VERIFICATION RUN. . . . .	77
5	EXPERIMENTAL PARAMETERS. . . . .	87
6	BREAKING WAVE HEIGHTS. . . . .	120
7	EROSION VOLUMES. . . . .	174
8	FRACTION OF EQUILIBRIUM EROSION FOR WAVE PERIODS . . . . .	177
9	FRACTION OF EQUILIBRIUM EROSION FOR SURGE LEVELS . . . . .	177

## LIST OF FIGURES

<u>Figure</u>	<u>Page</u>
1: EDELMAN'S METHOD APPLIED TO ACTUAL AND IDEALIZED BEACH PROFILES. . . . .	9
2: FACILITY LAYOUT AND CROSS SECTION . . . . .	22
3: WAVE GAUGE. . . . .	27
4: INSTRUMENT CARRIAGE . . . . .	28
5: BOTTOM PROFILING INSTRUMENT . . . . .	31
6: PROFILE R-41 LOCATION MAP . . . . .	58
7: PROFILE R-41 AS SCALED IN MODEL . . . . .	59
8: USE OF GRAIN-SIZE DISTRIBUTION TO FIND $d_e$ . . . . .	62
9: MODEL AND PROTOTYPE GRAIN-SIZE DISTRIBUTIONS. . . . .	68
10: ATTEMPTED MODEL VERIFICATION USING WAVE SPECTRUM. . . . .	71
11: VERIFICATION RUN 1, FINAL PROFILE ON CENTERLINE . . . . .	76
12: VERIFICATION RUN 2, FINAL PROFILE ON CENTERLINE . . . . .	79
13: ERODED BEACH-DUNE, RUN 2. . . . .	80
14: EXPERIMENTAL TEST SERIES PROFILE. . . . .	85
15: RUN 41 SEQUENTIAL EROSION . . . . .	95
16: INSTANTANEOUS VERSUS TIME-DEPENDENT SURGE LEVEL RISE. . . . .	98
17: INSTANTANEOUS SURGE COMPARISONS . . . . .	99
18: FIRST COMPARISON VARYING SURGE RISE DURATION. . . . .	100
19: SECOND COMPARISON VARYING SURGE RISE DURATION . . . . .	102
20: DUNE HEIGHT COMPARISONS . . . . .	103
21: SURGE LEVEL COMPARISONS . . . . .	106

<u>Figure</u>	<u>Page</u>
22: WAVE HEIGHT COMPARISONS. . . . .	107
23: WAVE PERIOD COMPARISONS. . . . .	109
24: NEARSHORE PROFILE COMPARISONS. . . . .	110
25: BREAKER HEIGHT VERSUS BAR DEPTH. . . . .	119
26: BAR CREST DISTANCE . . . . .	125
27: BAR TROUGH DISTANCE. . . . .	130
28: RATIO OF BAR CREST DISTANCE TO BAR TROUGH DISTANCE . . . .	132
29: GALVIN'S BREAKING WAVE PLUNGE DISTANCE DATA. . . . .	134
30: PLUNGE DISTANCE DEFINITION SKETCH. . . . .	137
31: VALUES OF "A" FOR NEARSHORE CURVE FIT. . . . .	142
32: BAR TROUGH DEPTH VERSUS BAR CREST DEPTH. . . . .	146
33: CALCULATED RUNUP VERSUS MEASURED RUNUP . . . . .	150
34: VERTICAL WAVE RUNUP PARAMETER. . . . .	152
35: OFFSHORE CURVE FIT . . . . .	156
36: CALCULATED BARRED PROFILE COMPARISONS. . . . .	162
37: TIME-DEPENDENT EROSION TRENDS. . . . .	168
38: TIME-DEPENDENT EROSION FROM PEAK SURGE TO EQUILIBRIUM. . .	179

Abstract of Dissertation Presented to the Graduate Council  
of the University of Florida in Partial Fulfillment of the Requirements  
for the Degree of Doctor of Philosophy

## BEACH AND DUNE EROSION DURING SEVERE STORMS

By

Steven Allen Hughes

August 1981

Chairman: Bent A. Christensen

Co-Chairman: Tsao-Yi Chiu

Major Department: Civil Engineering

With the increasing development of our coastal areas, it becomes necessary to understand the long and short term behavior of the dynamic beach-dune system in order to arrive at sound engineering decisions regarding future use of these regions, and to protect existing development threatened by beach erosion. One aspect which would greatly assist these efforts is the ability to accurately predict the amount of dune recession which would occur during extreme storm events.

This research has been directed toward a semi-empirical solution through the use of a small-scale movable-bed physical model. Based on the principles of hydraulic similitude, a new model law has been derived and verified. The verification involved the reproduction of an actual storm event to a degree of realism never before attempted, and the resulting erosion in the model almost exactly reproduced that which occurred in the prototype.

In order to determine the effects of wave period, wave height, surge level, surge duration, and dune height, these parameters were systematically varied in 41 experimental model tests. Beginning with an equilibrium profile, the surge level was increased over a typical

time span and then maintained at the peak level until near-equilibrium conditions prevailed. Qualitative comparisons between the resulting profiles indicated that it is necessary to employ a time-dependent surge level increase in order to more accurately simulate an actual storm event. In addition, it was found that each set of conditions appeared to form an equilibrium barred storm profile which could be shifted relative to the prestorm profile to obtain a sediment balance between erosion and deposition, and thus, determine dune recession.

Analysis of the experimental data provided a means of calculating the equilibrium barred storm profile in terms of the wave period, breaking wave height, surge level, and profile sediment grain-size. In most instances, the empirical expressions used in determining this profile have physical interpretations in terms of the incoming wave energy flux per unit width.

Finally, a method was developed which corrects the maximum dune recession in cases when equilibrium conditions are not reached.

## CHAPTER I

### INTRODUCTION

Nature has provided delicate measures at the land and sea boundary on a sandy coast to maintain a balance of forces under ever changing wave conditions. While the sloping beach and beach berm provide the first "line of defense" for the absorption of normal wave energy, the coastal dunes are the last zone of defense in the advent of storm (hurricane) waves and the accompanying storm surge which succeeds in overtopping the berm. In essence, the beach-dune system constitutes the natural coastal structure which effectively adjusts its shape in the form of erosion or accretion to cope with any weather condition. Left in its natural state, this system functions in a most efficient "give and take" fashion to provide a coastal defense mechanism. However, in recent years, increasing concentration of population and industry in coastal areas has resulted in developments which encroach upon the dynamic beach-dune zone and therefore interfere with the natural shore processes described above. The recent disastrous destruction of water front, man-made structures and the magnitude of sediment required by nature (in the form of beach-dune erosion) in adjusting its defense posture against Hurricane Eloise in Bay and Walton Counties on the northwest Florida coast serves as a good example of what could and did happen to structures placed within this dynamic zone (Chiu, 1977; Frank, 1976).

Realizing that the ever increasing development of Florida's beaches was interfering with natural shoreline processes and that the Florida coastline is in a high risk hurricane area (Neumann et al., 1978), the legislature established a Coastal Construction Control Line Law in September 1971 (Purpura, 1972). The purpose of the law was to prevent construction or excavation seaward of a control line for the protection of the beach-dune system and for the protection of upland structures from storm activity. The establishment of such an important line depends on a number of factors, however. One of the most important factors to be considered is the landward erosion distances of the beach-dune system that could be expected during a severe storm. A capability of predicting beach-dune erosion distance, caused by storm activity, with a reasonable degree of accuracy would not only be an enormous benefit to the State of Florida, but would also address itself to this great problem on all the world's sandy coasts.

The investigation of any specific problem in the field of applied engineering usually proceeds in the following manner:

- 1) Identification of the problem and its important parameters,
- 2) Development of the physics of the problem and formulation of suitable assumptions and simplifications based on observations and common sense,
- 3) Development of a mathematical theory from the simplified physics of the system including all the relevant parameters (predictive in nature and quite often highly empirical), and
- 4) Theory verification using known prototype data or by small-scale model testing.

A review of the currently available literature on the subject of surf zone dynamics quickly leads to the conclusion that a purely

theoretical approach to the problem of dune erosion based on the Navier-Stokes equations is presently beyond our grasp. Among other things, this approach would require an understanding of wave transformation within the surf zone and its associated time-dependent vertical water particle velocity distribution, the turbulent fluctuations and energy losses beneath a breaking wave, bottom friction effects, sediment transport (both suspended and bed-load) throughout the surf zone, and consideration of random seas. At present, no suitable solution exists for any of these problems. However, experience tells us that nature does indeed have "order," and that many natural phenomena can be accurately analyzed through empirically derived expressions relating the important parameters.

Faced with this insurmountable theoretical "wall" the investigation of the dune erosion problem necessarily becomes one of a parametric study involving empirically verified relationships with the inclusion of known physics when possible. A successful solution of this type would not only provide a suitable engineering solution, but would also help further our understanding of the basic, underlying physics which control this process.

There have been two basic approaches to the problem to date, the gross simplification of the governing physics involved in dune erosion and the use of small-scale model testing to aid in the parameterization of the process. These methods are discussed in Chapter II, but it should be noted here that none provide results in agreement with field measurements. This lack of verification is a result of oversimplification of the process to the point that several important observed aspects have been omitted, such as offshore bar formation and time-dependent surges.



Because current methods of predicting dune recession during severe storms are unsuitable, there remains an immediate need for the development of an accurate, predictive engineering solution of the problem to aid coastal zone planners in the orderly development of the coastal communities without hindering the natural "storm defense" provided by the beach-dune system. This is the primary goal toward which this research was directed.

#### Important Factors and Assumptions

Our present knowledge of the dune erosion process, derived mainly from observations combined with common sense, make it possible to list the important parameters involved:

- 1) Primary dynamic factors:
  - a) the storm surge water level,
  - b) the storm surge duration, and
  - c) the incoming wave period and wave height and their spectral distribution.
- 2) Primary geometrical factors:
  - a) the configuration of the prestorm dune, beach, nearshore and offshore zones, and
  - b) the grain-size distribution on the beach.

No predictive model at present incorporates all of these parameters. In fact, most models are of a steady-state nature, which is a condition seldom reached during the short duration of a storm event. This indicates that any predictive model must give transient beach-dune response.

Secondary factors of importance are given as:

- 1) Strong onshore-directed winds,
- 2) Oblique wave attack,
- 3) Heavy rains,
- 4) Beach and dune vegetation, and
- 5) Interaction with structures.

While the secondary factors listed certainly have some effect upon the amount of erosion which could occur, it is felt that the small refinements resulting from inclusion of these factors into the analysis are not warranted due to the difficulties involved.

In pursuing a solution to the dune erosion process, the following, almost universally applied, assumptions have been invoked in this study:

- 1) Natural beaches with sand-sized sediment distributions;
- 2) Fairly uniform offshore depth contours and straight beaches;
- 3) No interactions with coastal structures or tidal inlets;
- 4) A two-dimensional onshore-offshore sediment transport situation involving no net sediment losses or gains to the system, implying an absence of longshore currents (which field data indicate is a reasonable assumption for severe storm conditions; and
- 5) Sufficiently high coastal dune as to prevent wave overtopping at the peak surge level.

### Objectives

The overall objective of this study has been to develop the capability of predicting the magnitude of beach-dune erosion as a result of given storm conditions. More specifically the objectives include the following:

- 1) Develop and verify the necessary small-scale movable-bed modeling relationships for use in an experimental test series,
- 2) Determine the characteristics of the poststorm barred profile,
- 3) Evaluate the effects of storm surge rise duration,
- 4) Compare and quantify the relative importance of the main factors listed above, and
- 5) Evaluate the effect of storm duration on the transient erosion condition.

## CHAPTER II

### PREVIOUS RESEARCH AND EXPERIENCE

The specific problem of being able to predict the amount of beach-dune erosion during severe storm conditions has drawn the interest of investigators from the fields of coastal engineering, geology, and land use planning as well as local, state, and federal agencies. And while the destructive potential resulting from dune erosion is well recognized, descriptions of the phenomenon, even in the simplest qualitative evaluation, provide little insight into the actual physical process.

At present there are no verified methods for the prediction of dune erosion during severe storms, even under the limiting assumptions of a two-dimensional process without bar formation, net erosion due to longshore currents, or dune overwash.

There are three basic approaches to finding a solution for a hydraulic process:

- 1) A complete physical analysis based on the equations of fluid flow and sediment transport when suitable simplifying assumptions, based upon observation and common sense, are utilized;
- 2) A numerical representation of the governing equations and boundary conditions which are solved in an iterative fashion and verified with extensive field data;

- 3) The verification and operation of a small-scale model of the process carried out with the hopes that the dominating forces have been successfully scaled down.

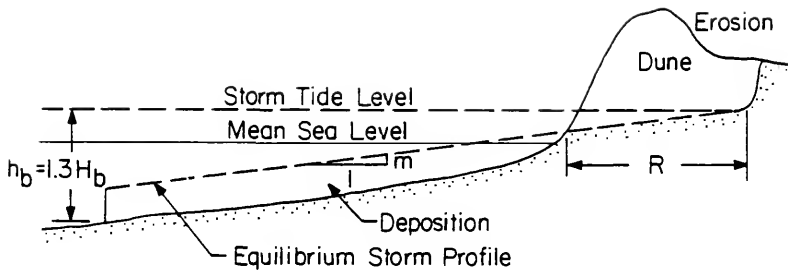
The complete physical analysis of the problem is presently out of the question due to the almost total lack of understanding of the fluid flow details within the surf zone. Likewise, numerical methods are limited by the lack of detailed prototype measurements before, during, and immediately following a major storm event. Modeling in a small-scale wave facility appears to be the most practical, but this too has its drawbacks, which will be discussed in detail in Chapter IV.

### Previous Simplified Physical Solutions

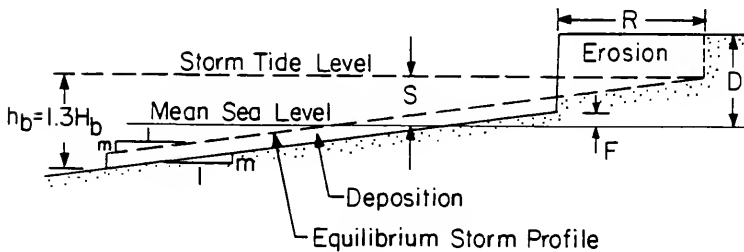
#### Edelman's Method

It appears that the first attempt at quantifying the amount of dune erosion and the resulting recession of the dune field was given by Edelman (1968). He assumed that the poststorm nearshore profile could be approximated by a straight line with a slope of about 1:50 for beaches typical to those found in the Netherlands. Under the assumption of onshore-offshore sediment transport where the eroded volume equals the deposited volume, Edelman's method could be used to predict erosion for an actual beach profile as illustrated in Figure 1a, or for "ideal conditions" as shown in Figure 1b.

For the actual beach profile, recession,  $R$ , is obtained by shifting the equilibrium storm profile until erosion area equals deposition area. For the "ideal condition" the dune recession is calculated by



1a: ACTUAL PROFILE APPLICATION.



1b: IDEALIZED PROFILE APPLICATION.

FIGURE 1: EDELMAN'S METHOD APPLIED TO ACTUAL AND IDEALIZED BEACH PROFILES.

$$R = \frac{-\beta + \sqrt{\beta^2 + 2\delta}}{m}, \quad (1)$$

where

$m$  = beach slope,

$\beta = D - S + \mu$ ,

$\mu = 1.3H_b - S + F$ ,

$\delta = 1.3H_b\mu - \mu^2$ ,

$F$  = vertical distance from mean sea level to the base of the dune, and

$S$  = storm surge level.

The other assumptions are given as: (a) the width of the surf zone is defined by breaking wave height  $H_b = 1.5(S)$  and breaking depth  $h_b = 1.3H_b$ , where  $S$  is the storm surge level; (b) the deposition is evenly spread over the surf zone; (c) the slope of the poststorm profile is the same as the original slope; and (d) the eroded dune toe is slightly lower than the highest surge level reached. Both (c) and (d) above are based upon field observations.

The main weaknesses of Edelman's method lie in the assumption that the nearshore beach profile is a straight line with the same slope as the prestorm profile, and in the assumptions for the limiting depth  $h_b = 1.3H_b$  and the surf zone width. In addition, the wave period and the sediment grain-size have not been taken into account, and the assumption is made that an equilibrium is reached.

Edelman (1972) later conceded that the beach profiles have a more intricate shape than he assumed, and that storms never lasted long enough to produce the equilibrium condition.

The Edelman method was modified by Vallianos (1974) and used to design dune cross sections. One modification included the recognition of a flatter beach slope after the storm than that of the prestorm profile.

A modified version of Edelman's method has also been used by the University of Florida's Department of Coastal and Oceanographic Engineering to estimate erosion distance for use in establishing coastal construction setback lines for the State of Florida. Although Edelman's method was used successfully by the Department to test an eroded profile in St. Johns County, Florida, during a three day northeast storm in early February, 1973, it predicts too much erosion for Hurricane Eloise. This points to the influence of storm duration since Eloise was a fast moving storm with a peak surge lasting only about half an hour to an hour.

#### Dean's Method

Besides Edelman's assumptions, Dean (1976) considered uniform energy dissipation and uniform shear stress across the surf zone to establish an equation for the equilibrium beach profile given as

$$\frac{h}{h_b} = \left(1 - \frac{x}{w}\right)^\alpha, \quad (2)$$

where

$x$  = the horizontal coordinate directed onshore from the  
breaker line,

$w$  = the width of the surf zone,



$h$  = the water depth,

$h_b$  = the breaking depth,

and  $\alpha$  depends upon the assumed energy dissipation mechanism.

By assuming different profile shapes before and after the storm, and considering the limiting depth and wave assumptions of Edelman, Dean gave the following dimensionless relationship for beach recession:

$$R' = S' - \frac{h'_{b2}}{1 + \alpha} [1 - (1 - R')^{1 + \alpha}] \quad (3)$$

in which

$$R' = \frac{R}{w_1 (h_{b2}/h_{b1})^{2.5}},$$

$S' = S/B$  where  $B$  is dune height above prestorm mean sea level,

$S$  = surge level,

$$h'_{b2} = h_{b2}/B,$$

and the subscripts 1 and 2 refer to prestorm and storm conditions, respectively. Here again a balance between erosion volume and deposition volume is assumed. Dean did a comparison between his method and Edelman's, and while similar trends were observed, the two methods differed significantly. He also pointed out that a more valid and verified method is needed which would include the presence of an offshore bar, the transient effects, and the fact that surges will never last long enough to produce equilibrium conditions.

#### Previous Experimental Research

While much experimental research has been done regarding the general aspects of beach response to wave conditions, those which have

addressed the specific problem of dune erosion during storm conditions are relatively few.

### Qualitative Model Tests

Van der Meulen and Gourlay (1968) performed two-dimensional small-scale model tests to examine the influence of dune height, wave steepness, and wave period using a sediment grain-size of  $d_{50} = 0.22$  mm. Due to their uncertainty regarding the correctness of the model law implemented for these tests, the conclusions drawn were given as qualitative observations which should be considered for the selection of future scale-model studies.

These observations include the following:

- 1) The recession of a sand dune increases as the height of the dune decreases;
- 2) For given wave conditions, storm surge water level, and sediment, the equilibrium profiles seem to be independent of the dune shape;
- 3) The dune erosion is a function of wave steepness, wave length, sediment size, storm surge level, dune shape, and initial beach profile;
- 4) The dune foot recession is greater for wind waves than for regular waves with the same energy and modal wave period;
- 5) Bar formations are less predominant for wind wave experiments;
- 6) Dune erosion is very rapid in the early stages of the tests (a direct result of using an instantaneous surge level rise).

All of these observations are basically correct, and later chapters will attempt to physically explain and quantify each point given above.

### Model Tests to Determine Scaling Relationships

Van de Graaff (1977) conducted a series of dune erosion experiments with the twofold purpose of developing a design criterion for the Dutch coastline and developing relationships for scaling between model and prototype as well as between models of different dimensions. All the tests were performed using an instantaneous surge level rise and a single prototype storm condition represented by a Pierson-Moskowitz energy density spectrum.

An empirical correlation of the data resulted in the scaling relations of

$$N_T = 1$$

and

$$N_\lambda = N_\mu^{1.28}$$

where

$N_T$  = morphological time scale,

$N_\lambda$  = horizontal length scale, and

$N_\mu$  = vertical length scale,

valid between the ranges of  $26 < N_\mu < 150$  when the same bottom material in the prototype is used in the scale model.

More extensive tests by Vellinga (1978) using the same prototype design conditions as Van de Graaff concluded that the best scale-model

relationship was achieved when the dimensionless fall velocity parameter  $H/\omega T$  was held constant between prototype and model. When this could not be met, the profile could be distorted using the relationship

$$N_{\lambda} = \frac{N_{\omega}^{1+\alpha}}{N_{\omega}^{2\alpha}} \quad (4)$$

where  $\alpha = 0.5$  for fine sand and  $N_{\omega}$  = grain fall-velocity scale. The morphological time scaling in this case was given as

$$N_T = N_{\omega}^{1/2}, \quad (5)$$

which is the same as the hydrodynamic time scale.

Unfortunately, both of these experimental series concentrated on the development of the scaling relationships for one prototype condition, and then relied upon correlations to determine the distortion without any physical arguments to support them. Hence, it is quite possible that the given relationships are valid only for the tested prototype condition. Furthermore, the use of a fairly wide-banded spectrum, such as the Pierson-Moskowitz in shallow water, could be criticized since shallow water spectra are typically more narrow-banded. This subject will be touched upon again in Chapter IV. Finally, the testing of only one prototype condition gives no information as to the effects of varying the storm parameters. In addition, the instantaneous surge level rise negates any type of time-dependency analysis which could be carried out upon their data. It will be shown in the present study that the storm surge must rise over a finite period in order to more accurately predict prototype response from model experiments.

Ma (1979) carried out a series of dune erosion experiments at the University of Florida as a preliminary to the present research. The main thrust of the work was directed towards identifying the scaling effects present in small-scale models. The tests were designed holding the dimensionless fall velocity parameter constant between three different vertical scales. The prestorm profile used in the model was selected to represent an average beach-dune profile existing on the coast of the Florida Panhandle; and the model series included two different wave heights, wave periods, and storm surge levels. The scale-model law developed by Van de Graaff was utilized, and three different sediment grain sizes were tested.

Upon scaling the results for both fine and coarse grains up to prototype, Ma found good agreement between the differently scaled models for the same prototype storm conditions. Unfortunately the comparison between model and actual prototype erosion caused by Hurricane Eloise was not too successful since the test program did not include a time-dependent surge level increase. However, this research did lend some credibility to the idea of preserving the parameter  $H/\omega T$ , and it pointed out some of the difficulties to be expected in future modeling efforts. In addition, some qualitative insight was gained with regard to the dune erosion process, and some of the problems with the wave flume were uncovered and rectified.

#### Predictive Techniques Based on Model Tests

An exhaustive effort by Swart (1974a, 1974b) examined the results of many model tests carried out at the Delft Hydraulics Laboratory

over the years. He proposed that the beach profile be characterized by three distinct zones, each with its own transport mechanism. These zones are the backshore above the wave run-up limit in which "dry" transport takes place, the developing profile where a combination of bed-load and suspended-load transport occurs, and the transition area where only bed-load transport takes place.

Swart wisely avoided the internal mechanisms of sediment concentrations and bottom velocities by making a schematization of the external properties of the profile development in order to predict rates of offshore sediment transport. The final empirical relationships given by Swart provided a means of determining both the equilibrium profile characteristics and the time-dependent sediment transport rates.

Swart subsequently realized that the computational method he described was too complicated for normal use, prompting him to modify the technique in order to ease the computations without significantly affecting the results (Swart, 1976).

However, even with these simplifications, the method remains fairly complex and has several drawbacks which preclude it from use in determining dune erosion during storms:

- 1) The model law used in the testing has never been fully verified as representing actual prototype behavior;
- 2) The tests used primarily a fixed water level which does not simulate storm surge rise;
- 3) The empirically derived expressions offer no physical explanation for the interaction of the parameters such as wave height and period;

- 4) The time-dependent rates for erosion, when scaled to the prototype, are assumed to be correct, but never verified;
- 5) Many of the initial profiles did not represent near-equilibrium beach conditions;
- 6) Barred profiles are not predicted by the method but are usually observed in nature during the offshore sediment transport phenomenon.

### Discussion

As can be seen in the above literature review, the problem of coastal dune erosion during storms has been approached by two different methods. On one hand are the simplified physical models offered by Edelman and Dean, and on the other are small-scale model testing programs seeking to provide some insight into the process.

The physical models suffer due to the lack of understanding of the actual complex physics of surf zone and the resultant effects upon the coastal dunes. There has not even been sufficient field data of poststorm erosion to indicate that these methods provide even an order of magnitude estimate of the dune erosion.

The model testing programs, to present, have been concerned mainly with the establishment of suitable model laws, to be used in small-scale testing, which would provide accurate results when scaled up to prototype. In addition, a time-variable surge level increase has not been used, which later will be shown to be a pertinent factor.

Thus, it is seen that this is an area requiring immediate examination in order to both identify the important parameters and their

relationship to the process, and to provide an accurate and reliable means of calculating the dune erosion as a result of selected storm conditions.

#### Proposed Method of Problem Solution

Drawing upon the previous experience discussed above, the following steps are proposed in order to logically examine and formulate a solution method for determining dune erosion during a storm:

- 1) Derive a suitable small-scale movable-bed model law based upon sound physics and past experiments which will provide a basis for the operation of a laboratory model, simulating storm conditions and the resulting dune erosion.
- 2) Verify the model law by the approximate reproduction of a prototype event for which field data are available.
- 3) Conduct an extensive series of model experiments in which the important storm parameters are varied within their expected ranges. The series will attempt to closely reproduce actual storm conditions by including such factors as a varying storm surge level and an initial equilibrium profile.
- 4) The test results will be initially examined overall in an effort to identify the effects of the important parameters in a qualitative sense, and to gain some insight into the entire process. From this overview it may be possible to recognize the primary physical mechanisms which influence erosion.
- 5) From the above step, decisions can be made as to which aspects of the phenomenon can be parameterized in such a



way that some physical justification for the parameters could be offered.

- 6) Correlations will be sought for the dominant features present in the erosion process in terms of the chosen parameters, and physical explanations will be given when possible. While the physical explanations will, for the most part, be qualitative in nature, it is expected that a good amount of insight will be gained to further add to the present poor understanding of the process.
- 7) Finally, a proposed engineering solution will be constructed, based upon the analysis, with the hope that it will provide an accurate method until the time the process is fully understood and analyzed in physical terms. Along with the proposed solution will be a summary of the restrictions imposed by the assumptions and an outline of the range of applications for which the solution can be deemed reasonably accurate.

## CHAPTER III

### WAVE TANK FACILITY

#### Air-Sea Wave Tank

The Coastal and Oceanographic Engineering wind and wave facility was dedicated in 1957 and used primarily as a wave tank. Under a grant awarded in 1967, the Air-Sea tank was updated and improved, giving it the capability of being used for advanced research into air-sea interactions. These improvements, along with a detailed description of the facility, are given by Shemdin (1969).

#### The Wave Channel

Figure 2 gives a general layout of the wave facility which is 6 feet wide and has a total length of 150 feet. The mechanical wave generator section occupies 11 feet, while the wave absorbing beaches occupy 19 feet of the total length. The remaining 120 feet are divided into two bays, each 34 inches wide and 6'4" deep. The maximum water depth for wave generation is 3 feet. The dune erosion tests were conducted in the eastern bay since the entire length of the test section has full height glass observation windows.

While the tank could be filled from a well at the rate of 500 gallons per minute, the water used for this series of experiments came through a 2-inch city water line equipped with a calibrated valve.

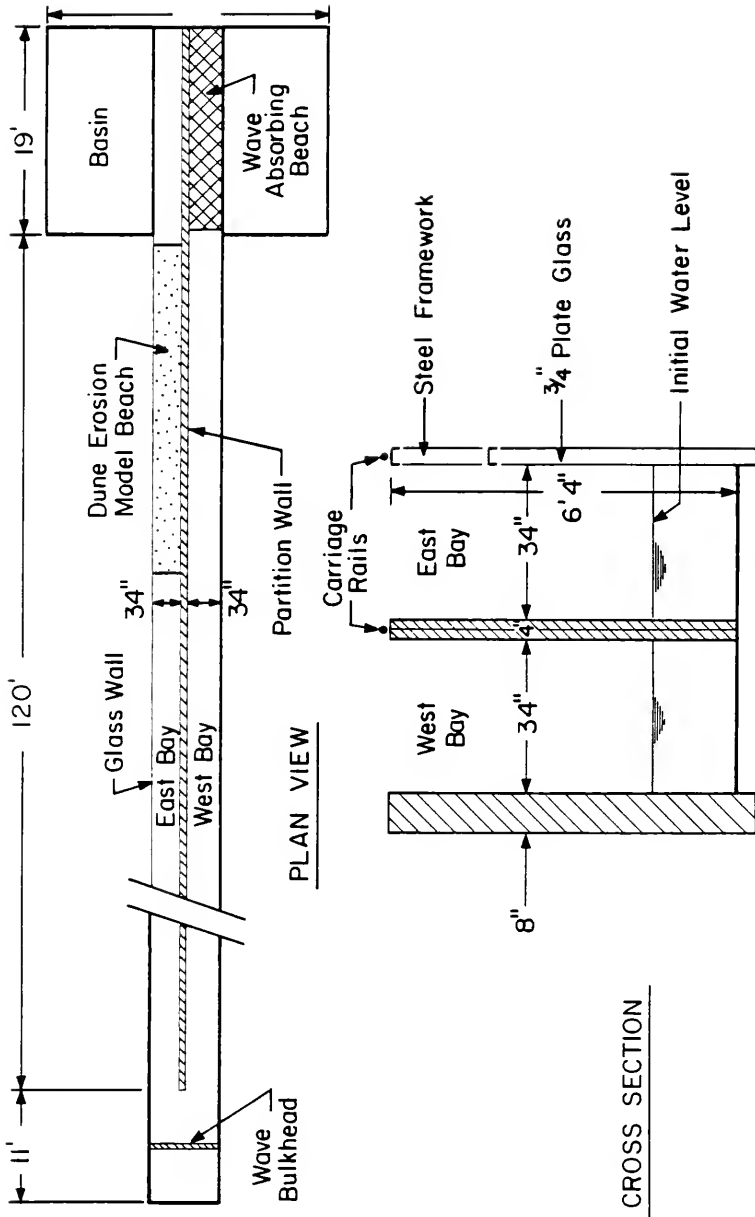


FIGURE 2: FACILITY LAYOUT AND CROSS SECTION.

This provided a controlled means of increasing the surge level during the experiments, and the water was of greater clarity than the well water, providing for better observation of the sediment movement.

#### Mechanical Wave Generator

Wave generation in the Air-Sea tank is achieved through an electronically controlled, hydraulically driven wave paddle measuring 6 feet wide and 4 feet high. Identical waves are generated in both bays.

The wave generator bulkhead is mounted on a carriage and is driven by two hydraulic rams governed by hydraulic servo-valves. The system provides independent control of the top and bottom rams in such a way that the bulkhead can move either as a piston on the carriage or as a paddle. Any combination of piston and paddle motion is possible. For the dune erosion tests, the bulkhead motion consisted of a piston motion combined with a paddle motion about the bottom of the bulkhead. This gave the upper water particles a greater displacement than the lower particles, which more closely represents the vertical velocity distribution found in water waves.

Sinusoidal wave motion was produced by sending an analog sine-wave signal from a function generator to the servo-valves with the wave amplitude being controlled by varying the input amplifier gain.

Prior to the experiments, new servo-valves and solid-state electronic controls were installed in order to provide better frequency response and system reliability. Throughout the entire testing program, the new system performed without any problems.

### Computer

As is the case with most modern wave facilities, a digital computer has been employed to aid in the gathering and processing of experimental data. This not only speeded up the process, it also provided a more accurate means of data acquisition, with a smaller chance of error. To guard against errors, methods were developed to immediately check and confirm the accuracy of the computer-made measurements.

Two further benefits of using the computer are that the speed of profile measuring and recording allowed for a greater number of experiments to be conducted within the time constraints of the project, and that data reduction and analysis programs could be run immediately following each experiment on an instantaneous "turn-around" basis.

In the early stages of the project the computer was used to generate random time-series to a given power spectrum, to operate the wave paddle to produce these random waves in the tank, to monitor and record wave data on command, and finally to analyze the recorded wave data. During the actual test series, when regular waves were used, the computer was used only to measure and record the beach profiles and to analyze the data for erosion volume. Listings of these programs are given in Appendix A.

### Hardware

The computer used in the experimental program was the DECLAB-11/03 with a CPU memory of 28 K bytes and programmable in the Fortran IV language, complete with diagnostics. The system includes 1) a real-time clock, 2) an analog-to-digital converter capable of handling 16

single-ended or 8 differential analog signal inputs, 3) a digital-to-analog converter capable of outputting 4 different analog signals on command, and 4) an RX01 dual floppy disk drive for program and data storage.

Two terminals were interfaced to the computer. A Tektronix 4006-1 Graphics video terminal was used for writing and editing programs, while a TI Silent 700 hard-copy terminal was remotely located nearer to the wave tank for executing profiler programs and data analysis.

### Software

The system software included the standard components of: 1) an editing program for writing or editing Fortran programs, 2) a Fortran compiler, 3) a linking program which creates the final machine language program including any hardware input/output commands, 4) a peripheral exchange program for transferring programs or data to different devices such as tape or hard disk, 5) an extensive Fortran Scientific Subroutine package, and 6) support routines for the laboratory peripherals.

The computer realized only a small percentage of its potential during the dune erosion experiments, and it is expected that many more applications will be found in future studies involving movable-bed models.

### Wave Gauge

The wave gauge used for monitoring the waves in the tank was a capacitance-type gauge designed and built by the Coastal and

Oceanographic Engineering Laboratory at the University of Florida.

Figure 3 shows the gauge in position.

The capacitance wave gauge uses the water as one plate of a varying capacitor; hence the capacitance of the sensing portion of the instrument changes as the water level fluctuates during wave motion. The signal is sent to the control room in the form of a varying frequency where it is then converted to an analog signal and recorded as a continuous record on a strip chart recorder. A detailed calibration at the beginning of the experiment confirmed the linearity of the gauge (see Appendix B), and the resulting conversion factor for volts to centimeters was confirmed prior to every experimental run. The gauge is electronically isolated to eliminate any interaction between other electrical signals present in the laboratory.

#### Rail Mounted Movable Carriage

A horizontally moving instrument carriage was installed in the eastern bay of the wave tank to provide a variable-speed platform on which sensing instruments could be mounted for the monitoring and recording of experimental data. In this research program the carriage was used solely for the purpose of transporting the beach profiling instrument over the length of the profile in a controlled fashion. Figure 4 shows the carriage with profiler in place from several angles.

The rails for the carriage have been installed with a horizontal tolerance of  $\pm 0.001$  inches, providing an excellent platform from which to measure beach profiles. The carriage drive train is powered by a  $\frac{1}{2}$ HP electric motor capable of moving the carriage at speeds between 0 to 20 feet per second.

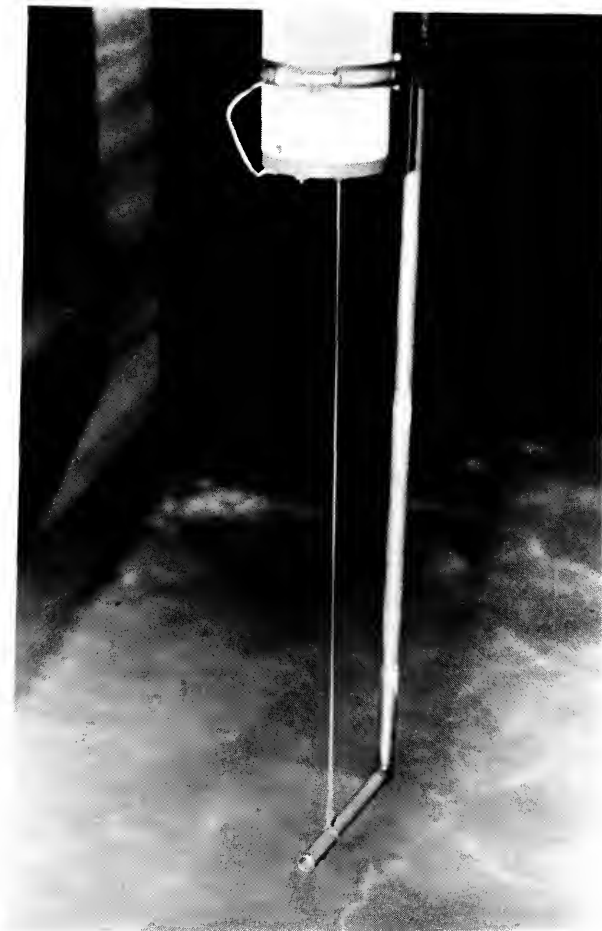
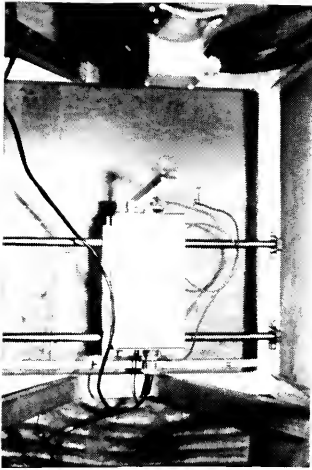


FIGURE 3: WAVE GAUGE.

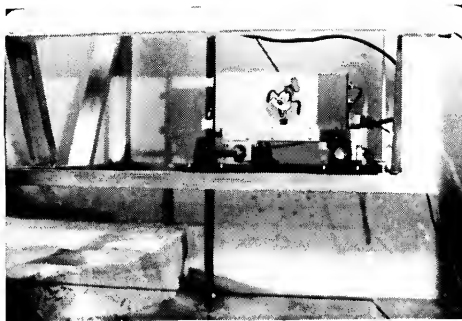




TOP VIEW



END VIEW



SIDE VIEW

FIGURE 4: INSTRUMENT CARRIAGE.

A hand-held remote control unit allows the drive motor to be started or stopped, activates the automatically operated bottom-following probe on the profiling instrument, and also allows the manual vertical positioning of the probe.

The horizontal movement of the carriage is monitored by a "follower wheel" which has a ring of magnets equally spaced around it. A sensor is activated each time a magnet passes by, and this produces a voltage variation similar to a square wave between zero and five volts as the carriage proceeds down the rail. The computer can "count" the number of downsteps in the voltage signal, and by applying a conversion factor, it can determine relative horizontal carriage displacement. The approximate conversion factor was 0.42 inches of horizontal travel per voltage downstep.

The horizontal displacement can be referenced to any initial or final carriage location by inputting the appropriate value read from a measuring tape mounted on the upper portion of the tank side-wall.

The signals from the horizontal position indicator and from the profiling instrument were relayed to the computer through a cable connected between the carriage and a junction box mounted on the side of the tank.

#### Profiling Instrument

The MK-V Electronic Profile Indicator was developed at the Delft Hydraulic Laboratory in Holland for the purpose of continuously

measuring bed levels in hydraulic movable-bed models. The instrument and its mounting on the carriage is illustrated in Figure 5.

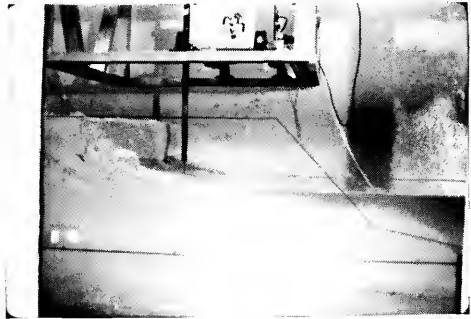
#### Probe Description

The instrument probe is placed vertically in the water where a feedback servo-mechanism maintains the tip of the probe at a constant distance (adjustable between 0.5 mm to 2.6 mm) above the sediment bedform. When the instrument is placed on the carriage and moving horizontally, the probe continuously follows the bottom profile configuration.

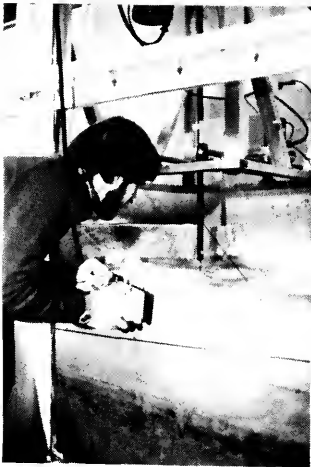
Monitoring of a ten-turn potentiometer connected to the vertical shaft holding the probe produces a continuous record of the bottom variations in terms of voltage. This voltage is easily converted to vertical distance through the very nearly linear potentiometer calibration constant determined to be 8.25 inches/volt. This calibration is shown in Appendix B. The vertical probe stroke is about 36 inches, and the instrument is placed on the carriage so that it can reach within 1 inch of the bottom of the wave tank.

#### Carriage Mounting

A sliding track on the carriage allows the profiler to be placed in any desired lateral position across the width of the tank. For the dune erosion experiments the profile was measured down the tank centerline with the thought that this position gave the most representative profile and was least affected by the side walls.



PROFILER ON CARRIAGE



PROFILER IN  
OPERATION



VERTICAL PROBE

FIGURE 5: BOTTOM PROFILING INSTRUMENT.

### Profiler Operation

The profiler is normally operated in conjunction with a computer program which automatically records the vertical position every time the horizontal carriage position indicator senses a voltage drop. This translates to a set of profile coordinates every 0.42 inches.

Since it was felt that this much data were not necessary, the program was operated in a different mode which allowed the operator to take profile data only where it was deemed necessary.

The recording of the above water portion of the profile was complicated by the fact that the bottom-seeking servo-mechanism is non-functioning when the probe is out of the water. However, since the probe potentiometer still produces a voltage signal, the computer program was written in a way as to permit the taking of a data point when an external trigger was pressed.

The procedure followed in recording the above-water profile was to place the carriage in the desired horizontal position, lower the probe manually by remote control to the beach surface, press the trigger, and then move the cart, using the remote control, to a new position where the procedure was repeated. Once the profile was below the water level, the bottom-seeking feature was activated, and the points were recorded where desired by stopping the horizontal movement of the carriage and pressing the trigger of the hand control. The computer kept track of the horizontal positions where data were taken and paired them with their respective beach elevations. The data were then stored on floppy disks along with the necessary initial references and conversion factors needed to convert the digitized

voltage to linear ranges and elevations, both referenced to the initial intersection point of beach and water level.

The operator was careful to record all the data necessary to accurately describe the profile features and variations. The typical profile measuring consisted on the average of 35 to 40 profile data pairs and covered a horizontal range of 14 feet and a vertical range of 12 inches. In all cases the measured profiles extended seaward past the region of any net sediment transport.

While recording the underwater profile, the carriage moved at about 8 feet/minute, and, after experience was gained, the operator found that the measuring and recording of the entire profile could be completed in under 5 minutes from the time the wave action was halted.

## CHAPTER IV

### MODEL LAW

Small-scale physical model testing of both natural phenomena and man-made structures has long been accepted as a useful engineering aid for the analysis and prediction of the prototype behavior. The first known hydraulic scale-model experiments were conducted by an English engineer during the period 1752-53 to determine the performance of water wheels and windmills (Hudson et al., 1979). The earliest known tests of a river model using a movable-bed were conducted in France in 1875 and in England by Reynolds in 1885. Since that time great advances have been made in the development of the model laws which govern hydraulic similitude, the instrumentation used in the models, and modeling techniques in general. Perhaps more importantly, many years of experience and basic research by many fine hydraulic laboratories throughout the world have made the simulation of more complex phenomena possible, with more confidence given to the test results.

Many hydraulic problems are fairly simple in nature and can be adequately solved by analytical methods to a reasonable degree of accuracy. However, there are many more cases where the problem being considered is far too complex to be handled analytically. Often our understanding of the physics of the problem is very limited or even nonexistent. In these cases simple approximations are insufficient and other means of obtaining engineering solutions are necessary. This

is when small-scale modeling of a hydraulic phenomenon can prove beneficial by aiding in the development of a physical solution or by helping us to arrive at parametric relationships which can aid in our understanding of the hydraulic process under consideration. This is because scale models of hydraulic phenomena are essentially a means of replacing the analytical integration of the differential equations governing the process, including initial and boundary conditions. Often model testing provides enough insight into the physics of the process so that refinements can be made to simple mathematical models.

Physical models allow the investigator to observe the process in action and distinguish certain characteristics of the flow patterns which might have been neglected in the analytical approach. In addition, the model provides a tight control of the important parameters, a control which is not available in the prototype. Examples include extreme events where accurate prototype data will be lacking, such as hurricanes, dam bursts, and flooding. Using the model to predict the results of these extreme events can provide invaluable information which more than justifies the high cost of building and operating the model.

Of all the hydraulic engineering models which can be performed, movable-bed scale-model investigations of coastal erosion and coastal sediment transport phenomena are probably the most difficult. In fact, so many different model laws have been proposed, modeling of this type should be considered more of an art than a science! However, by carefully identifying the major forces involved, it should be possible to derive a model law which can be verified and which will provide reasonable, quantitative results.



### Previous Scale-Model Relationships

Numerous papers have been written proposing similitude relationships for movable-bed coastal models. For a rather complete bibliography of the subject, see page 308 of "Coastal Hydraulic Models" (Hudson et al., 1979). These relationships range from those which were derived solely by theoretical considerations to those which were established on a strictly empirical foundation. In each case the relationship is assumed valid for a given set of specific flow characteristics. For example, a model law which attempts to scale the dominant forces involved in incipient motion of sediment in a tidal inlet over the tidal cycle will not be valid for sediment transport in the surf zone, where a completely different set of forces dominate the regime. For this reason it is necessary to first have an understanding of the dominant dynamic forces at work for a given coastal hydraulic problem, and then to examine the proposed scale-model relationships to determine if these are the forces being scaled.

Perhaps the most thorough investigation using known relationships of beach processes to determine the proper scaling law for coastal movable-bed models was that of Fan and LeMehaute (1969). Their result was a table containing eight proposed scaling relationships, each being a combination of three or more derived similitude conditions based on the known beach process relationships. One important point to note is that all of the proposed model laws satisfied the condition of the time scale being equal to the square root of the vertical scale. Using available data, a tentative model law was chosen to be verified by extensive experiments.

The experimental program was carried out the following year with the results reported in 1971 (Noda, 1971). Noda conducted the experiments to determine the validity of the proposed model law, and he then proceeded to derive a completely empirical model law based on similitude of equilibrium beach profiles in the breaker zone. Unfortunately, while good reproduction was given in the surf zone, the corresponding dune and beach erosion was not reproduced. Hence, this model law is not really applicable to the modeling of dune erosion.

The literature appears to contain no reported studies regarding model similitude relationships which were physically derived specifically for the case of dune erosion during storms. However, two recent studies conducted by the Delft Hydraulic Laboratory in the Netherlands provided a totally empirical model law for dune erosion (Van de Graaff, 1977; Vellinga, 1978).

Without going into details, these studies derived a model law by empirical correlations of tests done at different scale dimensions when compared to a single prototype condition. Several questions can be raised as to the validity of the derived relationships:

- 1) Since very little physical reasoning has been applied in the model law derivation, it is more than likely that a prototype condition other than that tested could not be reproduced.
- 2) Tests were conducted with a fixed surge level instead of a variable surge similar to what occurs in the prototype.  
Hence, there is no solid evidence that the morphological time scaling is correct.
- 3) The hydraulic time scale was derived by Froude scaling and is equal to the square root of the vertical scale, the same as

Noda's derivation. It will be shown shortly that this is not necessarily correct when modeling dune erosion.

- 4) The Pierson-Moskowitz energy density spectrum was used as the wave climate for the tests. This spectrum is representative of deep-water wave fields, while the experiments were carried out in water depths equivalent to 70 feet in the prototype. At these water depths, energy density spectra are decidedly narrower than the P-M spectrum. In addition, prototype spectra contain wave grouping which is not understood, but definitely is important. These model tests did not attempt to reproduce this phenomenon. This point will be discussed in the following chapter in further detail.
- 5) Attempts to apply this model law in the initial verification stages of the current research failed to even come close to reproducing prototype erosion. In fact, accretion of the beach above mean sea level occurred for both regular and random wave conditions. This also will be discussed in the following chapter.

These factors, combined with the apparent lack of any other suitable model law for dune erosion, have led to the following development of a new scale-model relationship.

#### Proposed Model Law for Dune Erosion

The requirements for similarity between hydraulic scale-models and their prototypes are found by the application of several relationships generally known as the laws of hydraulic similitude. These laws,

which are based on the principles of fluid mechanics, define the requirements necessary to ensure correspondence between model and prototype (Hudson et al., 1979).

Complete similarity between model and prototype requires that the system in question be geometrically, kinematically, and dynamically similar. Geometric similarity implies that the ratios of all linear dimensions between model and prototype are equal, kinematic similarity is similarity of motion, and dynamic similarity between two geometrically and kinematically similar systems requires that the ratios of all forces in the two systems be the same. From Newton's Second Law the dynamic similitude is achieved when the ratio of inertial forces between model and prototype equals the vector sums of the active forces, which are recognized as gravity, viscous, elastic, surface tension, and pressure in the coastal regime. An additional requirement is that the ratios of each and every force must be equal. Or, in equation form,

$$\frac{(F_i)_p}{(F_i)_m} = \frac{(F_g)_p}{(F_g)_m} = \frac{(F_v)_p}{(F_v)_m} = \frac{(F_t)_p}{(F_t)_m} = \frac{(F_e)_p}{(F_e)_m} = \frac{(F_p)_p}{(F_p)_m} \quad (6)$$

where subscripts p and m are for prototype and model, respectively. Five of these force ratios are taken as independent, with one (usually pressure) being determined after establishment of the others.

Since it is considered impossible to satisfy equation (6) except with a full-scale model, it is necessary to examine the flow situation being modeled to determine which forces contribute little or nothing to the phenomenon. These forces can then be safely neglected with the goal of reducing the flow to an interplay of two major forces from

which the pertinent similitude criterion may be theoretically developed (Rouse, 1950).

For models of wave action and ensuing sediment transport the elastic forces and the surface tension forces are sufficiently small that they can be neglected, provided that the water wave length in the model is greater than about 10 centimeters. Since inertial forces are always present in fluid flow, the condition for dynamic similitude reduces to equating the ratio of inertial forces to the ratio of either gravity forces or viscous forces.

For the particular case of dune erosion the main area of interest is not the offshore zone, but the surf zone and beachface. Here the waves rush up the beach and then return down the slope, eroding and/or depositing sediment in their wake. During this process, particularly during severe storm conditions, the fluid particle velocities near the bed are well in excess of the critical velocity for incipient motion, and sediment is in a state of nearly constant motion. Thus, over the wave cycle, the fluid process can be idealized as unsteady, unidirectional, open channel flow up a slope followed by flow down the slope. Of course this simplification can not be used in an analytical approach due to the complexities involved. However, through this visualization, it is easy to recognize that the two major forces acting on a sand grain are the inertia forces, due to the turbulent flow fluctuations near the bed, and the nearly horizontal component of gravity acting parallel to the beach slope. The viscous forces are small compared to the forces due to the turbulent fluctuations and thus can be neglected in this instance.

Before deriving the scale-model relationships, it is important to point out that the horizontal and vertical length scales will be different, providing a distortion of the model. This is necessary because the reduction of size of the sand grains, as required to obtain geometric similarity, would result in sand particles so small that cohesive forces not present in the prototype would be present in the model. When sediment material of nearly the same size and specific weight as found in the prototype is used in the model, distortion of the model will occur naturally in the mathematical derivation. Sometimes choosing a lighter material to use as the sediment in the model will result in an undistorted model, but the expenses and difficulties which arise are seldom worth the effort.

#### Derivation of Dynamic Similarity Condition

For convenience it is customary to introduce the notation

$$N_a = \frac{\text{value of parameter "a" in prototype}}{\text{value of parameter "a" in model}}$$

to represent the scale ratio of a given parameter between the prototype and model. Using the symbols:

L = horizontal length,

B = horizontal width,

D = vertical depth,

T = time, and

F = force;

the fundamental model scale ratios can be defined as:

$$\text{Horizontal Length Scale: } N_\lambda = \frac{L_p}{L_m} = \frac{B_p}{B_m} \quad (7)$$

$$\text{Vertical Length Scale: } N_\mu = \frac{D_p}{D_m} \quad (8)$$

$$\text{Time Scale: } N_T = \frac{T_p}{T_m} \quad (9)$$

$$\text{Force Scale: } K = \frac{F_p}{F_m}, \quad (10)$$

where again the subscripts p and m are for prototype and model, respectively. From these four scales, all other model scales can be derived.

Following the development of Christensen and Snyder (1975), the force due to gravity in the nearly horizontal direction of the principal flow may be written as

$$F_g = \rho g(\text{volume})(\sin\beta)$$

where  $\rho$  is the fluid density,  $g$  is the gravitational acceleration, and  $\beta$  is the beach slope. For small beach slopes,  $\sin\beta \approx \beta \approx \frac{D}{L}$ , so the force scale for gravity can be written as

$$K_g = \frac{\rho_p g_p (L_p B_p D_p) (\frac{D_p}{L_p})}{\rho_m g_m (L_m B_m D_m) (\frac{D_m}{L_m})} = \left(\frac{\rho_p}{\rho_m}\right) \left(\frac{g_p}{g_m}\right) N_\lambda N_\mu^2 \quad (11)$$

The inertial force is best represented as a horizontal, or nearly horizontal, area multiplied by the shear stress acting over this area, or

$$F_{\text{inertial}} = \text{Area} \times \text{Shear Stress}.$$

For the turbulent flow experienced next to the bed, which is in the rough range, the shear stress depends on the rate of momentum transfer and can be expressed as the Reynold's shear stress which is proportional to the fluid density and the time mean value of the product of a vertical velocity fluctuation and the velocity fluctuation in the direction of the time mean flow. Consequently, the inertial force is

$$F_i = \overline{\rho u'v'}(\text{area}) ,$$

and the inertial force scale ratio can be written as

$$K_i = \frac{\rho_p \left(\frac{L_p}{T_p}\right) \left(\frac{D_p}{T_p}\right) (L_p B_p)}{\rho_m \left(\frac{L_m}{T_m}\right) \left(\frac{D_m}{T_m}\right) (L_m B_m)} = \left(\frac{\rho_p}{\rho_m}\right) \frac{N_\lambda^3 N_\mu}{N_T^2} . \quad (12)$$

For dynamic similitude requiring  $K_{\text{inertial}} = K_{\text{gravity}}$ , and noting that  $g_p = g_m$ , equations (11) and (12) yield the time scale, i.e.,

$$N_\lambda N_\mu^2 = \frac{N_\lambda^3 N_\mu}{N_T^2}$$

or

$$N_T = \frac{N_\lambda}{(N_\mu)^{1/2}} . \quad (13)$$

Equation (13) is essentially the same as a similarity of the Froude number between prototype and model, when the Froude number is based on a vertical length and a horizontal velocity, i.e.,

$$F^* = \frac{V_{\text{horizontal}}}{(g D_{\text{vertical}})^{1/2}} . \quad (14)$$



Physically, this can be interpreted as a measure of near-horizontal displacement of a sand grain being held up just above the bed by turbulent fluctuations. The grain is moved horizontally by a velocity as it falls back to the bed vertically.

It should also be noted that in the case of an undistorted model where  $N_\lambda = N_u$ , equation (13) reduces to

$$N_T = (N_u)^{1/2}, \quad (15)$$

which is the time scale for wave motion used in the previous modeling attempts. It also arises from scaling of the Froude number. However, the distortion required due to the use of beach-size sand in the model means that equation (13) must be used for dynamic similarity.

#### Sediment Transport Similarity Criterion

Besides having dynamic similarity in the model, it is necessary to find some method of determining the required distortion of the model arising from the use of natural-sized beach sand. The lack of physical understanding with regard to this question has led many investigators to propose a variety of parameters to be scaled in the model which result in a distortion relationship (Kemp and Plinston, 1968; Noda, 1971). Others have used an empirical approach (Van de Graaff, 1977; Vellinga, 1978), as already mentioned.

Currently, the most promising parameter used for the prediction of equilibrium beach slopes is the dimensionless fall velocity, as presented by Dean (1973). The physical significance of this parameter, herein designated by

$$P = \frac{H}{\omega T}, \quad (16)$$

where

H = wave height,

T = wave period, and

$\omega$  = fall velocity of the sediment,

is whether a sediment particle thrown into suspension by the passage of a wave will settle to the bed during the time that the water particle motion is shoreward or seaward, resulting in onshore or offshore movement of the particle. This parameter has proven to be a good predictor of onshore-offshore sediment transport (Dean, 1973).

More recent investigations have shown that the dimensionless fall velocity parameter is also a good predictor of several other surf zone features. Dalrymple and Thompson (1976) demonstrated that this parameter could be used successfully to predict the foreshore slope when H was given as the deepwater wave height. While significant scatter was present in the data representation, they reported a much better correlation than when the same data were plotted versus  $H_0/L_0$  and a third parameter pertaining to grain-size. They concluded that the parameter  $H_0/\omega T$  should be preserved between the model and the prototype in order to reproduce the same equilibrium profile.

Noda (1978) investigated both full-scale and small-scale model results for profile similarity and found that a much closer similarity could be obtained when the  $H/\omega T$  parameter was conserved than when wave steepness,  $H_0/L_0$ , was held constant. He also offered an empirical relationship for the selection of model grain-sizes and concluded that movable-bed coastal models could be distorted, but the validity still needed to be confirmed.

Saville\* (1980) compared prototype model tests using sand against small-scale tests employing coal as the sediment. The tests were designed so that the fall velocity of the sediment would be correctly scaled. His preliminary findings indicated that profile similarity was best in the surf zone and on the beachface, where settling velocity might be expected to be a major parameter affecting the modeling. The comparison seaward of the surf zone is not as good, possibly because a shear stress modeling relationship would be more appropriate in this region.

As pointed out in Chapter II, comparisons by Ma (1979) indicate that scaling between models of different dimensions and sediment is best achieved by preservation of the dimensionless fall velocity parameter. In this way there appears to be a profile similarity, and consequently, erosion volume similarity.

Based on this growing amount of evidence it becomes increasingly clear that the parameter  $H/\omega T$  should be the same in the model as in the prototype for profile similarity. This will also allow the sediment grain-size and specific weight to be incorporated into the model law as a single variable,  $\omega$ . This requirement becomes

$$\frac{H_p}{\omega_p T_p} = \frac{H_m}{\omega_m T_m} \quad (17)$$

or

$$N_T = \frac{N_H}{N_\omega} \quad (18)$$

---

\*Personal communication with Saville indicates that this research has not been completed as of June, 1981, and thus was not included in the 17th Coastal Conference Proceedings.

# Dune Erosion Model Law

Since the time scale for wave motion is the same as the time scale for the resulting turbulent velocity fluctuations, equation (18) can be equated to the dynamic similarity criterion of equation (13), yielding

$$\frac{N_{\lambda}}{(N_{\mu})^{1/2}} = \frac{N_{\mu}}{N_{\omega}} \quad (19)$$

Rearranging gives the final scale-model relationship for the model distortion as a function sediment fall velocity, i.e.,

$$N_{\lambda} = \frac{N_{\mu}^{3/2}}{N_{\omega}} \quad (20)$$

which combined with equation (13), given again below,

$$N_T = \frac{N_{\lambda}}{N_{\mu}^{1/2}} \quad (13)$$

provides the complete requirements for scale-model testing of dune erosion during storms using a movable-bed model. Actually, equations (13) and (20) should fulfill the modeling requirements for the determination of any profile alterations due to wave action in the surf zone, not just those due to storm conditions.

It is interesting to note that equation (20) is identical to the empirically derived distortion given by Vellinga (1978) for fine sand (see equation (4), Chapter II), with the only difference between the model laws being the time scale (equation (5) and compared to equation (13)).

### Morphological Time Scale

Making the morphological time scale the same as the hydraulic time scale will conserve the number of incoming waves per unit time, thus conserving the incoming wave energy per unit time, and this seems most plausible, in view of the scaling of the particle fall velocity and the length scale distortion. The time scaling of the surge duration should also be to the same scale.

Unfortunately not enough is known about beach process reaction times to determine the morphological time scaling unequivocally. However, results from Saville (1980) indicate that better time-dependent profile comparisons are given if the time scale is distorted since the small-scale model beach in Saville's experiments deformed faster than would be expected when scaled up to prototype using the time-scale relationship

$$N_T = N_\mu^{1/2} \quad (15)$$

It is easily seen that the proposed time scaling given by equation (13) can be expressed as

$$N_T = \Omega N_\mu^{1/2}, \quad (21)$$

where

$$\Omega = \frac{N_\lambda}{N_\mu} = \text{model distortion.}$$

Hence, the time scale has the same distortion as the lengths in the model. If the model distortion is increased, the beach process will occur in a shorter time in the model.

While the above reasoning appears to be qualitatively correct, a further confirmation of the morphological time scale for beach processes is needed. However, the results of the model verification, given in Chapter V, indicate that the assumed time scaling is quite reasonable.

#### Discussion of the Model Law

The scale-model relationships just derived have resulted from a combination of basic physics and an observed parametric relationship which results in a model distortion as a function of the sediment grain-size scale ratio. The two equations given, equation (13) and equation (20), are expressed in terms of four variables,  $N_\lambda$ ,  $N_\mu$ ,  $N_T$ , and  $N_\omega$ . This allows the experimenter the freedom of selecting two of the scaling ratios to suit the model facility.

The main difference between this model law and previous attempts is the derived time scaling relationship. The other model laws have expressed, for the most part, the time scaling as

$$N_T = N_\mu^{1/2},$$

which usually arises as a result of trying to preserve the wave steepness parameter  $H_0/L_0$ . However, the wide range of values of wave steepness found for transition between summer and winter profiles by numerous investigators (Johnson, 1949; Watts, 1954; Rector, 1954; Saville, 1957a; etc.) indicates that wave steepness may not be such a good parameter to preserve.

In contrast, this proposed model law preserves the dimensionless fall velocity parameter, which has been shown to be a better indicator of beach processes. This results in a time scale given by

$$N_T = \Omega N_\mu^{1/2},$$

where

$$\Omega = \text{model distortion} = \frac{N_\lambda}{N_\mu}.$$

Likewise, the wave steepness is scaled as

$$\left. \frac{H_o}{L_o} \right\}_p = \left. \frac{H_o}{\frac{g}{2\pi} T^2} \right\}_p = \left. \frac{N_\mu H_o}{\frac{g}{2\pi} N_T^2 T^2} \right\}_m = \left. \frac{N_\mu}{N_T^2} \frac{H_o}{L_o} \right\}_m$$

or

$$\frac{\left. \frac{H_o}{L_o} \right\}_p}{\left. \frac{H_o}{L_o} \right\}_m} = \frac{N_\mu}{N_T^2} = \frac{N_\mu^2}{N_\lambda^2} = \frac{1}{\Omega^2}. \quad (22)$$

One drawback that might arise from this distortion is that the reflection of the incipient waves may become significantly greater in the model than in the prototype, and care must be taken to minimize this effect by selection of scales which give a small distortion. For example, reflection is not appreciable for beach slopes milder than about 1:20, so a prototype beach having a slope of 1:40 could be modeled with a distortion up to  $\Omega = 2$  without much effect due to wave reflection.

It is possible to have an undistorted model, using these proposed relationships, by the proper selection of sediment for the model. This

represents the ideal condition, as long as the resulting model sediment size is still outside of the cohesive sediment range. Using equations (13) and (20) with  $N_\lambda = N_\mu$ , the requirement becomes

$$N_\omega = N_\mu^{1/2} = N_T, \quad (23)$$

with both the parameters  $H_0/L_0$  and  $H/\omega T$  being conserved. However, this condition is more often than not impossible to satisfy due to the fairly large length scale ratio,  $N_\mu$ , required to model typical sandy beaches.

It is worth noting that Battjes' (1974) surf similarity parameter, given as

$$\xi = \frac{\tan\beta}{\left(\frac{H}{L_0}\right)^{1/2}}, \quad (24)$$

is preserved by the proposed model law. Representing  $\tan\beta = \frac{D}{L}$  as before, and  $L_0 = \frac{g}{2\pi} T^2$ , then

$$\frac{\xi_p}{\xi_m} = \frac{\frac{D_p}{L_p} \left(\frac{g_p}{2\pi}\right)^{1/2} \frac{T_p}{H_p^{1/2}}}{\frac{D_m}{L_m} \left(\frac{g_m}{2\pi}\right)^{1/2} \frac{T_m}{H_m^{1/2}}} = \frac{N_T N_\mu^{1/2}}{N_\lambda},$$

when  $(g_p/g_m) = 1$ .

Substitution of equation (13) for  $N_T$  yields

$$\frac{\xi_p}{\xi_m} = \frac{N_\lambda}{N_\mu^{1/2}} \cdot \frac{N_\mu^{1/2}}{N_\lambda} = 1. \quad (25)$$



Thus, similarities which Battjes noted were related to the similarity parameter should be successfully scaled using the proposed model law.

An interesting aspect of the power relationship in the scale-model law between the horizontal and vertical scales is that it is the same as was derived by Dean for equilibrium beach profiles (Dean, 1977) and further examined by Hughes (1978). Dean proposed an equation for the equilibrium beach profile, given as

$$h = Ax^{2/3}, \quad (26)$$

where

$h$  = depth below mean sea level,

$x$  = horizontal distance seaward from the intersection of the beach and the water level, and

$A$  = function of sediment characteristics,

developed from the theoretical concept of uniform wave energy dissipation per unit volume of water in the surf zone. An examination of a large number of profiles by both Dean and Hughes lent credibility to this proposed equation. Rewriting equation (26) as

$$\frac{Ax^{2/3}}{h} = f(x,h) = 1$$

and requiring similarity of this parameter between prototype and model gives

$$\frac{A_p x_p^{2/3}}{h_p} = \frac{A_m x_m^{2/3}}{h_m}$$

or

$$\frac{A_p}{A_m} \cdot \frac{x_p^{2/3}}{x_m^{2/3}} = \frac{h_p}{h_m} \quad (27)$$

Replacing  $x_p/x_m$  with the horizontal length scale  $N_\lambda$ , and  $h_p/h_m$  with the vertical length scale  $N_\mu$ , and rearranging gives

$$N_\lambda = \frac{N_\mu^{3/2}}{\left(\frac{A_p}{A_m}\right)} \quad (28)$$

which results in the same distortion power as was found in the model law equation (20). In essence, the proposed model law is also preserving the equilibrium beach profile as given by equation (26). It is quite possible that the similarity is only coincidental, but later analysis in Chapter VIII seems to indicate that this is not the case.

Finally, as a sampler of what follows in the next chapter, it seems appropriate to mention that attempts to reproduce a prototype event in the wave tank resulted in complete failure when previous model laws based on the time scaling  $N_T = N_\mu^{1/2}$  were tried, while a quite reasonable verification was achieved using the proposed relationships. This fact, plus the seemingly logical development of the model law, makes it appear that the proposed model relationships given by equations (13) and (20) provide a viable means of investigating dune erosion using a small-scale movable-bed model.

## CHAPTER V

### MODEL VERIFICATION

Complete verification of a movable-bed scale-model is perhaps the most difficult task in the whole realm of modeling. The main principle behind verification is that of being able to reproduce in the model the results of a prototype event by the scaling of the known parameters of the event in the model.

Major difficulties arise in two areas:

- 1) In most cases, complete data on all the important parametric values during the prototype event are lacking or unreliable.
- 2) Small-scale testing can introduce secondary effects caused by the model facility itself. For example, many erosion experiments are done in two-dimensional wave tanks, whereas, the process may, in fact, be a three-dimensional phenomenon, complete with rip-currents and longshore sediment transport.

The first of these difficulties, the lack of complete data, will probably never be resolved for the case of dune erosion during storms, due simply to the fact that prior knowledge of a storm landfall is not known in time to install all the necessary instrumentation for recording wave climate, surge level rise, profile changes, etc. Even if all instrumentation were in place, the severity of a hurricane-related storm has the habit of destroying or misplacing the equipment.

The second difficulty, scaling effects, can often be resolved by the careful examination of these effects and the magnitude of change they cause in the model. In the case of dune erosion, the assumption is made that the process is strictly that of onshore-offshore sediment movement. While perhaps not totally correct, the general feeling among most investigators is that onshore-offshore motion is the primary mechanism at work during storms, and thus, the process can be successfully modeled in two dimensions with the hope that the other effects are small.

Model verification proceeds loosely in the following order:

- 1) Select a prototype event with as much available data as possible.
- 2) Select the model scales to give the best performance and range of the facility. For instance, a wave tank must be able to produce good wave forms over the frequency and wave height ranges determined to represent the upper and lower extremes expected for the phenomenon.
- 3) Attempt to reproduce the prototype results by running the model with the given input conditions scaled as accurately as possible.
- 4) After reproducing the desired end condition to reasonable satisfaction, repeat the experiment to show that the same result can be obtained for the same conditions.
- 5) Investigate the sensitivity of the model by examining the effects of perturbing the input parameters.
- 6) Select a different set of scale ratios, as determined by the model law, and repeat the verification.

Verification of the scale model is a time-consuming but essential step in an experimental program. With a verified model the experimenter can proceed with a carefully planned series of model tests designed to shed light on the importance of each independent parameter with reasonable confidence that the results accurately depict what would happen in the prototype under the same conditions.

#### Selection of Prototype Conditions

When Hurricane Eloise struck the Florida Panhandle in September, 1975, its storm surge and accompanying destructive wave action eroded large sections of the relatively undeveloped natural beach-dune system of Walton County to the right of the storm's landfall, in addition to the havoc it played with the highly developed Panama City area (Chiu, 1977).

Under the Florida Coastal Construction Setback Line Program (Purpura, 1972), the coastal areas primarily affected by Hurricane Eloise were surveyed about two years before, with beach-dune profiles taken approximately every 1000 feet and offshore soundings every 3,000 feet (Coastal and Oceanographic Engineering Laboratory, 1974; Sensabaugh et al., 1977). Immediately after the passage of Eloise, survey teams from the Florida Department of Natural Resources (DNR) resurveyed the profiles in the areas most affected by the storm, and these 195 sets of beach-dune profiles were made available by DNR for selection of a suitable profile to be modeled.

### Profile Selection

Since the beach and dunes of Walton County came closest to representing the natural, undisturbed shoreline being considered in this study, these profiles were examined, and the decision was made to use the beach-dune profile designated as R-41. Selection was made based on a number of factors:

- 1) A 26 feet high dune, which means no wave overtopping occurred.
- 2) A fairly simple dune geometry making remolding of the dune in the wave tank considerably easier.
- 3) Profile R-41 is located almost exactly on the track of the hurricane's eye, which allows use of existing methods for calculation of peak storm surge.
- 4) The other Walton County profiles to the right of the storm landfall seem to exhibit pretty much the same erosion characteristics as R-41, thus indicating the decision was fairly arbitrary with regards to poststorm profile configuration.
- 5) Sand samples taken in the immediate vicinity of profile R-41 were available from DNR for analysis.

The profile location is shown in Figure 6, and the profile selected for verification tests is given in Figure 7 with the poststorm profile also shown. Since there was no offshore profile taken at this range, the offshore portion to be modeled was obtained by averaging profiles R-39 and R-42 where such data were recorded.

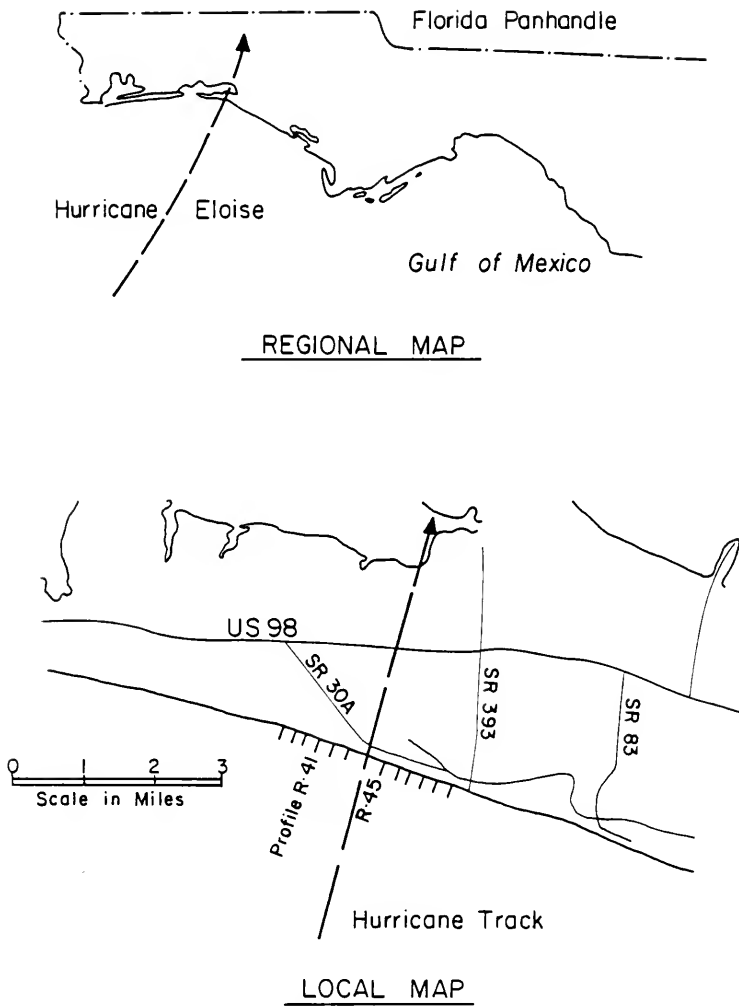


FIGURE 6: PROFILE R-41 LOCATION MAP.

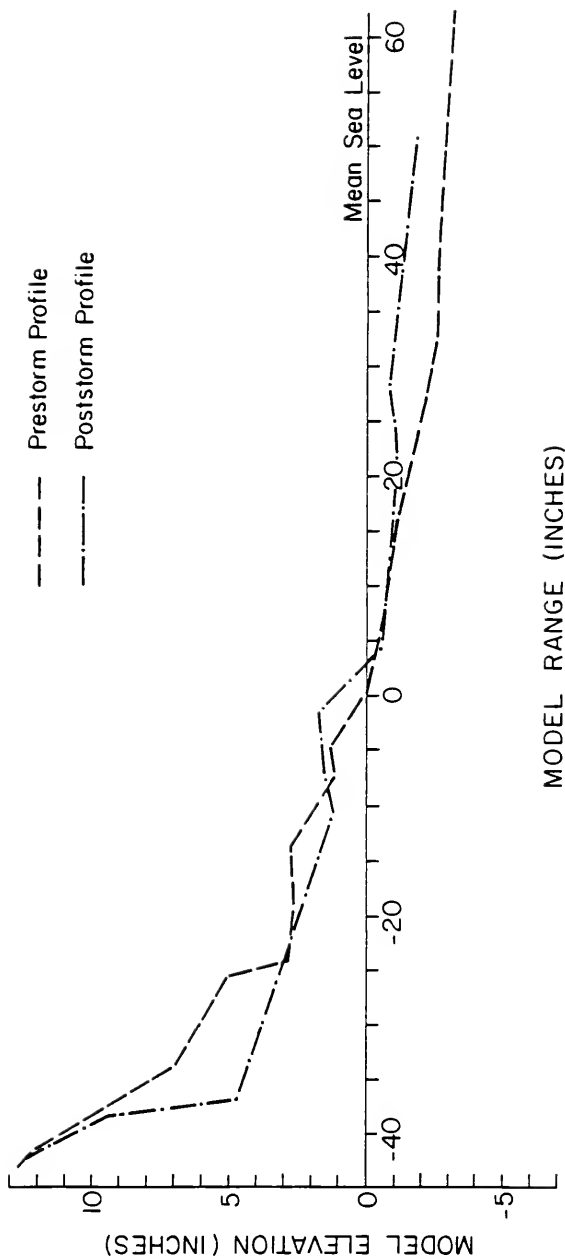


FIGURE 7: PROFILE R-41 AS SCALED IN MODEL.



# Profile Sediment Analysis

Sand samples taken in the immediate vicinity of profile R-41 were obtained from DNR and analyzed, in order to arrive at a representative grain size for the profile. The sieve analysis used standard sieves numbered 10, 18, 25, 35, 45, 60, 80, 120, 170, and 230, which gave a linear progression in  $\phi$  units.\* The results of the analyses are shown in Table 1 below.

TABLE 1  
WALTON COUNTY SAND ANALYSES

Parameter in (mm)	Dune	Mean High Water	Mean Low Water	Profile
$d_{50}$	0.226	0.215	0.330	R-39
$d_e$	0.2199	0.2092	0.3202	
$d_{50}$	0.260	0.280	0.270	R-42
$d_e$	0.2517	0.2705	0.2627	
$d_{50}$	0.260			R-45
$d_e$	0.2511			

In the above table,  $d_{50}$  is given as the mean grain-size diameter taken from the distribution curve at the point where 50 percent of the sample is finer than that size. The parameter  $d_e$  has been defined by

---

\* $\phi = -\log_2 d_{mm}$ : definition with diameter,  $d_{mm}$ , given in millimeters.

Christensen (1969) to be the effective grain-size of a nonuniform natural sediment. It represents the grain-size of a uniform spherical sediment that behaves in the same way as the natural nonuniform sediment from which it was derived, and as such, provides a convenient means for expressing well-sorted sediment distributions. Calculation of  $d_e$  is done using equation (29) when the grain-size distribution is a straight line.

$$\frac{d_e}{d_{50}} = \frac{2 Cu \ln Cu}{Cu^2 - 1} . \quad (29)$$

In equation (29),  $Cu = \frac{d_{60}}{d_{10}}$ , Hazen's uniformity coefficient, and the values for  $d_{10}$ ,  $d_{50}$ , and  $d_{60}$  are obtained from the sediment distribution as illustrated in Figure 8. Since the prototype grain-size distributions for Walton County were nearly straight lines (as can be seen in Figure 9),  $d_e$  was calculated using equation (29). As shown in Table 1, well-sorted, narrow grain-size distributions have an effective grain-size nearly equal to the mean. The average value of  $d_e$  for all seven samples is 0.255 mm, while the average of the three samples of profile R-42 is 0.262 mm. Since R-42 is only 1000 feet from the selected profile R-41, it was decided to use the value of  $d_e$  obtained from the R-42 samples. Actually the difference between that value and the overall average is quite insignificant.

#### Surge Hydrograph Selection

Since no comprehensive storm surge data exist for Hurricane Eloise, it was necessary to make a close approximation for the surge

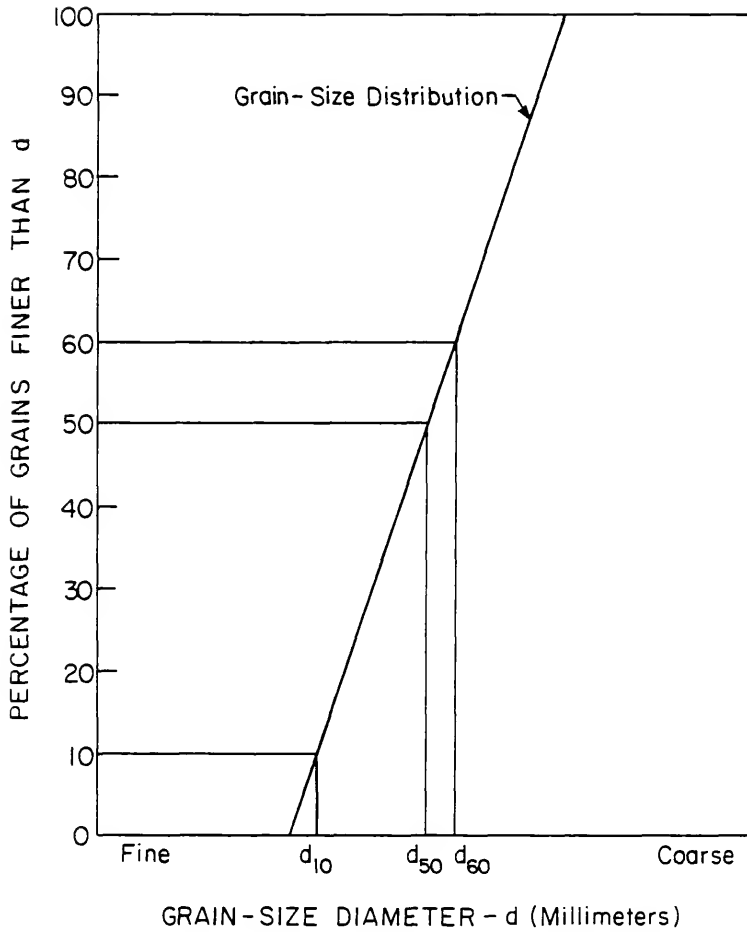


FIGURE 8: USE OF GRAIN-SIZE DISTRIBUTION TO FIND  $d_e$ .

hydrograph using a combination of existing prediction methods and logical arguments.

A first estimate of the peak surge level can be obtained by looking at the eroded dune profile shown on Figure 7. It is seen that the dune toe is located at a prototype elevation of about 10 feet above mean sea level. It is obvious that any surge level above 10 feet would have eroded the dune more than it did. Allowing for wave run-up would put the peak surge level at somewhere between 7 and 9 feet.

Using the nomogram method for prediction of peak surge for a storm moving onshore given in the Shore Protection Manual (Coastal Engineering Research Center, 1975), it was possible to calculate a first estimate of the surge on the storm track, which passed over the profile in question. Using the storm values of

$$V_F = 20 \text{ knots--forward speed,}$$

$$P = -1.72 \text{ inches } H_g\text{--pressure differential,}$$

$$R_{\max} = 15 \text{ naut. miles--radius of maximum winds,}$$

obtained from the National Weather Service, the peak surge was found to be approximately 7.7 feet.

Although the method cannot be considered accurate, it is at least in the neighborhood predicted by common sense.

Finally, a computer prediction for peak surge using the NOAA SPLASH data is shown in Figure V-5 of Pidgeon and Pidgeon (1977), as calculated for Hurricane Eloise. From this, the surge elevation of about 7.5 feet is given at the location of profile R-41.

The above reasoning, combined with observations during the verification runs as to the effects of varying the peak surge, has led to

the final estimate of slightly over 8 feet for the value of peak surge experienced at this location during Hurricane Eloise.

The time history of the surge level rise was approximated as a linear increase from mean sea level to peak surge over a time span of 12 hours, a constant peak surge for one hour, and a linear decrease over 6 hours. This was determined by examining the recorded surge time histories associated with storms of similar strengths as Eloise (Harris, 1963).

While the assumed surge hydrograph may not be exactly what occurred, it is felt that it is a very reasonable estimate, and hopefully the beach response in the model will bear this out. In fact, preliminary tests showed that the majority of erosion occurred around the peak surge value; thus the assumed duration is not quite as important as the peak elevation. Later observations from the experimental test series confirmed this.

#### Wave Climate Selection

While no nearshore wave data were taken precisely at the location of R-41, it was possible to estimate the probable wave climate using data recorded at other locations during Hurricane Eloise.

A wave-rider buoy operated by the National Oceanic and Atmospheric Administration recorded wave data in the middle of the Gulf of Mexico as the hurricane eye passed within 10 miles (Withee and Johnson, 1975). At the peak of the storm at that location, it was found that the dominant spectral wave period was 11 seconds, and it remained constant over a five hour period. Peak significant wave height was 29 feet. As

the storm made landfall, wave data were also being recorded on the Naval Coastal Systems Laboratory tower located 11 miles offshore of Panama City in 105 feet of water. Here the modal wave period was also 11 seconds for the two hours before power failure which occurred within an hour of the closest approach of the storm's eye (Pidgeon and Pidgeon, 1977). At that time the maximum significant wave height was found to be 14 feet.

From these two sets of data, it can be seen that the dominant wave period appears to be conserved while the storm moved into shallow water. Thus a dominant wave period of 11 seconds can confidently be nominated as a prototype parameter for profile R-41, located about 40 miles to the west of the Panama City tower.

Selection of significant wave height is a little less precise due to the effects of energy dissipation experienced by the wave field during shoaling. In addition, the significant wave height should be greater to the right of the track of the storm with the maximum at about the radius of maximum winds (20 miles in this case).

Some computer numerical models do exist which attempt to predict energy losses of spectra due to shoaling (Hsiao, 1978), but the expense and difficulty in running them make their use, in this case, unjustified.\* For this reason, the significant wave height (SWH) in shallow water (50 feet) at the R-41 profile site was estimated by assuming a 14 feet SWH existed 11 miles offshore, the same as Panama City, and that losses incurred in shoaling reduced the significant wave height to around 12 feet. This value represents the peak value at the

---

\*Dr. O.H. Shemdin, Department of Coastal and Oceanographic Engineering, University of Florida, personal communication.

height of the storm and associated surge. At lower surge levels, the SWH value was, of course, less.

While the chosen value for wave period is probably very close to what actually occurred during the storm, not as much confidence can be given to the selected SWH. However, the value of 14 feet represents a maximum, while values of under 10 feet seem slightly low for a category 3 hurricane at landfall. However, it was shown during the experimental phase that wave height perturbations do not significantly alter the amount of dune erosion.

#### Selection of Model Scales

In Chapter IV the scale-model relationships were derived, resulting in two equations in four unknowns: the vertical length scale ratio ( $N_\mu$ ), the horizontal length scale ratio ( $N_\lambda$ ), the sediment fall velocity scale ratio ( $N_\omega$ ), and the time scale ratio ( $N_T$ ). Having the freedom of selecting two of the ratios, it was found that choosing  $N_\omega$  and  $N_\mu$  was the most convenient. Originally it was hoped that the vertical scaling could be 1:16 (or  $N_\mu = 16$ ), but this placed a limitation on the range of wave heights which could be generated in the tank before extreme nonlinearities began to dominate the wave motion. As a consequence, the vertical scale ratio was chosen to be  $N_\mu = 25$ .

The sand used to mold the profile in the wave tank was first sifted to remove all sizes greater than 0.3 mm. This was done to reduce the effective grain-size diameter, which in turn increases  $N_\omega$  with the result of decreasing the model distortion. A second reason for removing the larger grains was to try to prevent "armoring" of the foreshore beach slope.

Two samples were sieve analyzed, producing nearly identical distributions. A composite using both sample results was plotted, and the values of  $d_{50} = 0.152$  mm and  $d_e = 0.147$  mm were found. The distribution of grain-sizes for the model sand compared very favorably with the prototype distributions, one almost appearing to be a linear offset of the other. Figure 9 shows both the model sand and the approximate prototype sand grain-size distributions.

The values of particle fall velocity for both the prototype and model effective grain-size diameters at 25°C are given in the Shore Protection Manual as:

$$\omega_p = 4.0 \text{ cm/sec for } d_e)_p = 0.262 \text{ mm}$$

$$\omega_m = 1.65 \text{ cm/sec for } d_e)_m = 0.147 \text{ mm ,}$$

which results in

$$N_{\omega} = \frac{\omega_p}{\omega_m} = 2.424 .$$

From equation (13) and (20) of Chapter IV, the scale ratios for horizontal length and time were calculated along with the model distortion,

$\Omega = \frac{N_{\lambda}}{N_{\mu}}$ . These values are listed in Table 2 below, and were used throughout the model verification and the experimental test series.

TABLE 2  
MODEL SCALE RATIOS

Vertical Length Scale	$N_{\mu}$	25
Horizontal Length Scale	$N_{\lambda}$	51.56
Time Scale	$N_T$	10.31
Model Distortion	$\Omega$	2.06



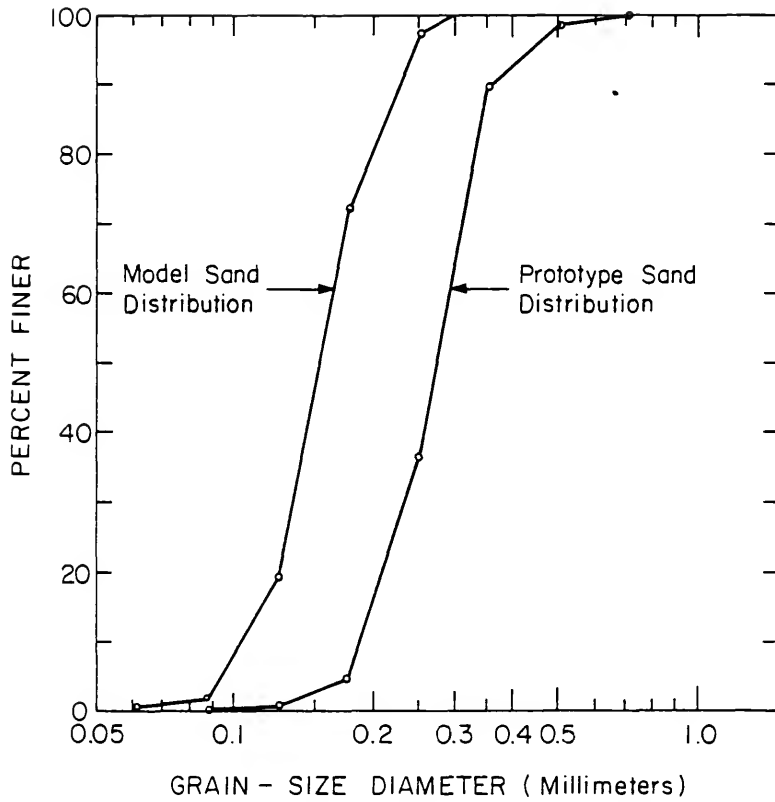


FIGURE 9: MODEL AND PROTOTYPE GRAIN-SIZE DISTRIBUTIONS.

### Requirements for Verification

There are three major characteristics of dune erosion which must be reproduced in the model test in order to satisfactorily obtain verification:

- 1) For the correctly scaled input parameters determined for the prototype, the total volume of dune material eroded above mean sea level in the model must approximate the same volume eroded in the prototype when the proper scale factors are applied.
- 2) This erosion must occur over the time span of the surge duration as scaled in the model.
- 3) The poststorm foreshore beach slope must duplicate that which existed in the prototype when the distortion factor is applied.

By doing this, the derived distortion of the model is verified.

Referring to Figure 7, the above three points essentially mean reproducing the poststorm profile in the region above mean sea level. It is not expected that the berm feature between ranges -10 inches to +5 inches will be reproduced since it was probably formed by low-steepness swell wave conditions which occurred between the end of the storm and the measurement of the profile several days later. The region above this elevation was not influenced after the surge elevation decreased. Reproduction of the profile in the surf zone is not necessary because the poststorm wave climate also caused changes in this region.

### Early Attempts at Model Verification

The first attempts to verify a model law were carried out using the scaling relationships as proposed by the Delft Hydraulics Laboratory (Vellinga, 1978). The first run was made using irregular waves with a vertical scale of  $N_u = 16$ . It was seen that this scale was too large to give proper waves which necessitated reducing the vertical scale to  $N_u = 25$ . Several tests were conducted at this scaling range using both regular and irregular waves. In all cases, sediment was moved from offshore and deposited on the beach as the surge level was raised. At this point it became obvious that preserving the wave steepness in the model, which results in the time scaling of  $N_T = N_u^{1/2} = 5$ , was not a proper technique. What perhaps worked for others, when an instantaneous surge level was applied, did not work when the water level rise occurred like it does in nature. In the latter case, the waves had time to transport sediment landwards and thus altered the beach configuration, which in turn affects the waves.

At this point in the verification program, a series of undocumented runs were made for the purpose of developing experience and intuition into the effects of varying the parameters and of gaining knowledge of the wave tank characteristics, an essential part of any experimental endeavor. Concurrently, the scale-model relationships presented in Chapter IV were developed, and the resulting distorted profile was remolded in the tank.

Following the establishment of the new model law, over 16 attempts were made at model verification using an irregular wave field. None of these runs produced results which satisfactorily fulfilled the requirements for verification. An example is shown in Figure 10.

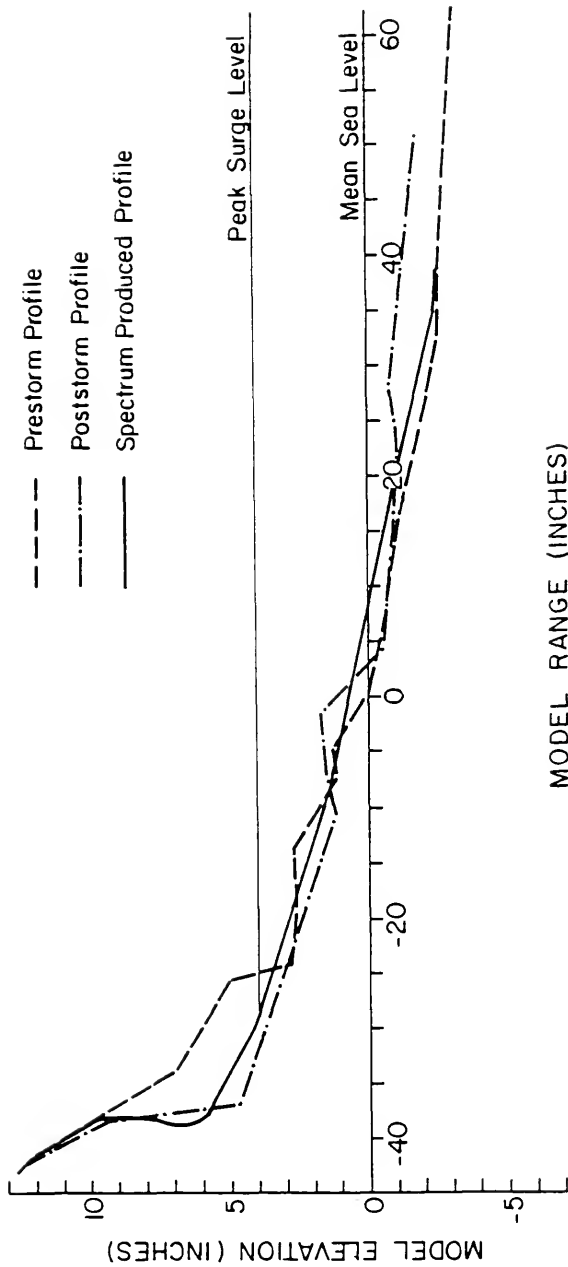


FIGURE 10: ATTEMPTED MODEL VERIFICATION USING WAVE SPECTRUM.

As can be seen, the amount of dune recession is good, and the resultant beach slope is nearly right; but the recurring problem was that the erosion was not deep enough, and the sand was not being transported offshore far enough.

Each of the input parameters was varied within reasonable limits to see if the estimation of the storm characteristics was inaccurate. None of these variations produced the desired result, although much was learned in the process. After looking at possible causes for this failure, from wave reflection to paddle response to spectral representations and so forth, it was finally decided that the problem was in trying to use irregular waves in the model. The next run after this conclusion was conducted using regular waves which gave an almost perfect verification of the model. Since it was only a trial, control was not very strict, and consequently this run was not documented. Knowing that verification of the model was possible with regular waves makes the explanation of the failures using irregular waves much easier. These arguments appear in the following section.

#### Irregular Versus Regular Waves

Ideally the operation of a small-scale wave model should include a random-type wave field as would exist in nature. In deep water it is possible to invoke the assumption of a Gaussian process in order to derive a suitable power spectrum representation of the wave heights and frequencies. However, as these waves propagate into shallow water, they become altered by such effects as shoaling, refraction, and reflection, thus turning the wave field into a very non-Gaussian phenomenon as individual waves begin to interact with each other in ways that are

still not understood. One of the main characteristics of shallow-water spectra is the presence of phase grouping, sometimes known as surf beat. This groupiness is a function of both space and time, with well grouped waves at one location becoming less well defined as they propagate in time. This must certainly have an effect upon the erosion of the beach and dune.

The narrow-band spectra generated for use in the model verification were developed under the assumption of a Gaussian process since research into shallow water waves is still in its infancy. And while the random time series conformed to the statistical representation given by the desired wave spectrum, there are an infinite number of different time series which will also conform, none of which depict the wave groupiness present in shallow-water random wave fields. This is the major argument against using spectral wave representations in a small-scale model until more is known about the resonance effect of nearshore wave spectra, and it probably was the cause of the failure to verify the model when spectral wave distributions were employed. This view is also supported in the reviewer's comments presented in a report by Jain and Kennedy (1979), where the statement is made that small-scale movable-bed modeling should be restricted to regular waves until more is known about nearshore random wave phenomena. Further confirmation of the importance of wave grouping was given by Johnson et al. (1978) who found that substantially more damage occurred to rubble mound structures for grouped waves than for nongrouped waves conforming to the same power spectrum distribution.

To further complicate matters, it has been shown that the generation of random waves in model facilities has the tendency of generating

long "parasitic" waves because the boundary conditions for second order wave effects are not satisfied at the wave paddle (Hansen and Hebsgaard, 1978). This fact was observed in the verification process on a strip chart recording of a random wave train, which illustrated a parasitic long wave with a period between 15 and 20 seconds. These long waves are reflected and continue to build in amplitude. Methods exist which will eliminate these long waves (Hansen et al., 1980; Hudspeth et al., 1978), but are primarily theoretical analyses which are difficult to apply with the present equipment in the Air-Sea wave flume.

For the above reasons, plus the fact that verification could be reasonably achieved using regular waves, it was decided that the model verification and ensuing experimental test series be conducted using regular wave trains. Perhaps future developments will allow the use of random waves in small-scale erosion tests.

#### Verification Runs

Two documented verification runs were performed using regular waves and reproducing nearly the same storm conditions. The second run was required in order to demonstrate that the results of the first run could be reproduced, and because a slight wave period variation was observed near the end of the first run. Both tests are detailed below.

#### First Verification Run

The parameters for the first run are given in Table 3 with both model and prototype values given.

TABLE 3  
FIRST VERIFICATION RUN

	Wave period (sec)	Maximum wave height	Peak surge level	Time to reach peak surge	Time at peak surge	Time of surge decrease
Prototype Value	11	8.5 ft.	8.3 ft.	12.4 hr.	1.9 hr.	5.2 hr.
Model Value	1.07	4.1 in.	4.0 in.	72 min.	11 min.	30 min.

The surge increase was approximately linear over the time span, and the wave period was held constant throughout. The prototype wave height of 8.5 feet gave the same wave energy density as a narrow-band spectrum with a significant wave height of about 12 feet; and while the surge level was on the increase, the wave height was gradually increased until the peak value was reached at 38 minutes into the run, or about when the surge was half its peak value. This value was maintained until the surge level began to decrease at which time the wave height was again reduced. This process hopefully typifies what happens in nature over the duration of a storm.

Figure 11 gives the measured profile taken down the wave flume centerline at the end of the verification run. Profiles measured near the glass wall and the back wall indicated that there was a slight lateral variation in the eroded profile. However, the erosion which occurred compared very favorably with the prototype, with the exception of the extra dune recession. A standard posttest check of the wave frequency revealed that the function generator knob had been bumped,



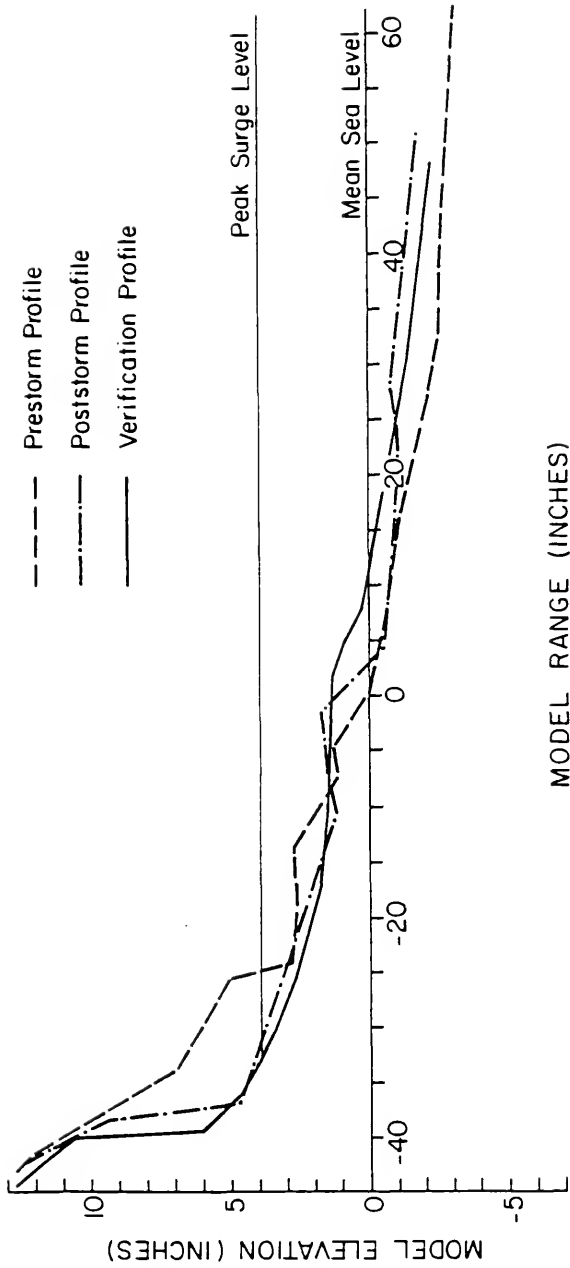


FIGURE 11: VERIFICATION RUN 1, FINAL PROFILE ON CENTERLINE.

causing an increased wave period (equivalent to 13 seconds in the prototype) during the latter portions of the peak surge duration. This was assumed to be the cause of the extra recession, a fact later confirmed by the experimental test series.

#### Second Verification Run

Table 4 gives the storm parameters for the second verification run which proceeded in much the same manner as the first run.

TABLE 4  
SECOND VERIFICATION RUN

	Wave period (sec)	Maximum wave height	Peak surge level	Time to reach peak surge	Time at peak surge	Time of surge decrease
Prototype Value	11	8.5 ft.	8.3 ft.	12 hr.	1.4 hr.	5.2 hr.
Model Value	1.07	4.1 in.	4.0 in.	70 min.	8 min.	30 min.

As before, the surge rise was approximately linear with the wave period being held constant throughout. The wave height was gradually increased to its peak value which occurred at about 48 minutes into the run, and the wave height was decreased as the surge level dropped, signifying the passage of the storm.

This time there was little discernible lateral variation in the eroded profile; and the eroded quantity and dune recession gave an

almost unbelievable reproduction of the prototype event as can be seen in Figure 12, which gives the posttest profile measured on the flume centerline. Near the glass, the profile was slightly elevated, but not by very much. Figure 13a shows the profile at the end of the peak surge duration, while Figure 13b was taken at the end of the surge decrease.

### General Observations

Several observations which provide some basic insight into the erosion process were made during the verification:

- 1) As the surge level began to rise, there was little change in the profile until the latter stages of the increase, when more of the dune was exposed to the erosive wave action. This points to the importance of the surge level in the erosion process.
- 2) The erosion that had occurred by the time the peak surge had been reached represented between 80 to 90 percent of the final erosion quantity. Thus it is seen that the most damage is done during the surge rise and the time the surge remains at its peak value.
- 3) The effect of lowering the surge level with decreased wave energy had only a minor effect on the profile, the most noticeable being the smoothing out of the profile as the water level dropped. This was caused by the deposition of sediment over the beachface and the transition from plunging breakers back to spilling breakers during the surge decrease.

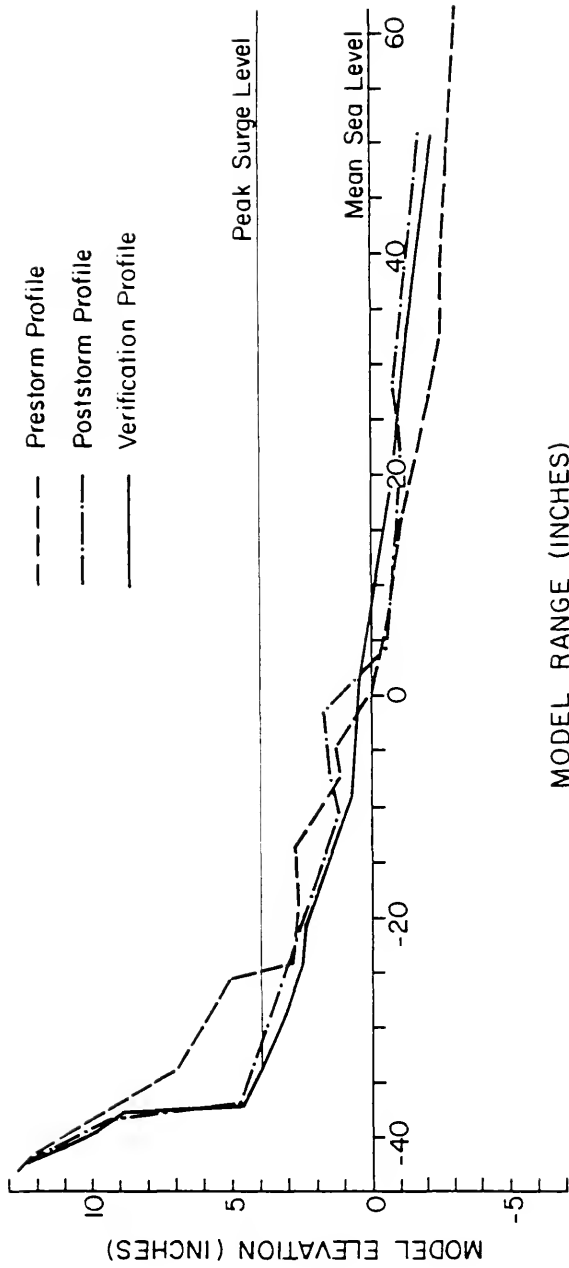


FIGURE 12: VERIFICATION RUN 2, FINAL PROFILE ON CENTERLINE.



13a: PROFILE AT END OF PEAK SURGE DURATION.



13b: PROFILE AT END OF SURGE LEVEL DECREASE.

FIGURE 13: ERODED BEACH-DUNE, RUN 2.

### Discussion

The verification of the proposed model law seems to have been successful based upon the above results. The estimation of the storm parameters was fairly reasonable in view of the limited data available, and the resultant eroded profiles obtained during the model testing closely resemble the actual prototype profile in terms of recession, eroded volume, and beachface slope. The offshore portion was not as good, due to the fact that this area was altered by the mild wave climate which prevailed between the end of the storm and the time the prototype profile was surveyed. The subsequent experimental series demonstrated that the erosion is most effected by surge level which was probably the most accurate of the estimated parameters. Thus the model would not be too sensitive to incorrect estimates in wave height, as long as they were within reason.

Of course there is always a need for further verification since the modeling laws have only been verified on one prototype event, but this must wait until more prototype data become available. Until such time, the derived small-scale movable-bed modeling relations presented in Chapter IV represent suitable modeling laws for use in small-scale investigations into dune erosion during severe storms. The relationships are based on physics and observations and have been verified in the laboratory by the reproduction of storm conditions to a degree of realism never before attempted, including a variable surge hydrograph and a varying wave height.

## CHAPTER VI

### EXPERIMENTAL TEST SERIES

The experimental test series to investigate the role of the primary factors involved in dune erosion by severe storms was designed in such a way as to cover the range of the storm parameters expected to occur during a hurricane making landfall on an undeveloped portion of the Florida coastline. The order of the test runs was usually arranged so that each successive run reproduced conditions more severe than the previous run. In this way the regrading of the beach and dune was optimized, and progressive patterns could be recognized early in the test series in order to make changes in the parameters if necessary. This chapter details the experimental test series, the parameters tested, and the procedures followed.

#### Profile Selection

The selected profile for the model series was chosen to be representative of an average Florida beach. From an analysis by Hughes (1978), it was found that a curve fit of the profile form

$$h = Ax^{2/3}$$

on over 400 actual beach profiles from the Florida each coast and panhandle indicated a modal value of  $A = 0.15$  when both depth ( $h$ ) and range ( $x$ ) are given in feet. Since these profiles probably exhibited

the characteristics of near-equilibrium beach profiles, it was decided to adopt this equation for the below mean sea level portion of the profile. This represents a better choice than a plane-sloped beach since it is desirable to begin the model tests with at least near-equilibrium conditions. In this way, the resultant changes would more closely duplicate nature.

Modeling the profile equation using the previously derived relationship obtained by comparing equations (20) and (28), i.e.,

$$\frac{A_p}{A_m} = \frac{\omega_p}{\omega_m}^{2/3},$$

where

$\omega$  = grain-size fall velocity,

p = prototype value, and

m = model value,

resulted in the equation

$$h_m = 0.19 x_m^{2/3}, \quad (30)$$

where both  $h_m$  and  $x_m$  have units of inches. Hughes also observed that beyond a certain depth the offshore profile became distinctly steeper, most probably a relic feature from the rising sea level over the past 4000 years (or from previous severe storms). An inspection of prototype profiles indicated that this portion could be well represented by a straight line with a prototype slope of 1:40 extending seaward from about the 13 foot depth.

The prestorm beachface was represented by a straight line having a prototype slope of 1:10 with a dune toe elevation of 7 feet above



mean sea level. These values were chosen after discussions with an individual familiar with Florida beaches.\* While slightly steeper than the average beachface calculated for Bay and Walton Counties in the Florida panhandle (Chiu, 1977), it was felt that the values used were a good representation of Florida beaches on the whole.

The dune was chosen with an initial height of 20 feet above mean sea level in the prototype with a dune face slope of 1:2. This slope is approximately the angle of repose for sediments in the range of grain sizes found in coastal dunes, and this slope was retained when the dune height was increased later in the test series.

The same sediment size as was used during the verification tests was used for the model series. Hence the prototype profile represents one with an effective grain-size of  $d_e = 0.27$  mm. For this reason all the scaling relationship values given for the model verification in Table 2 still apply for the test series. Figure 14 gives the initial profile used for the experimental series along with the model dimensions and slopes as determined by the scale-model relationships.

#### Storm Parameters

The storm parameters which were varied during the test series were as follows:

- 1) Wave period (10, 12, and 14 seconds in the prototype);
- 2) Wave height, when measured before shoaling began in the tank (6, 8, 10 feet in the prototype);
- 3) Peak surge level above mean sea level (8, 11, 14 feet in prototype);

---

\*Dr. T.Y. Chiu, Department of Coastal and Oceanographic Engineering, University of Florida, personal communication.

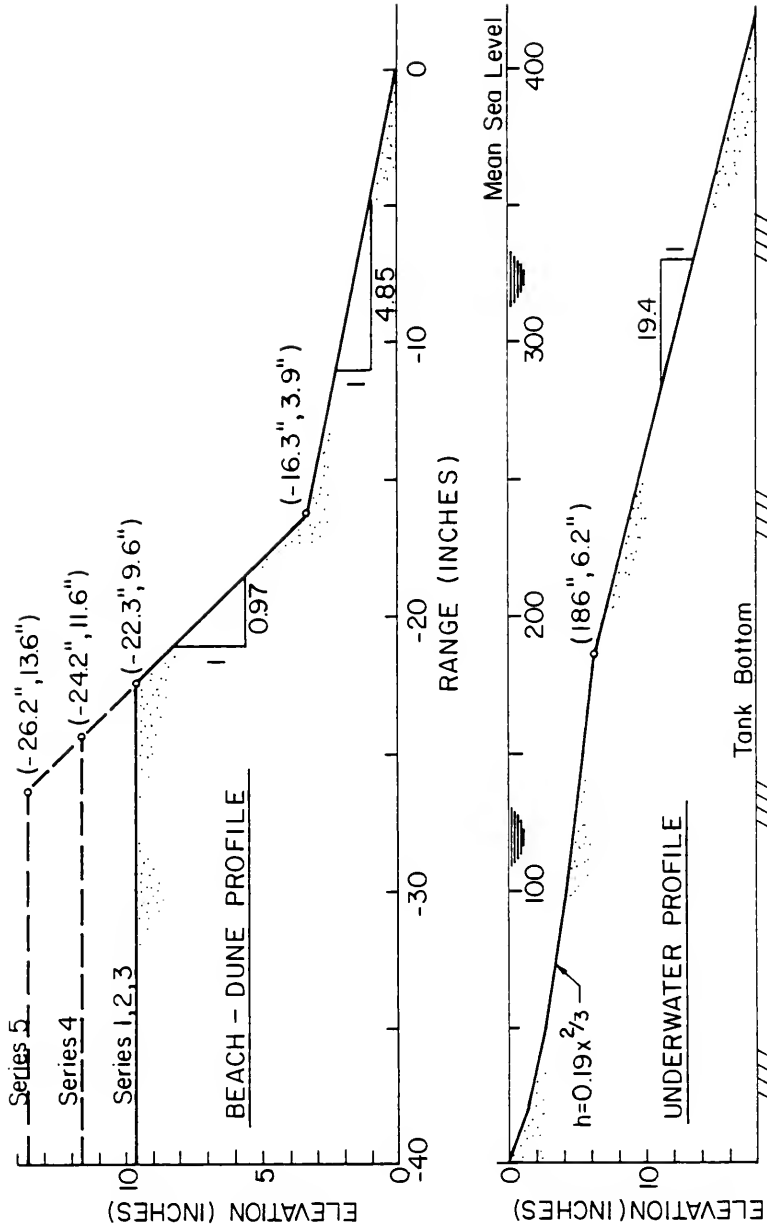


FIGURE 14: EXPERIMENTAL TEST SERIES PROFILE.

- 4) Instantaneous surge level rise as opposed to finite-time surge increases;
- 5) Surge level rise duration (4, 7, 15 hours in the prototype); and
- 6) Prestorm dune height (20, 24, 28 feet in the prototype).

Regular waves were used throughout the entire experimental program which began November 12, 1980, and ended January 20, 1981. The 38 experimental runs, involving a time-dependent surge level increase, approximated the surge as a linear increase over time. Table 5 lists both the model and prototype values for the parameters involved in the test series.

The experimental test runs can be divided roughly into five distinct series, as noted on Table 5. Series 1 compared three different wave heights at three different surge levels for a given wave period and dune height. In addition, the first 8 runs of the series investigated the effects of different time spans in bringing the surge level from mean sea level to its peak value. The first run used an instantaneous peak surge level in order to see if a finite surge is even required to obtain the final equilibrium. Runs 36 and 37 of series 4 repeated this test using different surge levels and initial dune heights.

Series 2 repeated series 1 at a different wave period, the only difference being that the effect of surge level rise duration had been established so further tests on this variation were not required.

Test series 3 was an abbreviated version of series 1 and 2 using yet another wave period, but maintaining the same initial dune height

TABLE 5  
EXPERIMENTAL PARAMETERS

Run #	Prototype Values					Model Values				
	Period $T_p$ (sec.)	Surge Level $S_p$ (ft.)	Wave Height $H_p$ (ft.)	Surge Duration $T_{sp}$ (hrs.)	Dune Height $D_p$ (ft.)	Period $T_m$ (sec.)	Surge Level $S_m$ (in.)	Wave Height $H_m$ (in.)	Surge Duration $T_{sm}$ (min.)	Dune Height $D_m$ (in.)
Series 1	1	8	6	0.0	20	.970	3.84	2.88	0.0	9.6
	2	8	6	7.7	20	.970	3.84	2.88	45	9.6
	3	8	6	14.6	20	.970	3.84	2.88	85	9.6
	4	8	6	4.3	20	.970	3.84	2.88	25	9.6
	5	8	10	12.2	20	.970	3.84	4.80	71	9.6
	6	8	10	4.3	20	.970	3.84	4.80	25	9.6
	7	8	10	8.4	20	.970	3.84	4.80	49	9.6
	8	8	8	8.8	20	.970	3.84	3.84	51	9.6
	9	11	6	9.1	20	.970	5.28	2.88	53	9.6
	10	11	8	9.1	20	.970	5.28	3.84	53	9.6
	11	11	10	9.5	20	.970	5.28	4.80	55	9.6
	12	14	6	9.6	20	.970	6.72	2.88	56	9.6
	13	14	8	10.3	20	.970	6.72	3.84	60	9.6
	14	14	10	9.8	20	.970	6.72	4.80	57	9.6
Series 2	15	8	6	8.4	20	1.163	3.84	2.88	49	9.6
	16	8	8	8.1	20	1.163	3.84	3.84	47	9.6
	17	8	10	8.6	20	1.163	3.84	4.80	50	9.6
	18	11	6	9.8	20	1.163	5.28	2.88	57	9.6
	19	11	8	9.6	20	1.163	5.28	3.84	56	9.6
	20	11	10	9.5	20	1.163	5.28	4.80	55	9.6
	21	14	6	10.3	20	1.163	6.72	2.88	60	9.6
	22	14	8	10.0	20	1.163	6.72	3.84	58	9.6
	23	14	10	9.6	20	1.163	6.72	4.80	56	9.6

TABLE 5  
CONTINUED

	Run #	Prototype Values					Model Values				
		Period $T_p$ (sec.)	Surge Level $S_p$ (ft.)	Wave Height $H_p$ (ft.)	Surge Duration $T_{sp}$ (hrs.)	Dune Height $D_p$ (ft.)	Period $T_m$ (sec.)	Surge Level $S_m$ (in.)	Wave Height $H_m$ (in.)	Surge Duration $T_{sm}$ (min.)	Dune Height $D_m$ (in.)
Series 3	24	14	8	6	8.6	20	1.357	3.84	2.88	50	9.6
	25	14	8	8	8.1	20	1.357	3.84	3.84	47	9.6
	26	14	11	6	9.1	20	1.357	5.28	2.88	53	9.6
	27	14	11	8	8.9	20	1.357	5.28	3.84	52	9.6
	28	14	14	6	9.5	20	1.357	6.72	2.88	55	9.6
	29	14	14	8	10.0	20	1.357	6.72	3.84	58	9.6
	30	12	8	6	8.3	24.2	1.163	3.84	2.88	48	11.6
Series 4	31	12	8	8	8.3	24.2	1.163	3.84	3.84	48	11.6
	32	12	11	6	9.6	24.2	1.163	5.28	2.88	56	11.6
	33	12	11	8	9.5	24.2	1.163	5.28	3.84	55	11.6
	34	12	14	6	9.5	24.2	1.163	6.72	2.88	55	11.6
	35	12	14	8	10.0	24.2	1.163	6.72	3.84	58	11.6
	36	12	11	8	0.0	24.2	1.163	5.28	3.84	0	11.6
	37	12	14	8	0.0	24.2	1.163	6.72	3.84	0	11.6
Series 5	38	12	11	6	10.1	28.3	1.163	5.28	2.88	59	13.6
	39	12	11	8	9.5	28.3	1.163	5.28	3.84	55	13.6
	40	12	14	6	10.1	28.3	1.163	6.72	2.88	59	13.6
	41	12	14	8	12.4	28.3	1.163	6.72	3.84	72	13.6

elevation. In this series only two different wave heights at 3 different surge levels were compared.

Series 4 and 5 repeated some of the earlier tests using different values of dune height.

Time-variation plots of the experimental profiles for each run are shown in Appendix C.

### General Observations

A few general observations are worth noting:

- 1) As the surge level began to rise, very little change in the original profile, outside of ripple formation, occurred until the surge level reached a height where the wave uprush reached the toe of the original dune. This was typically between 15 and 20 minutes into the run, depending upon the rate of rise being used. After this, dune erosion occurred quite rapidly.
- 2) In test series 1, as the surge approached its peak value, some unevenness in the profile across the width of the tank was observed. However, this was usually rectified by the wave action before the peak surge value was reached. The cause of this is the fact that the wave frequency was close to the fundamental mode of sloshing in a basin, and the wave crests could be seen exhibiting a rocking motion as they propagated down the tank toward the beach. On the gentle prestorm slope, this resulted in uneven uprush; but as the sediment moved offshore and built the bar system, the slope became steeper which acted to decrease this effect. The

profile then quickly became uniform across the width of the wave flume.

It is strongly felt that this phenomenon had little influence on the results. The other series sometimes exhibited this unevenness, but to a very small degree.

- 3) Wave reflection was most evident in test series 1, and when the bar formation became prominent, the monitored wave reflection sometimes approached the value of 15 percent. When this occurred, the test was temporarily halted and the water was allowed to settle before the test was resumed. The other series at higher values of wave period showed little sign of reflection, but subsequent data analysis indicated that reflection was present in all runs. It will be seen that this problem is overcome in the data analysis by considering only the properties of the transmitted wave instead of the deep water characteristics.
- 4) Dune erosion occurred very rapidly as the surge level increased. Typically 70 to 90 percent of the final "equilibrium erosion" occurred by the time the surge reached its peak value. However, the process was not one of passing through discrete steps of equilibrium. Chapter IX presents a more complete analysis of these observations.
- 5) The model waves initially were breaking in a spilling manner until the surge level increased to the point that the profile was steep enough to cause plunging breakers. The steepening of the profile was caused by a bar formation offshore.

- 6) It appeared, at least in the two-dimensional case, that all the sediment that went into building of the offshore bar during the experiments was derived solely from the coastal dune. This, however, may not be the case for offshore bar formation in the absence of a storm surge.
- 7) As the erosion was taking place, it was not uncommon for the dune to be substantially undercut before the weight of the overhanging dune brought it plunging down into the water. This was caused by the surface tension of the wet sand in the model. Since surface tension was not scaled in the model, this effect would not be present in nature where the weight of the sand would cause the dune to shear off before much undercutting could occur. In order to provide more reasonable results, it was at times necessary to tap the top of the dune to collapse it when the undercutting had become excessive. Surface tension did, however, work to the model's advantage since the nearly vertical sheared dune face closely resembled those found in nature where the roots of vegetation aid in maintaining a nearly vertical dune face during storm erosion.

#### Typical Test Procedures

Procedures are important in any experimental research in order to provide consistent results and to help eliminate human error. Whenever possible, procedures and standard practices should be established in advance of the testing program. The following is a brief outline of some of the procedures and techniques used during the experimental phase



of this project. By listing them here, future investigators might be able to identify the pitfalls and develop better methods for their work.

#### Regrading of the Prestorm Profile

After every run it was necessary to regrade the beach to the original prestorm profile. This profile was marked on the outside of the flume's glass wall with an indelible marking pen. It was found that the easiest method was to drain the water from the tank and then to immediately regrade the profile while the sand was still wet. This gave better sand compaction and a smoother profile. The grading was always begun offshore and proceeded toward the beach. Sighting the profile marking through the glass, the profile was graded using a timber 2 x 4 cut to slightly less than the tank width. The profile was kept uniform by checking with a "bubble-type" level across the width of the tank. Since it was found that the grading proceeded faster than the tank could be filled with water, the inlet water valve was open while the grading was being done. The process of draining, regrading, and filling the tank could be accomplished within 1½ to 2 hours.

#### Pretest

Before the start of each test, the experimental values for the run were recorded in a journal, the initial water level was checked, the peak surge point gauge was set, the wave gauge calibration was checked, the electronics were warmed up, the wave frequency was set or checked, and the stopwatch was wound and set.

### Beginning

After the hydraulic system was brought up to pressure, small waves were generated, and the inlet water valve was opened to its predetermined position to provide the nearly linear surge level increase over the stipulated time span. At this point, the timing of the experiment began. After a few minutes the wave amplitude was increased to that stipulated for the run. While a steadily increasing amplitude and period over the surge rise would more closely duplicate nature, it was felt that this introduced too many factors into the present analyses. During the surge rise, the wave amplitude was frequently checked and adjusted to compensate for the increasing hydrostatic pressure on the wave paddle. Any irregularities were noted in the journal.

### Peak Surge

As the time for peak surge approached, the wave height was closely watched, and the water level was monitored on a preset point gauge located in the stilling basin to the rear of the tank. When peak surge was reached, the water valve was closed, the wave generation was terminated, the time was noted, and the profile was measured and recorded. The computer immediately listed all values for spot checking for accuracy.

### Equilibrium

At this fixed peak surge level, the same wave condition was then run until near-equilibrium appeared to be reached. This time varied between 30 and 45 minutes, with profiles being recorded every 15 minutes.

Equilibrium was assumed when the dune toe position had not shifted and the nearshore beachface did not appear to be changing over a period of at least 5 minutes. As a check of these criteria, one test was allowed to continue running for several hours with very little noticeable change.

#### Posttest

Immediately following the measurement of the final profile, the drainage valves were opened, and the tank was drained. Simultaneously, the profiles were plotted and compared with previous results to confirm trends recognized earlier. After the drainage valves were closed, the water valve was opened, the profile regraded, and the water level brought up to its initial level.

Using this method, it was possible to conduct two tests in one working day; however, other factors sometimes prevented this.

The series of photographs shown in Figure 15 depict the dune erosion that occurred during run 41. The times given are those from the start of the surge level increase.



T=0 MIN.



T=20 MIN.



T=30 MIN.



T=40 MIN.



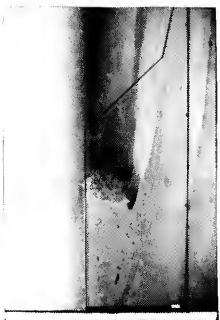
T=45 MIN.



T=50 MIN.



T=55 MIN.



T=60 MIN.



T=65 MIN.



T=72 MIN., PEAK SURGE



T=87 MIN.



T=102 MIN.

## CHAPTER VII

### QUALITATIVE ANALYSIS OF EQUILIBRIUM PROFILES

It is instructive to first examine the resulting experimental profiles, recorded when near-equilibrium conditions were reached, for general trends before attempting an analytical parameterization. This provides an insight into the relative importance of each of the tested parameters, as well as providing a view of the overall general mechanism involved in the process. In this comparison, only the last profile recorded for each run will be examined in an effort to visualize the final steady-state condition. The time-dependent trends will be discussed in Chapter IX. For some aspects of the comparison, it is possible to involve a fairly large number of profiles. In these instances, representative examples are given with the remainder shown in Appendix D.

#### Surge Level Rise Duration

Paramount to the entire experimental series was the establishment of the effects of the surge level rise duration. Definite knowledge on this subject had to be obtained before the test series could progress into the investigation of other parameters.

Firstly, a comparison was made between the equilibrium profile obtained for given wave conditions when the peak surge level was reached

instantaneously and a profile formed under the same wave conditions but with a finite-time surge level rise.

Figure 16 compares run 1, where the peak surge was fixed before the waves began, and run 2 where the surge level was raised to its peak value over 45 minutes and then allowed to run until near-equilibrium was established. As can be seen, the variable surge level run experienced more dune recession, apparently because sediment can be moved further offshore while the water rises and thus allows more sediment to be eroded from the dune. In the case of the instantaneous surge, the seaward slope of the offshore bar is steeper, indicating that the depth limit for significant sediment transport prohibits sand from being moved as far offshore. Later tests conducted using a different dune height and two additional surge levels confirmed this trend as shown in Figure 17. Details of the runs are given in Table 5 of Chapter VI. Thus, the first important conclusion to be drawn is that a time-dependent surge level rise allows more erosion to take place than could occur when the surge rise is instantaneous. This comes about quite simply because the limiting depth for sediment transport covers a wider range of the profile when the water level is gradually increased. Since time-dependent surge increases occur in nature, then they must also be reproduced in the model experiments.

The next question to be answered about surge level rise regards the time span over which the rise takes place. Runs numbered 2 through 7 were conducted with this question in mind. Figure 18 compares runs 2, 3, and 4 which were conducted using the same wave condition but with surge level rise times of 45, 85, and 25 minutes, respectively. As can be seen, the profiles are very similar at peak surge but show some variation 30 minutes later.

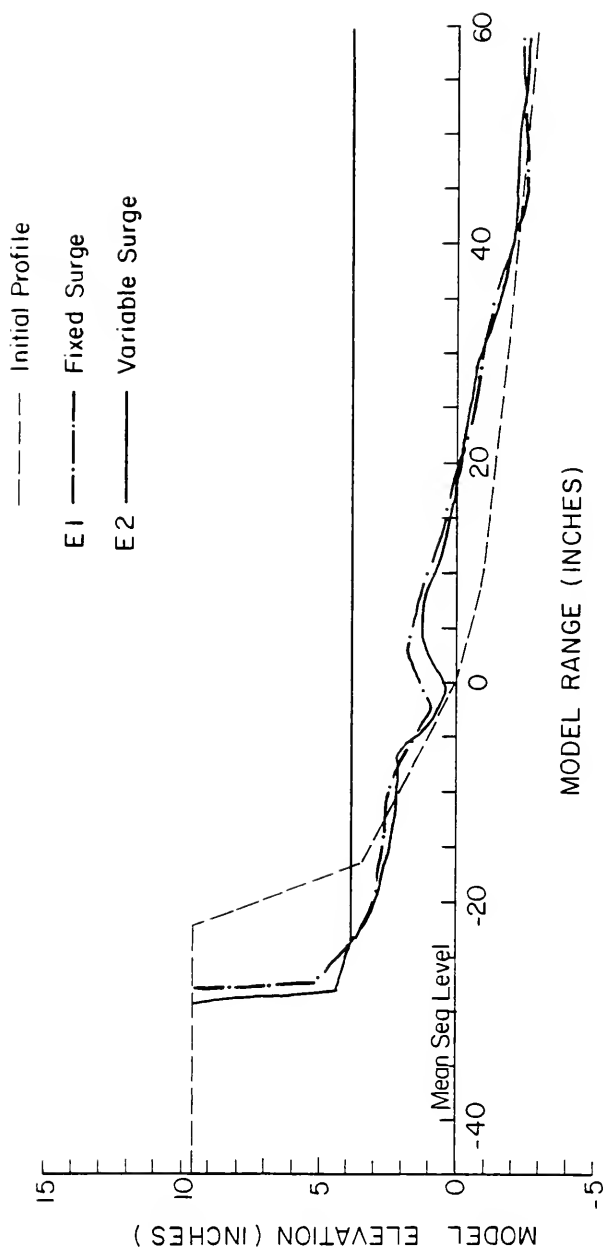


FIGURE 16: INSTANTANEOUS VERSUS TIME-DEPENDENT SURGE LEVEL RISE.

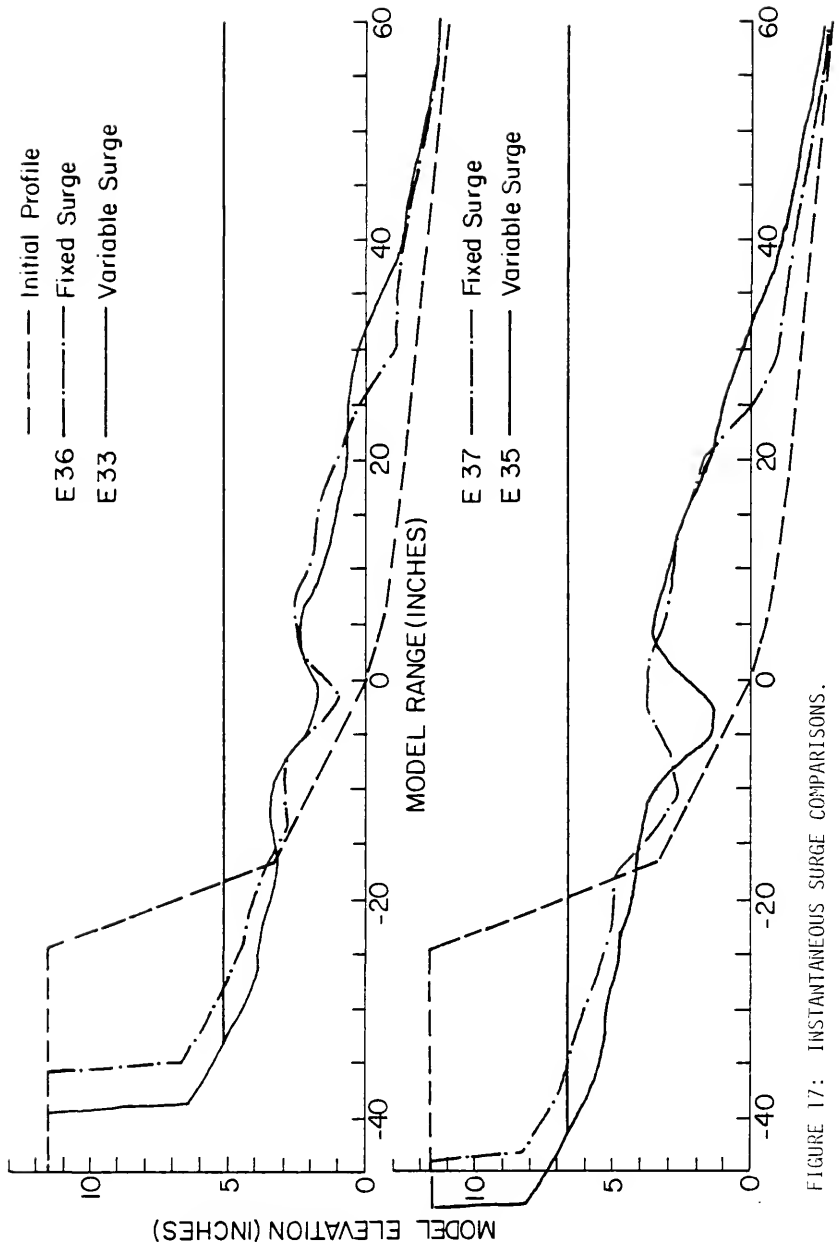


FIGURE 17: INSTANTANEOUS SURGE COMPARISONS.



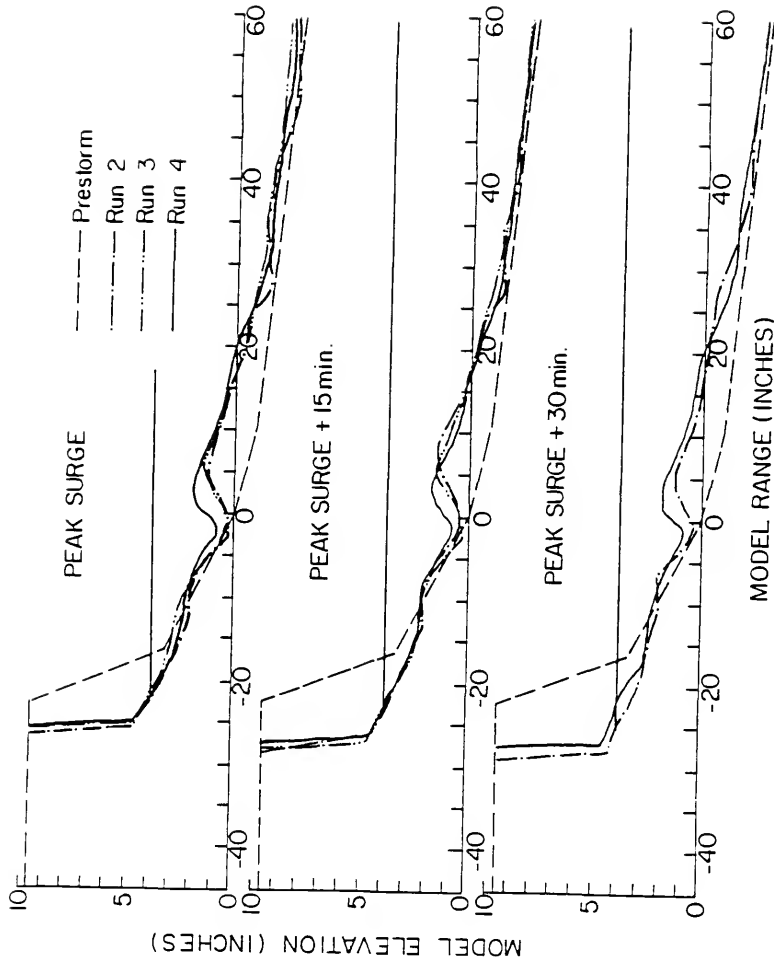


FIGURE 18: FIRST COMPARISON VARYING SURGE RISE DURATION.

Since these runs proved inconclusive, runs 5, 6, and 7 were conducted using a different wave height. As can be seen from Figure 19, the profiles show good similarity with the single exception of the peak surge profile of run 6 representing a rise time of 25 minutes, which simulated the prototype condition of an 8 foot surge rise over a 4 hour period.

Experience tells us that a surge rise as rapid as given by run 6 is highly unlikely to occur in nature. However, the close similarity shown between runs 5 and 7, which represent prototype surge rise times of 12 and 8 hours, respectively, point to the fact that the finite surge increase duration is not an important consideration, as long as it is within reasonable ranges expected in the prototype.

From this evidence it is concluded that the analysis of the dune erosion need not be concerned with the duration time of the surge level rise, but instead only with the peak surge value and the length of time the peak value is maintained.

For the remainder of the tests, the surge level rise was accomplished usually between 50 and 60 minutes (8.6 to 10.3 hours, prototype). It was felt that this was fairly typical of most hurricanes making landfall.

#### The Effect of Dune Height

Comparisons of the final recorded profiles from test series 2, 4, and 5 were made to investigate the effects of different dune height elevations on the erosion process. Figure 20 gives the comparison in two instances where wave height, wave period, and peak surge level were the same. The remaining comparisons are given in Appendix D.1.

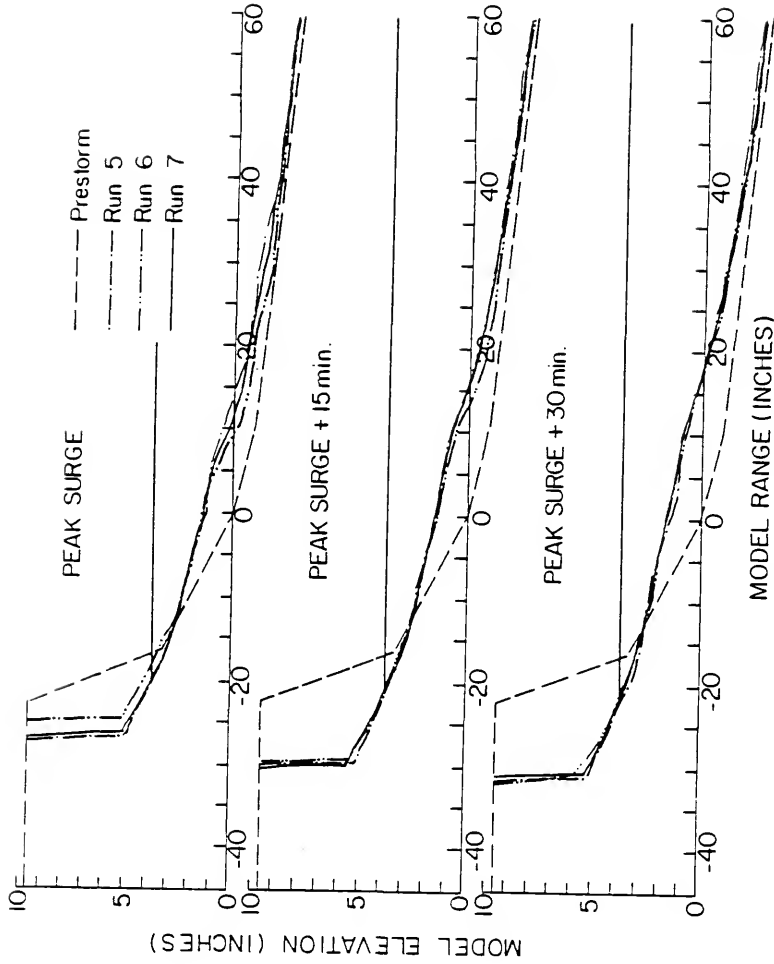


FIGURE 19: SECOND COMPARISON VARYING SURGE RISE DURATION.

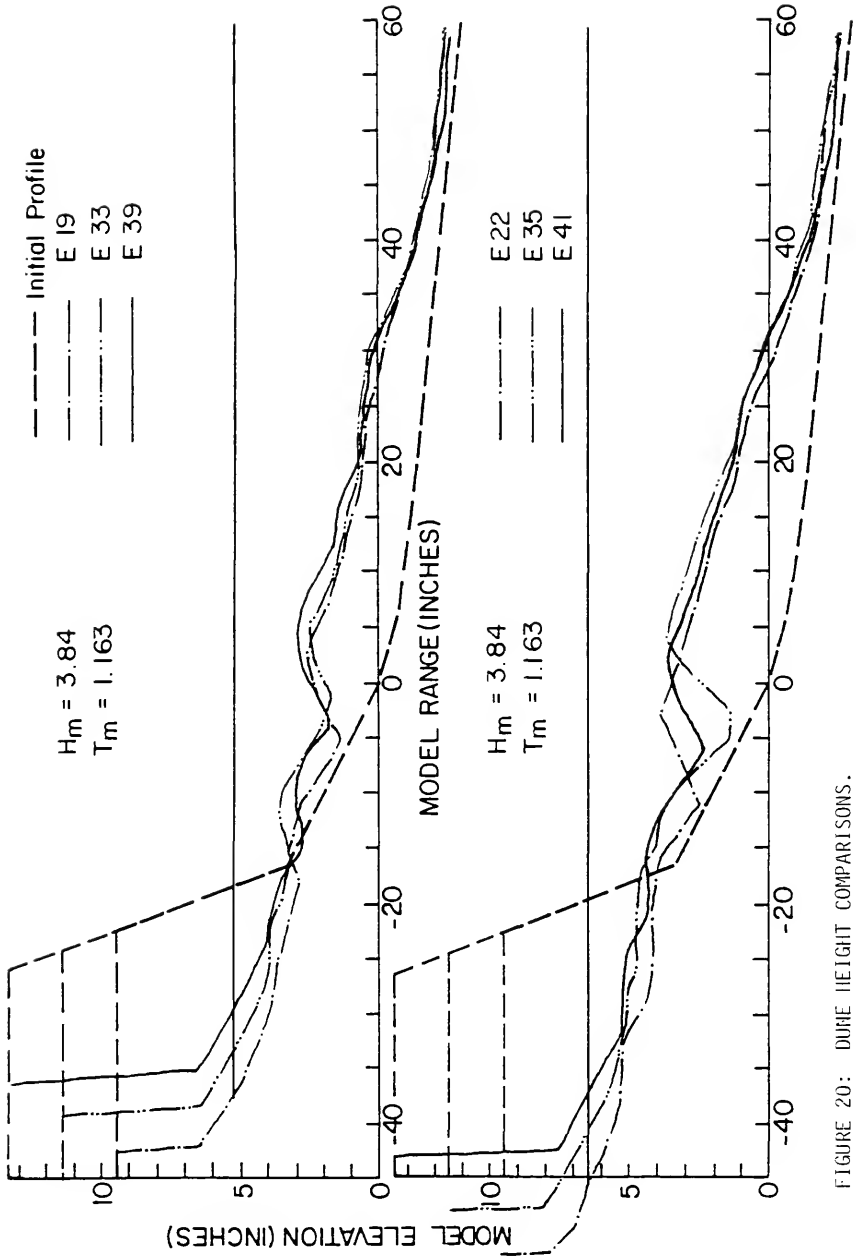


FIGURE 20: DUNE HEIGHT COMPARISONS.

It is seen that while the nearshore section and the dune recession show significant variation, the offshore profiles from the bar trough seaward are almost identical. While some variation is present, due to experimental effects, the strong trend is toward similar offshore bar features. Also in every case it is plainly evident that the higher dunes have less recession than the lower dunes. These two observations lead to the interesting hypothesis that, for a given prestorm beach-offshore profile and given storm condition, there appears to be a maximum sediment storage capacity in the offshore bar for equilibrium conditions. In other words, the storm will continue to move sediment from the dunes to the offshore bar until this "storage capacity" has been reached at which time the dune recession ceases. Since higher dunes provide more sediment, the dune recession would be less in that case.

This concept implies that there exists an equilibrium barred storm profile configuration which is characteristic of wave conditions, prestorm profile, and sediment grain-size. Once this profile is determined, it would be possible to shift the profile horizontally along the prestorm profile (relative to peak surge level) until a sediment balance between erosion and deposition is achieved, thus determining the equilibrium erosion which could occur. Obviously a higher dune will mean less dune recession. The peak surge level will be the most important factor since the barred storm profile is taken relative to the peak surge. The analytical development presented in the following chapter is based upon this hypothesis.

### The Effect of Storm Surge

The effect of the peak surge level upon the dune erosion at near-equilibrium conditions is seen qualitatively in Figure 21 which gives comparison of runs of the same wave period, wave height, and dune height but with different peak surge levels. Typically it is seen that a surge level increase of 3 feet in the prototype is responsible for dune recessions on the order of 30 to 40 feet in the prototype, for this particular beach-dune configuration. Another interesting aspect is that the portion of the profiles seaward of the offshore bar seem to coincide, indicating that the "storage capacity" of the offshore bar is directly related to the surge level, as it should be. However, this point will not be stressed because the other comparisons, shown in Appendix D.2, do not always illustrate this trend as strongly. The two following sections show that while wave height and wave period have some effect upon the dune recession, neither exhibits the large variations caused by different surge levels.

Therefore, it can be concluded that the surge level acts as a vehicle for exposing greater portions of the dune to the incoming wave energy, and that the surge level remains the single most important parameter involved in the process.

### The Effect of Wave Height

The comparisons of runs involving the same wave period, surge level, and dune height, but different wave heights, are given in Figure 22 and Appendix D.3. An increasing wave height has the effect of increasing the dune recession but to a much lesser extent than an

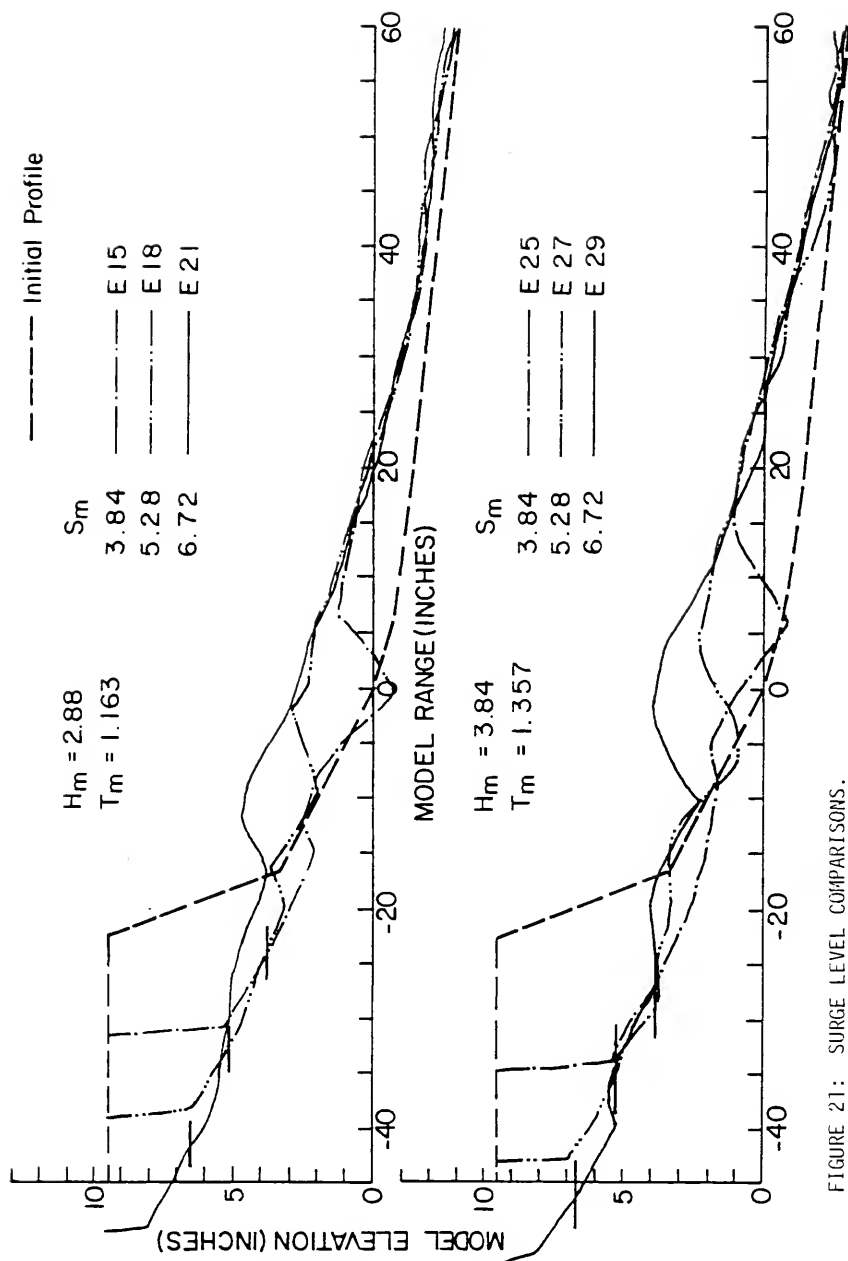


FIGURE 21: SURGE LEVEL COMPARISONS.

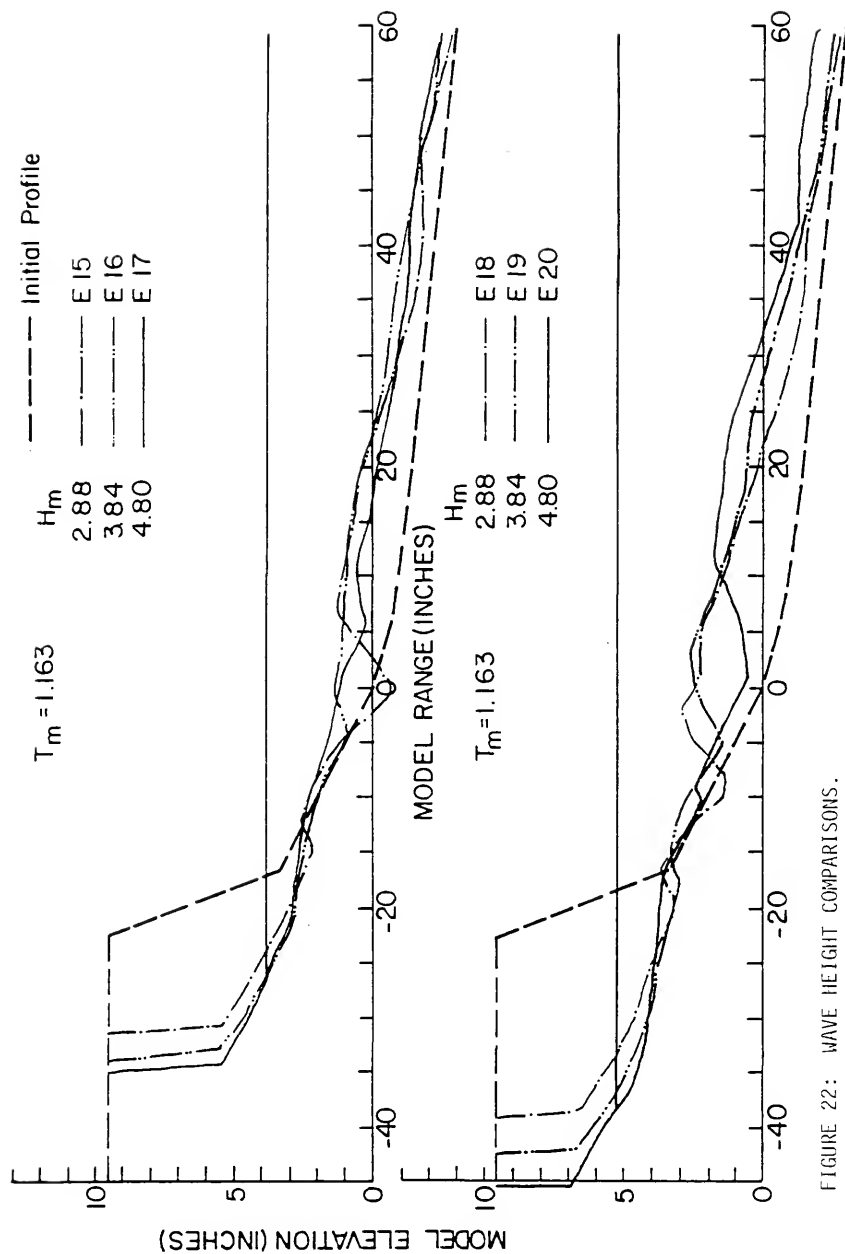


FIGURE 22: WAVE HEIGHT COMPARISONS.



increase in surge level. The interesting thing to note is that increasing the wave height lengthens the distance between the eroded dune toe and the crest of the offshore bar, as well as increasing the depth of the bar crest. These two points are quantified in Chapter VIII to help establish some important characteristics of the equilibrium barred profile.

#### The Effect of Wave Period

Comparisons between runs where the wave period was varied, while the surge level, wave height, and dune elevation were held constant, indicate that increasing the wave period increases the amount of dune recession, but once again, not by a large amount (see Figure 23 and Appendix D.4). This effect is attributed to the fact that the longer period waves run further up the beach and are thus capable of eroding more of the dune. This relationship is quantified in the following chapter and used in determining the equilibrium barred profile. The form of the remaining portion of the profile, especially in the offshore sector, does not seem to be particularly affected by variations in wave period.

#### Nearshore Beach Profile

One additional profile comparison was conducted by superimposing the near-equilibrium profiles, formed under the same wave condition at different surge levels, in such a way that the common reference point was the intersection of the beachface and the still peak surge level. Representative examples are shown in Figure 24 with the remainder

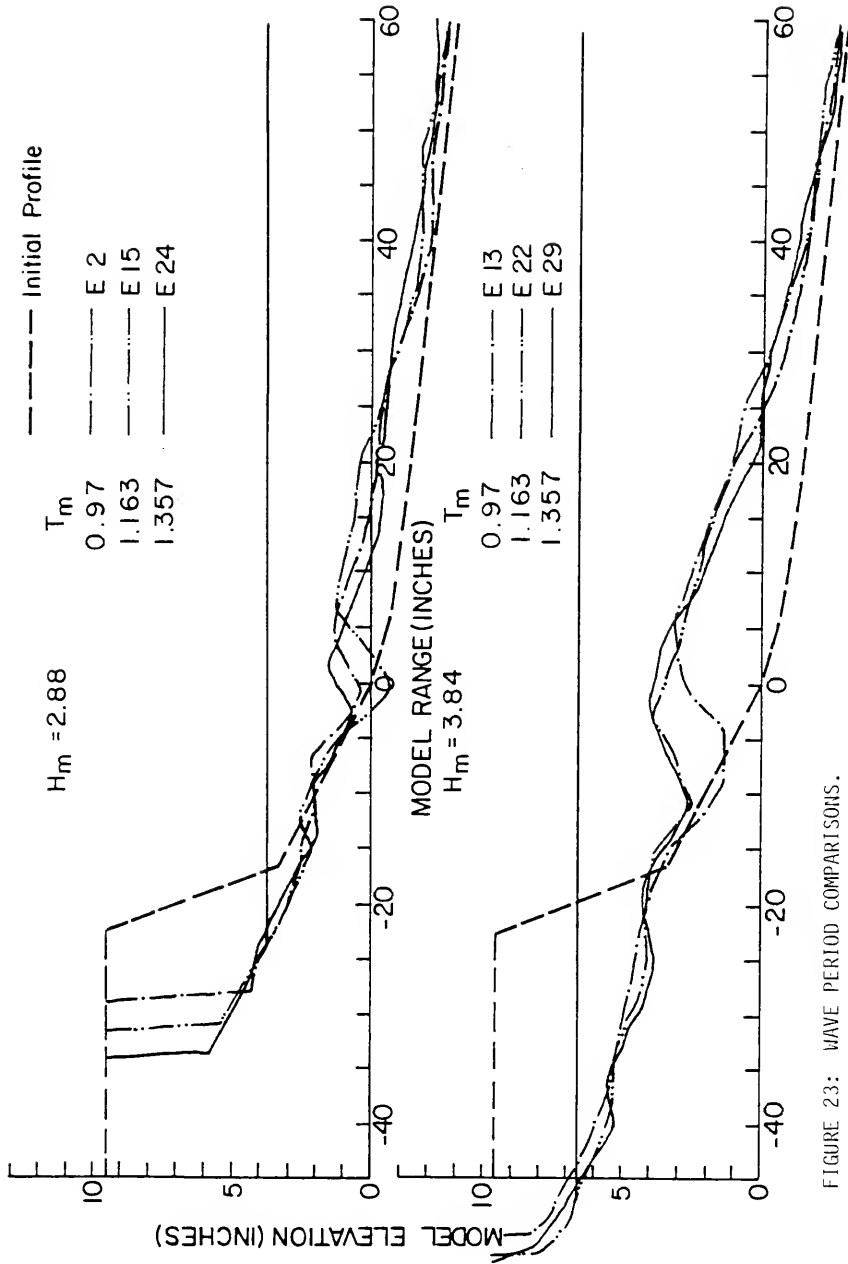


FIGURE 23: WAVE PERIOD COMPARISONS.

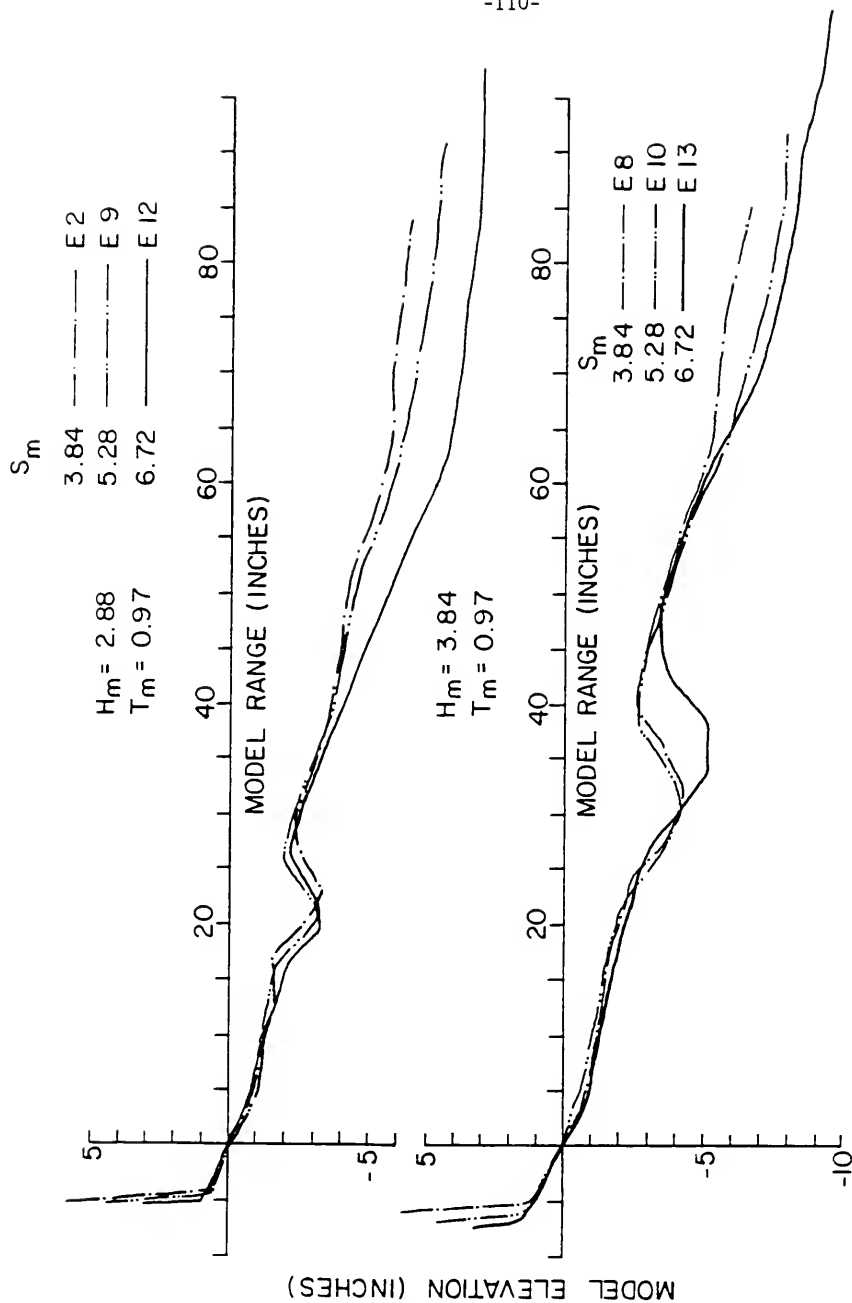


FIGURE 24: NEARSHORE PROFILE COMPARISONS.

given in Appendix D.5. From these comparisons it is seen that the nearshore profile shape is independent of the surge level and initial prestorm profile, while the profile seaward of the offshore bar is definitely related to the initial profile and surge level. It is also encouraging to note that the location of the dune toe and the location of the trough and crest of the bar show a good similarity under the same wave conditions. This is an indication of the repeatability of the experimental results.

From the above qualitative look into the effects of the primary factors involved in dune erosion, it has been possible to draw several conclusions which give valuable insight into the erosion of dunes and formation of barred profiles. Using these conclusions as guidelines, it is now possible to begin the quantitative analyses using the experimental test results. However, a general discussion on the overall topic of dune erosion is warranted in order to place everything in its proper perspective.

#### Dune Erosion in General

Besides the assumptions listed in Chapter I, there are several additional aspects regarding storms and the resulting erosion of the beach-dune system which need to be examined in the hopes of recognizing some of the limitations or failures of the ensuing analysis.

#### Waves

The experimental test series were run using regular waves of a "nonforced" type, i.e., gravity was the only force determining wave

motion. It is well known that, as these waves shoal, they steepen and break, most often in a spilling or plunging mode. The transition between these two types of breaking depends upon wave steepness and beach slope (Galvin, 1972) with plunging occurring for steeper waves and beach slopes. Galvin relates these two steepnesses through a parameter given as

$$B_o = \frac{H_o}{L_o (\tan \beta)^2}, \quad (31)$$

where  $\tan \beta$  is the beach slope. Since this parameter can be easily shown as being conserved by the model law given in Chapter IV, it is reasonable to believe that the model waves behaved in a similar fashion to prototype waves when it came to breaking. Thus the type of wave breaking which occurred during the various stages of the experimental run should be the same as what would be expected in nature. For example, the waves initially were spilling breakers due to the mild prestorm beach slope, but changed to the plunging type as the surge level rose and the offshore bar began to form, resulting in a steepening of the offshore beach slope.

During storms, however, the waves are "forced" by strong onshore-directed winds. So, instead of breaking strictly under the force of gravity, the waves never reach their maximum steepness because the wind blows the tops off, causing the waves to appear to be of the spilling type.

This "forced" condition may cause the final erosion obtained in the prototype to be somewhat less than indicated by the small-scale model since plunging waves cause more turbulence and hence move more

sediment. In addition, the offshore bar features are less predominant for spilling breakers.

For the present it must be assumed that this "forcing" condition either contributes little to the final erosion, or that it is offset by another natural phenomenon not reproduced in the laboratory experiments, such as spectral distribution.

### Spectral Distribution

The reasons that regular waves were chosen over a narrow-banded spectrum of waves for use during the model tests are given in Chapter V, the main reason being the inability to reproduce the "surf beat resonance" phenomenon. In nature, where the incoming wave field exhibits a variety of wave heights and frequencies, it would be expected that the bar feature would be a little less defined than with regular waves since the different height waves break at different depths, thus acting as a "smoothing" agent. The presence of resonance, however, helps to make the bar a little more well defined in addition to causing the wave runup to, at times, progress further up the beach than in the case of regular waves. This additional uprush causes more erosion and might possibly compensate for the "forced" wave condition discussed above.

Until more is understood about nearshore wave spectra and forced wave conditions, it must be assumed that the results obtained by the experimental series are close to reproducing natural events with the error being in favor of overestimation of the dune recession.

### Nonbarred Profiles

There are several instances where the formation of an equilibrium barred profile would not occur:

- 1) When conditions are such that the waves always break in a spilling fashion, a bar formation would be less likely.
- 2) If the prestorm beach slope is very mild and the surge level rise is not too severe, the lengthy surf zone would dissipate a considerable amount of energy, leaving less energy available to move sediment and build up the bar. While some erosion would take place and equilibrium conditions could be obtained, the development in the following chapter is not addressed to this particular condition since it does not represent the severe erosion condition.
- 3) A similar condition to that described above is the case of fairly low elevation dunes. For a substantial surge level rise, the dune recession will be tremendous as the storm moves sediment offshore. It may be that the lengthened surf zone could reach its "storage capacity" without the formation of an offshore bar. The verification of the small-scale model discussed in Chapter V is an example of such a case.

### Discussion

In view of the above points, it is necessary to restrict the definition of an equilibrium profile by stating that the equilibrium storm profile is one in which all the incoming wave energy is completely

dissipated over the length of the surf zone. This profile may or may not include an offshore bar feature.

Concentration for the remainder of the analysis will be given to barred storm profiles since they were most prevalent in the experimental tests and represent the most severe prototype conditions.

### Summary

Before becoming entangled in the quantitative analysis of the next chapter, it is beneficial to briefly review the conclusions reached in this overview of the final near-equilibrium test profiles.

- 1) In model testing, it is necessary to employ a time-dependent surge level increase of sufficient duration, in order to obtain more realistic erosion results.
- 2) There appears to be an offshore bar "sediment storage capacity" for a given prestorm profile and set of storm conditions. This is in the form of an equilibrium barred profile taken relative to the peak surge level.
- 3) Dune erosion can be found by shifting this barred profile horizontally until the erosion area equals the deposition area.
- 4) The storm surge level is the most important parameter in determining erosion, while wave height and period have a lesser effect.
- 5) The profile between the dune toe and offshore bar is independent of surge level, and thus, independent of prestorm profile configuration.



## CHAPTER VIII

### EQUILIBRIUM BARRED STORM PROFILE

It was seen in the preceding chapter that an equilibrium barred profile can be formed under storm conditions if the process is allowed to continue indefinitely. This profile appears to exhibit three distinct regions: the nearshore profile, the bar feature, and the offshore profile. While very few storms are of sufficient duration to allow establishment of the final equilibrium state, the equilibrium condition lends itself to analytical development since the transient effects may be discarded.

Once the equilibrium profile for a given set of storm conditions has been established, it will be possible to then determine the maximum expected erosion and dune recession which could occur. This is done by simply shifting the storm profile relative to the prestorm profile until a sediment balance is achieved between the eroded quantity and the deposited quantity. With the "equilibrium erosion" solution in hand, it will then be possible to investigate the amount of erosion which occurs from the time that peak surge is reached until the time that a near-equilibrium is established. The quantity of erosion which occurs over this time span approximately equals 20 percent of the total final equilibrium volume.

The actual physics of the bar formation are understood only in the overall general description of the phenomenon. The increased wave

energy and water level rise associated with storm activity act to upset the beach equilibrium established during normal weather conditions because the surf zone cannot dissipate this increased energy over its length. As a consequence, a large volume of water is transported onto the beachface. The upflow provides a quick-sand effect which sets the stage for rapid removal of beach material, and the downflow drags sediment seaward from the surface of the beachface. The large volume of water reaching the beach must return to the sea in order to maintain a balance. This return flow is sediment-laden and continues to carry its load offshore until the flow velocity is sufficiently reduced to the point that the load is dropped. Through this mechanism an offshore bar is formed by the deposition of sediment removed from the beachface and dune. This bar continues to grow and migrate seaward until its crest becomes high enough to steepen and break the majority of the incoming storm waves. When this dissipation mechanism is fully developed, and the incoming wave energy is completely dissipated through breaking and turbulent propagation over the extended length of the surf zone, the equilibrium barred storm profile is then established. From this description, the importance of the bar in providing the ultimate defense against beach-dune erosion can be seen, making the inclusion of the bar feature in the analysis imperative.

#### Breaker Depth Versus Breaker Height

When dealing with waves in the surf zone, it is an almost universally accepted practice to relate the water depth at breaking ( $h_b$ ) to the breaking wave height ( $H_b$ ) through the simple relationship

$$h_b = 1.28 H_b , \quad (32)$$

as derived by Munk (1949) using a modified solitary wave theory. Subsequent observations of both lab and field data by Iversen (1952a, 1952b), Galvin (1969), and Goda (1970), just to name a few, have established a slight dependency of the ratio  $h_b/H_b$  on beach slope and deep water wave steepness  $H_o/L_o$ . However, the data were somewhat scattered, and it is felt that the use of the simpler form of equation (32) gives satisfactory results as illustrated in Figure 25 which was reproduced from an unpublished report by James H. Balsillie of the Florida Department of Natural Resources, Bureau of Beaches and Shores.

Munk also derived an expression for the breaking wave height in terms of deep water wave characteristics which is given by

$$\frac{H_b}{H_o} = 0.30 \left( \frac{H_o}{L_o} \right)^{-1/3}, \quad (33)$$

where

$H_o$  is deepwater wave height and

$L_o = \frac{g}{2\pi} T^2$  = deepwater wave length.

Van Dorn (1978) gives a slightly different expression for  $H_b$  given as

$$\frac{H_b}{H_o} = 0.4 \left( \frac{H_o}{L_o} \right)^{-1/3}, \quad (34)$$

which varies from Munk's theoretical derivation only by the constant, and which seems to fit the available data a bit better.

For the model experiments, the values of  $H_b$  obtained from equations (32), (33), and (34) are shown in Table 6 along with the value of  $H_o$ , calculated using linear wave theory from the intermediate depth where the wave height was measured in the tank. The calculation allows

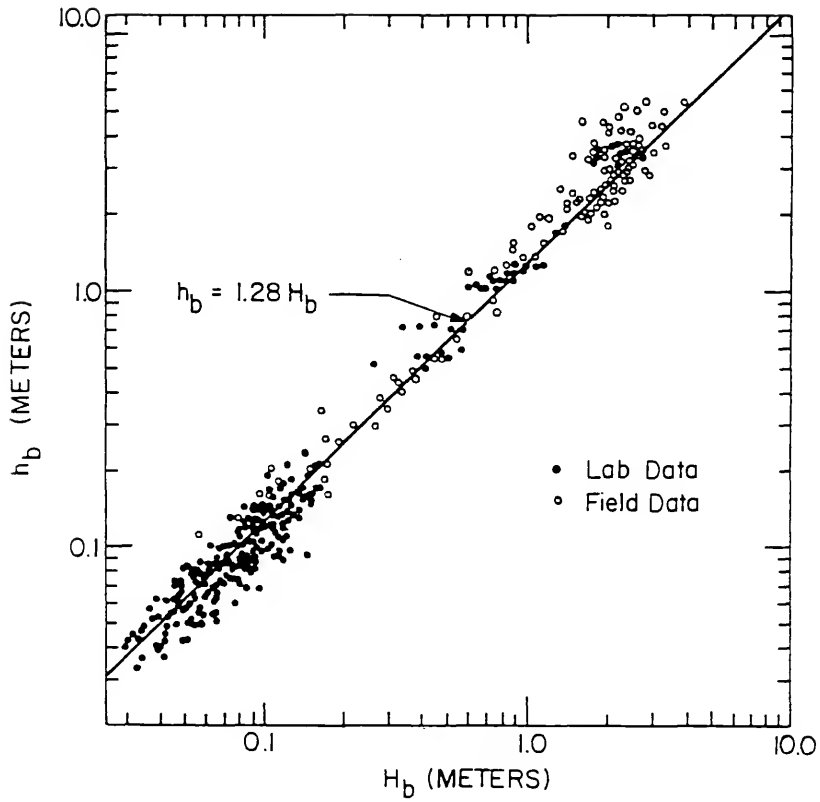


FIGURE 25: BREAKER HEIGHT VERSUS BAR DEPTH.

TABLE 6  
BREAKING WAVE HEIGHTS

Run #	Period $T_m$ (sec.)	Surge Level $S_m$ (in.)	Wave Height $H_o$ (in.)	Breaking Wave Height-- $H_b$ (in.)		
				Eq. (32)	Eq. (33)	Eq. (34)
2	0.970	3.84	2.97	1.96	2.39	3.19
8			3.95	1.96	2.9	3.87
9			2.95	1.58	2.39	3.18
10		5.28	3.93	2.29	2.89	3.85
11			4.92	2.89	3.35	4.47
12			2.94	1.73	2.38	3.17
13		6.72	3.19	2.16	2.88	3.84
14			4.89	2.64	3.35	4.46
15	1.163	3.84	3.08	1.96	2.77	3.69
16			4.11	1.96	3.35	4.47
17			5.13	1.51	3.89	5.19
18		5.28	3.06	1.69	2.76	3.68
19			4.08	2.12	3.34	4.45
20			5.09	2.82	3.88	5.17
21		6.72	3.04	1.62	2.75	3.66
22			4.05	2.25	3.33	4.44
23			5.06	2.73	3.86	5.15
24	1.357	3.84	3.14	1.77	3.11	4.15
25			4.19	2.21	3.77	5.03
26		5.28	3.13	1.18	3.11	4.14
27			4.18	2.26	3.77	5.02
28		6.72	3.12	1.65	3.10	4.13
29			4.16	2.13	3.76	5.01
30	1.163	3.84	3.08	1.86	2.77	3.69
31			4.10	1.91	3.35	4.47
32		5.28	3.06	1.62	2.76	3.68
33			4.08	2.20	3.34	4.45
34		6.72	3.04	1.82	2.75	3.66
35			4.05	2.30	3.33	4.44
38	1.163	5.28	3.06	1.62	2.76	3.68
39			4.08	1.89	3.34	4.45
40		6.72	3.04	1.90	2.75	3.66
41			4.05	2.36	3.33	4.44

for surge level increase and applies to the final near-equilibrium beach profiles. The value of  $h_b$  was taken to be the minimum offshore bar depth with respect to still water surge level.

Of these three relationships, the values calculated using  $H_b = h_b/1.28$  are probably the most accurate in view of the large amount of supporting data for this relationship, and the fact that the values are determined at the break point independently of the shoaling characteristics of the deep water wave.

The large discrepancy between the predicted values of  $H_b$  using either equation (33) or (34) from the probable value of  $H_b$  found from equation (32) undoubtedly is a result of the laboratory scale effects, more specifically, wave reflection.

The distortion inherent in the modeling law gives offshore slopes twice as steep as those found in nature. As a consequence, a greater proportion of the incoming wave energy ended up being reflected in the wave tank, resulting in smaller wave heights at breaking.

Additionally, equations (33) and (34) are not preserved in the model law, so there exists some doubt as to whether prototype or model values of  $H_o$  and  $L_o$  should be used to calculate  $H_b$ .

Since the main concern in this effort deals with the area extending from the dune toe to just offshore of breaking, it was decided to use values of  $H_b$  calculated from equation (32).

#### Location of Bar Crest

One of the more important factors in constructing an equilibrium barred profile is the determination of the bar location with respect to the dune toe, representing the limit of wave uprush.

Two previous papers touching upon this point were those of Kemp (1960) and Sunamura and Horikawa (1974).

Kemp's experiments were conducted in a three-dimensional wave tank measuring 15 feet by 9 feet, with a water depth of 6 inches. For sand ranging between 0.45 mm and 2.0 mm, Kemp gave an empirical relationship for the distance between the dune toe and the bar crest,  $X_{bc}$ , as

$$X_{bc} = \frac{24H_b^{3/2}}{d^{1/2}}, \quad (35)$$

where  $H_b$  and  $X_{bc}$  are given in feet and the grain size,  $d$ , is in millimeters.

Some doubt can be cast upon the validity of this expression due to the very small size of the wave facility employed and the large grain-sizes used. Data collected in the current dune erosion experiments did not match when plotted along with Kemp's results. However, the difference is not too great, indicating that the basic form of equation (35) may be nearly correct (as will be shown shortly).

The more recent work of Sunamura and Horikawa (1974) detailed experiments in a 25 meter long wave tank using a water depth of 1.5 meters. Sand grain-sizes employed were 0.2 mm and 0.7 mm, and the authors gave the expression for bar crest location in non-dimensional form as

$$\frac{X_{bc} L_o}{H_b} = 0.018 \left( \frac{H_b}{d} \right)^2. \quad (36)$$

Their experiments began with a plane-sloping beach which was eroded by the ensuing wave action.

The main objection to equation (36) is that  $H_b$  is given as the breaker height at the onset of the erosion when the profile is still a plane slope. Since nature does not form barred profiles from plane-sloped beaches, equation (36) has no real application outside of model testing. To be more practical,  $H_b$  must be the breaker height when the final equilibrium profile is reached.

In addition, neither of the two above mentioned papers gives any physical interpretation of the predictive equation for  $X_{bc}$ .

#### Development of the Equation for Bar Crest Distance, $X_{bc}$

The important characteristics which determine the equilibrium position of the offshore bar formed by plunging breakers obviously are the wave period, the breaking wave height, and the sediment grain-size. Formulation of an expression using the breaking wave characteristics rather than the deepwater wave parameters eliminates any need for consideration of the shoaling of the waves, the surge level, or the pre-storm profile. Since it is desirable to nondimensionalize the breaker distance,  $X_{bc}$ , the most logical choice is the breaker wave length,  $L_b$ , since it incorporates both wave period and breaker wave height, and the ratio  $X_{bc}/L_b$  is preserved between model and prototype. Experimental results indicate that this "dimensionless breaker distance" is not constant, but instead it varies directly with  $H_b$  and inversely with wave period,  $T$ . This corresponds with recent results obtained by Noda (1978) and Saville (1980), who point out that profile similarity can be obtained when the dimensionless fall velocity parameter is conserved, thus implying that  $H_b/\omega T$  is indeed an important parameter for



determination of the breaker distance. It should then be expected that

$$\frac{X_{bc}}{L_b} = f\left(\frac{H_b}{\omega T}\right),$$

where

$X_{bc}$  = breaker distance (distance from bar crest to uprush limit),

$L_b$  = breaking wave length,

$H_b$  = breaking wave height,

$T$  = wave period, and

$\omega$  = sediment fall velocity.

Using the expression given by Van Dorn (1978) for the breaking wave length, expressed as

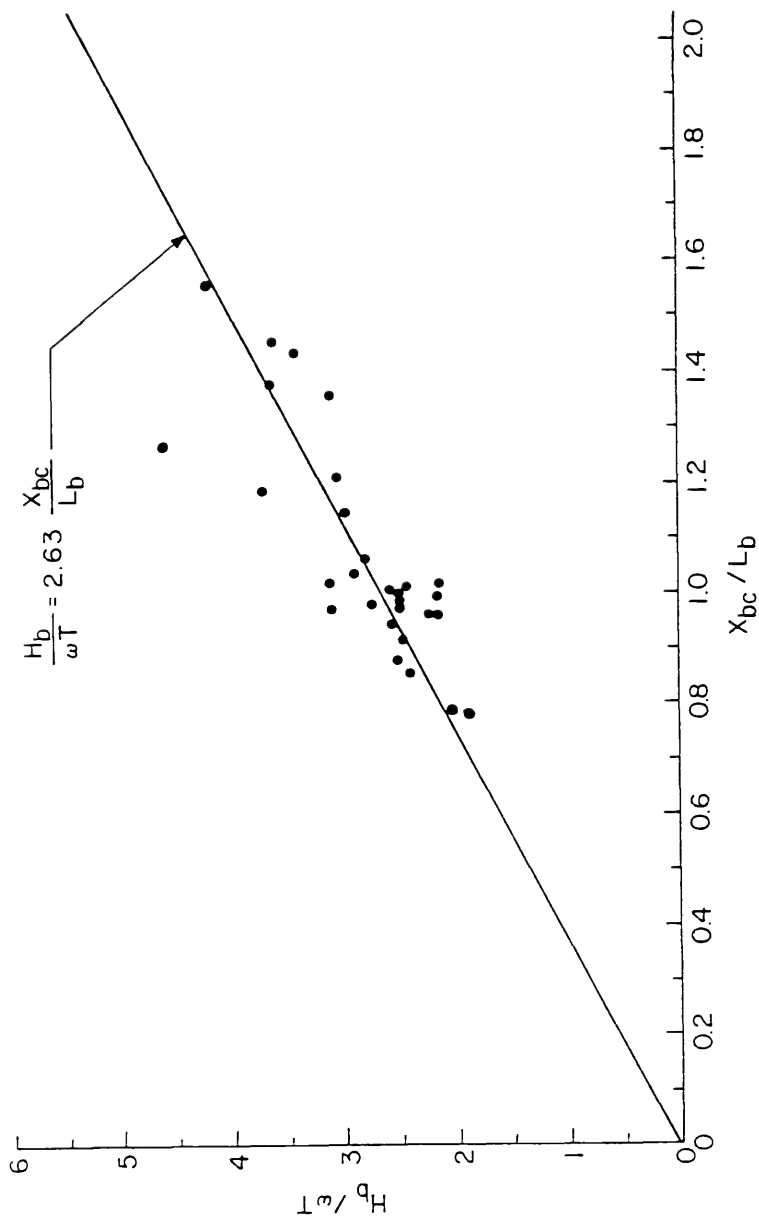
$$L_b = C_b T = T[(2g)(0.77H_b)]^{1/2}, \quad (37)$$

values of  $X_{bc}/L_b$  were plotted in Figure 26 against  $H_b/\omega T$  for the 29 experiments where the offshore bar feature was clearly discernible. While the data contain considerable scatter, a linear relationship appears to exist, which was found to be

$$\frac{H_b}{\omega T} = 2.691 \frac{X_{bc}}{L_b} - 0.068 \quad (38)$$

by the method of least-squares. The coefficient of determination for this curve fit was  $r^2 = 0.684$ , which is not as good as hoped for, but still indicates a strong trend.

The scatter of the data can be attributed to the difficulty in selecting the actual position of the bar crest, which is a gently



sloping crown, and also to the possibility that a full equilibrium condition had not been reached at the time of final data taking. Nonetheless, it is felt that this relationship is basically correct.

In equation (38) it is seen that the linear offset of 0.068 is quite small, and that the data can be represented almost as well by a least-squares fit through the origin given as

$$\frac{H_b}{\omega T} = 2.63 \frac{X_{bc}}{L_b} . \quad (39)$$

It should be noted that attempts to locate prototype data to further verify equation (39) proved fruitless. Data obtained from nature typically do not represent severe storm conditions since milder wave climates have altered the bar features before poststorm measurements could be taken. In addition, grain-size and wave period data are generally lacking in the prototype. Large scale model tests, such as those by Rector (1954) and Watts (1954), were conducted using an initially plane-sloped beach, and the resulting barred profiles did not exhibit a reasonably well-defined location for the bar crest and the uprush limit. Thus, they could not be used either.

#### Physical Interpretation

A physical interpretation of equation (39) can be obtained by rearranging it into the form

$$\omega X_{bc} = 0.38 \frac{H_b L_b}{T} .$$

By replacing  $L_b$  with

$$L_b = C_b T$$

and multiplying both sides by  $H_b$ , the equation becomes

$$\omega H_b X_{bc} = 0.38 H_b^2 C_b .$$

By noting that the average wave energy flux (or wave power) per unit width of surf zone perpendicular to the beach at breaking is given by linear wave theory as

$$\bar{P} = \frac{\gamma}{8} H_b^2 C_b , \quad (40)$$

equation (39) finally becomes

$$\omega H_b X_{bc} = \frac{3.04 \bar{P}}{\gamma} . \quad (41)$$

In equation (41) the product  $H_b X_{bc}$  represents a water volume per unit width in the surf zone which is directly related to the total volume of water per unit width contained in the surf zone. Thus, equation (41) indicates that the incoming breaking wave energy flux per unit width, entering the surf zone across a vertical plane located at the bar crest, is directly proportional to the product of the surf zone volume and the sediment fall velocity.

Considering that for equilibrium conditions this energy must be totally dissipated, primarily through turbulence associated with the wave breaking and its propagation as a bore up the beach, it can be logically seen that an increase in energy flux must also increase the breaker distance in order to provide a larger surf zone volume to dissipate this increased energy input.

It can also be seen that for a given energy flux, increasing the grain-size of the sediment increases the fall velocity, which in turn decreases the breaker distance. This is because the larger grains take more energy to be turbulently tossed about, and they settle more rapidly, resulting in greater energy dissipation. As a consequence, beaches with coarser grains will have a shorter breaker distance, and hence they will be steeper. This fact has long been known from both model and prototype observations.

For nonequilibrium conditions, such as were observed in the current dune erosion experiments, the breaker distance,  $X_{bc}$ , steadily increased until the time when near-equilibrium was established. Since more energy flux per unit width was entering the surf zone than could be dissipated over the shorter breaker distance, there was an "excess of energy" which was expended through erosion of the dune and the offshore movement of sediment. Eventually the equilibrium breaker distance was established, and erosion of the dune ceased.

A further interesting aspect of equation (39) can be seen by rearranging the equation and replacing  $L_b$  with equation (37), which yields

$$X_{bc} = \frac{0.47g^{1/2}H_b^{3/2}}{\omega} . \quad (42)$$

Equation (42) closely resembles the empirical equation proposed by Kemp (equation (35)), with  $H_b$  being raised to the same power. The main difference lies in Kemp's choice of grain-size diameter instead of grain-size fall velocity. However, it should be pointed out that in the turbulent flow range,  $\omega$  is proportional to  $d^{1/2}$ , so Kemp's equation is essentially of the same form as equation (42).

It should also be pointed out that wave period does not appear explicitly in equation (42); but  $H_b$  is certainly a function of wave period, as seen in equations (33) and (34) which relate  $H_b$  to  $L_0$ .

A final feature of equation (39) is the fact that it is preserved when scaling from the model to the prototype, due to the fact that both  $X_{bc}/L_b$  and  $H_b/\omega T$  are preserved in the model law. In other words, equation (39) is valid as it stands for either the model or the prototype.

In conclusion, the relationship given by equation (39) appears to be a reasonable estimate of the breaker distance,  $X_{bc}$ , between the offshore bar crest and the limit of uprush on the beach. The physical interpretation seems logically sound, and it is felt that further developments and measurements will bear this out. Finally it should be reiterated that this analysis applies only to plunging breakers in storm conditions.

#### Location of Bar Trough

The location of the bar trough was also assumed to be related to the breaking wave length since the plunging distance of a breaking wave determines the location of the trough and this distance must be a function of wave length. Denoting the distance between the bar trough and the dune toe as  $X_{bt}$  and assuming

$$\frac{X_{bt}}{L_b} = f\left(\frac{H_b}{\omega T}\right),$$

29 data points representing near-equilibrium conditions were obtained from the model experiments and plotted as shown on Figure 27.

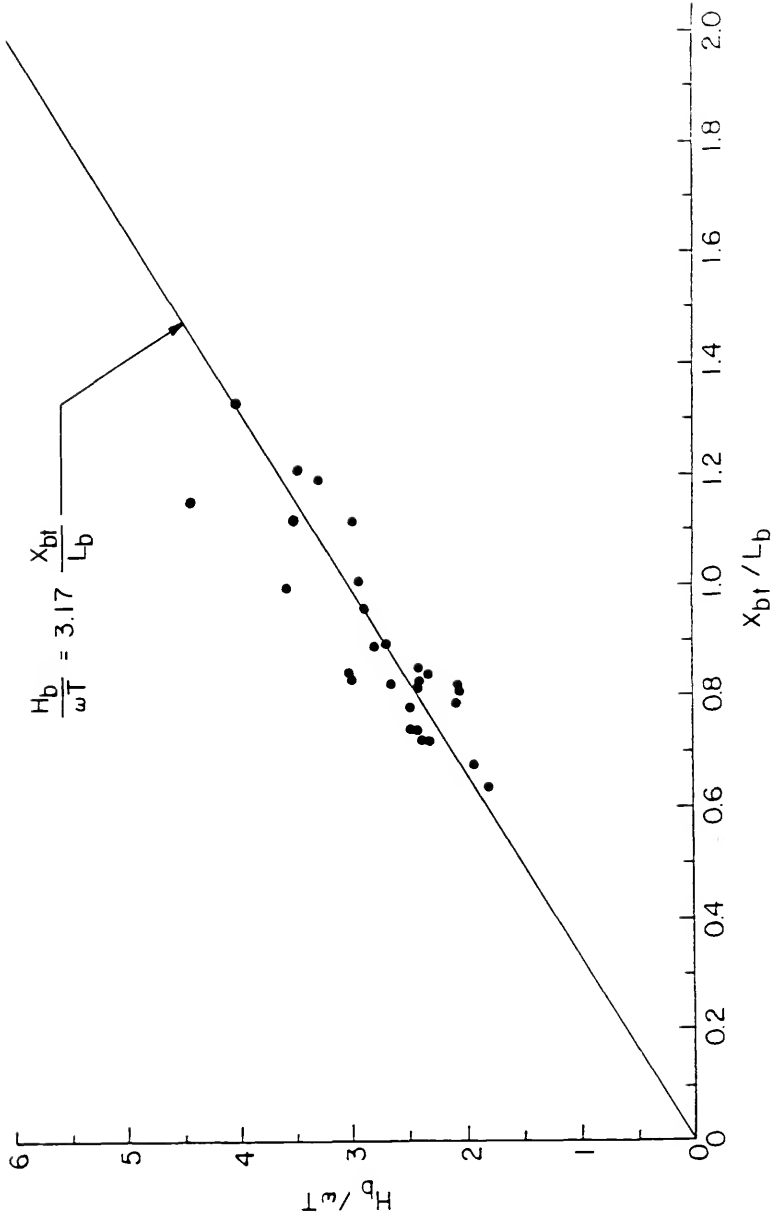


FIGURE 27: BAR TROUGH DISTANCE.

Once again the scatter is disturbing, but it appears that a linear relationship does exist. The least-squares best fit is given by

$$\frac{H_b}{\omega T} = 3.166 \frac{X_{bt}}{L_b} + 0.004 , \quad (43)$$

with the coefficient of determination being  $r^2 = 0.722$ .

Since the linear offset is very small, it is more convenient to force the best-fit through the origin yielding

$$\frac{H_b}{\omega T} = 3.17 \frac{X_{bt}}{L_b} . \quad (44)$$

The scatter can once again be attributed, somewhat, to the difficulty in selection of the actual position of the bar trough.

As was the case for equation (39), equation (44) is preserved in the model law, thus it can be used for either model or prototype predictions.

Dividing equation (39) by equation (44) gives the interesting result that

$$\frac{X_{bc}}{X_{bt}} = 1.21 . \quad (45)$$

Or as  $X_{bc}$  increases so does  $X_{bt}$ , proportionately. Figure 28 shows the variation in  $X_{bc}/X_{bt}$  as recorded from the model experiments. The average of all points, not surprisingly, is 1.21 with a root-mean-square (RMS) error of 0.039.

Building upon the physical interpretation given for the breaker distance,  $X_{bc}$ , it can be seen that equation (44) and the resulting equation (45) imply that an increase in the wave energy flux per unit



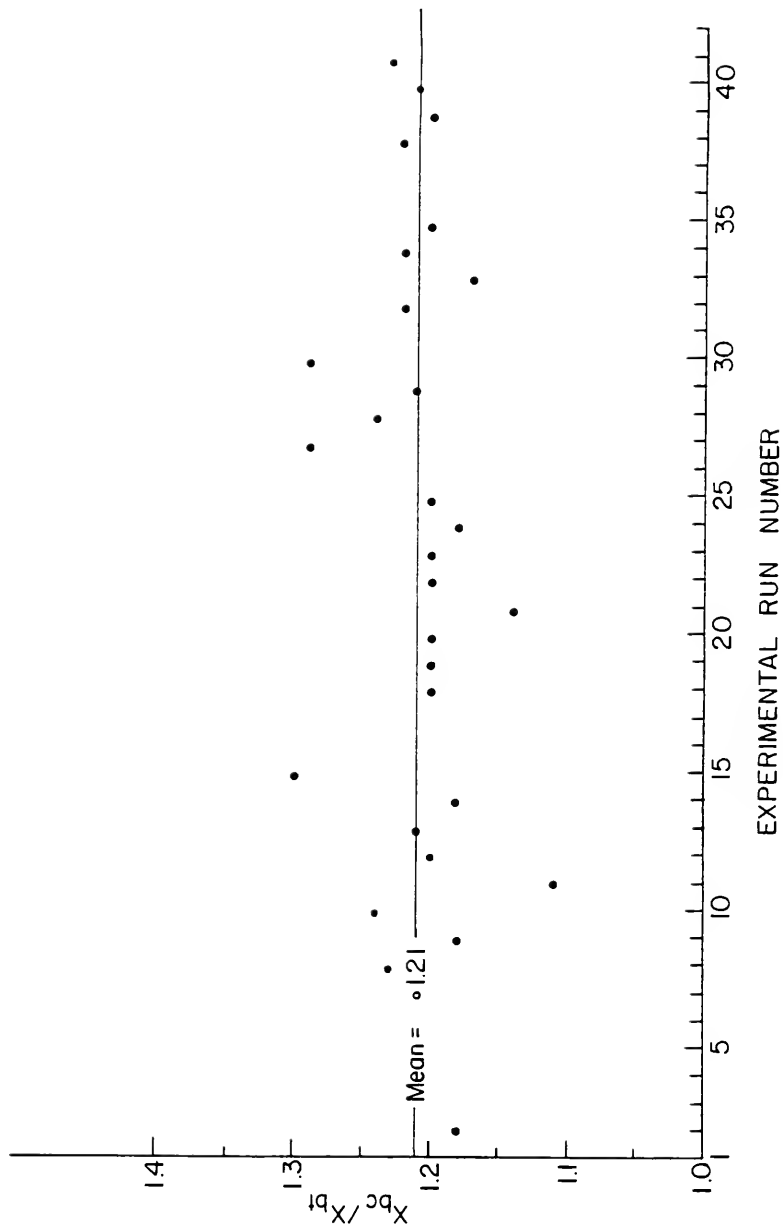


FIGURE 28: RATIO OF BAR CREST DISTANCE TO BAR TROUGH DISTANCE.

width entering the surf zone increases the breaker distance,  $X_{bc}$ , which in turn increases  $X_{bt}$  in such a way that the ratio of  $X_{bc}/X_{bt}$  remains constant. This can only be done if the breaking wave plunging distance increases with the wave energy flux per unit width, as would logically be expected. This aspect is enlarged upon in the following section.

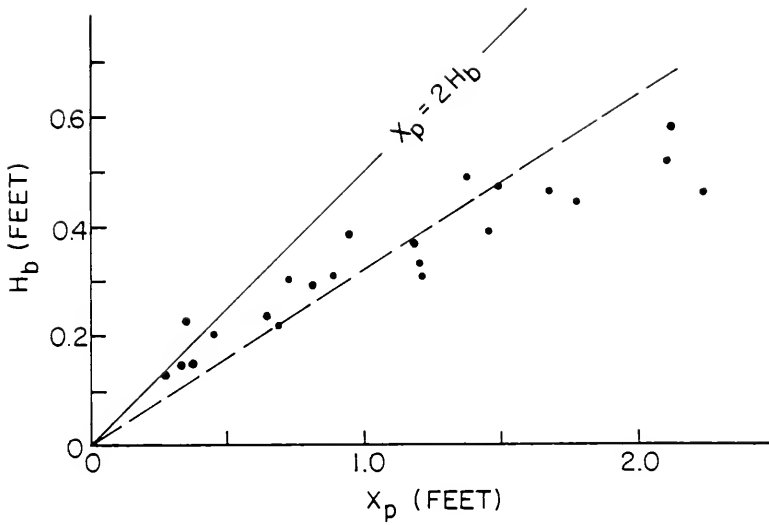
### Plunge Distance Hypothesis

Galvin (1969) developed an elementary expression for the plunging wave plunge distance,  $X_p$ , given as

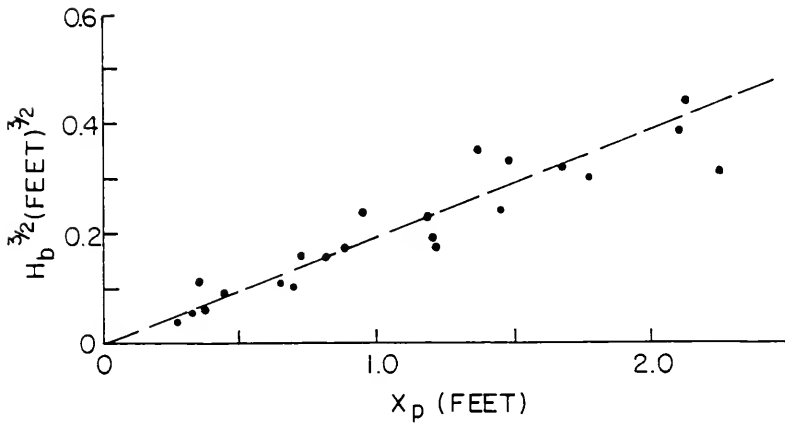
$$X_p \approx 2H_b . \quad (46)$$

This development assumes that at breaking the water particles at the crest are moving forward with the speed of the wave,  $C_b$ , and the particles are moving vertically subject only to the acceleration of gravity. However, Galvin's experimental results, conducted using a rigid, plane beach slope, gave plunge distances which were as large as  $4.5H_b$ , with an average of about  $3H_b$ . Galvin's data are shown plotted on Figure 29a. As can be seen, an attempt to sketch a straight line through the origin fitting the data meets with limited success. Galvin attributed this poor fit to the simple assumptions made in the "free-fall" analysis. As he correctly pointed out, there is a significant upward vertical particle velocity present as the wave breaks, which further complicates matters.

By approximating the plunge distance as the distance between the bar crest and the bar trough, equation (39) and equation (44), when subtracted, result in



29a:  $H_b$  VERSUS  $X_p$ .



29b:  $H_b^{3/2}$  VERSUS  $X_p$ .

FIGURE 29: GALVIN'S BREAKING WAVE PLUNGE DISTANCE DATA.

$$\frac{x_p}{L_b} = \frac{x_{bc} - x_{bt}}{L_b} = 0.065 \frac{H_b}{\omega T}, \quad (47)$$

which is the nondimensional equation for plunge distance, and which is also "preserved" between prototype and model. Equation (47) carries the same physical interpretation as before. The plunge distance is proportional to the wave energy flux per unit width crossing the bar crest. Rearranging equation (47) and substituting for  $L_b$  from equation (37) gives

$$x_p = \frac{0.081g^{1/2}H_b^{3/2}}{\omega}. \quad (48)$$

So instead of  $x_p$  being proportional to  $H_b$ , it is seen that  $x_p$  is related to  $H_b^{3/2}$ . Figure 29b shows Galvin's results replotted as a function of  $H_b^{3/2}$ . It is clearly seen that the values more closely follow the linear relationship as suggested by equation (48). The straight line was sketched in to illustrate this trend.

The fact that Galvin's data, which were obtained on a rigid plane slope with no bar formation, exhibit a trend toward  $H_b^{3/2}$  adds further credibility to the physical interpretations given thus far.

Pursuing a simplified theoretical development in the same fashion as Galvin, assume that the trajectory of a water particle at breaking is that of a free-falling body under the force of gravity. However, the horizontal velocity of the wave crest is not  $C_b$ , the breaking wave celerity, but  $C_b'$ , which is larger than  $C_b$ . This comes about by virtue of the upward vertical accelerations under the crest. As a wave breaks in a plunging fashion, these vertical accelerations transfer

momentum to the upper portion of the wave crest, acting like a "thrust" in the horizontal direction. For this simplified analysis, it is assumed that this "thrust" results only in an increase of the horizontal velocity at the crest.

From the equations of uniformly accelerated motion, and in accordance with the sketch given in Figure 30, the equation for the vertical distance becomes

$$H_b = \frac{1}{2} g t^2 , \quad (49)$$

while the horizontal motion is described by

$$X_p = C_b' t , \quad (50)$$

where  $t$  = time. Solving equation (49) for  $t$ , and placing the result into equation (50), yields

$$X_p = C_b' \left[ \frac{2H_b}{g} \right]^{1/2} . \quad (51)$$

Solving equation (47) for  $X_p$ , equating the result to equation (51), and solving for  $C_b'$  gives

$$C_b' = \frac{0.065}{\omega} \left( \frac{g}{2} \right)^{1/2} H_b^{1/2} C_b . \quad (52)$$

Replacing  $H_b^{1/2}$  in equation (52) with the relationship obtained from equation (37), i.e.,

$$H_b^{1/2} = \frac{C_b}{[2(.77)g]^{1/2}} ,$$

it is seen that

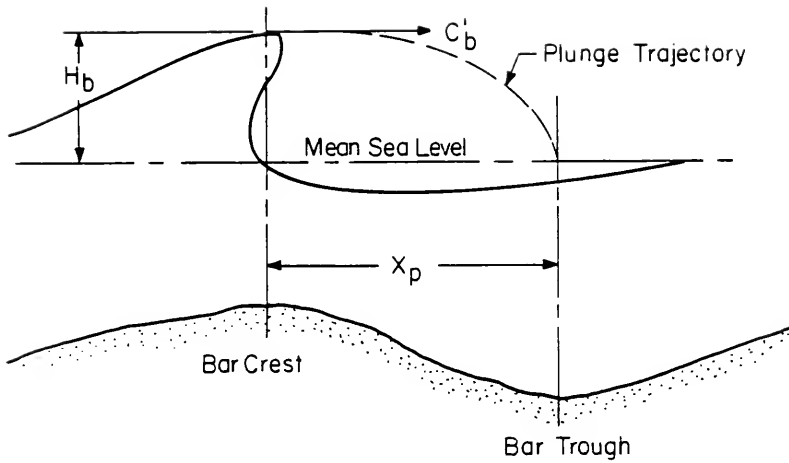


FIGURE 30: PLUNGE DISTANCE DEFINITION SKETCH.

$$C_b' = 0.037 \frac{C_b^2}{\omega} . \quad (53)$$

This simply states that, in the range of plunging breakers, the "wave thrust velocity" at breaking varies as the square of the breaking wave celerity.

A further interpretation of equation (53) can be given by assuming that  $C_b'$  is proportional to  $C_b$  through the simple relationship of

$$C_b' = K_C C_b , \quad (54)$$

where  $K_C$  is greater than 1 and is somehow related to the vertical water particle accelerations. From equations (53) and (54) it is immediately recognized that

$$K_C = \frac{0.037 C_b}{\omega} , \quad (55)$$

which is a dimensionless function relating  $K_C$  to the breaking wave celerity. Thus, as the wave celerity increases,  $K_C$  increases, which implies that the vertical accelerations responsible for the horizontal "thrust velocity" also increase. The presence of the sediment fall velocity has come about from the use of equation (47), and it could possibly be interpreted as a measure of bottom friction or as a damping agent acting upon the vertical water particle accelerations.

While the above analysis is quite simplistic and is not intended to be an accurate physical description of plunging breakers, the hypothesis put forth seems to provide at least a heuristic model which could serve as a basis for further research.

### Nearshore Curve Fit

Examination of the nearshore portion of the near-equilibrium barred profiles clearly indicates that the profile is not a straight line, but instead a curve which usually exhibits the characteristics of having an increasing slope as the water depth decreases. While it is impractical to determine every minor feature of the nearshore profile, caused by any number of complex phenomena, it is possible to derive a semi-empirical relationship for this portion based on some rather simplified physics.

Dean (1977) gave three derivations for equilibrium beach profiles in the nearshore region between the surf zone and the beach. He assumed that the ratio of breaker height to water depth is constant, landward of the point of first wave break, thus restricting the formulations to spilling breakers. The first model assumed the beach profile was due to a uniform alongshore shear stress. Since dune erosion is considered here only as an onshore-offshore sediment transport problem, this model is not applicable. Dean's second model considered that the profile was a result of uniform energy dissipation per unit surface area of the sea bed, with the energy first being transferred into turbulence and then, through viscous action, into heat. The final result was an equation of the form

$$h = Ax^{2/5} ,$$

where

h = depth below mean sea level,

x = horizontal range directed seaward, and

A = a function primarily of grain-size.



The third derivation proceeded along the same lines, only this time the profile was formed by uniform energy dissipation per unit volume of water within the surf zone. This resulted in an equation of the form

$$h = Ax^{2/3} . \quad (56)$$

Subsequent evaluation of a large number of actual beach profiles by both Dean and Hughes (1978) found that equation (56) provided the best fit to the prototype data in a substantial majority of the cases, the implication being that the mechanism of beach profile formation within the surf zone is best described as a uniform energy dissipation per unit volume, in the simplest of approximations.

It was seen earlier in this chapter that the breaker distance (or surf zone length) can be expressed as a function of wave power per unit width, which is also proportional to  $h_{bc}$ .

Multiplying the left-hand side of equation (41) by  $b/b$ , where  $b$  = unit width of surf zone perpendicular to the beach, leads to the conclusion that the incoming energy flux per unit width is proportional to some surf zone volume per unit width. Since the same conclusion can be reached for the bar trough distance, it can be reasoned that the energy present after the initial plunging wave break is dissipated over the volume of the remaining surf zone, as is the case for Dean's third derivation.

After the initial plunge, which results in a significant energy loss, the remaining wave energy moves as a bore toward the beach. So, from the bar trough to the shoreline, the wave can be considered as a spilling breaker, and Dean's profile derivation may be used. For completeness, Dean's derivation is briefly outlined in Appendix E.1.

### Experimental Results

Using a direct power-curve fitting technique as described by Hughes (1978), the "best-fit" of the equation  $h = Ax^{2/3}$  was performed on the nearshore beach portion for 33 of the experimental, near-equilibrium profiles. The curve-fitting extended from the dune toe position seaward to the offshore bar trough, and the method employed the technique of least-squares.

Figure 31 presents the calculated values of "A" for each of the runs, which show only slight deviation from the computed average, as given by the straight line. In fact, the root mean square error about the mean value is only 0.0386.

The RMS errors, calculated for each profile by the formula

$$\text{RMS}_{\text{error}} = \left[ \frac{1}{n} \sum_{i=1}^n (h_{\text{measured}} - h_{\text{calculated}})^2 \right]^{1/2},$$

varied between 0.142 inches to 0.634 inches with an average RMS error equal to 0.336 inches. This corresponds to 0.7 feet in the prototype. Errors of this magnitude are certainly tolerable and are much better than the errors found when the profile is approximated by a straight line in the nearshore region.

### Discussion

From the results of the curve-fitting, it is plainly evident that "A" is neither a function of breaking wave height,  $H_b$ , or wave period, T. This was also pointed out by Hughes when he examined the values for "A" taken from natural beach profiles representing three different wave

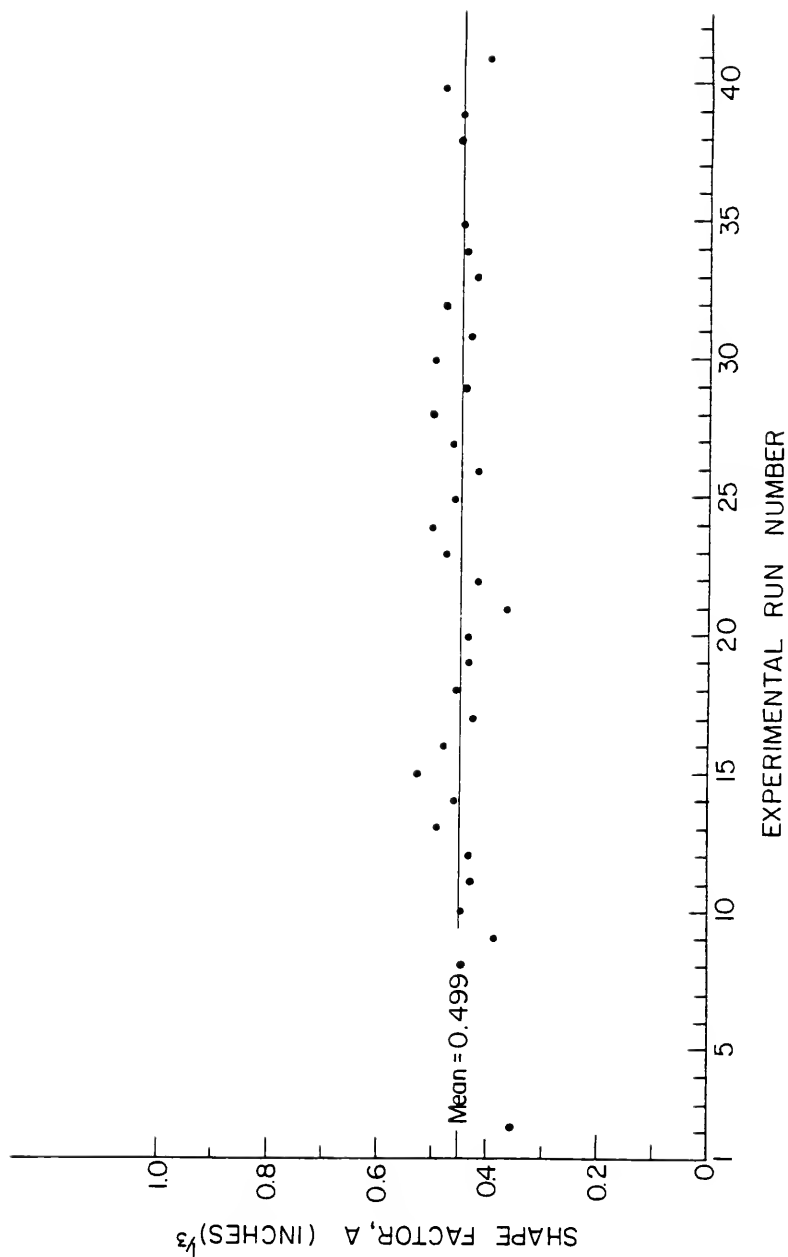


FIGURE 31: VALUES OF "A" FOR NEARSHORE CURVE FIT.

energy conditions. This can be reasonably explained by the fact that the extra surf zone volume, necessary to dissipate an increased incoming wave energy flux, is obtained by a lengthening of the surf zone. In addition, as will be seen shortly, increased energy flux per unit width also increases the depth of the bar crest and bar trough with respect to still water level in such a manner that the ratio of the depths appears to be constant.

Thus for increasing wave energy, the position of the bar trough moves offshore and becomes deeper in such a manner that the curve

$$h = Ax^{2/3}$$

can be extended seaward to intersect this position without changing the value of "A." The increased energy is dissipated by the longer plunge distance and the increased surf zone volume.

However, it can be stated that "A" is a function of grain-size fall velocity,  $\omega$ , since a larger value of  $\omega$  will dissipate more energy and permit a shorter surf zone length. Because the depth of the bar trough will remain the same, it will be necessary for "A" to increase as some function of  $\omega$ . Thus, there seems to be some sort of trade-off between grain-size and surf zone volume since an increased  $\omega$  decreases volume by decreasing surf zone length, but it also increases volume by providing a steeper profile out to the bar trough. It is qualitatively felt that the net volume change will bring about a decrease in total surf zone volume for increasing grain-size, with the larger grain-sizes dissipating more energy.

It is therefore concluded that the shape factor, A, in the near-shore beach profile equation, given by  $h = Ax^{2/3}$ , is independent of the

wave climate and is dependent only upon the grain-size, more specifically, the grain-size fall velocity. Furthermore, "A" probably increases as  $\omega^{2/3}$  as was indicated in the derivation of Appendix E.1. Results by Hughes also illustrate this trend, but only in a general sense because the grain-size range covered was not sufficient to quantify the results.

#### Offshore Bar Crest Depth Versus Bar Trough Depth

Several studies involving both model experiments and prototype measurements have been conducted with regard to offshore bar geometry.

In one of the earliest experimental studies, Keulegan (1948) pointed out that natural bars seemed to be somewhat longer and flatter than those produced in model experiments. As already demonstrated, this is a direct cause of the need to use model sediments similar in size to those found in nature, making it necessary to use a distorted model when the parameter  $H/\omega T$  cannot be scaled. Keulegan, however, did point out that the ratio of bar crest depth ( $h_{bc}$ ) to bar trough depth ( $h_{bt}$ ) was similar in both model and prototype, and it appeared to be practically independent of the wave characteristics or the beach slope. He computed an average value of

$$\frac{h_{bt}}{h_{bc}} = 1.69$$

for his model experiments.

Shepard (1950) examined this ratio using a large number of beach profiles along the California coast. While the scatter is significant, the data do indicate a trend, given by Shepard as

$$\frac{h_{bt}}{h_{bc}} = 1.16 .$$

A study of beach profiles from three locations along the Texas coast by Herbich (1970) gave values of  $h_{bt}/h_{bc}$  ranging between 1.25 and 1.35.

In the current dune erosion experiments, the values ranged between 1.16 and 1.97, with the average at

$$\frac{h_{bt}}{h_{bc}} = 1.52 .$$

The 29 values obtained are shown plotted on Figure 32, along with the averages given by the other investigators.

While the relationship seems to be somewhere between 1.2 and 1.7, it is felt that too much variation exists for this to be used for prediction of bar trough depth. It is interesting to note that the laboratory tests give higher values for  $h_{bt}/h_{bc}$  than those found in nature. This can be primarily attributed to the fact that the laboratory tests were conducted using monochromatic waves, while the wave trains in nature contain a spectrum of waves which act to "smooth" the bar features due to the fact that the different height waves will break in different locations above the bar. A secondary influence is the tidal variations found in the prototype, which also help to smooth the bar features.

It can be concluded that the ratio of bar trough depth to bar crest depth is not necessarily a constant because of the considerable variation shown on Figure 32. This ratio is more than likely a function of the plunging wave and of the huge turbulent vortex it generates, which scours out the bar trough.

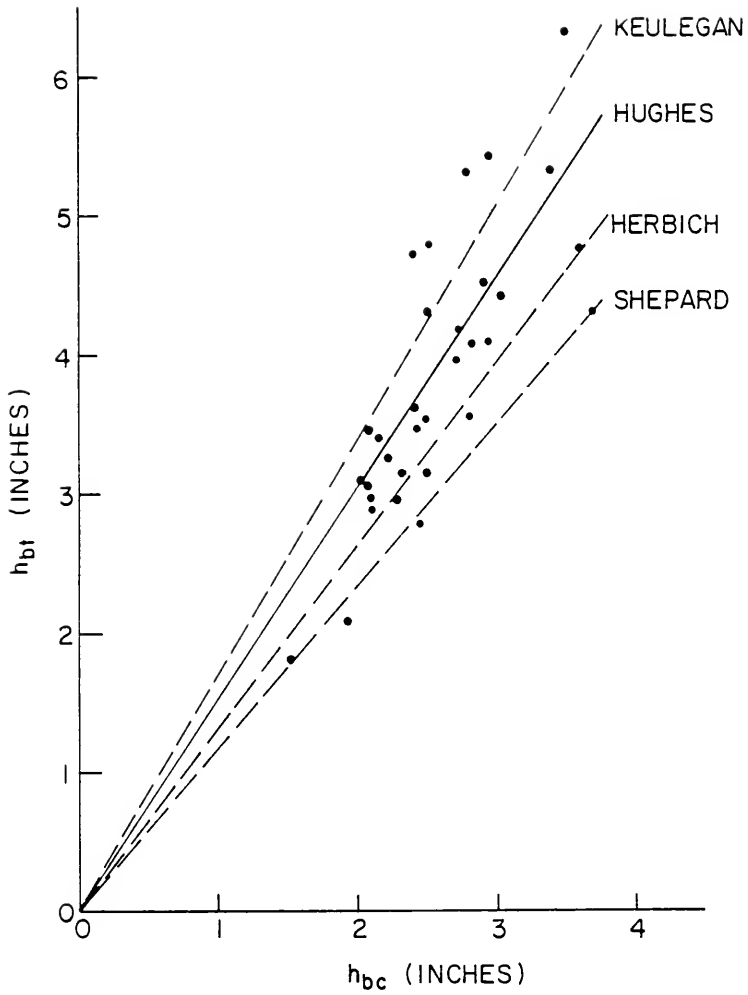


FIGURE 32: BAR TROUGH DEPTH VERSUS BAR CREST DEPTH.

### Wave Runup

Since the nearshore profile is calculated referenced to the dune toe, which corresponds to the point of maximum wave runup, it is necessary to be able to predict the elevation of the maximum runup above the still surge level in order to construct the equilibrium barred profile. The vertical runup elevation was selected over the horizontal runup distance because the experiments demonstrated much more consistency than when the horizontal distance was chosen. This was caused by the gentle beach slopes which necessitated a linear interpolation between profile data points to determine the intersection of still surge level and the beachface. Thus, small errors in elevation could cause significant errors in the horizontal position of this intersection point, and consequently, give errant values for the horizontal runup distance.

Most previous experimental work dealing with wave runup was conducted using plane, rigid beach slopes. A simple, reliable expression for runup on smooth plane-slopes was given by Hunt (1959) and can be written as

$$\frac{R_v}{H} = \frac{\tan \alpha}{\left(\frac{H}{L_0}\right)^{1/2}}, \quad (57)$$

where

$R_v$  = vertical runup distance above still water level,

$\tan \alpha$  = beach slope,

$H$  = wave height, and

$L_0$  = deep water wave length.

Unfortunately, equation (57) is not valid for cases other than plane-sloped beaches. As has been seen, actual beaches have curving profiles



which get progressively steeper nearer to the beach. In addition, the rigid bottom must alter the wave characteristics from those present on natural, barred profiles.

A method for calculating wave runup on composite slopes was given by Saville (1957b). While perhaps better than Hunt's formula, the method requires an iteration procedure, and unfortunately it still deals only with rigid beds.

In the present experiments, the values of vertical wave runup with respect to still surge level were calculated from the profile measurements and then examined for any significant trend. No apparent relationship could be seen as a result of variations in the breaking wave height, which is related to energy flux. However, a definite trend was seen to exist with regard to wave period. As wave period increased, the vertical runup increased, which is a pretty common observation.

It also seems logical that  $R_v$  should somehow be directly related to beach slope, as it is in equation (57).

Rearranging Hunt's formula into the form

$$R_v = (HL_0)^{1/2} \tan \alpha$$

and replacing  $L_0$  with

$$L_0 = \frac{g}{2\pi} T^2 ,$$

yields

$$R_v = \left[ \frac{gH}{2\pi} \right]^{1/2} T \tan \alpha . \quad (58)$$

For gentle beach slopes,

$$\tan \alpha = \frac{dh}{dx} ,$$

but the profile has been shown to be  $h = Ax^{2/3}$ , from which it is easily shown that

$$\frac{dh}{dx} = \frac{2}{3} \frac{A^{3/2}}{h^{1/2}} = \tan \alpha . \quad (59)$$

Placement of equation (59) into equation (58) yields

$$R_V = \frac{2}{3} \left[ \frac{g}{2\pi} \right]^{1/2} \left[ \frac{H}{h} \right]^{1/2} TA^{3/2} . \quad (60)$$

But within the surf zone, it is assumed that  $H = Kh$ , where  $K \approx 0.78$ , and equation (70) becomes

$$R_V = 0.235g^{1/2}TA^{3/2} , \quad (61)$$

which is independent of the wave height. Figure 33 gives the runup calculated when placing the value of "A" found for each experiment into equation (61), as compared to the actual runup value. As can be seen, equation (61) typically gives larger values for vertical runup, which indicates that either the assumed value for K is too large or, more likely, effects such as bottom friction and percolation on the beach-face aid in reducing, slightly, the value of  $R_V$ .

Writing equation (61) as

$$R_V = TA^{3/2} \times \text{constant}$$

and noting that A is proportional to  $\omega^{2/3}$ , as shown in Appendix E.1, the final expression for vertical runup on a natural beach slope can

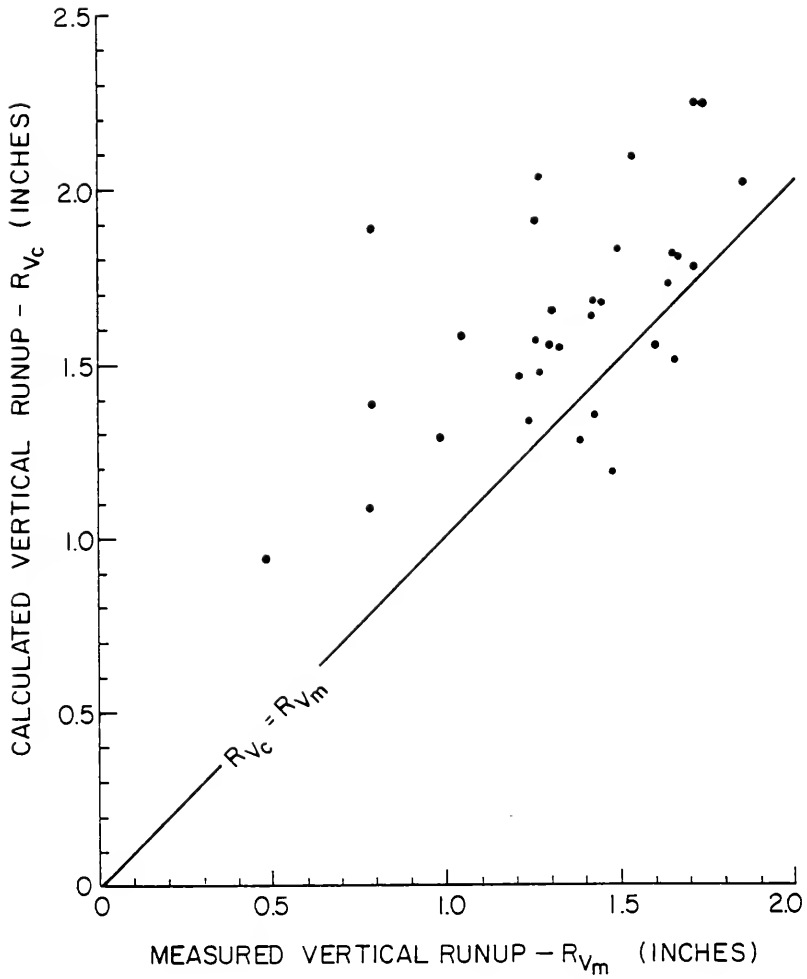


FIGURE 33: CALCULATED RUNUP VERSUS MEASURED RUNUP.

be given as

$$\frac{R_v}{\omega T} = \text{constant} . \quad (62)$$

This runup parameter has the features of being dimensionless and also of being preserved in the model law. In other words, the value of the constant will be the same in both the prototype and the model.

Physically, equation (62) states that the vertical runup distance is influenced only by the wave period for a given beach. Therefore, period must be the only characteristic wave parameter which is carried all the way across the surf zone. The wave height characteristics are lost in the process of forming and maintaining the equilibrium nearshore profile.

It is also seen that the sediment fall velocity influences the runup, since runup increases as  $\omega$  increases. This could be interpreted in the following manner. As the grain-size increases,  $\omega$  increases and the beach becomes steeper, as was seen earlier in this chapter. This steeper beach profile must dissipate slightly less wave energy through turbulence, which means slightly more energy must be dissipated in the final wave runup, thus giving larger values for  $R_v$ .

For the dune erosion experimental series, the values of  $R_v/\omega T$  have been calculated and are shown on Figure 34. A certain amount of scatter exists, but not enough to distract from the apparent trend of  $R_v/\omega T = \text{constant}$ . Three factors could contribute to the scatter:

- 1) Measurement error, which probably does not amount to very much since the profiling instrument calibration is quite good.

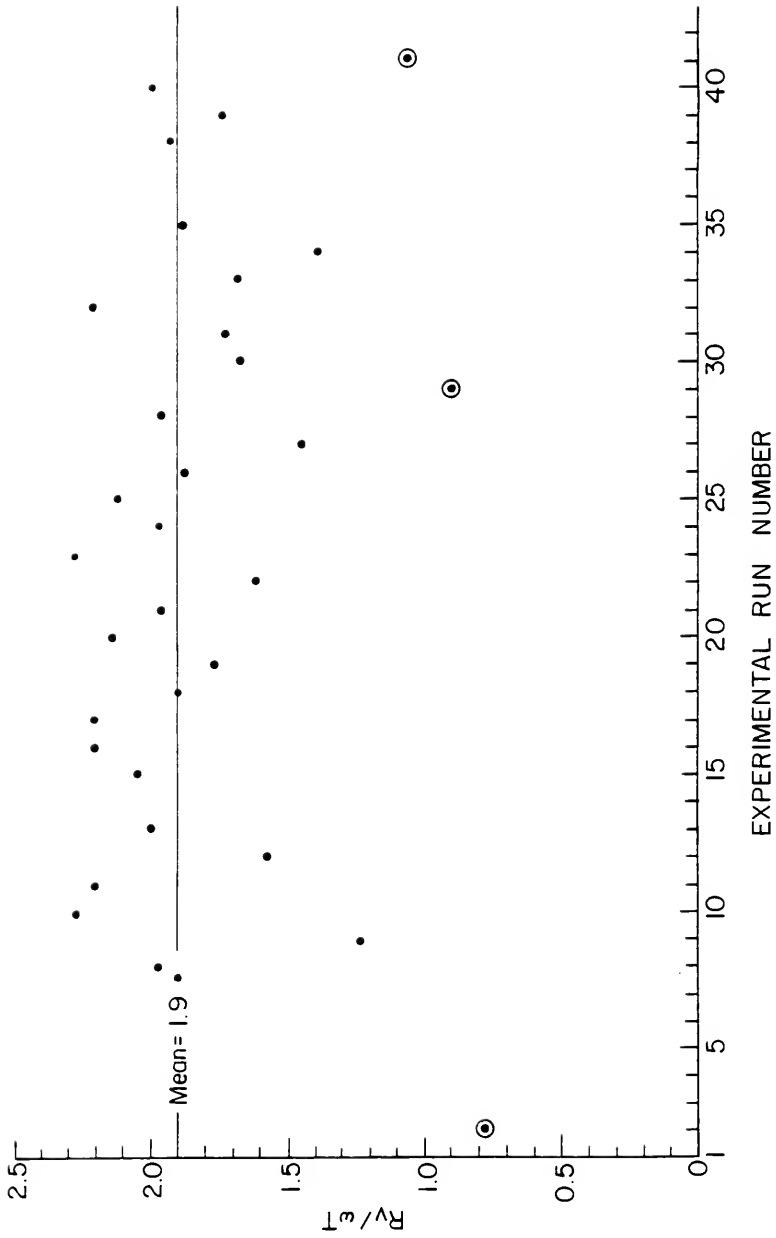


FIGURE 34: VERTICAL WAVE RUNUP PARAMETER.

However, the manual placement of the probe could create errors on the order of  $\pm 0.1$  inch. This error translates to approximately  $\pm 0.13$  in the value of the constant, 1.9.

- 2) It is very likely that the final profile, while near equilibrium, had not reached a final equilibrium in some instances, thus contributing to the error.
- 3) While the profile remained quite uniform across the width of the wave tank, there sometimes appeared to be minor variations in the profile as a result of the side wall effects.

Taking these effects into account, it would appear that  $R_v/\omega T$  does remain nearly constant.

The average for all data points shown on Figure 34, excluding the three circled points which fall way below the trend, is given by

$$\frac{R_v}{\omega T} = 1.9 . \quad (63)$$

The calculated RMS error was 0.267, which is about 14 percent.

An examination of Ma's (1979) results for different grain-sizes gave values for  $R_v/\omega T$  in the neighborhood of 1.9, but they varied considerably, due mostly to the difficulty of determining  $R_v$  from the profiles.

Due to the above physical agreements and experimental results, it is concluded that the dimensionless parameter  $R_v/\omega T$  is a constant, and represents a simple means for the determination of vertical wave runup for either prototype beaches or movable-bed models.

### Offshore Curve Fit

In the region seaward of the offshore bar the bottom equilibrium profile, arising from storm activity, exhibits features similar to the nearshore profile. Comparisons of the near-equilibrium profiles for the experimental runs indicate two obvious trends which can aid in the analysis of this portion of the barred profile, the profile becomes progressively steeper as the depth decreases, and the overall profile steepens as the peak surge level increases. From the first of these observations comes the fact that the profile can best be described as a power curve rather than as a straight line. This corresponds with the same conclusion found for the nearshore region. The second observation makes it necessary to incorporate the surge level into the analysis.

Making use of some known physical relationships for sediment transport in this region, combined with a few simplifying assumptions, it was possible to derive a simple power curve relationship for the profile in the immediate offshore region, given by the expression

$$h = A_0(x - x_i)^{2/3}, \quad (64)$$

where

$h$  = depth relative to peak surge level (feet),

$x$  = horizontal range (feet),

$x_i$  = reference range where the curve intersects the water level (feet), and

$A_0$  = shape factor (feet<sup>1/3</sup>).

The complete derivation is presented in Appendix E.2 along with the assumptions and reasoning implemented. Equation (64) is of the same form as equation (56), which was used for the nearshore profile. This

implies a similarity of profiles between these two regions, a fact that intuitively seems correct.

### Experimental Results

Using the method of least-squares curve fitting, the power curve of equation (64) was applied to the experiment profiles in order to find the values for  $A_0$ . As can be seen from Figure 35a, the values of  $A_0$  appear to be independent of wave height and wave period, but they are definitely a function of surge level. While not proven in this research, it is also felt that  $A_0$  will have some dependence on grain-size, as was the case for the nearshore profile. The profile should become steeper for an increased value of sediment fall velocity.

The values of vertical RMS error calculated for each profile varied between 0.136 inches to 0.583 inches, with the average RMS error for all profiles being 0.304 inches. This average corresponds to a value of 7.6 inches in the prototype.

Figure 35b illustrates the linear trend given by the averages of all values at each surge level, at least for the surge range tested. This linear trend is given by the best-fit of

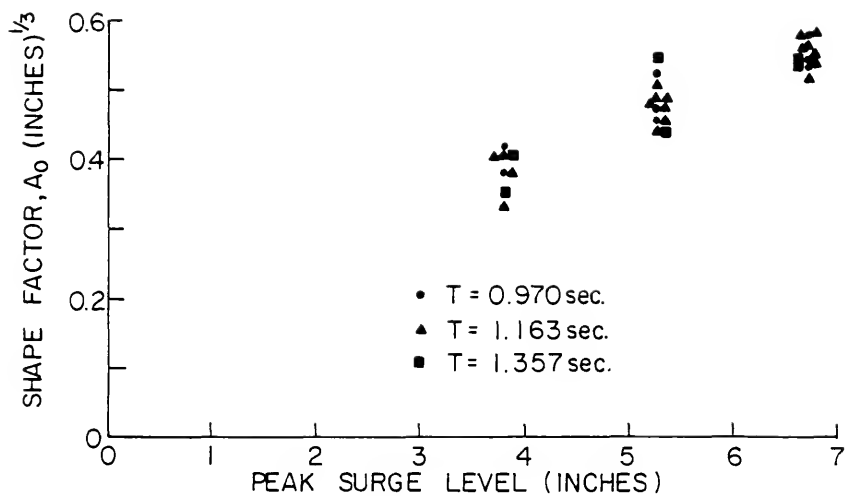
$$A_0 = 0.167 + 0.058S_m ,$$

which leads to the offshore profile equation for the model given as

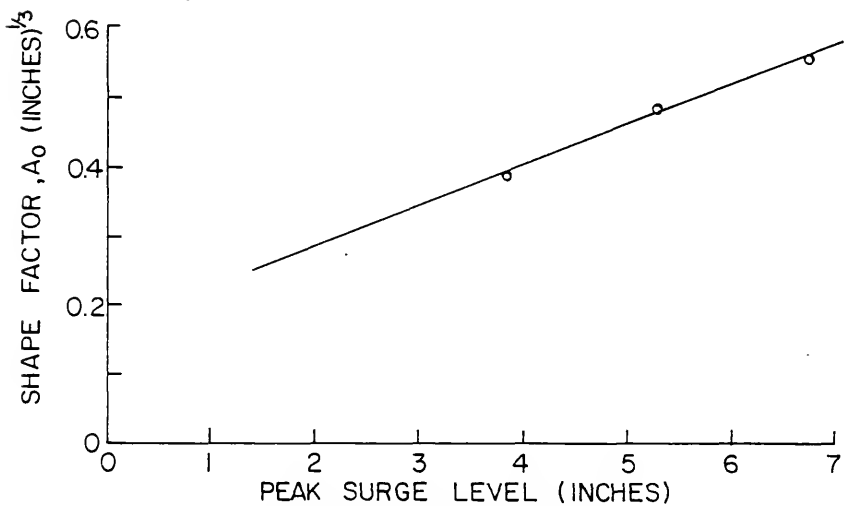
$$h_m = (0.167 + 0.058S_m)(x_m - x_i)^{2/3} , \quad (65)$$

where  $S_m$  is the surge level in inches, and  $h_m$ ,  $x_m$ , and  $x_i$  are also in inches. The equivalent equation for the prototype is scaled up as





35a:  $A_0$  VALUES FOR EACH RUN.



35b: AVERAGE  $A_0$  VALUES AT EACH SURGE LEVEL.

FIGURE 35: OFFSHORE CURVE FIT.

$$h_p = (0.132 + 0.022S_p)(x_p - x_i)^{2/3} . \quad (66)$$

Here

$h_p$  = depth in feet,

$x_p$  = range in feet,

$x_i$  = reference range in feet, and

$S_p$  = surge level in feet.

Unfortunately, equations (65) and (66) have some rather severe limitations placed on their usage. These are discussed below.

### Applications

There are two major constraints placed upon the empirically derived offshore profile equations given above.

Because the experimental test series did not attempt to investigate the effects of different prestorm offshore profiles, the results cannot be universally applied. During the storm surge rise, sediment is being transported offshore and finally deposited when the bottom velocities are sufficiently decreased. As the surge rises, some sediment deposited at lower surge levels can no longer be moved because the limiting-depth of transport has been exceeded. So, in essence, the process of profile formation is actually a series of discrete steps which take place as the water level rises. The portion which developed at lower surge levels is incremented as the surge level increases, thus making the profile steeper. This explains why the values of  $A_0$  appear to be related to surge level.

In the same manner it can be seen that an initially steeper prestorm profile will give a higher value of  $A_0$ , indicating a steeper

offshore storm profile. This comes about because the eroded sediment cannot be carried as far offshore before it is dropped, when compared to the milder prestorm profile.

The second constraint is the prototype grain-size. Because equation (66) was scaled up using the modeling relationships derived earlier, it can only be applied to profiles having a similar grain-size of around 0.26 mm. This ties into the first constraint since the initial prestorm profile steepness will be a function of sediment fall velocity. In addition, it should be expected that the increased stability of larger grain-sizes, when exposed to erosive conditions, should allow a steeper equilibrium offshore storm profile.

On the brighter side, however, the experimental test series were designed to approximate the average Florida beach in terms of grain-size and prestorm profile; thus, the results from the offshore curve fitting, given by equation (66), could be used with a higher degree of confidence when applied to the Florida coastline.

To reiterate, the empirically derived prototype relationship for the offshore portion of the equilibrium barred storm profile, given by equation (66), should only be applied to beaches exhibiting the same prestorm underwater configuration as that given by the expression

$$h = 0.15x^{2/3} ,$$

where 0.15 has the units of (feet)<sup>1/3</sup>, which is typical of Florida beaches. The prototype effective grain-size diameter should be in the neighborhood of 0.26 mm, and it is doubtful that the relationship could be extrapolated much past a peak surge value of 16 feet in the prototype.

### Summary

This chapter has been concerned with the parameterization of certain characteristics of the equilibrium barred storm profile. By determining this profile, it then becomes possible to determine the maximum amount of dune erosion and recession which would be expected on any prestorm beach-dune configuration for a given set of storm parameters. This is done simply by shifting the calculated storm profile relative to the prestorm profile until a balance is established between eroded and deposited sediment.

It was demonstrated that the distance between the dune toe and bar crest, as well as the distance between dune toe and bar trough, can be found as a function of breaking wave height, wave period, and sediment fall velocity. Physical explanations were given for these expressions.

A hypothesis was developed for plunging distance, but only to demonstrate a possible direction for further research.

The nearshore profile between the dune toe and the bar trough was found to fit a curve given by

$$h_m = 0.50x_m^{2/3} \quad (67)$$

in the model, where  $h_m$  and  $x_m$  are in inches. The equivalent prototype equation for the nearshore region scales up to be

$$h_p = 0.39x_p^{2/3}, \quad (68)$$

where  $h_p$  and  $x_p$  are given in units of feet. Equation (68), however, is restricted to use on beaches having an effective grain-size diameter in the vicinity of 0.26 mm.

An investigation into the relationship between the water depths over the bar and crest proved inconclusive.

A simple means of calculating wave runup was derived and empirically calibrated for use in either the model or the prototype. It appears that the vertical runup is principally a function only of wave period and sediment size.

Finally, an analysis of the offshore portion of the barred profile was undertaken, which yielded results applicable to the average Florida beach but needs to be further analyzed to determine the effects of grain size and of a different prestorm profile.

From the foregoing analyses, it is now possible to construct the equilibrium barred profile from the incoming wave parameters.

#### Sample Prototype Calculation

Given the deep water wave height,  $H_0$ , the wave period,  $T$ , the peak surge level,  $S$ , and the sediment fall velocity,  $\omega$ , the determination of the equilibrium barred storm profile proceeds as follows:

- 1) Calculate  $H_b$  from equation (34).
- 2) Determine  $L_b$  from equation (37).
- 3) Calculate  $h_b$  from equation (32).
- 4) Calculate the vertical runup,  $R_v$ , from equation (63).
- 5) Using equation (68), replace  $h_p$  with the value for  $R_v$  and solve for  $x_{pi}$ . This is the distance between the dune toe and the intersection of the still surge level with the beach. Using this intersection point as the zero reference, plot the position of the dune toe as  $(-x_{pi}, R_v)$ .

- 6) Determine the distance between the dune toe and bar trough using equation (44). The horizontal range of the bar trough, relative to the reference point, is given as  $(x_{bt} - x_{pi})$ .
- 7) Using equation (68), calculate the nearshore profile pairs  $(x_p, h_p)$  and reference them to the chosen coordinate system through the transformations

$$x = x_p - x_{pi} \quad \text{and} \quad y = R_v - h_p .$$

- 8) The shearface of the eroded dune is drawn in as a nearly vertical line.
- 9) Calculate the bar crest distance from the dune toe  $(x_{bc})$  using equation (39); then plot the bar crest, relative to the coordinate system as  $(x_{bc} - x_{pi}, -h_b)$ . Connect the bar crest and trough with a straight line.
- 10) Using equation (66) for the offshore portion, replace  $h_p$  with the value for  $h_b$  and solve for  $(x_{bc} - x_{pi} - x_i)$  from which the value of  $x_i$  can be found. Placing this value for  $x_i$  back into equation (66) then allows the calculation of the offshore depths relative to the intersection of surge level and profile.

By the above method, the equilibrium barred profile can be calculated, and ultimately the maximum dune recession can be found as discussed earlier.

This method was used to calculate the profiles for runs 18 and 34 of the experimental series, chosen arbitrarily, and the comparisons with the actual measured profiles are shown in Figure 36. As can be

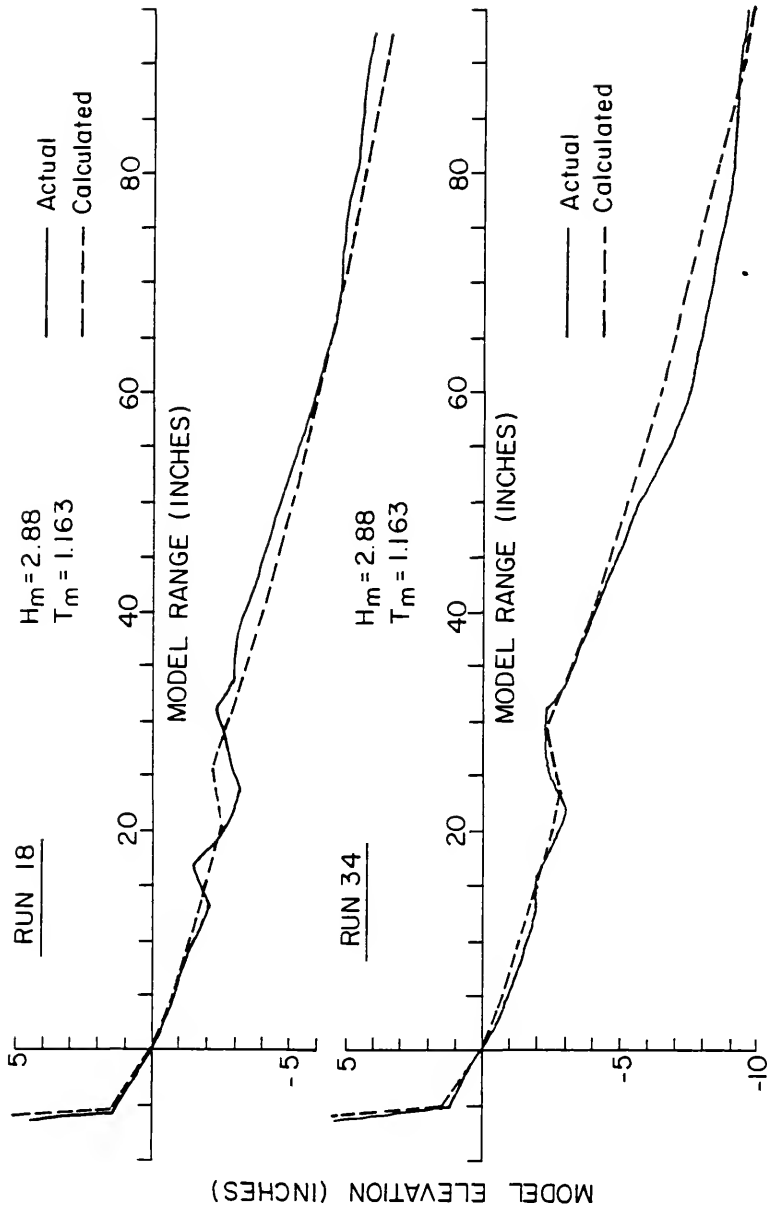


FIGURE 36: CALCULATED BARRED PROFILE COMPARISONS.

seen, the comparisons are very favorable. It should be noted that the model-value equations (65) and (67) were used in this case.

The next step is to determine the effect of peak surge duration, which is examined in the following chapter.



## CHAPTER IX

### TRANSIENT EROSION EFFECTS

The quantitative analyses presented in Chapter VIII provide a means of calculating the near-equilibrium erosion which would occur for a given set of storm conditions acting on a given prestorm profile. However, the resulting erosion values represent the maximum dune recession which would occur if the storm conditions persisted indefinitely at the peak surge level. While a severe "northeaster" lasting three days might well approximate this condition, hurricanes move much faster, with the surge water level remaining at its peak value often only several hours. As a consequence, the erosion experienced by the beach-dune system during a hurricane, while severe, never reaches a full equilibrium. Hence, there remains the need of being able to estimate the effects of the peak surge duration and then to adjust the calculated dune recession accordingly.

Essentially, what is required in determining the transient erosion is a partitioning, with respect to time, of the dune erosion which occurs from the time that the peak surge level is reached until the time that near-equilibrium is established. By doing this, it then becomes possible to determine the effect of peak surge duration, since no further dune recession can take place once the surge level begins to drop.

A further advantage of developing a transient dune erosion model is that future refinements are possible as more prototype data become available. Verification of an "equilibrium-type" model, such as Edelman's, requires equilibrium prototype storm erosion, which seldom occurs. On the other hand, a transient model can be adjusted to suit any peak storm surge duration with the advantage that, every time storm data are collected, further verification and refinement of the model will be possible.

### Theoretical Development

As was the case for the development of the equilibrium barred storm profile, the actual physics involved in the transient dune erosion phenomenon are beyond our grasp. Therefore, the investigation must become a parameterization of the important factors, strengthened by physical reasoning where possible.

### Energy Concepts

During normal conditions, a beach is able to reach a state of quasi-equilibrium when subjected to a nearly constant incoming wave field. In addition, the beach is able to rapidly adjust to small variations in the incoming waves and the tidal fluctuations in water level. In this case the incoming wave energy flux is totally dissipated over the length of the surf zone by the mechanisms of wave breaking, bottom friction, wave transformation, turbulence, and to-and-fro sediment transport, with the final small amount of wave energy being converted to wave uprush. Essentially, there is no remaining wave energy left over at the uprush limit.

However, during a severe storm, the water level and the incoming wave energy increase dramatically over a short period of time, so rapidly in fact that the beach is unable to adjust quickly enough to totally dissipate this energy increase. The result is an "excess of energy" left over at the uprush limit which can only be dissipated by further wave uprush and the corresponding erosion of the dune sand, now exposed to the wave action by virtue of the surge level rise. In time, the beach profile will be eroded to the point that equilibrium will once again be reached, and the incoming wave energy will be totally dissipated over the length of the new surf zone, with no excess energy reaching the eroded dune toe. In actual fact, this time never arrives because the storm event ends before equilibrium can be reached.

Based upon the above description, it is possible to write a mathematical statement, given as

$$\frac{dE_t(t)}{dt} = \beta(t) \frac{dE_b(t)}{dt} , \quad (69)$$

where

$E_b$  = average wave energy density per unit width at the breaking,

$E_t$  = average wave energy density per unit width arriving at the dune toe, and

$\beta$  = a time dependent proportionality.

Equation (69) states that, during a storm, the time-rate of wave energy per unit width reaching the dune toe is proportional to the time-rate of wave energy per unit width reaching the breaking point. The quantities  $dE/dt$  have units of wave power per unit width, while  $\beta(t)$  is dimensionless.

Since the "excess energy" is such a difficult parameter to work with, it is necessary to recast it into a more useful form. This is done by reasoning that energy is a form of work, and that a certain amount of work will be required in order to erode a certain amount of sediment. Under the assumption that the time-rate of erosion (per unit width of beach) occurring at the dune toe is directly proportional to the excess energy available at the dune toe, it is possible to write

$$\frac{dV_e}{dt} = K \frac{dE_t}{dt}, \quad (70)$$

where

$V_e$  = eroded volume of sediment per unit width of beach, and

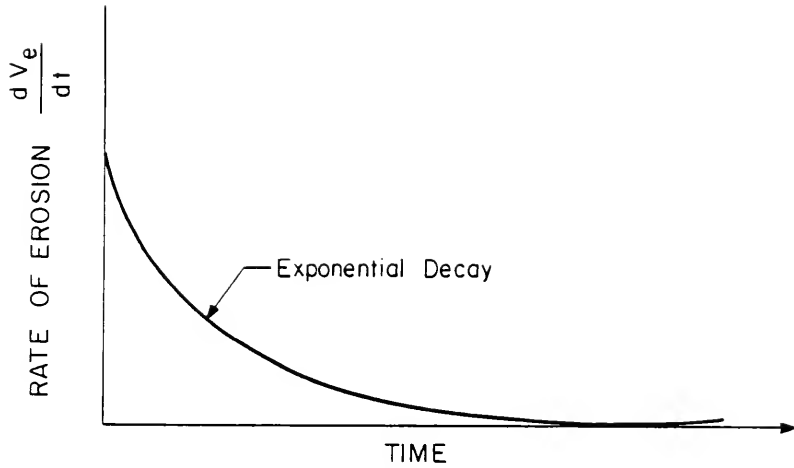
$K$  = proportionality constant having units of inverse stress.

It is reasonably expected that the rate of volumetric erosion should be a function of the shear stress acting on the sand grains. Thus, the factor  $K$  should be a function of the sediment characteristics, such as grain size, grain shape, and specific weight.

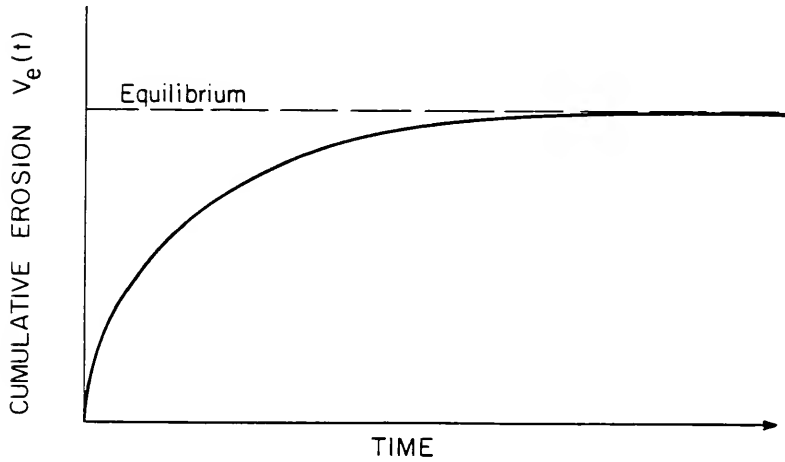
Combining equations (69) and (70) yields

$$\frac{dV_e}{dt} = K\beta(t) \frac{dE_b}{dt}. \quad (71)$$

To find a form for  $\beta(t)$ , consider the case of an instantaneous sea level rise with a constant incoming wave energy. For this case, it has been well observed in model experiments that the rate of erosion is initially large and then decreases in time, as shown in Figure 37a. This curve exhibits the characteristics of an exponential decay.



37a: RATE OF DUNE EROSION.



37b: CUMULATIVE DUNE EROSION.

FIGURE 37: TIME-DEPENDENT EROSION TRENDS.

Assuming the exponential form of

$$K\beta(t) = A + Be^{-\alpha t}$$

and applying the boundary condition of  $dV_e/dt$  approaching zero as  $t$  approaches infinity, the result is

$$\beta(t) = \frac{Be^{-\alpha t}}{K} . \quad (72)$$

By placing equation (72) back into equation (69), and by then assuming that, at time  $t = 0$ , the rate of energy arriving at the beach is a fraction,  $\eta$ , of the incoming energy, i.e.,

$$\frac{dE_t(0)}{dt} = \eta \frac{dE_b(0)}{dt} ,$$

it is then seen that  $B = \eta K$  and

$$\beta(t) = \eta e^{-\alpha t} . \quad (73)$$

Finally, equation (73) can be placed into equation (71) to yield

$$\frac{dV_e(t)}{dt} = K\eta e^{-\alpha t} \frac{dE_b}{dt} , \quad (74)$$

which is a parametric equation for the rate of dune erosion at a fixed surge level.

Continuing the special case of instantaneous sea level rise and constant incoming wave energy, equation (74) can be integrated, if  $K$ ,  $\eta$ , and  $\alpha$  are not functions of time. This integration gives

$$V_e(t) = \frac{K\eta}{\alpha} (1 - e^{-\alpha t}) \frac{dE_b}{dt} , \quad (75)$$

which has the general form as illustrated in Figure 37b. As shown, the erosion is initially very rapid, and then it slows down as equilibrium is approached. Finally, the cumulative erosion curve approaches the equilibrium erosion value asymptotically, as would be expected.

While the form of equation (75) is intuitively correct for the case of an instantaneous surge increase with constant incoming wave energy, the equation cannot be used to describe an actual event where wave energy varies with time.

#### Empirical Coefficients

The factor,  $K$ , will be a function of sediment characteristics alone, i.e.,

$$K = K(d_e, \gamma_s, C_d, \dots) ,$$

where

$d_e$  = effective grain diameter,

$\gamma_s$  = sediment specific weight, and

$C_d$  = grain drag coefficient.

The proportion of breaking wave energy to initially reach the dune toe,  $\eta$ , has a value between zero and one, and it is probably a function of surge level, wave period, wave height, and beach-dune configuration, i.e.,

$$\eta = \eta(S, T, H_b, \text{profile}) .$$

Likewise, it should perhaps be expected that

$$\alpha = \alpha(S, T, H_b, \text{profile}) .$$

### Complete Equation

In an actual storm, the surge level, wave height, and wave period are all functions of time, which make  $\eta$ ,  $\alpha$ , and  $dE_b/dt$  functions of time. Thus, the differential equation (74) becomes

$$\frac{dV_e(t)}{dt} = K\eta(t)e^{-\alpha(t) \cdot t} \frac{dE_b(t)}{dt}, \quad (76)$$

which will be most difficult to integrate until more is known about the storm parameter time-variations, and how they effect  $\eta(t)$  and  $\alpha(t)$ .

If the erosion process could be considered as passing through discrete steps of equilibrium as the surge level rises, it might be possible to find functions for  $\eta$  and  $\alpha$  in order to complete a numerical integration of equation (76). However, comparisons of the experimental test results strongly indicate that this is not the case. So, for the present, it will not be possible to predict the transient erosion taking place while the surge level rise is on the increase.

### Discussion

The development just completed cannot be put into use at this time due to the difficulties in determining the empirical coefficients. The only portion of the present experiments where portions of the analysis might hold would be from the time of peak surge until the time of near-equilibrium. In this case, the arguments used in arriving at the integrated equation (75) apply to the process. Given enough data, it would be possible to perform a curve-fit in order to determine  $\eta$  and  $\alpha$ . However, most of the experiments provided only 3 data points,



which make curve-fitting somewhat unreliable. Attempting to record more data would not really help the cause since the erosion occurs in "chunks" as large sections of the dune break away and collapse into the water. Thus, the actual process is not strictly continuous. Another factor to be considered is the continuous starting and stopping of the wave paddle in order to make measurements. This must certainly have an adverse effect, if done too often.

Physically, the preceding development seems to fit in with the results given in Chapter VIII. In that case, it was seen that the surf zone length was determined by the incoming wave power. For the equilibrium case, this power was dissipated over the length of the surf zone. The concept of "excess energy" implies that the surf zone is not of sufficient length necessary to dissipate all of the incoming wave power. Thus, during the transient erosion, it would be expected that the distance between the bar crest and the dune toe would be less than the final, equilibrium distance. This trend can be observed for all the time-dependent experimental profiles shown in Appendix C.

Thus, the theoretical development presented has physical roots, and it might possibly lend itself to further development in the future. At present, though, it must be regarded as an heuristic model at best.

Fortunately, the present experimental results do allow a simplified development which can provide an engineering estimate of the effect of peak surge duration. This analysis is presented in the following sections.

### Experimental Results

As previously mentioned, the beach profiles were recorded for each experiment when peak surge was reached, and then at 15 minute intervals, maintaining a constant peak surge level. All runs were continued at peak surge until a near-equilibrium appeared to be established. This typically took about 30 minutes, which represents 5.2 hours in the prototype. Very few storms will have a peak surge duration of this length, but those that do will probably reach a storm equilibrium.

The profiles obtained for each experimental run are given in Appendix C. A quick inspection of these profiles gives a good indication of the large amount of erosion which did occur by the time the peak surge level was reached. A simple computer program was used to calculate the volume of sediment eroded per inch of beach width. These results are presented in Table 7.

### Preliminary Data Analysis

Assuming that the erosion obtained from the final profile for each experiment (involving time-dependent surges) represents the equilibrium erosion, the erosion values given at peak surge, and at peak surge plus 15 minutes, can be expressed as a percentage of the equilibrium erosion. For the 33 runs used in this analysis, it was found that, at the time of peak surge, the percentage of total erosion which had occurred ranged between 60 percent and 91 percent with the overall average being 79 percent. Similarly, the percentages, 15 minutes after peak surge had been reached, ranged between 80 percent and 98 percent, with an overall average of 90 percent. Table 8 presents a further breakdown of percentage values when averaged by wave period. As can be seen,

TABLE 7  
EROSION VOLUMES

Run #	T <sub>m</sub> (sec.)	S <sub>m</sub> (in.)	H <sub>m</sub> (in.)	Elapsed Time (min.)	Total Erosion (in <sup>3</sup> /in)	Run #	T <sub>m</sub> (sec.)	S <sub>m</sub> (in.)	H <sub>m</sub> (in.)	Elapsed Time (min.)	Total Erosion (in <sup>3</sup> /in)
1	0.970	3.84	2.88	5 20 40	35.56 46.37 47.14	10	0.970	5.28	3.84	53 68 83 89.02	78.38 82.65 87.01 89.02
2	0.970	3.84	2.88	45 60 75	45.17 50.97 56.25	11	0.970	5.28	4.80	55 70 85	72.63 86.28 97.16
3	0.970	3.84	2.88	85 100	35.90 50.99	12	0.970	6.72	2.88	56 71 86	72.86 80.52 89.40
4	0.970	3.84	2.88	25 40 55	37.77 46.54 49.79	13	0.970	6.72	3.84	60 75 90	94.37 107.12 117.28
5	0.970	3.84	4.80	71 86 101	41.85 53.56 63.35	14	0.970	6.72	4.80	57 72 83	96.39 113.97 117.74
6	0.970	3.84	4.80	25 40 55	28.25 49.69 57.89	15	1.163	3.84	2.88	49 64 79	49.18 55.59 70.94
7	0.970	3.84	4.80	49 65 80	39.65 55.31 59.22	16	1.163	3.84	3.84	47 62 77	50.71 74.63 85.08
8	0.970	3.84	3.84	51 66 81 96	44.38 56.57 69.39 70.23	17	1.163	3.84	4.80	50 65 80 95	60.43 69.16 82.58 87.17
9	0.970	5.28	2.88	53 68 83 98	61.84 71.01 76.27 76.84	18	1.163	5.28	2.88	57 72 87	77.23 84.45 89.76

TABLE 7

CONTINUED

Run #	T <sub>m</sub> (sec.)	S <sub>m</sub> (in.)	H <sub>m</sub> (in.)	Elapsed Time (min.)	Total Ergston (in <sup>3</sup> /in)	Run #	T <sub>m</sub> (sec.)	S <sub>m</sub> (in.)	H <sub>m</sub> (in.)	Elapsed Time (min.)	Total Ergston (in <sup>3</sup> /in)
19	1.163	5.28	3.84	56 71	86.41 106.77	28	1.357	6.72	2.88	55 70	95.29 101.80
20	1.163	5.28	4.80	86 55	116.85 79.63	29	1.357	6.72	3.84	85 58	106.49 115.38
21	1.163	6.72	2.88	70 85	104.69 121.11	30	1.163	3.84	2.88	73 88	123.54 126.53
22	1.163	6.72	3.84	60 75 90	95.29 102.51 106.05	31	1.163	3.84	3.84	48 63 78	51.32 64.56 76.80
23	1.163	6.72	4.80	58 73 88	112.94 124.62 130.11	32	1.163	5.28	2.88	48 63 78	58.36 79.08 86.37
24	1.357	3.84	2.88	56 71 86	108.56 132.22 142.00	33	1.163	5.28	3.84	56 71 86	91.62 94.05 105.74
25	1.357	3.84	3.84	50 65 80	65.59 67.80 77.37	34	1.163	6.72	2.88	55 70 85	92.07 111.63 123.85
26	1.357	5.28	2.88	47 62 77	70.93 84.75 87.00	35	1.163	6.72	3.84	55 70 85	84.22 94.43 104.79
27	1.357	5.28	3.84	53 68 83 96	66.75 77.49 84.85 88.14	36	1.163	5.28	3.84	58 73 88 103	120.41 125.97 143.72 153.72
				52 67 82	89.60 100.90 109.91					15 30 45	77.00 87.28 92.42

TABLE 7

CONTINUED

Run #	T <sub>m</sub> (sec.)	S <sub>m</sub> (in.)	H <sub>m</sub> (in.)	Elapsed Time (min.)	Total Erosion (in <sup>3</sup> /in)	Run #	T <sub>m</sub> (sec.)	S <sub>m</sub> (in.)	H <sub>m</sub> (in.)	Elapsed Time (min.)	Total Erosion (in <sup>3</sup> /in)
37	1.163	6.72	3.84	15	100.97	40	1.163	6.72	2.88	59	103.47
				30	107.58					74	113.17
				45	113.33					89	121.93
38	1.163	5.28	2.88	59	91.62	41	1.163	6.72	3.84	72	132.02
				74	101.91					87	146.60
39	1.163	5.28	3.84	89	111.68					102	156.25
				55	104.17						
				70	111.16						
				85	118.50						

there appears to be no distinguishable trend, and the values vary by only 7 percent at the most.

TABLE 8  
FRACTION OF EQUILIBRIUM EROSION FOR WAVE PERIODS

Period (sec)	Average at Peak Surge	Average at Peak Surge + 15 minutes
0.970	0.788	0.904
1.163	0.774	0.895
1.357	0.840	0.930

When the erosion percentages were averaged according to surge level, however, a definite trend was observed, as can be seen in Table 9.

TABLE 9  
FRACTION OF EQUILIBRIUM EROSION FOR SURGE LEVELS

Surge Level (inch)	Average at Peak Surge	Average at Peak Surge + 15 minutes
3.84	0.714	0.863
5.28	0.798	0.908
6.72	0.838	0.930

At peak surge, there was a 12 percent variation, with a 7 percent variation given for the values obtained 15 minutes later.

This trend indicates that a higher surge level promotes a larger percentage of erosion during the surge level rise.

Fortunately, it may be possible to neglect this dependency, for the present analysis, because the variations given in Table 9 are within 7.5 percent of the average at worst, and this amount of error can certainly be tolerated in a time-dependent erosion solution.

### Engineering Guidelines

Using the overall averages calculated for the percentage of equilibrium erosion obtained at peak surge and 15 minutes after peak surge had been reached, it was possible to obtain a nearly linear relationship as shown in Figure 38.

This linear approximation is given as

$$\frac{V(t)}{V_e} = 0.794 + 0.007 t_m \quad (77)$$

for the model, where  $t_m$  has units of minutes. The corresponding prototype equation becomes

$$\frac{V(t)}{V_e} = 0.794 + 0.041 t_p, \quad (78)$$

where  $t_p$  is the prototype peak surge duration expressed in hours. In both of the above equations,  $V(t)$  is the transient erosion volume per unit width of beach, while  $V_e$  is the equilibrium erosion volume per unit width obtained using the method presented in Chapter VIII.

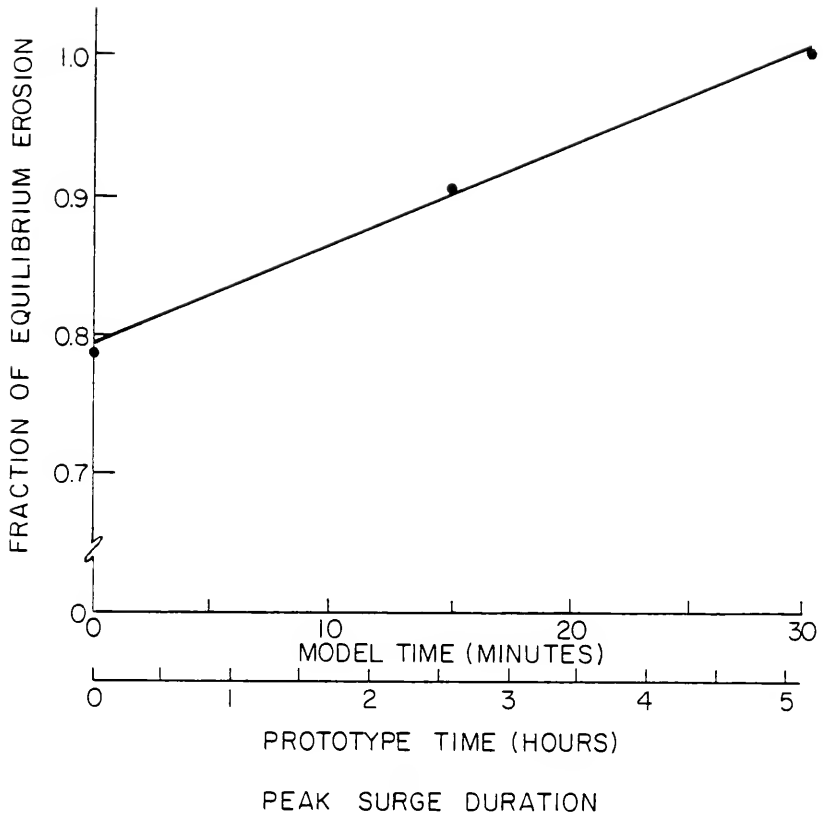


FIGURE 38: TIME-DEPENDENT EROSION FROM PEAK SURGE TO EQUILIBRIUM.



### Discussion

The experimental results have yielded a simple means of adjusting the dune erosion with respect to peak surge duration. While there exists some variation in the percentages of erosion given at peak surge, these variations are within 10 percent. When considering the range of parameters tested in the model series, these results are quite satisfying. The important point to notice is that a large percentage of erosion had occurred by the time the storm reached peak surge. Thus, the difference in erosion between a fast-moving and a slow-moving storm is only about 15 percent of the total equilibrium erosion.

From this observation, it can be concluded that peak surge duration plays an important role only when the dune heights are at a relatively low elevation. In this case, a greater dune recession must take place in order to erode the volume of sediment necessary to achieve an equilibrium. This is readily seen in the Appendix C profiles when the surge level is high or the dune elevation is low.

This whole analysis is based on the assumption that the morphological time scaling is the same as the hydraulic time scaling. Arguments supporting this assumption appear in Chapter IV, and the verification results of Chapter V seem to support this claim. This aspect, however, urgently needs to be further verified, and as such, becomes a top priority for further research.

For the present, it is felt that the linear partitioning of surge duration-dependent erosion, given by equation (78), represents a workable method of estimating dune erosion during severe storms.

### Application

For a given storm for which the peak surge duration is known (along with the storm parameters needed to apply the results of Chapter VIII), the erosion estimation is carried out in the following manner:

- 1) Calculate the equilibrium barred storm profile using the procedure outlined in Chapter VIII.
- 2) Transpose this profile, relative to peak surge, along the prestorm profile until a balance is obtained between erosion and deposition. This configuration represents the maximum dune erosion expected to take place.
- 3) Calculate the equilibrium erosion volume,  $V_e$ .
- 4) For the given peak surge duration (less than 5 hours), calculate the transient erosion volume,  $V(t)$ , using equation (78).
- 5) Find the difference between  $V_e$  and  $V(t)$ , and reduce the dune recession distance until this difference in erosion volume has been "replaced." This will depend upon the prestorm dune elevation.

A first estimate can be found by assuming the transient beachface profile is the same as the near-equilibrium profile. While not correct, the Appendix C profiles indicate that this assumption is fairly reasonable.

The method only gives an estimation of the transient dune recession. The rest of the calculated profile represents equilibrium conditions.

For high elevation dunes, the method should provide fairly accurate results. As the dune elevation decreases, this accuracy will fall off somewhat.

## CHAPTER X

### SUMMARY AND CONCLUSIONS

The ability to accurately predict the amount of dune recession during extreme storm events, such as hurricanes, is one of the most important problem solutions required by coastal planners. This ability would assist coastal engineers in providing safe recommendations for the increasing coastal construction being experienced on many portions of the coastline. This research has been directed toward the establishment of a reliable engineering method for the prediction of beach-dune erosion under any specified storm condition.

#### Model Law

Movable-bed small-scale modeling of coastal erosion has been historically a very inexact science. The modeling relationships developed in Chapter IV were derived through the consideration of the inertial forces, represented by the turbulent shear stress, and the gravity force in the nearly horizontal direction of the principal flow. This resulted in a dynamic scaling relationship for a distorted model. The profile similarity criterion was based on the preservation of the dimensionless fall velocity parameter, which has been shown to be an important factor. Combining of these two criteria resulted in a model law which is similar to previous results, differing primarily in the hydrological time scaling. By proper selection of model grain size,

it is possible to have an undistorted model, but this will rarely be possible.

It is concluded that the modeling relationships presented represent a plausible means of scaling beach-dune erosion in the small-scale physical model. The results of the model verification further add to the strength of this conclusion.

#### Model Verification

The verification of the derived modeling relationships was performed in the wave flume by the close approximation of an actual prototype event. By careful examination of the limited data available, it was possible to reasonably estimate the prototype storm parameters. Reproduction of these parameters in the wave tank gave an almost exact reproduction of the actual erosion experienced in the prototype. Further credibility can be given to the verification by the fact that the procedure involved a time-dependent storm surge hydrograph and an increasing wave height as the storm progressed. To the author's knowledge, this was the first time that these features had been incorporated into an erosion model verification.

Attempts to verify the model using a randomly produced irregular wave train, fitting the spectral requirements, proved unsuccessful. Arguments against the use of irregular waves have been given, but later developments may make their use feasible.

It is concluded that the model verification has been successful in, at least, one instance for which prototype data were available. The reproduction of the storm event, to a degree of realism never before attempted, certainly adds weight to this conclusion.

### Experimental Test Series

The experimental test series was designed around a typical Florida beach profile with sand grain-size in the vicinity of 0.26 mm. The series looked at the effects in varying the wave period, wave height, peak surge elevation, dune height, and surge level rise duration. The parameters were chosen to represent the upper and lower values for a severe storm. The variable-surge experiments began with an equilibrium profile and then elevated the surge level over a typical time span expected to occur. Upon reaching the peak surge level, the test was continued until near-equilibrium conditions prevailed.

These time-dependent surge rise experiments represent the first of this type, and the results indicated that the finite surge rise is necessary to more accurately depict the dune erosion phenomenon.

The testing procedure was carefully monitored and controlled, and the conclusion is made that the results represent the most valid dune erosion experiments to date.

### Qualitative Profile Analysis

Qualitative comparisons between the resulting near-equilibrium profiles resulted in several conclusions: It is necessary to employ a time-dependent surge level increase, there appears to exist an equilibrium barred profile which is characteristic of the storm parameters, erosion can be found by shifting the barred profile to obtain a sediment balance, the storm surge level is the most important factor in dune erosion, and the profile between the dune toe and the offshore bar is independent of surge level and prestorm profile configuration. In

addition, some aspects of the dune erosion process were discussed in general terms.

### Equilibrium Barred Storm Profile

In Chapter VIII it was shown that several features of the equilibrium barred storm profile could be expressed in terms of the dimensionless fall velocity parameter, thus adding further strength to the modeling profile similarity criterion.

Relationships were established for the bar crest and bar trough distances from the dune toe in a nondimensional form, which is preserved by the model law. It was seen that these relationships could be physically explained in terms of incoming wave energy flux, per unit width, entering the surf zone.

The nearshore profile was found to fit a power curve representation with a coefficient based solely on grain-size fall velocity. It was seen earlier that this form also was characteristic of the model law.

A simple nondimensional parameter was developed and correlated for the vertical runup distance. Having nearly the same form as the dimensionless fall velocity parameter, the runup parameter is also preserved by the model law.

An analysis into the offshore portion of the barred profile yielded results applicable to the average Florida beach, but further research needs to be conducted before applying the method elsewhere.

Finally, a method was given for use in calculating the equilibrium barred profile, using the given storm parameters. With this calculated

profile, it becomes possible to determine the maximum equilibrium erosion expected to occur for any specified storm on any given beach profile.

It is concluded that the method provides results superior to the previous, simplified methods. This was the first analysis to include the offshore bar feature.

### Transient Dune Erosion

An examination of the experimental profiles revealed that between 70 and 90 percent of the final equilibrium erosion had taken place by the time the peak surge level had been reached.

A theoretical development, based on energy concepts, was presented, but it was found that it could not be applied in this instance. However, a simple engineering approximation was given for the linear partitioning of the erosion which occurs during peak surge duration. Using this method, it becomes possible to predict the dune recession as a function of peak surge duration, making it possible to allow for situations where equilibrium could not be reached over the time span of the storm event.

### Application and Assumptions

The proposed method for the prediction of dune erosion is limited in its application by the following assumptions:

- 1) Natural beaches with sand grain-size distributions having a mean diameter of around 0.25 mm. While the relationships

contain provision for different grain-sizes, they have not been fully proven, as yet.

- 2) Straight beaches with fairly uniform offshore depth contours.
- 3) No interactions with tidal inlets or coastal structures.
- 4) Onshore-offshore sediment transport with no alongshore currents.
- 5) No dune overtopping.

In addition, the offshore prestorm profile must be similar to that modeled in the experimental test series. While small variations in this profile would probably have little effect, major differences would certainly effect the predictive ability of the method. Fortunately, many undeveloped Florida beaches fall into the above stipulations; thus, the method may be used to aid in the analyses of the Coastal Construction Setback Line.

### Summary

It is felt that this method represents an advance in the parameterization of the dune erosion process, and it provides an improved means of determining dune erosion resulting from severe storms. In addition, several surf zone characteristics can now be described by physically plausible relationships.

The research has also provided a new small-scaling movable-bed modeling law which has been verified under realistic conditions. It is hoped that further research will add greater confidence to the modeling relationships, and thus, pave the way for routine physical modeling of coastal processes.



### Recommendations for the Future

It is most imperative that work continue into the verification of the modeling relationships. This research should confirm the existence of profile similarity between models of different scale and different grain-sizes. It would also be beneficial to determine how small the model can be made.

Further verification of prototype events should be attempted whenever accurate prototype data become available. This would further enhance the reliability of the model law and give a more complete understanding of the scaling effects. When it becomes practical to use wave spectra in a movable-bed model, then they must be employed.

More testing should be done using different grain-sizes and different offshore profiles to confirm the empirically derived expressions used in the calculation of the equilibrium-barred storm profile, and to generalize the method for the application to any sandy shoreline.

After the above research has been conducted, and the method has been improved upon, it would be possible to examine the effects of waves overtopping the dune, man-made structures, tidal inlets, and three-dimensional processes involving alongshore currents.

APPENDIX A  
COMPUTER PROGRAM LISTINGS

```

C      PROFILE DATA TAKING PROGRAM
C
C      THIS PROGRAM WILL RECORD THE DUNE PROFILE WHEN THE PROBE IS
C      MANUALLY PLACED AT THE RIGHT ELEVATION AND THE BUTTON IS PUSHED.
C      THE CART MUST THEN BE MOVED TO THE NEXT POINT, AND THE PROCESS
C      REPEATED.
C
C      IT WILL ALSO RECORD THE UNDERWATER PROFILE AUTOMATICALLY.
C
C      THE CART SHOULD ALWAYS MOVE FROM THE MOST LANDWARD PORTION OF
C      THE DUNE TOWARD THE WAVE PADDLE OFFSHORE.
C
C      STEVE HUGHES  3-JUNE-1980
C
C      LOGICAL*1 IVAL,Y
C      DIMENSION IPOINT(2048)
C      INTEGER*2 CMONTH,CDATE,CYEAR,IEXP,IProf,HDRWD1
C      BYTE DIA(9)
C      BYTE FILENM(14)
C      DATA FILENM/'D','X','1',':','E','X','X','P','X','X',
C      1','.','P','R','O'/
C      DATA Y/"131/"
C
C      CHECK FOR DATE
C
C      CALL IDATE(CMONTH,CDATE,CYEAR)
C      IF(CMONTH.EQ.0) STOP 'ENTER SYSTEM DATE'
C
C      IDENTIFY PROGRAM TO USER
C
C      TYPE 1
C      1 FORMAT(' *****',/,
C      1' * PROFILE DATA TAKING PROGRAM *,/,
C      2' *****',//)
C
C      OUTPUT CURRENT SYSTEM DATE
C
C      CALL DATE(DIA)
C      TYPE 400,DIA
C      400      FORMAT(3X,9A1)
C
C      GATHER INFORMATION FROM OPERATOR
C
C      TYPE 2
C      2 FORMAT(3X,'ENTER CURRENT EXPERIMENT NUMBER:',$,)
C      ACCEPT 3,IEXP
C      3 FORMAT(I2)
C      TYPE 4
C      4 FORMAT(3X,'ENTER THE CONSEQUITIVE PROFILE NUMBER',/,
C      13X,'FOR THIS EXPERIMENT:',$,)
C      ACCEPT 3,IProf
C      IEXP1=IEXP/10

```

```

      IEXP2=IEXP-(10*IEXP1)
      IPROF1=IPROF/10
      IPROF2=IPROF-(10*IPROF1)
      FILENM(6)=IEXP1+48
      FILENM(7)=IEXP2+48
      FILENM(9)=IPROF1+48
      FILENM(10)=IPROF2+48
      TYPE 5
5  FORMAT(3X,'ENTER REAL VALUE (F6.2) OF ELAPSED',/
      13X,'TIME IN MINUTES SINCE START OF EXPERIMENT:',$,)
      ACCEPT 6,ELAPTM
6  FORMAT(F6.2)
C
C  OUTPUT FILE NAME
C
      TYPE 7,FILENM
7  FORMAT(3X,'FILE NAME IS: ',14A1)
      TYPE 700,IEXP,IPROF,ELAPTM
700  FORMAT(3X,'EXPERIMENT #:',I2,2X,'PROFILE #:',I2,2X,'ELAPSED TIME:'
      1,F6.2,1X,'MINUTES',/)
C
C  OPEN UNFORMATTED OUTPUT FILE
C
      CALL ASSIGN (1,FILENM,14,'NEW')
      DEFINE FILE 1 (1,2048,U,INEXT)
      HDRWD1=-1
C
C  DEFINE VERITICAL CALIBRATION CONSTANT
C
      CVERT=8.25
C
C  DETERMINE MEAN SEA LEVEL
C
      TYPE 10
10  FORMAT(3X,'PLACE PROBE AT MEAN SEA LEVEL POSITION')
      PAUSE 'TYPE <CR> WHEN READY.'
      JOE=0
      DO 45 I=1,5
45  JOE=JOE+IADC(14)
      IFIRST=INT(JOE/5.0)
C
C  DUNE OR OFFSHORE PROFILE?
C
      L=1
      TYPE 90
90  FORMAT(3X,'ARE YOU TAKING DUNE PROFILE? (Y OR N):',$,)
      ACCEPT 91,IVAL
91  FORMAT(A1)
      IF(IVAL.NE.Y)GO TO 805
C
C  DUNE PROFILE MEASUREMENTS
C
      TYPE 92

```

```

92 FORMAT(3X,'MOVE CART TO INITIAL DUNE POSITION AND INPUT INITIAL',/
1,3X,'HORIZONTAL CART POSITION (NEGATIVE INCHES F6.2):',$,)
ACCEPT 6, HORIZ
TYPE 93
93 FORMAT(3X,'PUSH BUTTON TO MANUALLY RECORD DUNE PROFILE',/,
13X,'TYPE <CR> ON COMPLETION')
70 IHI=0
CALL TAKE(IHI)
IF(IHI)72,73,74
72 JOE=0
DO 46 II=1,5
46 JOE=JOE+IADC(14)
IPOINT(L)=INT(JOE/5.0)
GO TO 70
73 L=L+1
IPOINT(L)=0
GO TO 70
74 CONTINUE
C
C OFFSHORE PROFILE?
C
TYPE 81
81 FORMAT(3X,'ARE YOU TAKING OFFSHORE PROFILE? (Y OR N):',$,)
ACCEPT 91,IVAL
IF(IVAL.NE.Y)J=L
IF(IVAL.NE.Y)GO TO 40
TYPE 82
82 FORMAT(3X,'MOVE CART TO INITIAL OFFSHORE POSITION, TYPE <CR> WHEN
1 IN POSITION')
ICHAR=0
86 IHI=0
CALL TAKE(IHI)
IF(IHI)83,84,85
83 GO TO 86
84 IPOINT(L)=0
L=L+1
GO TO 86
85 GO TO 802
C
C BRANCH FOR NO DUNE PROFILE
C
805 TYPE 801
801 FORMAT(3X,'MOVE CART TO INITIAL POSITION AND INPUT HORIZONTAL',/,
13X,'POSITION IN INCHES (F6.2):',$,)
ACCEPT 6,HORIZ
C
C RECORD UNDERWATER PROFILE
C
802 J=L
ICHAR=ITTNR()
TYPE 12
12 FORMAT(3X,'TURN ON PROFILER AND TYPE <CR> TO BEGIN PROFILE DATA',/
13X,'TAKING. WHEN COMPLETED, STOP CART AND TYPE <CR>.')

```

```

C      PAUSE 'TYPE <CR> TO START'
C
C      IHI=0
15 CALL TICK(IHI)
   IPOINT(J)=IADC(14)
   J=J+1
   IF(IHI.GT.0)GO TO 40
   GO TO 15
C
C      STORE HEADER WORDS AND PROFILE DATA ON DISK
C
40 K=J-1
   M=2048-11-K
C
C      CALCULATE HORIZONTAL CALIBRATION CONSTANT
C
   TYPE 560
560   FORMAT(3X,'INPUT FINAL HORIZONTAL POSITION (F6.2) IN INCHES:',$)
      ACCEPT 6,FINAL
      CHORIZ=(FINAL-HORIZ)/K
      WRITE(1,1)HDRWD1,ELAPTM,CHORIZ,CVERT,HORIZ,IFIRST,HDRWD1,
1(IPOINT(1),I=1,K),(HDRWD1,I=1,M)
      CALL CLOSE(1)
550   TYPE 300
300   FORMAT(3X,'OPTIONAL DATA DISPLAY! ',//,
13X,'TYPE [1] FOR NUMERICAL RESULTS',//,
23X,'TYPE [2] FOR GRAPHICAL DISPLAY',//,
33X,'TYPE <CR> TO EXIT PROGRAM')
      ACCEPT 301,IOP
301   FORMAT(11)
      IF(IOP.NE.1)GO TO 302
      CALL DATA(K,CHORIZ,CVERT,HORIZ,IFIRST,IPOINT)
      GO TO 550
302   IF(IOP.NE.2)GO TO 350
      CALL PLOT(K,CHORIZ,CVERT,HORIZ,IFIRST,IPOINT)
      GO TO 550
350   STOP
END
C
C
SUBROUTINE TICK(IHI)
10 IHI=IADC(15)
   ICHAR=ITTINR()
   IF(ICHAR.GT.0)GO TO 30
   IF(IHI.LT.2460)GO TO 10
20 IHI=IADC(15)
   ICHAR=ITTINR()
   IF(ICHAR.GT.0)GO TO 30
   IF(IHI.GT.2460)GO TO 20
   IHI=0
   RETURN
30 IHI=1
   RETURN

```

```

      END
C
C
      SUBROUTINE TAKE(IHI)
      IYES=0
10  IHI=IADC(15)
      IYES=IADC(13)
      ICHAR=ITTINR()
      IF(ICHAR.GT.0)GO TO 30
      IF(IYES.GT.2458)GO TO 40
      IF(IHI.LT.2460)GO TO 10
20  IHI=IADC(15)
      IYES=IADC(13)
      ICHAR=ITTINR()
      IF(ICHAR.GT.0)GO TO 30
      IF(IYES.GT.2458)GO TO 40
      IF(IHI.GT.2460)GO TO 20
      IHI=0
      RETURN
30  IHI=1
      RETURN
40  IYES=IADC(13)
      IF(IYES.LT.2458)GO TO 41
      GO TO 40
41  IHI=-1
      RETURN
      END
C
C
      SUBROUTINE DATA(J,CHORIZ,CVERT,HORIZ,IFIRST,IPOINT)
      DIMENSION IPOINT(2000)
C
C
      REQUEST DO-LOOP INCREMENT
C
      TYPE 5
5  FORMAT(3X,'ENTER VALUE OF [N] TO PRINT EVERY N-TH POINT (I2)')
      ACCEPT 6,N
6  FORMAT(I2)
      TYPE 7
7  FORMAT(3X,'DATA POINT',3X,'RANGE(INCHES)',3X,'ELEV.WRT.MSL (INCHES
1)')
      DO 10 I=1,J,N
      RANGE=HORIZ+(CHORIZ*(I-1))
      IF(IPOINT(I).EQ.0)GO TO 10
      VERT=(IFIRST-IPOINT(I))*CVERT/409.6
      TYPE 20,I,RANGE,VERT
20  FORMAT(8X,I3,9X,F7.2,11X,F6.2)
      GO TO 10
10  CONTINUE
      RETURN
      END
C

```

```

C      SUBROUTINE PLOT(J,CHORIZ,CVERT,HORIZ,IFIRST,IPOINT)
      LOGICAL*1 STARS(65)
      DIMENSION IPOINT(2000)
      DATA STARS/65*'*/
C
C      REQUEST DO-LOOP INCREMENT
C
      TYPE 1
1     FORMAT(3X,'ENTER VALUE OF [N] TO PRINT EVERY N-TH POINT (I2)')
      ACCEPT 2,N
2     FORMAT(I2)
C
C      TYPE OUT LABELS
C
      TYPE 3
3     FORMAT(2X,'RANGE ELEV. MSL',4X,'ABS. VALUE OF ELEV. (*=1/4 INCH)',
      1/,1X,' (INCH) (INCH) .',6X,'(N) DENOTES NO DATA TAKEN THIS RANGE')
      TYPE 4
4     FORMAT(1X,75(1H-))
C
C      PLOT DATA
C
      DO 10 I=1,J,N
      RANGE=HORIZ*(CHORIZ*(I-1))
      IF(IPOINT(I).EQ.0)GO TO 30
      VERT=(IFIRST-IPOINT(I))*CVERT/409.6
      IFT=INT((ABS(VERT)*4.0)+0.5)
      TYPE 20,RANGE,VERT,(STARS(M),M=1,IFT)
20    FORMAT(1X,F6.2,1X,F6.2,1X,65A1)
      GO TO 10
30    TYPE 35,RANGE
35    FORMAT(1X,F6.2,3X,'--',3X,'N')
10    CONTINUE
      RETURN
      END

```



```
C THIS PROGRAM OPENS DATA FILES COLLECTED USING
C THE PROFILE PROGRAM AND ANALYSES THEM.
C
C STEVE HUGHES    NOV. 24, 1980
C
C   INTEGER*2 HDRWD1
C   DIMENSION IPOINT(2040),RANGE(100),VERT(100),E(100)
C   DIMENSION A(100),ATOT(100)
C   TYPE 1
1  FORMAT(3X,'ENTER DATA FILE NAME:',$,)
C   CALL ASSIGN (1,'XXXX.PRO',-8,'RDO','NC',1)
C   DEFINE FILE 1 (1,2048,U,INEXT)
C   INEXT=1
C
C READ IN DATA FILE
C
C   READ(1,INEXT)HDRWD1,ELAPTM,CHORIZ,CVERT,HORIZ,IFIRST,HDRWD1,
C   1(IPOINT(I),I=1,2037)
C
C CONVERT TO REAL VALUES
C
C   RIB=409.6
C   K=1
C   DO 3 I=1,2037
C   IF(IPOINT(I).EQ.-1)GO TO 5
C   IF(IPOINT(I).EQ.0)GO TO 3
C   RANGE(K)=HORIZ+((I-1)*CHORIZ)
C   VERT(K)=(IFIRST-IPOINT(I))*(CVERT/RIB)
C   K=K+1
3  CONTINUE
5  CONTINUE
C   L=K-1
C
C DETERMINE PRE-STORM DUNE HEIGHT
C
C   IF(VERT(1).LT.9.0)GO TO 28
C   IF(VERT(1).GT.20.0)GO TO 28
C   DUNHT=VERT(1)
6  FORMAT(F6.2)
C   GO TO 29
23  DUNHT=VERT(2)
C   VERT(1)=VERT(2)
29  CONTINUE
C
C CALCULATE PRE-STORM PROFILE ARRAY
C
C   E3=0.0
C   R3=0.0
C   E2=3.36
C   R2=-16.289
C   E1=DUNHT
C   R1=-(E1-E2)*0.969+R2
C   DO 7 I=1,L
```

```

      IF(RANGE(I).GT.R1)GO TO 10
      E(I)=E1
      GO TO 7
10  IF(RANGE(I).GT.R2)GO TO 11
      E(I)=-((RANGE(I)-R2)/0.969+E2
      GO TO 7
11  IF(RANGE(I).GT.R3)GO TO 12
      E(I)=-((RANGE(I)-R3)/4.847+E3
      GO TO 7
12  E(I)=-0.1903*(RANGE(I)**(2.0/3.0))
7   CONTINUE
C
C   INPUT VALUE OF HORIZONTAL REFERENCE
C
      TYPE 18
18  FORMAT(3X,'ENTER ELEVATION FOR NET EROSION (INCH.F6.2):',9)
      ACCEPT 6,ALEVEL
C
C   CALCULATE EROSION AREA
C
      K=L-1
      DO 13 I=1,K
      C=RANGE(I+1)-RANGE(I)
      IF(RANGE(I).LT.R1.AND.RANGE(I+1).GT.R1)GO TO 14
      IF(RANGE(I).LT.R2.AND.RANGE(I+1).GT.R2)GO TO 15
      IF(RANGE(I).GT.R3)GO TO 16
      ATOT(I)=(E(I)-VERT(I)+E(I+1)-VERT(I+1))*C/2.0
      IF(VERT(I+1).LT.ALEVEL)GO TO 17
      A(I)=ATOT(I)
      GO TO 13
17  A(I)=(E(I)+E(I+1)-2.0*ALEVEL)*C/2.0
      GO TO 13
14  CALL DISCON(VERT,RANGE,E,R1,E1,ALEVEL,TOT,RTOT,I)
      ATOT(I)=TOT
      A(I)=RTOT
      GO TO 13
15  CALL DISCON(VERT,RANGE,E,R2,E2,ALEVEL,TOT,RTOT,I)
      ATOT(I)=TOT
      A(I)=RTOT
      GO TO 13
16  T1=(2.0*(E(I)-VERT(I)-VERT(I+1)))*C/2.0
      T2=0.1142*(RANGE(I)**(5.0/3.0)-RANGE(I+1)**(5.0/3.0))
      T3=E(I)*C
      ATOT(I)=T1+T2-T3
      A(I)=0.0
13  CONTINUE
      ATOT(L)=0.0
      A(L)=0.0
      TOTPOS=0.0
      TOTNEG=0.0
      APOS=0.0
      DO 20 I=1,L
      IF(ATOT(I))21,21,22

```

```

21 TOTNEG=TOTNEG+ATOT(I)
   GO TO 23
22 TOTPOS=TOTPOS+ATOT(I)
23 IF(A(I).GT.0.0)APOS=APOS+A(I)
20 CONTINUE
C
C PRINT RESULTS
C
   TYPE 30
30 FORMAT(3X,'TYPE [1] TO SUPPRESS INTERMEDIATE VALUES:',$)
   ACCEPT 31,IWHAT
31 FORMAT(I1)
   IF(IWHAT.EQ.1)GO TO 35
   TYPE 32,ALEVEL
32 FORMAT(14X,'FINAL',4X,'INITIAL DISPLACED EROSION ABOVE'/4X,
1'RANGE',5X,'ELEV.',5X,'ELEV.',5X,'AREA',5X,F5.2,1X,'INCH. ELEV.'/
23X,'(INCH.) (INCH.) (INCH.) (SQ. IN.) (SQ. IN.)'/)
   DO 8 I=1,L
   TYPE 9,RANGE(I),VERT(I),E(I),ATOT(I),A(I)
9 FORMAT(3X,F7.2,3X,F7.2,3X,F7.2/32X,F8.2,3X,F8.2)
8 CONTINUE
35 TYPE 36,TOTPOS,TOTNEG,ALEVEL,APOS
36 FORMAT(3X,'TOTAL EROSION= ',F8.2,' SQ. IN. '/3X,
1'TOTAL DEPOSITION= ',F8.2,' SQ. IN. '/3X,
2'TOTAL EROSION ABOVE ELEV. ',F5.2,' = ',F8.2,' SQ. IN. ')
   CALL CLOSE(1)
   STOP
   END
C
C
C
SUBROUTINE DISCON(V,R,E,RR,EE,ALEVEL,TOT,RTOT,I)
DIMENSION V(100),R(100),E(100)
V1=(V(I)-V(I+1))*(R(I+1)-RR)/(R(I+1)-R(I))+V(I+1)
T1=(E(I)+EE-V(I)-V1)*(RR-R(I))/2.0
T2=(EE+E(I+1)-V1-V(I+1))*(R(I+1)-RR)/2.0
TOT=T1+T2
IF(V(I+1).LT.ALEVEL)GO TO 2
RTOT=TOT
GO TO 3
2 T1=(E(I)+EE-2.0*ALEVEL)*(RR-R(I))/2.0
T2=(EE+E(I+1)-2.0*ALEVEL)*(R(I+1)-RR)/2.0
RTOT=T1+T2
3 RETURN
END

```

APPENDIX B  
INSTRUMENT CALIBRATIONS

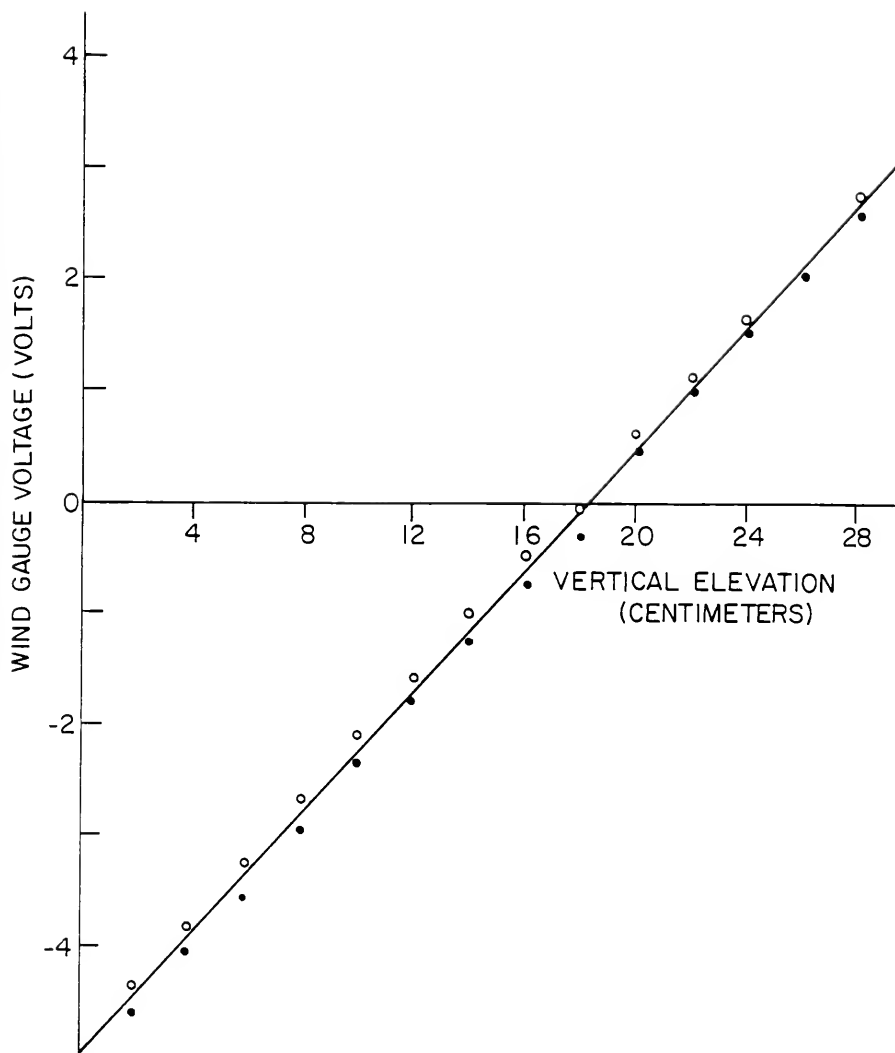


FIGURE 39: WAVE GAUGE CALIBRATION.

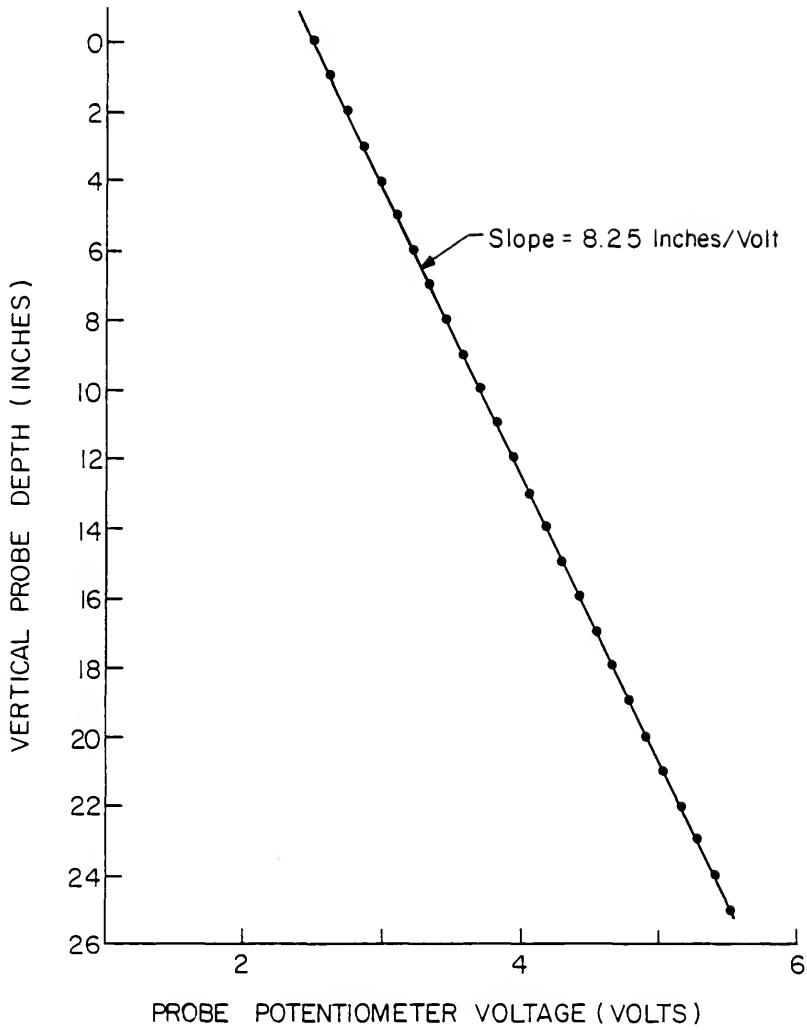


FIGURE 40: VERTICAL PROBE CALIBRATION.

## APPENDIX C

### TIME-DEPENDENT EXPERIMENTAL PROFILES

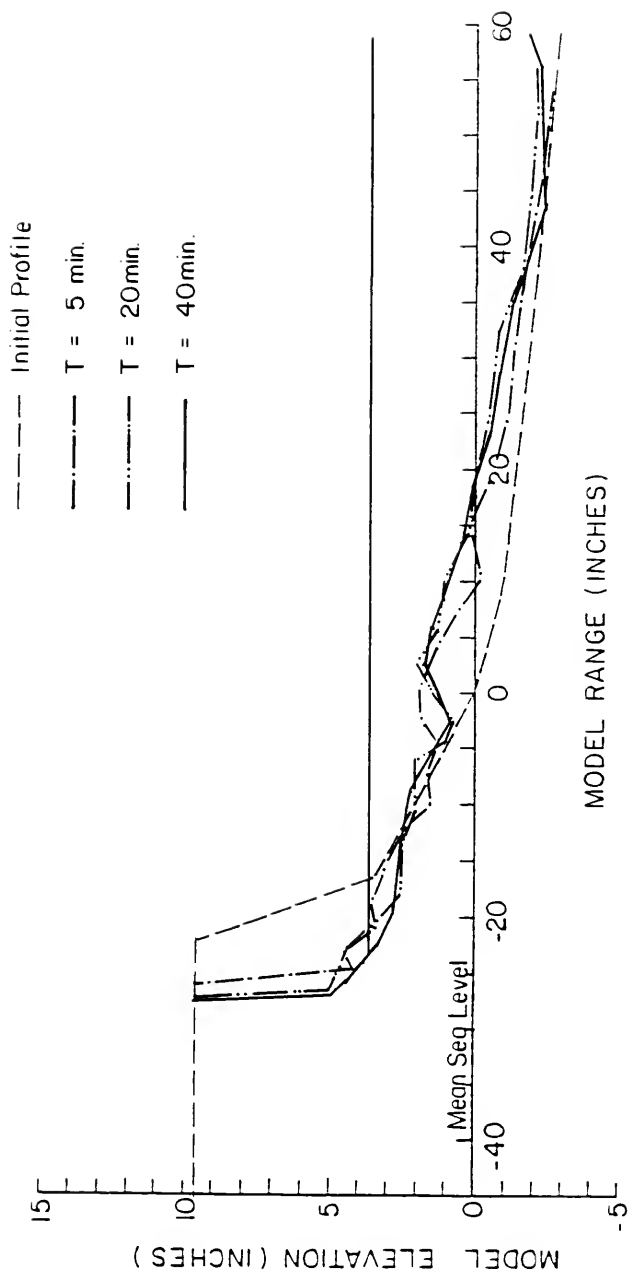


FIGURE 41: RUIN #1, FIXED SURGE LEVEL.



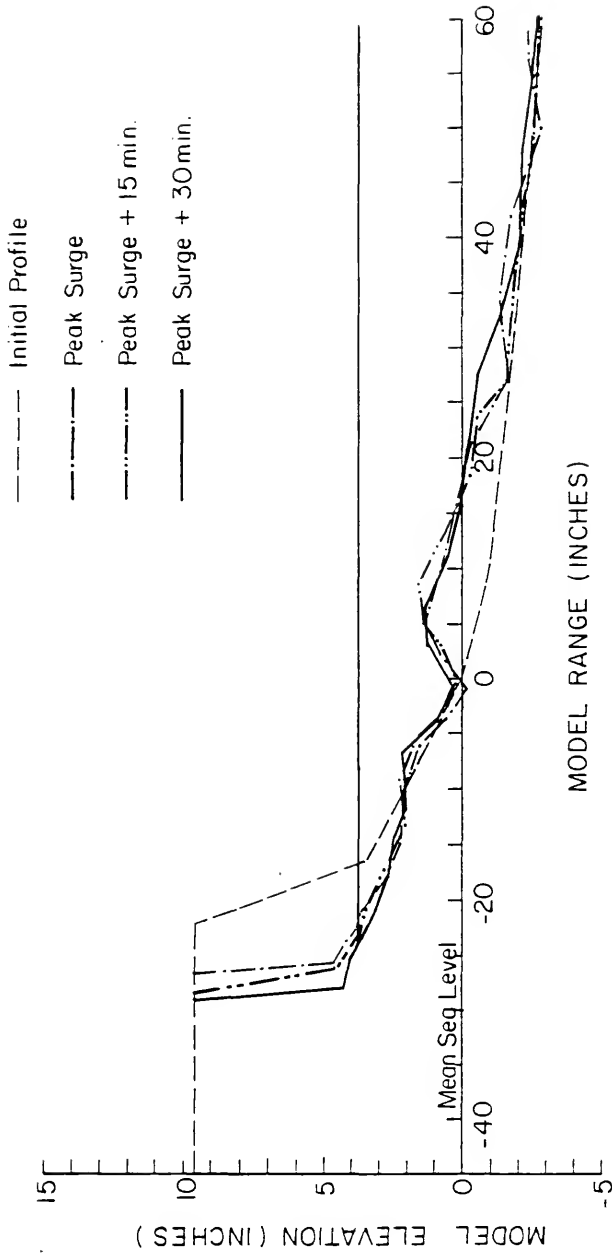


FIGURE 42: RUN #2.

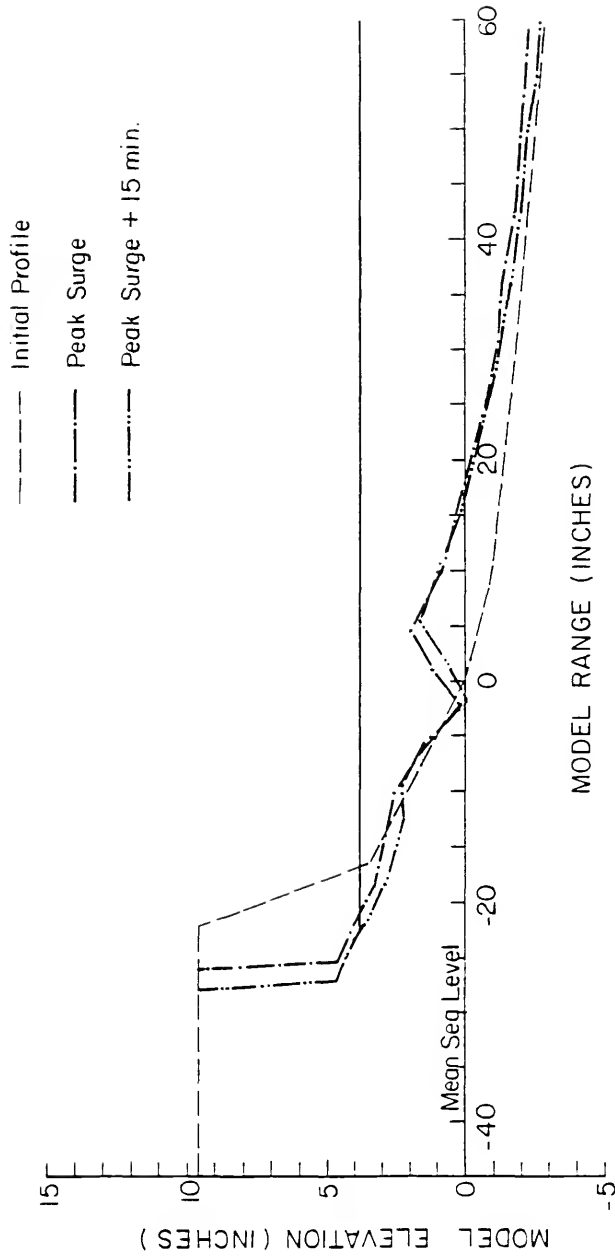


FIGURE 43: RUN #3.

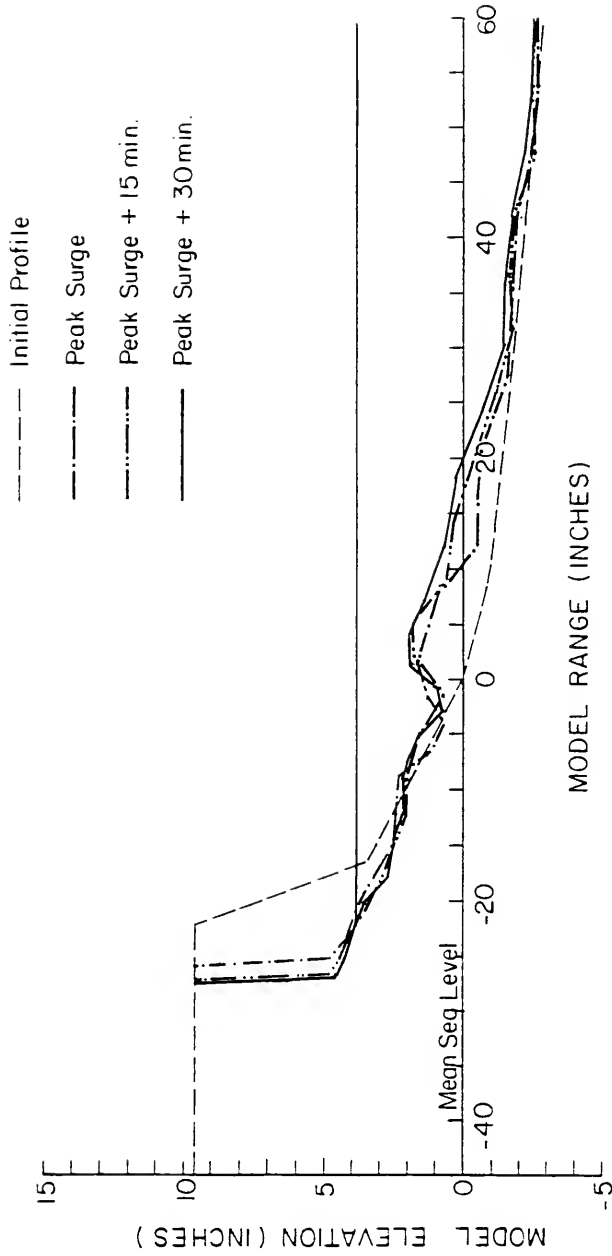


FIGURE 44: RUN #4.

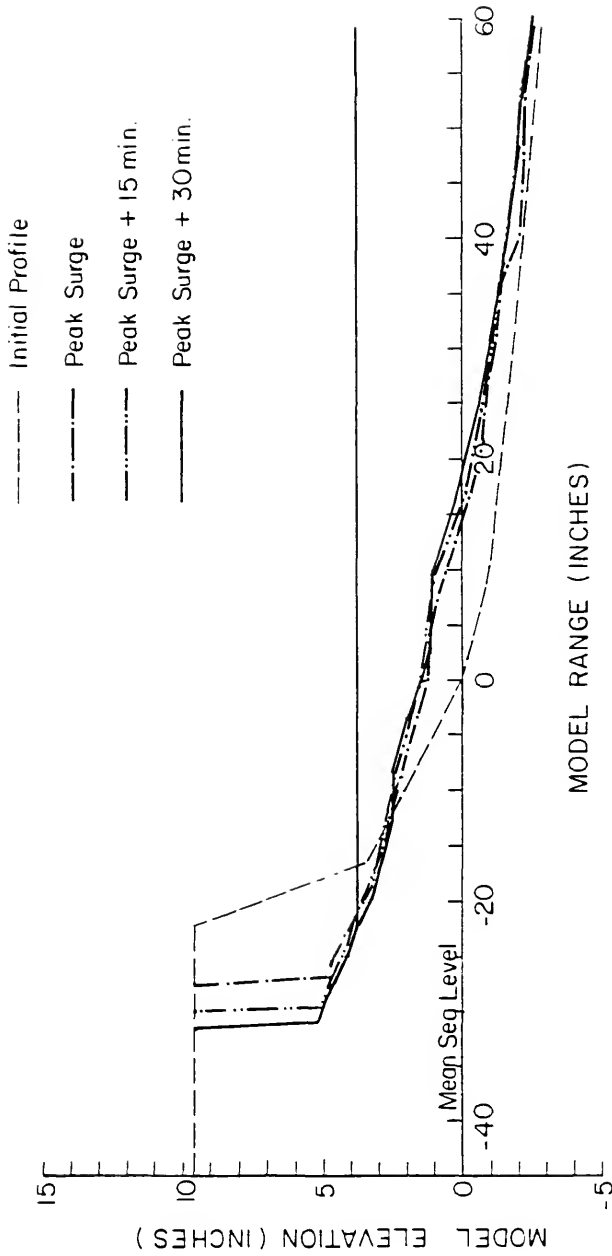


FIGURE 45: RUN #5.

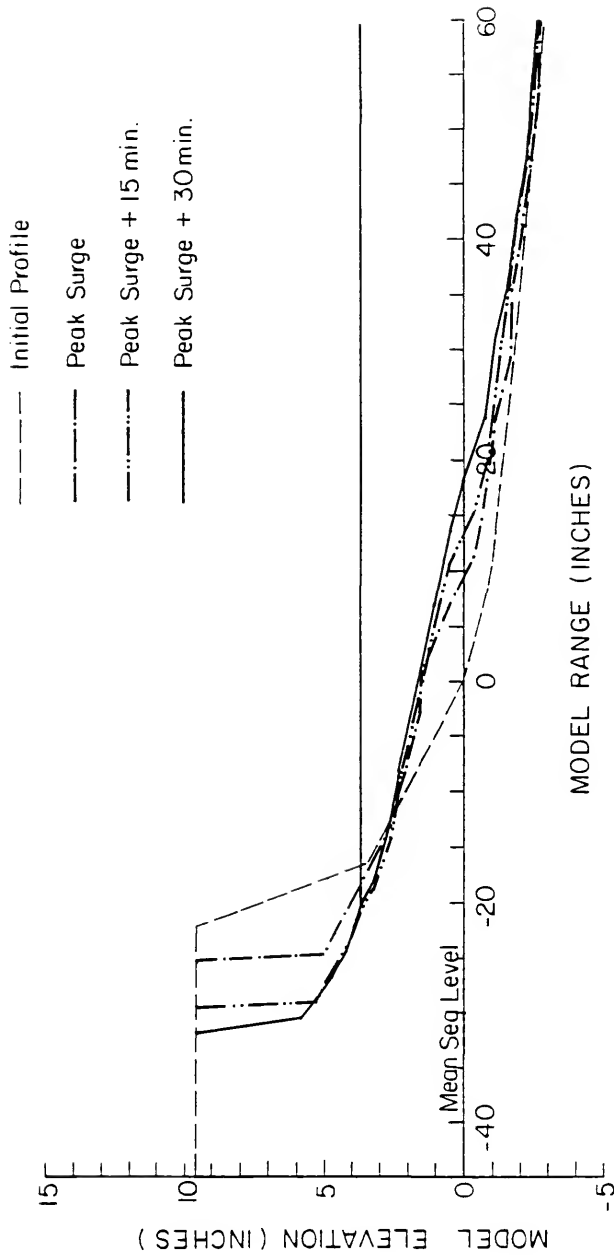


FIGURE 46: RUII #6.

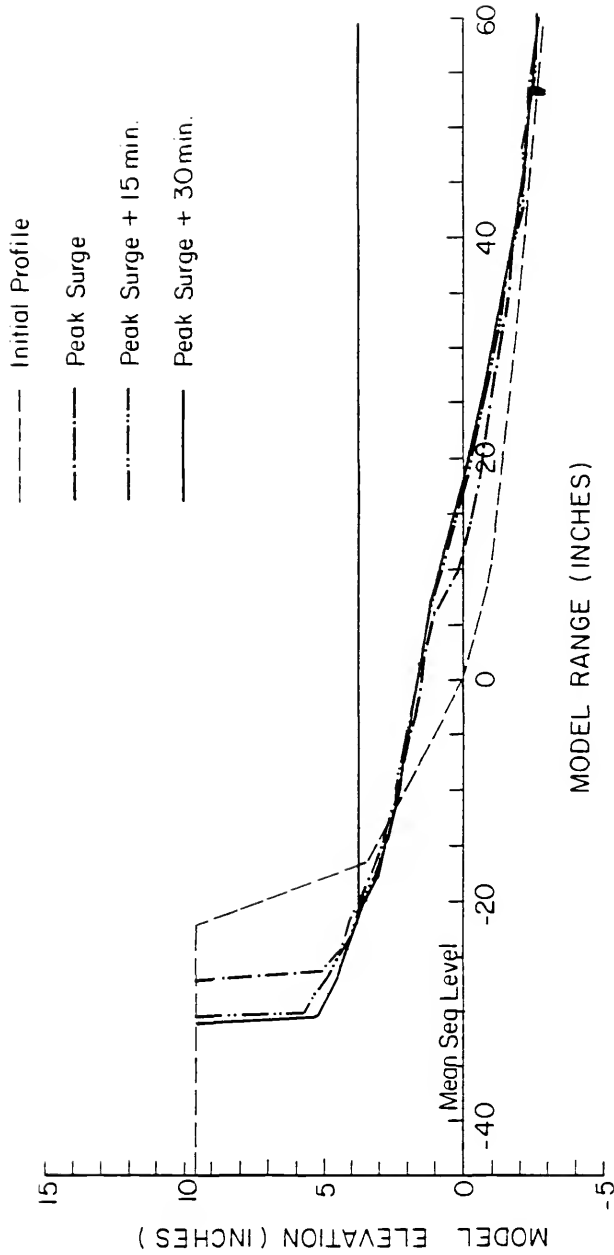


FIGURE 47: RUN #7.

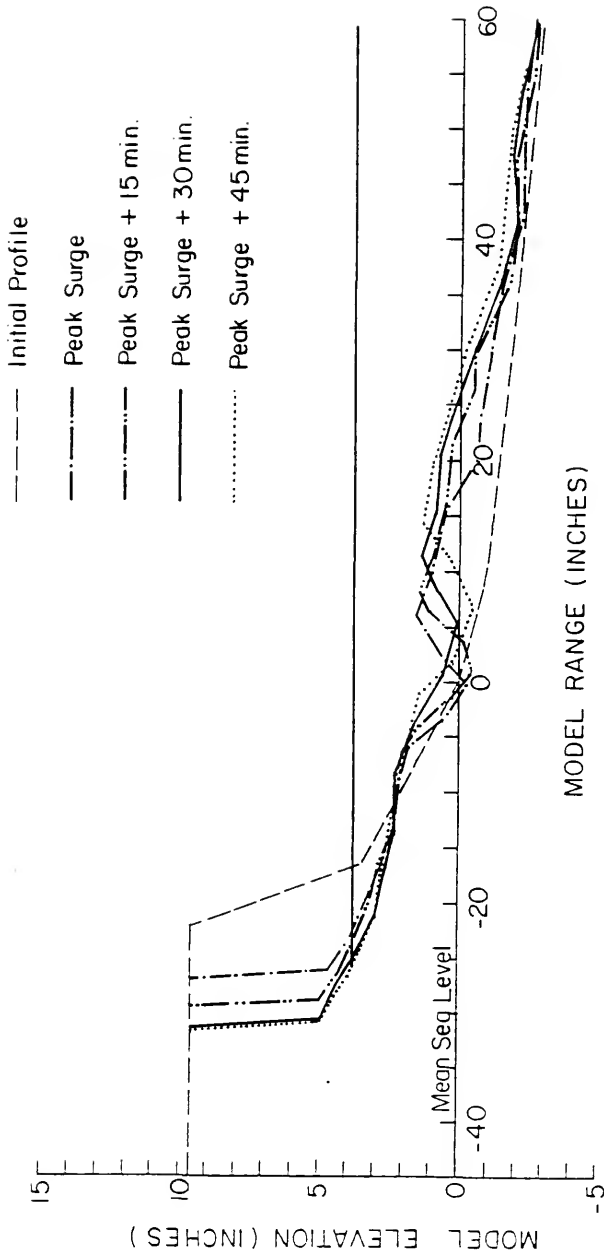


FIGURE 48: RUN #8.

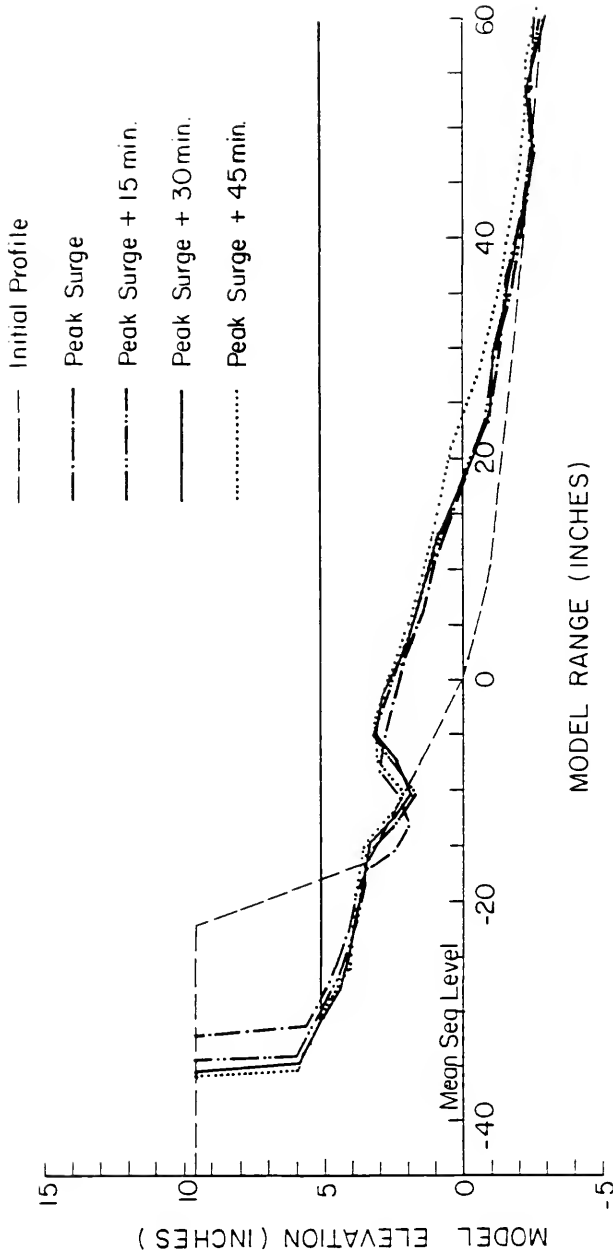


FIGURE 49: RUN #9.



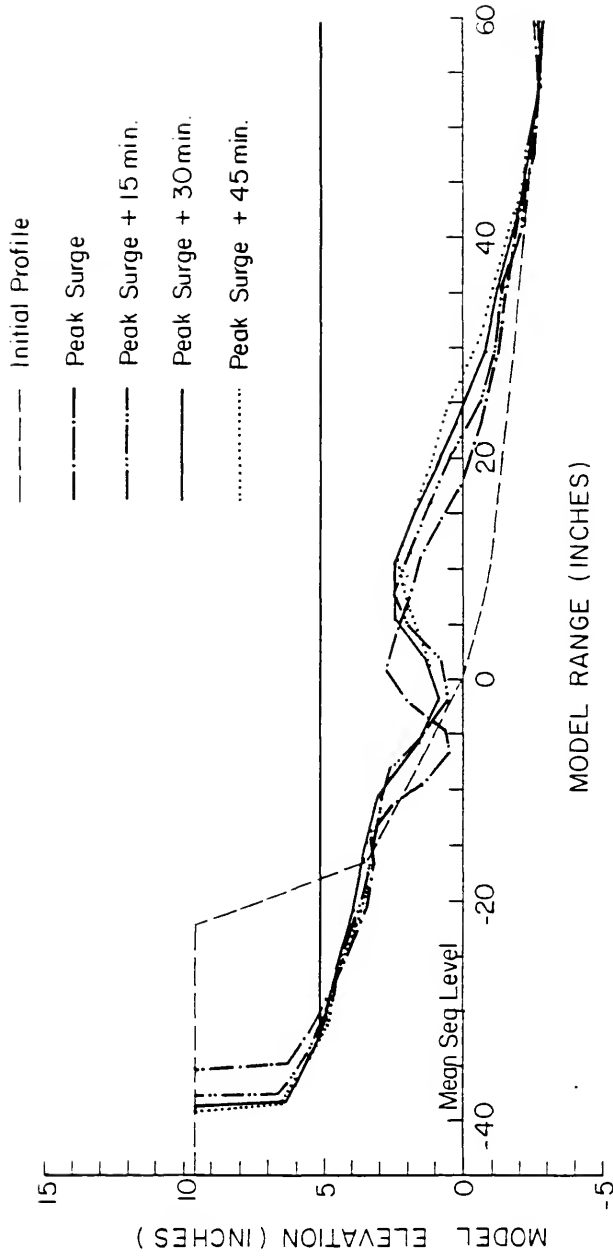


FIGURE 50: RUT #10.

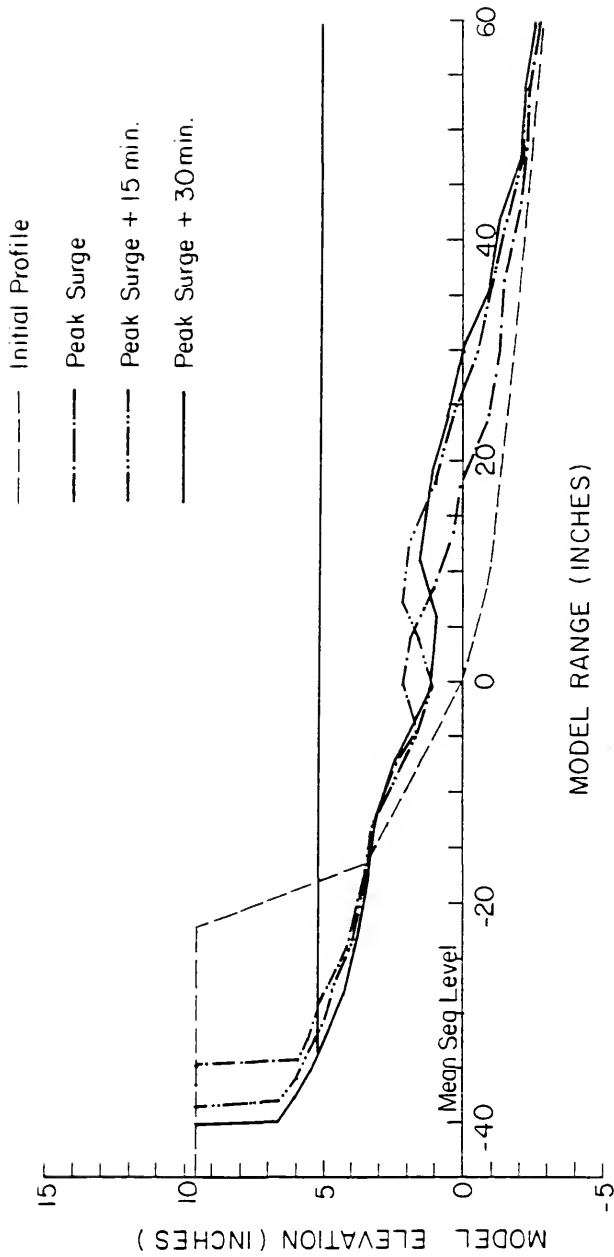


FIGURE 51: RUN #11.

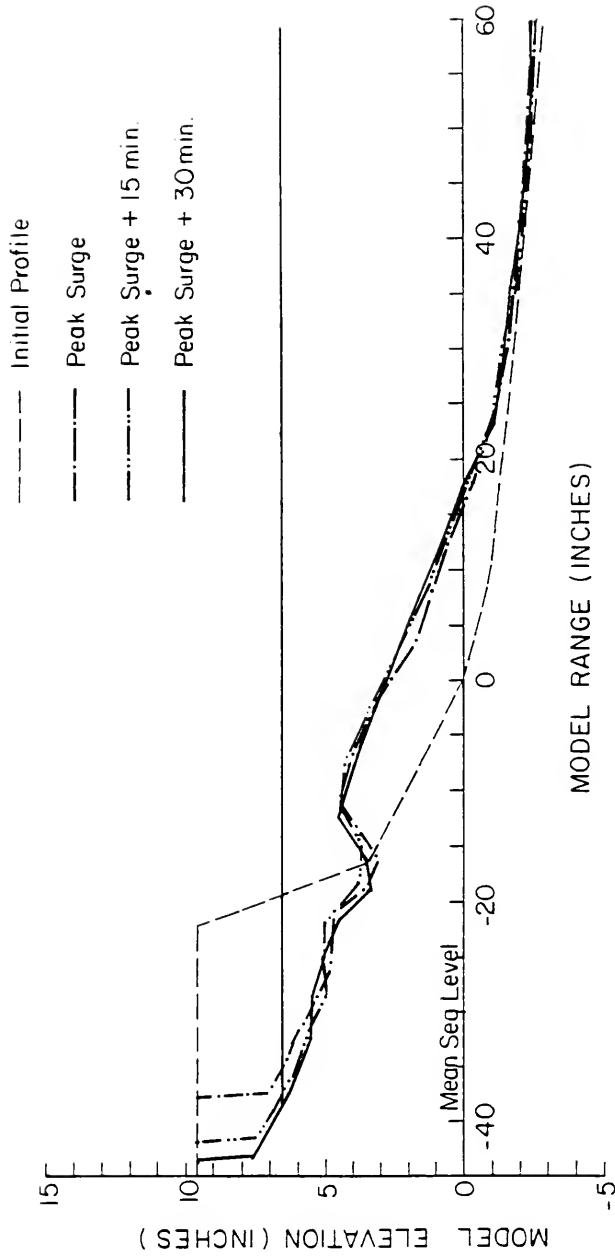


FIGURE 52: RUN #12.

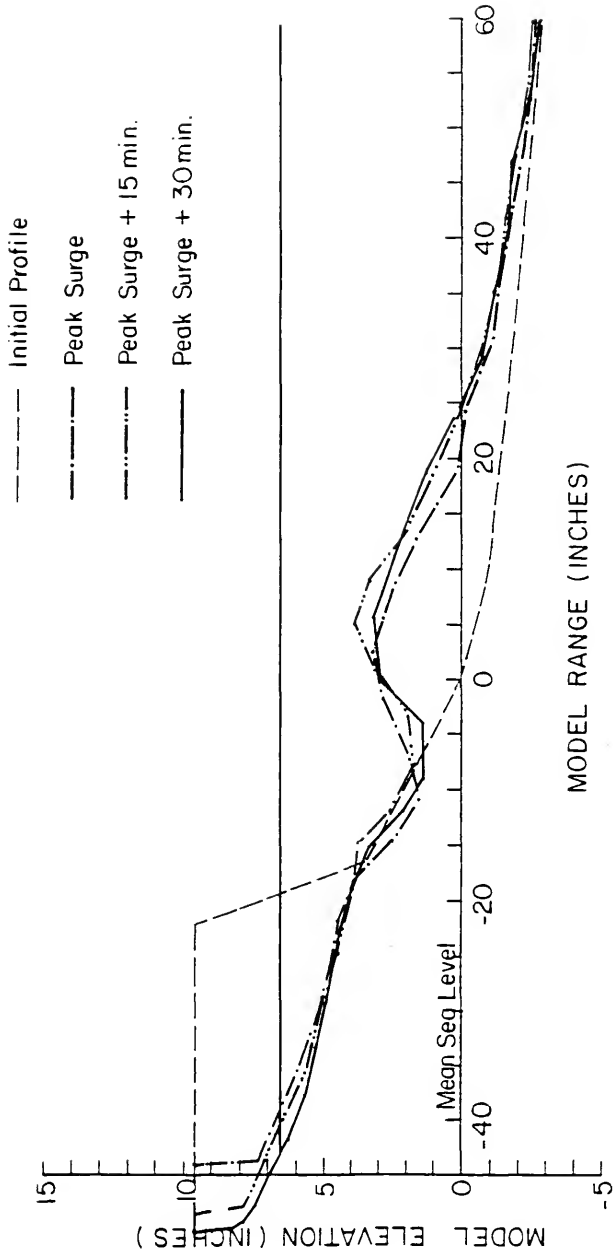


FIGURE 53: RUH #13.

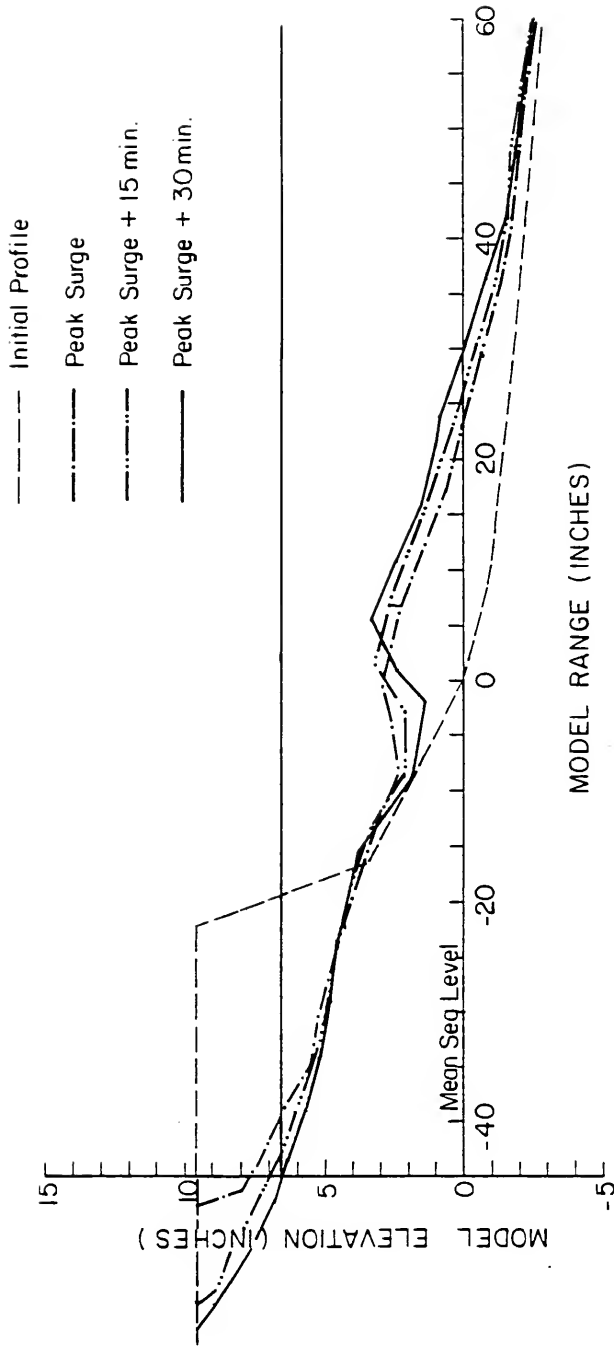


FIGURE 54: RUN #14.

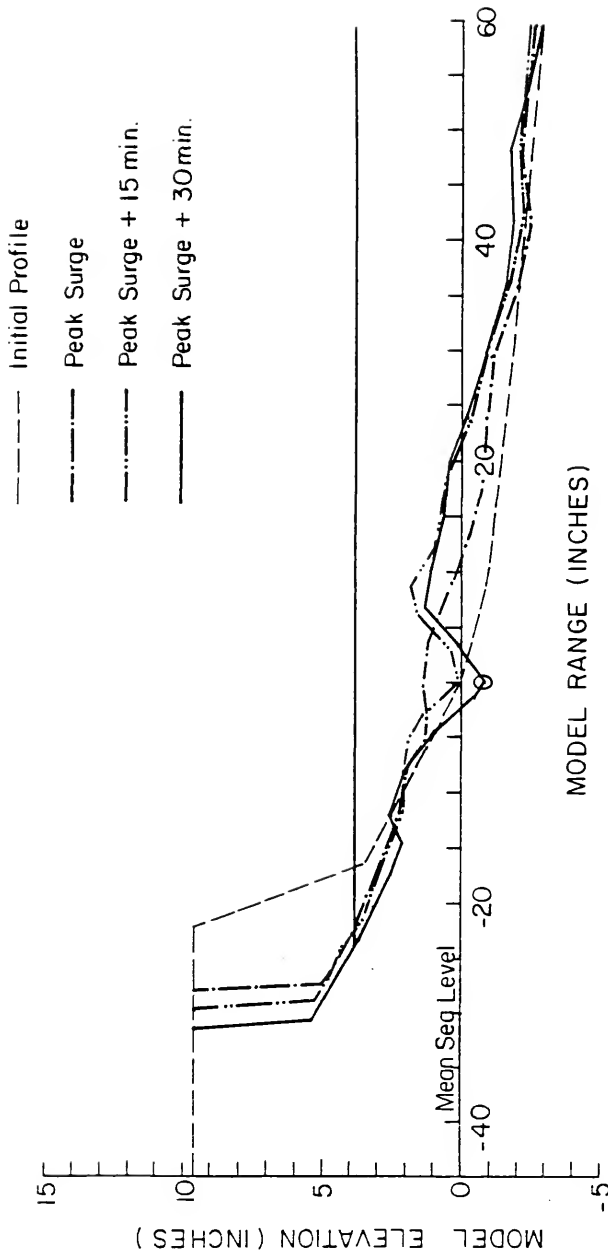


FIGURE 55: RUN #15.

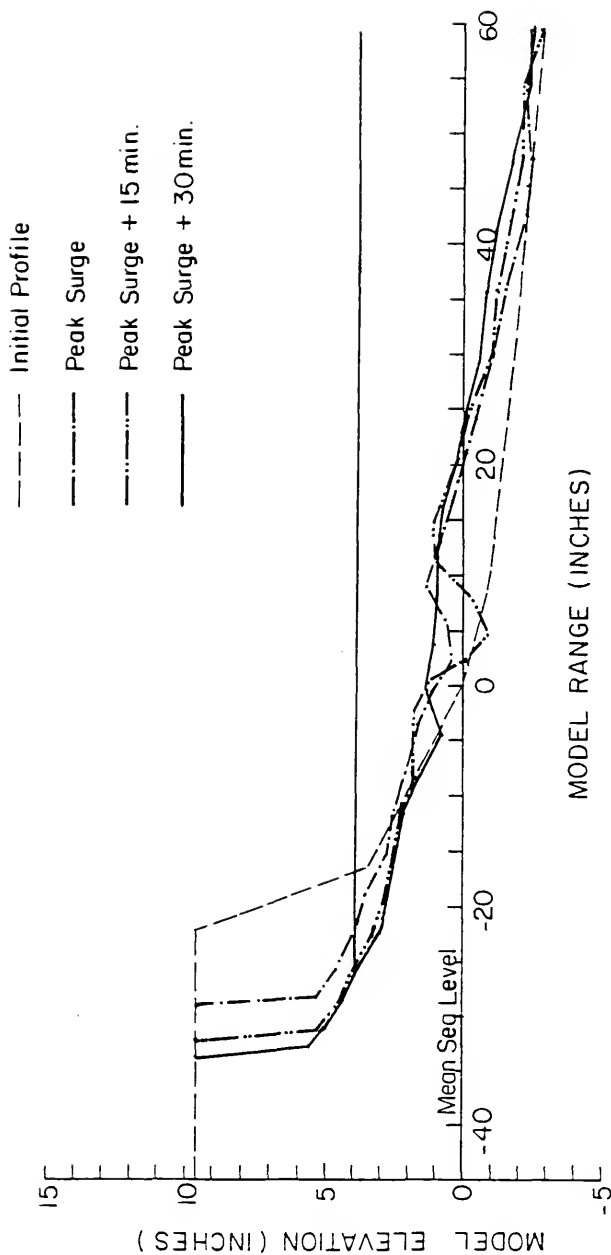


FIGURE 56: RUH #16.

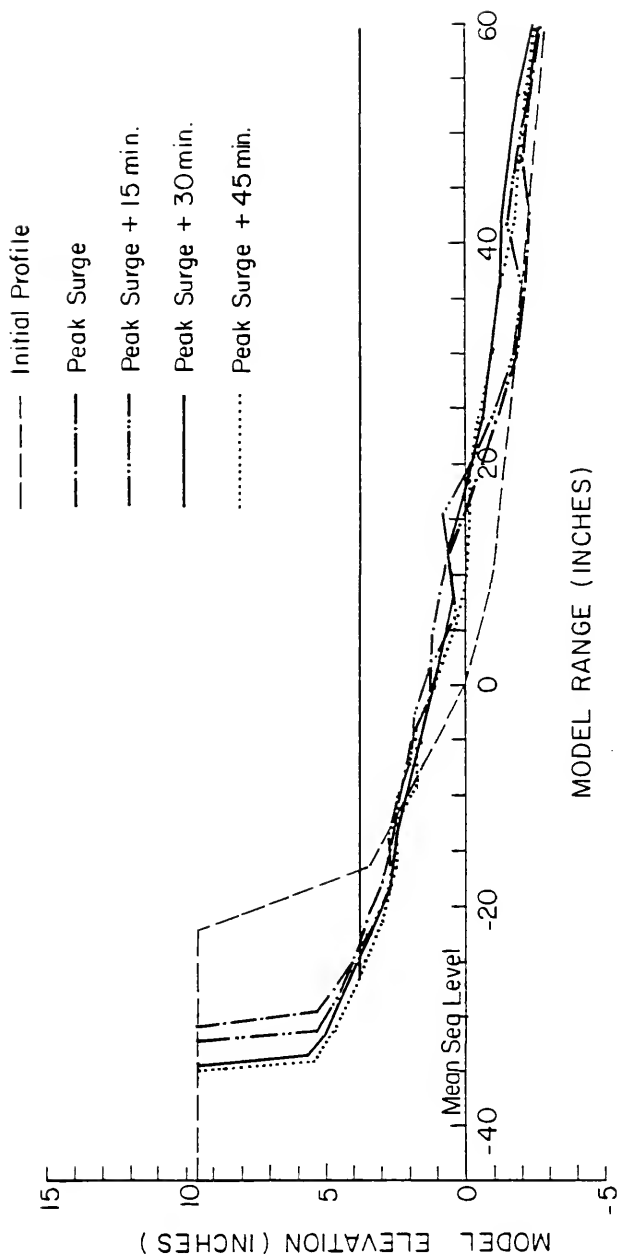


FIGURE 57: RUI #17.



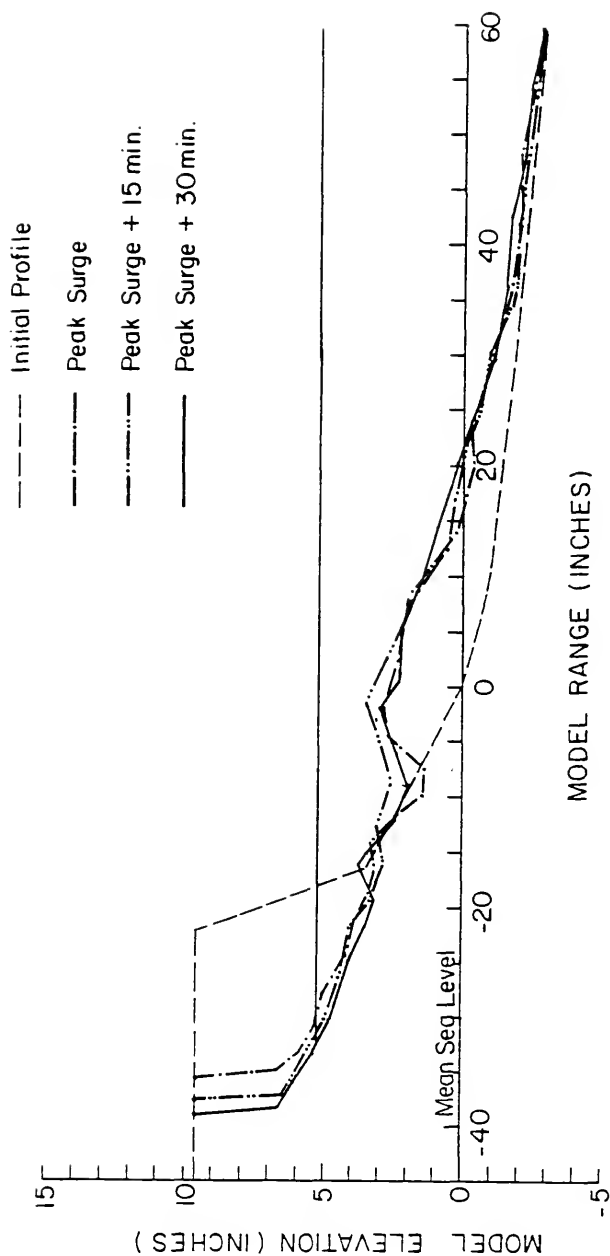


FIGURE 58: RUN #18.

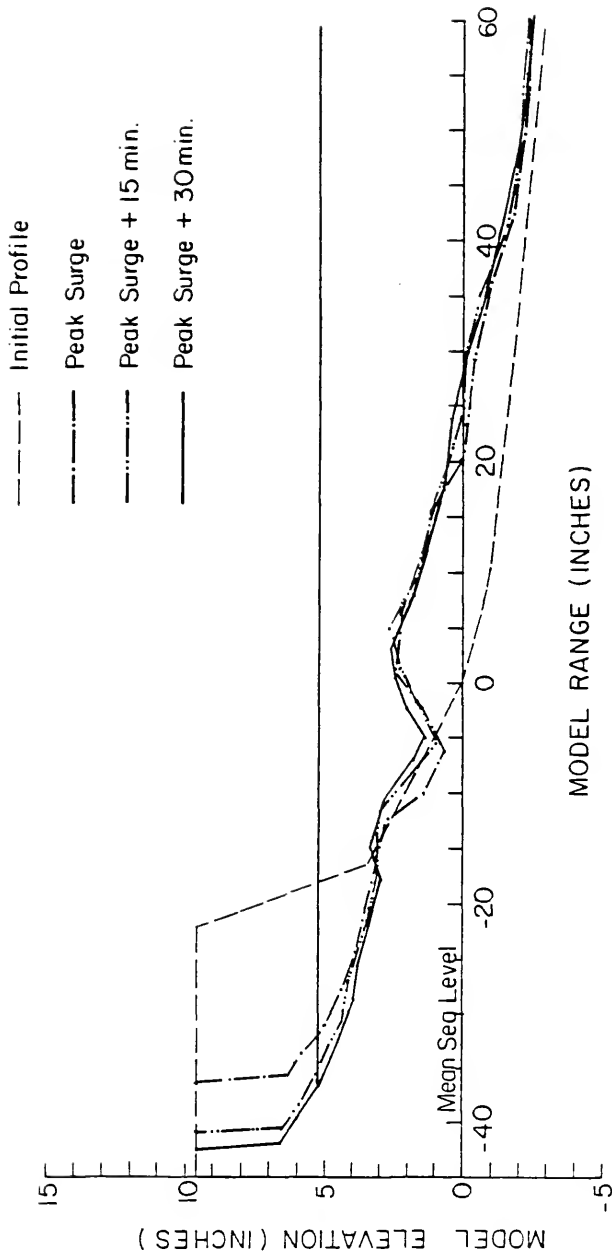


FIGURE 59: RUN #19.

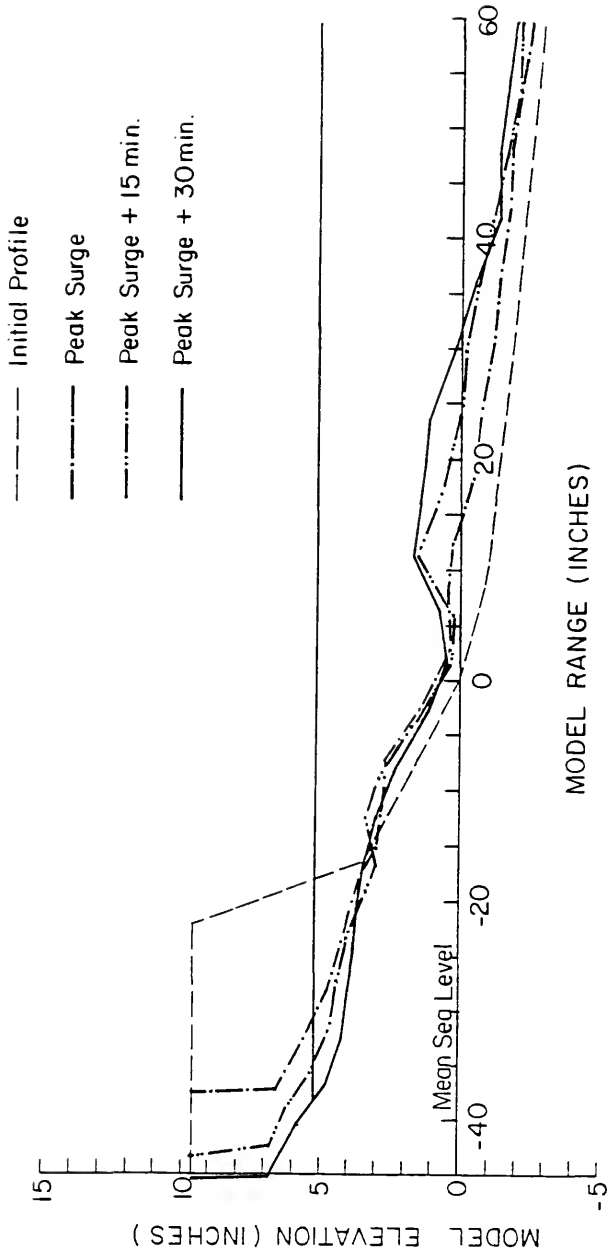


FIGURE 60: RUN #20.

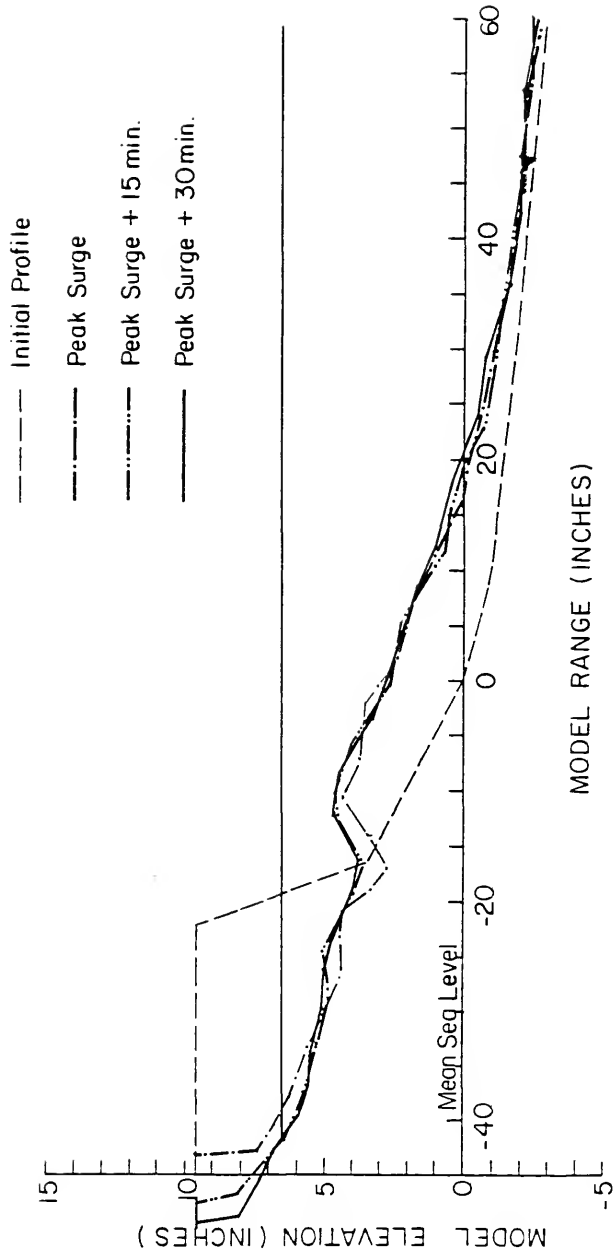


FIGURE 61: RUN #21.

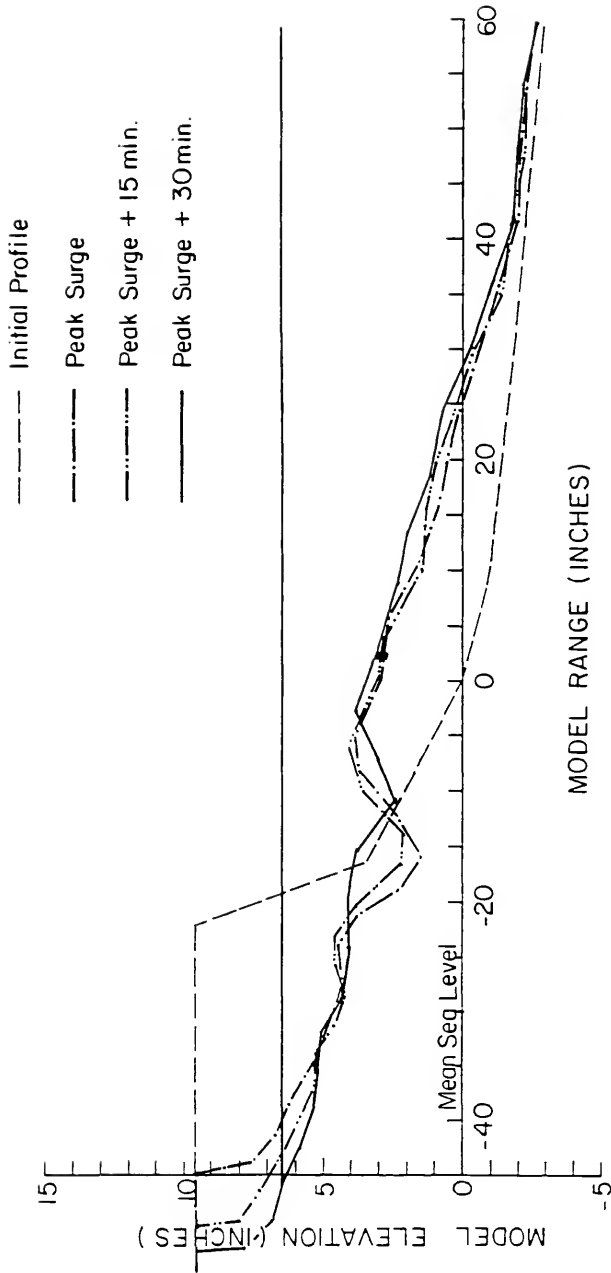


FIGURE 62: RUN #22.

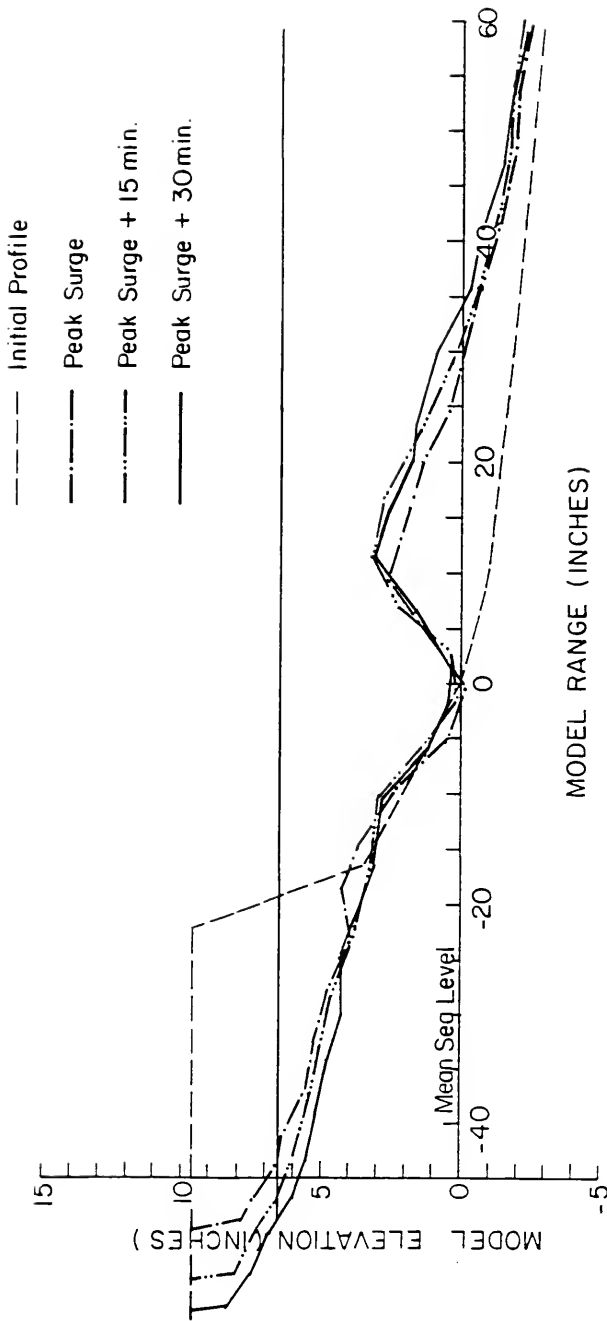


FIGURE 63: RUIN #23.

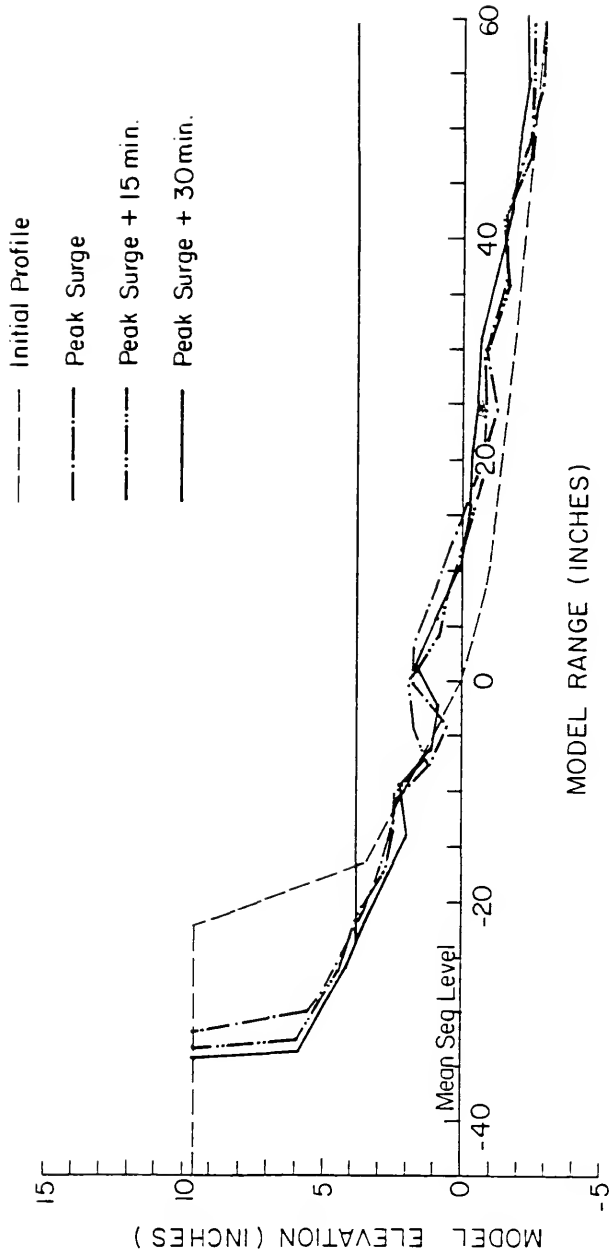


FIGURE 64: RUN #24.

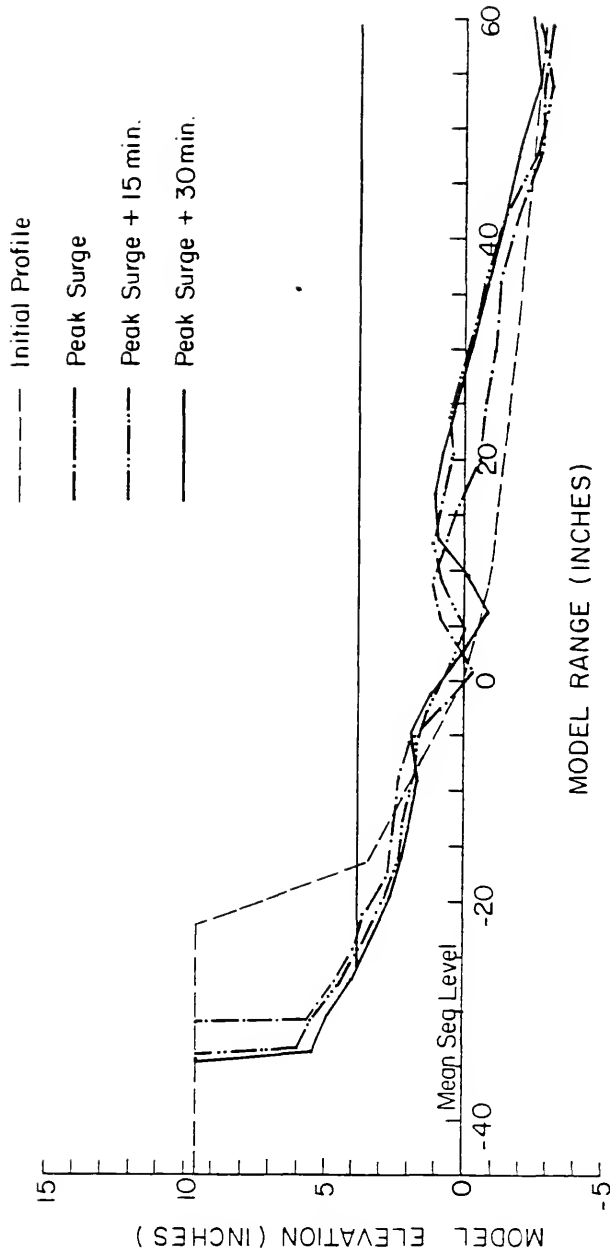


FIGURE 65: RUN #25.



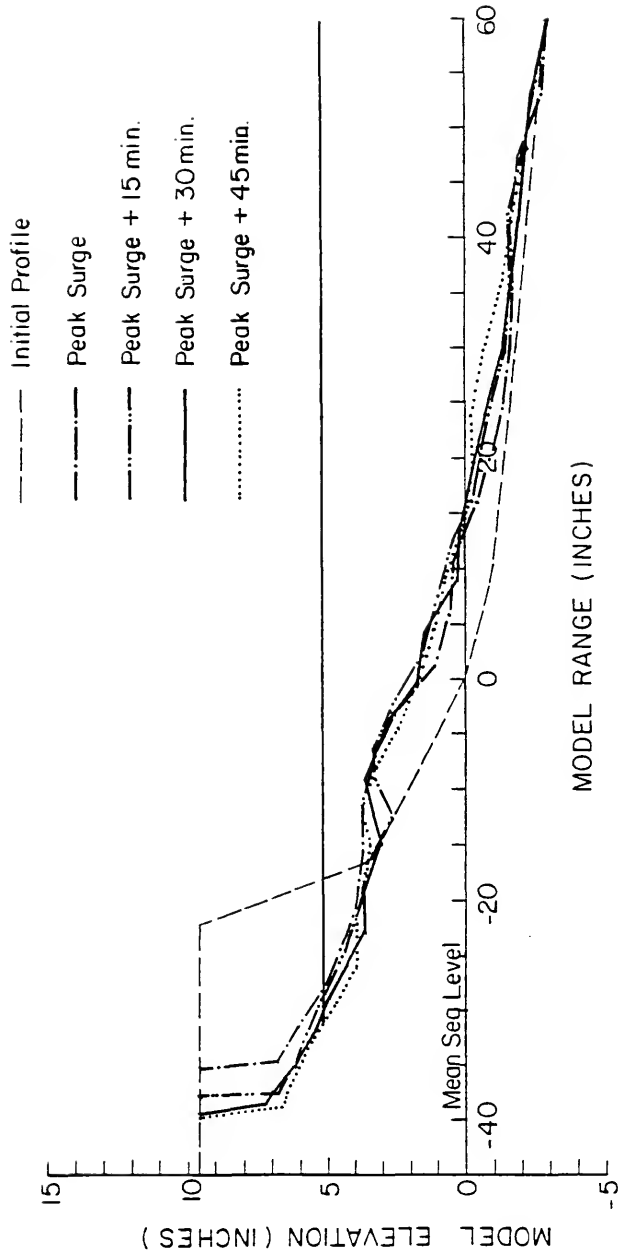


FIGURE 66: RUN #26.

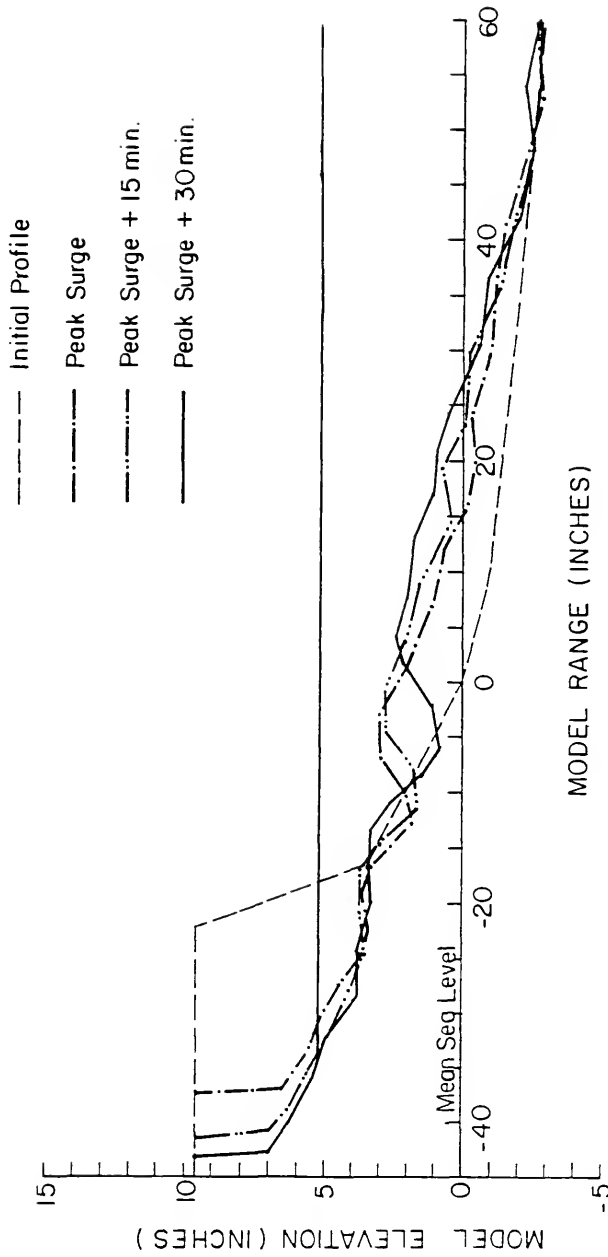


FIGURE 67: RUN #27.

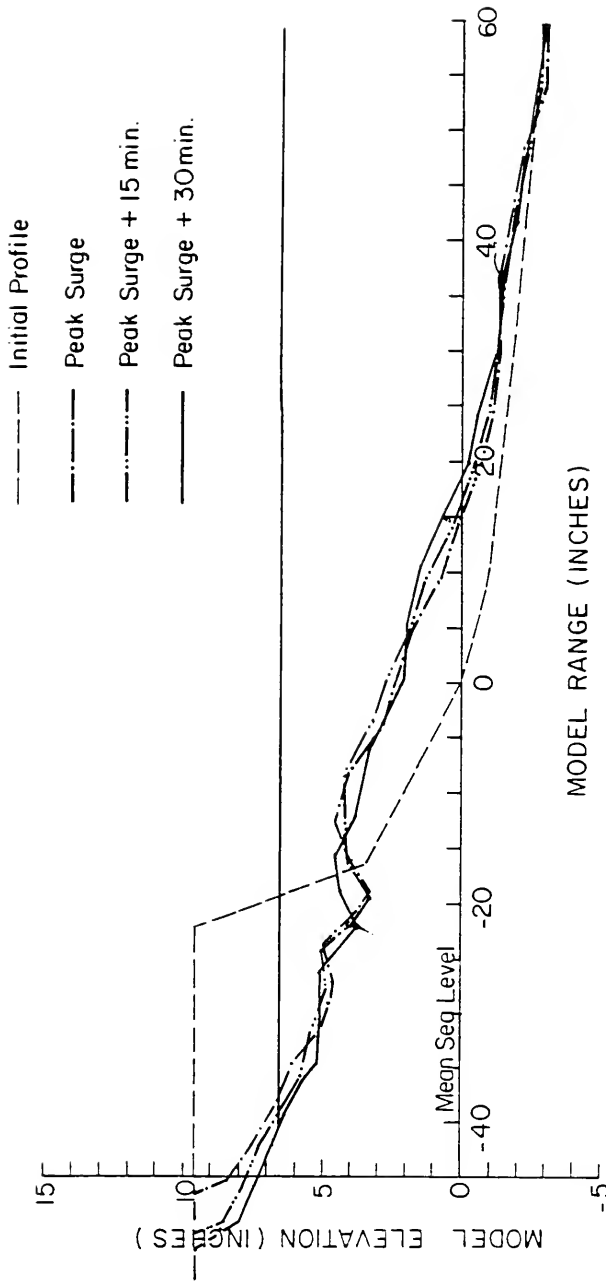


FIGURE 63: RUN #28.

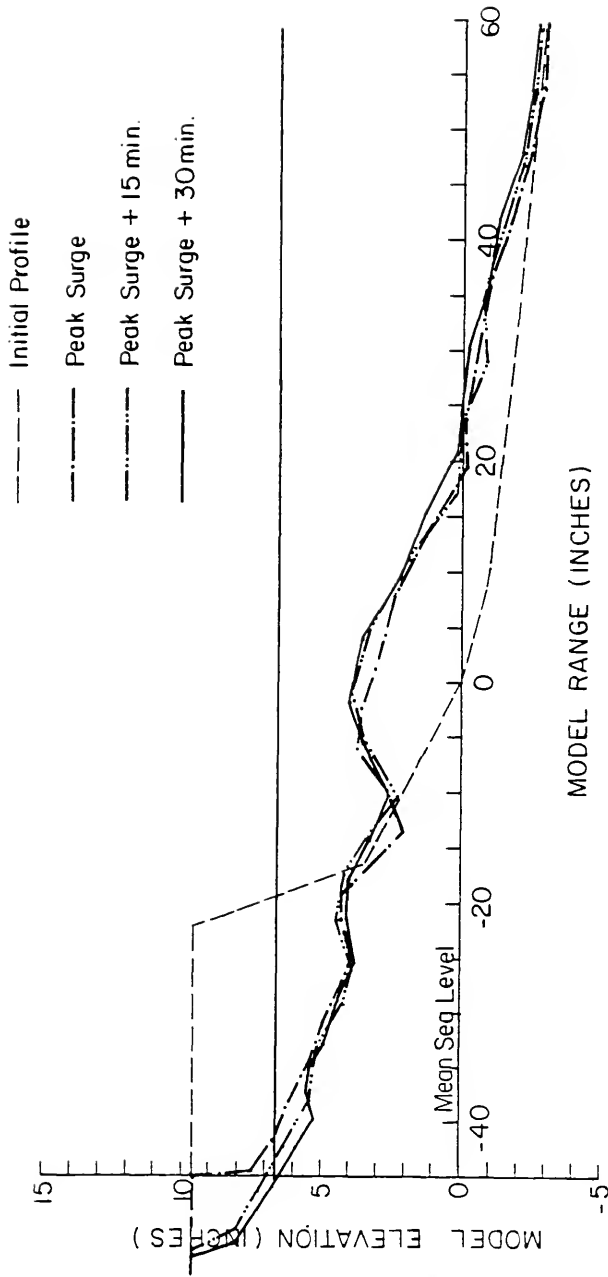


FIGURE 69: RUN #29.

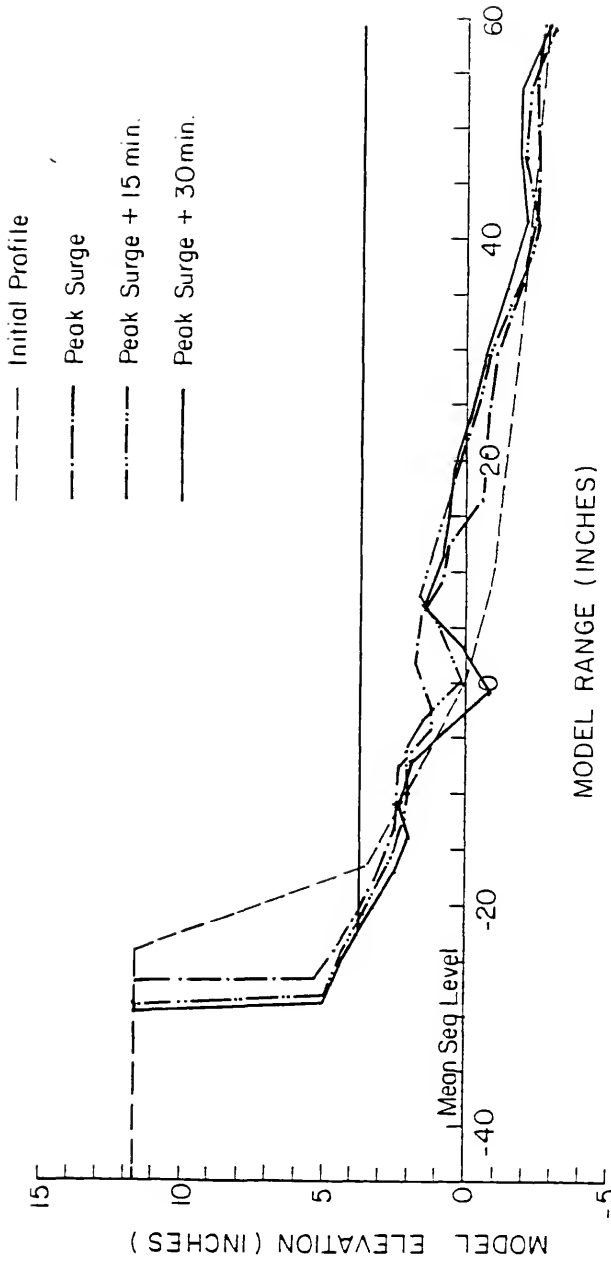


FIGURE 70: RUN #30.

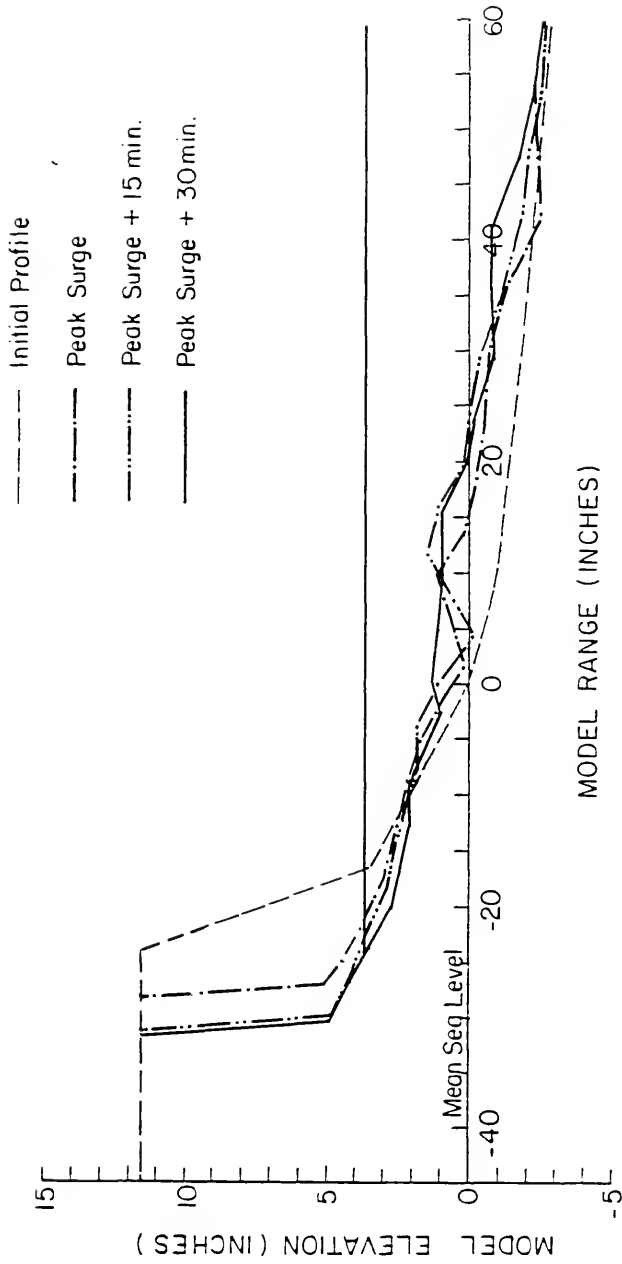


FIGURE 71: RUN #31.

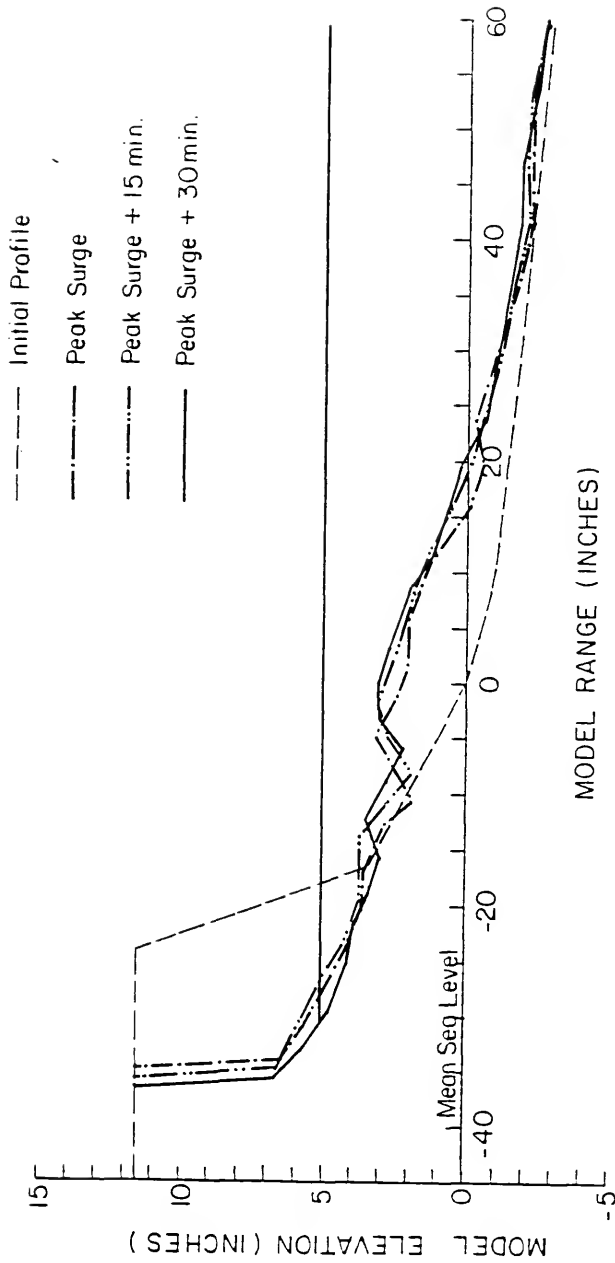


FIGURE 72: RUN #32.

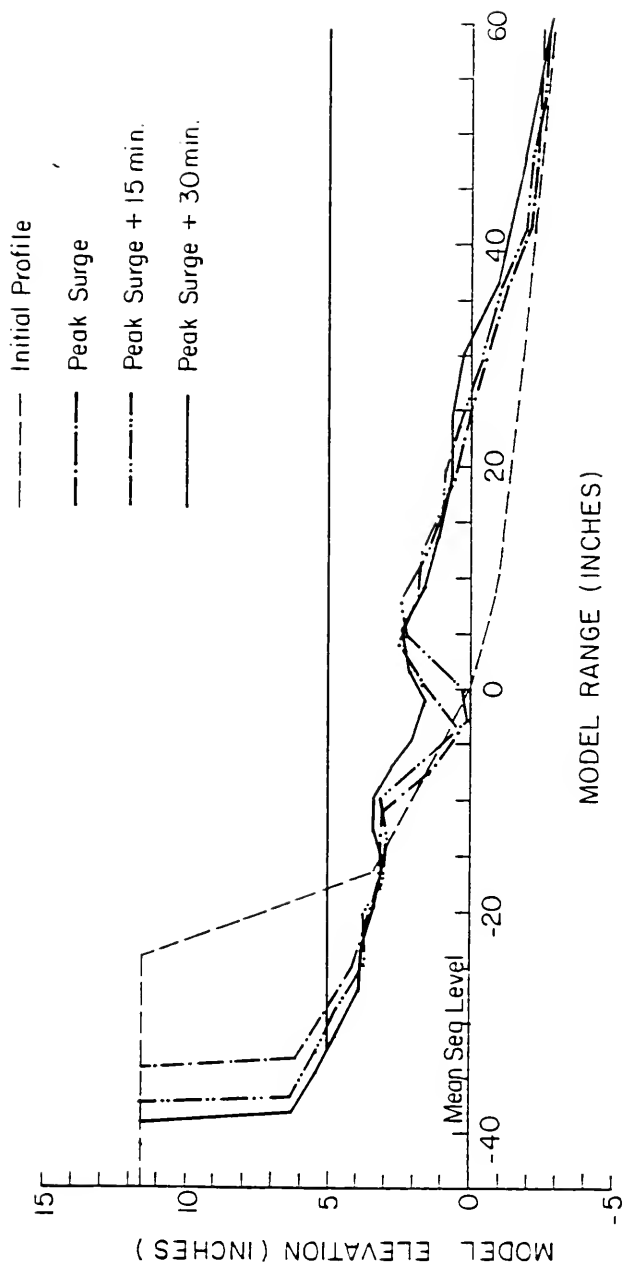


FIGURE 73: RUN #33.



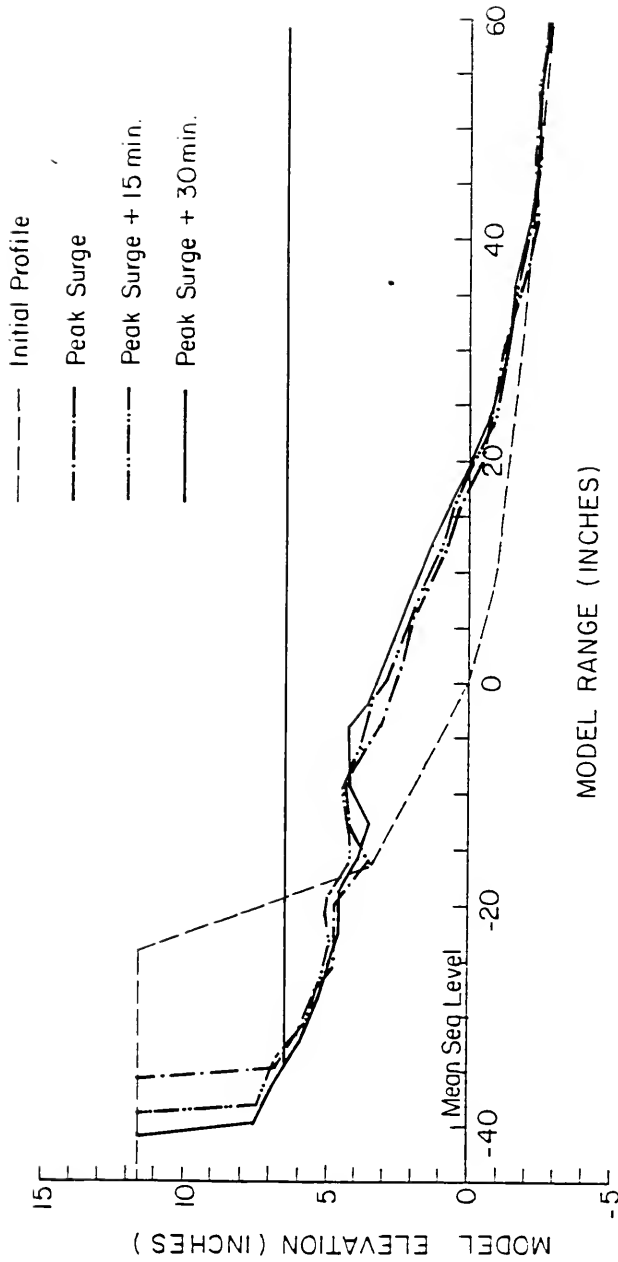


FIGURE 74: RUN #34.

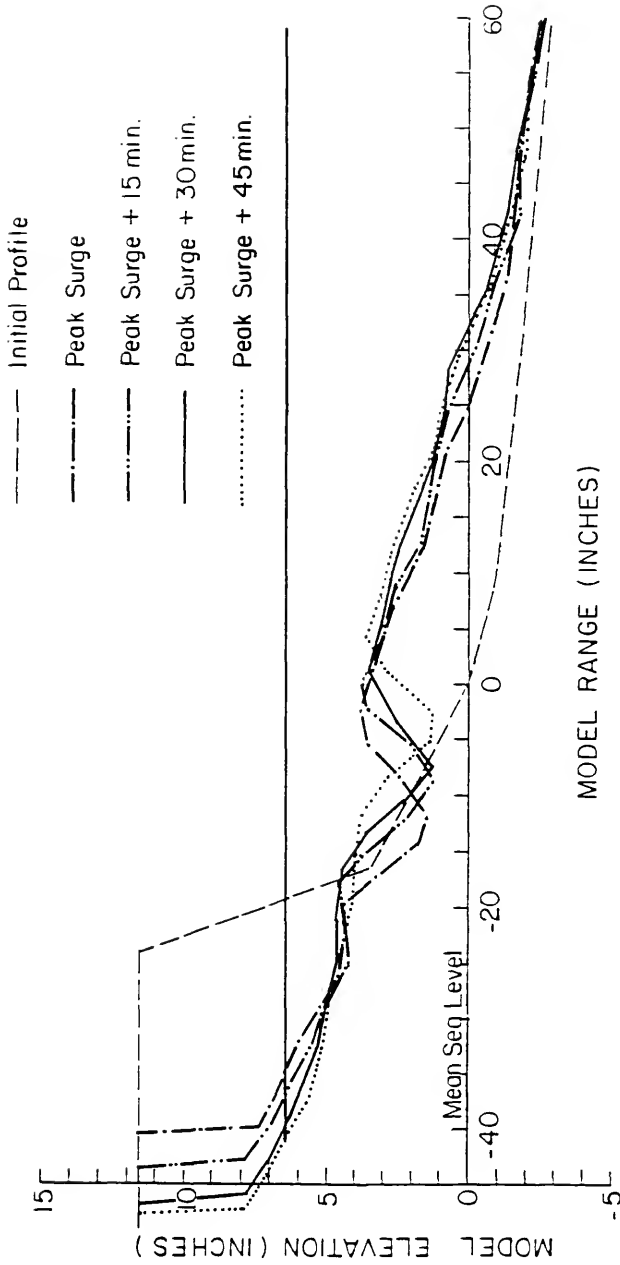


FIGURE 75: RUN #35.

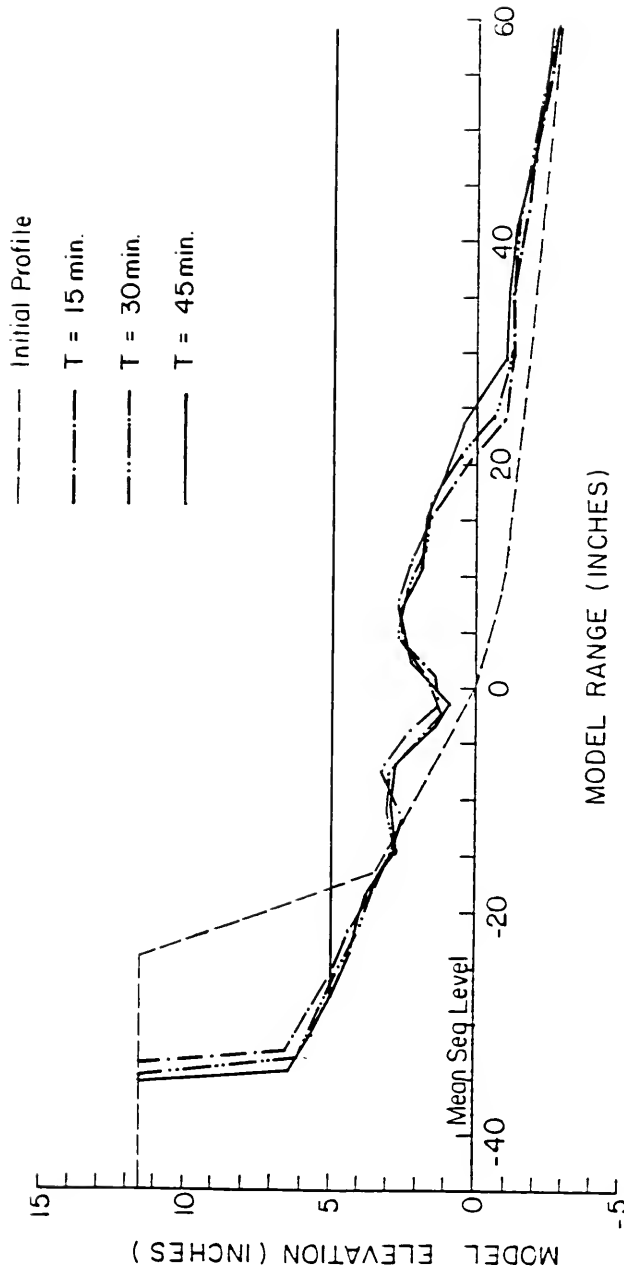


FIGURE 76: RUN #36, FIXED SURGE LEVEL.

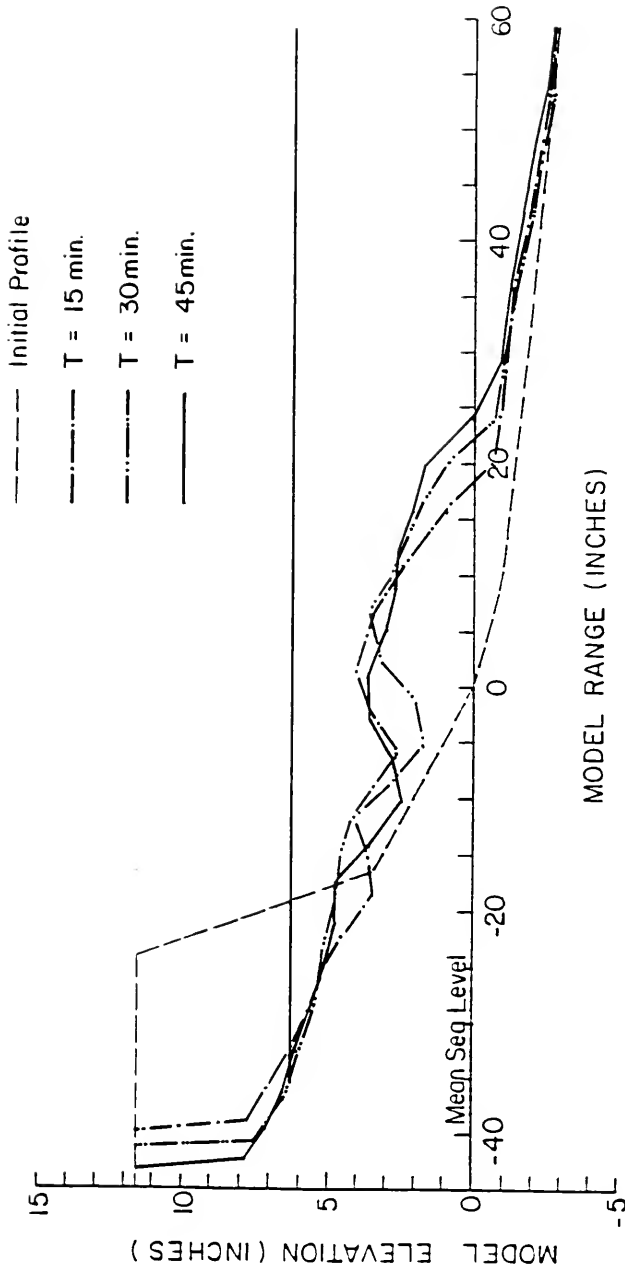


FIGURE 77: RUN #37, FIXED SURGE LEVEL.

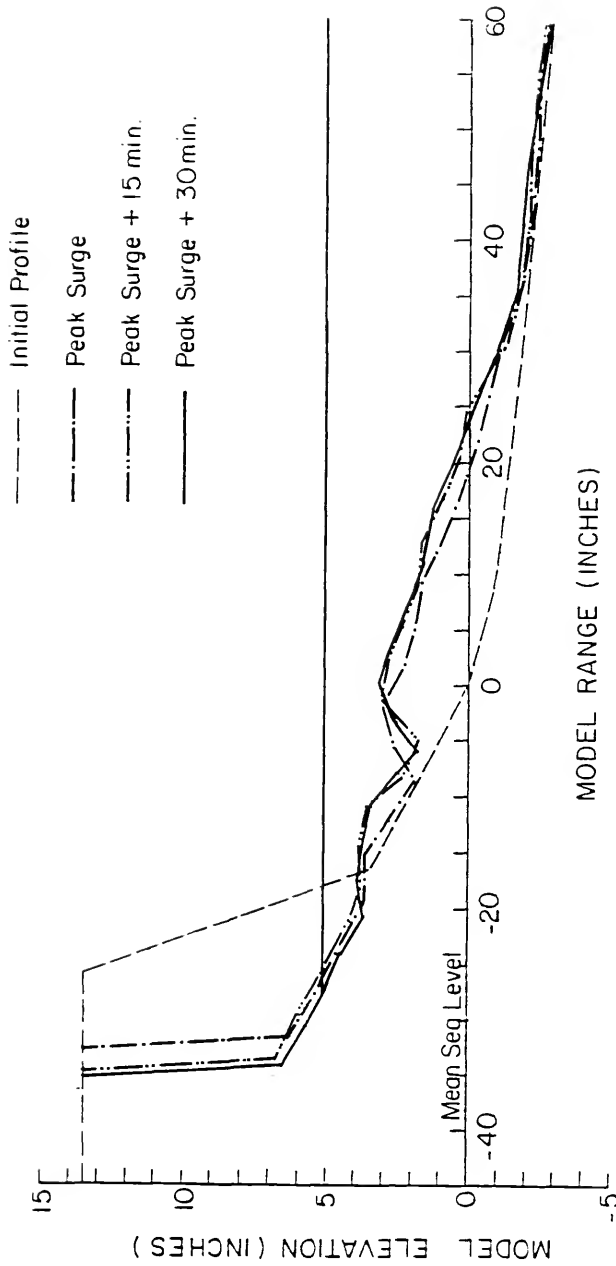


FIGURE 78: RUN #33.

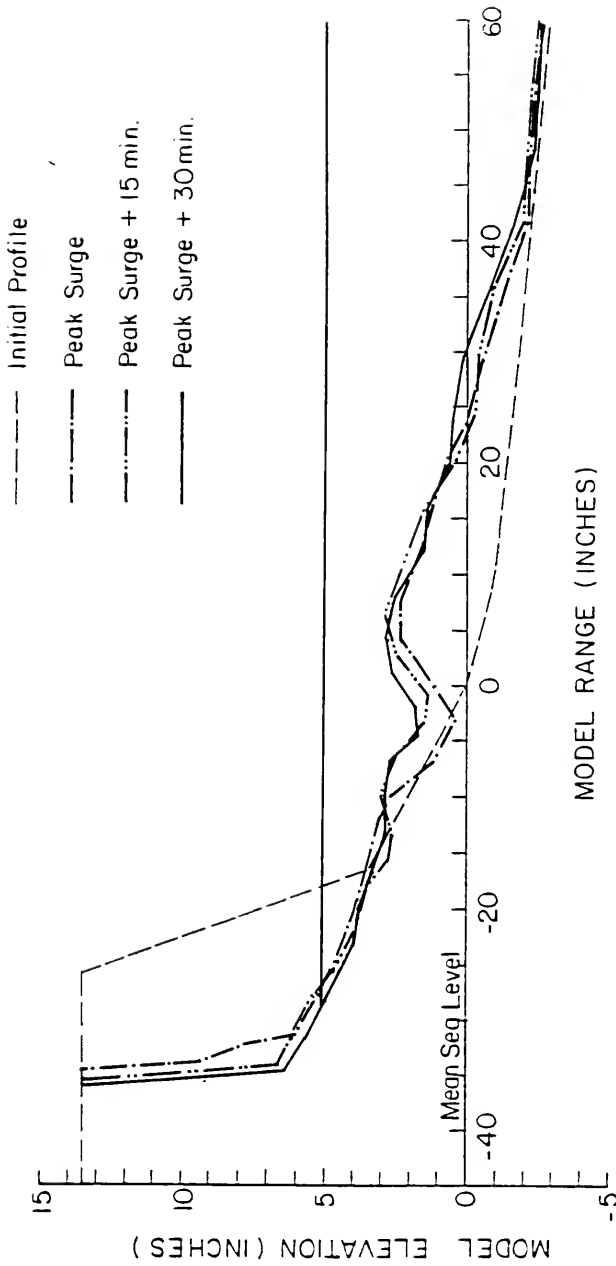


FIGURE 79: RUM #39.

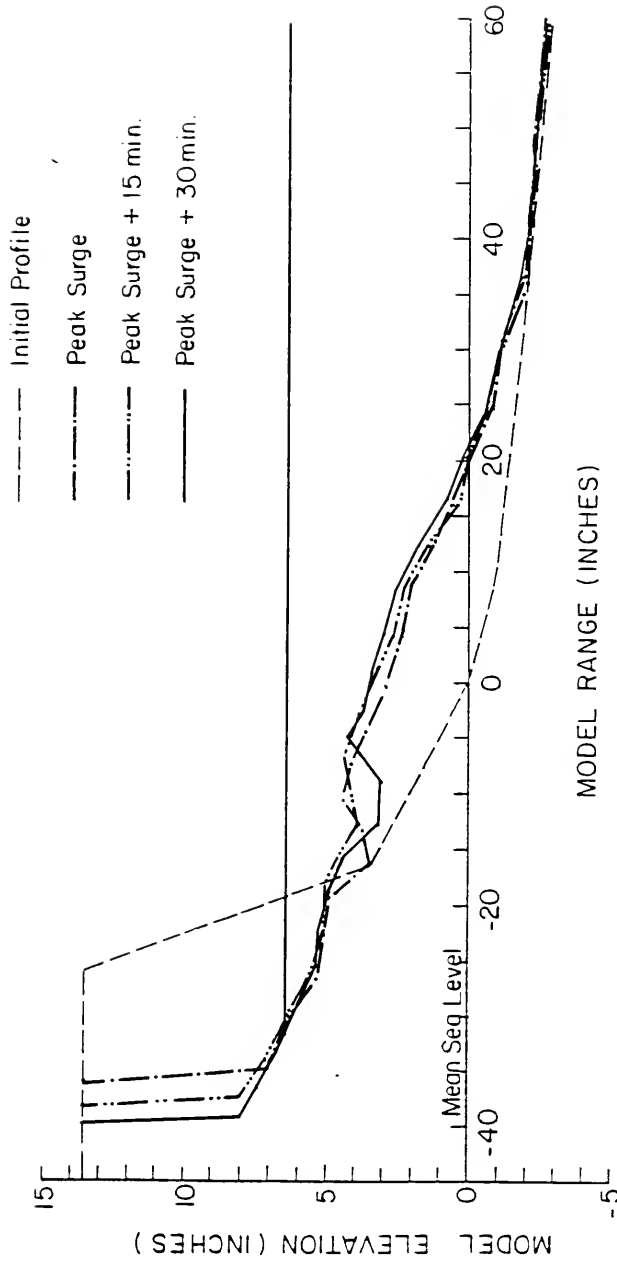


FIGURE 80: RUN #40.

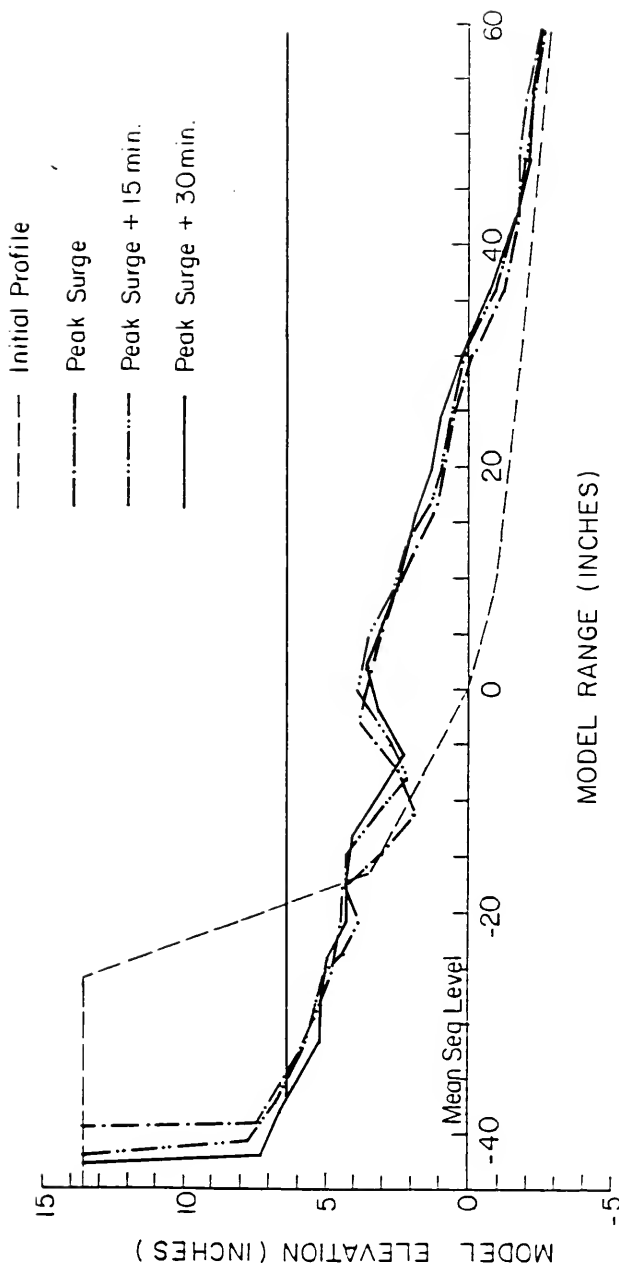


FIGURE 81: RHH #41.



APPENDIX D  
PROFILE COMPARISONS

APPENDIX D.1

DUNE HEIGHT COMPARISONS

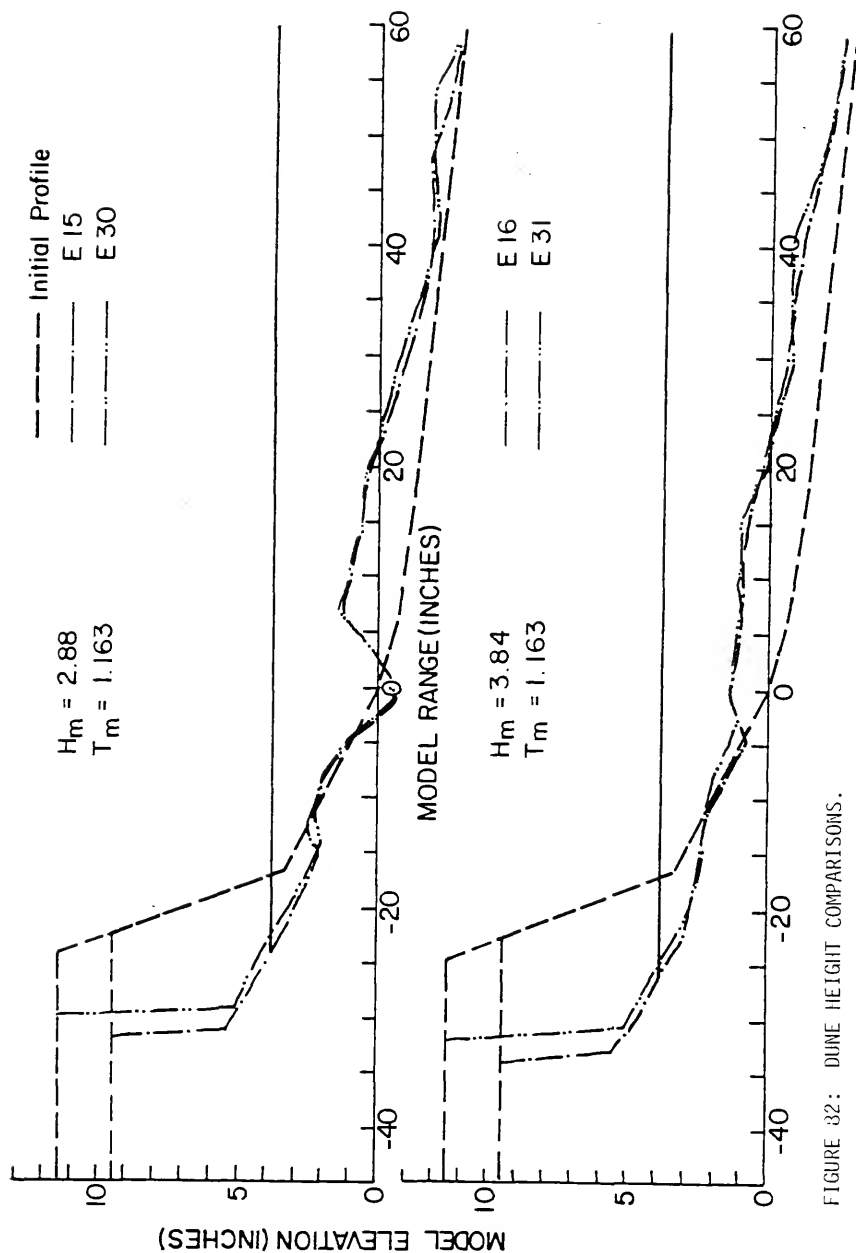


FIGURE 32: DUNE HEIGHT COMPARISONS.

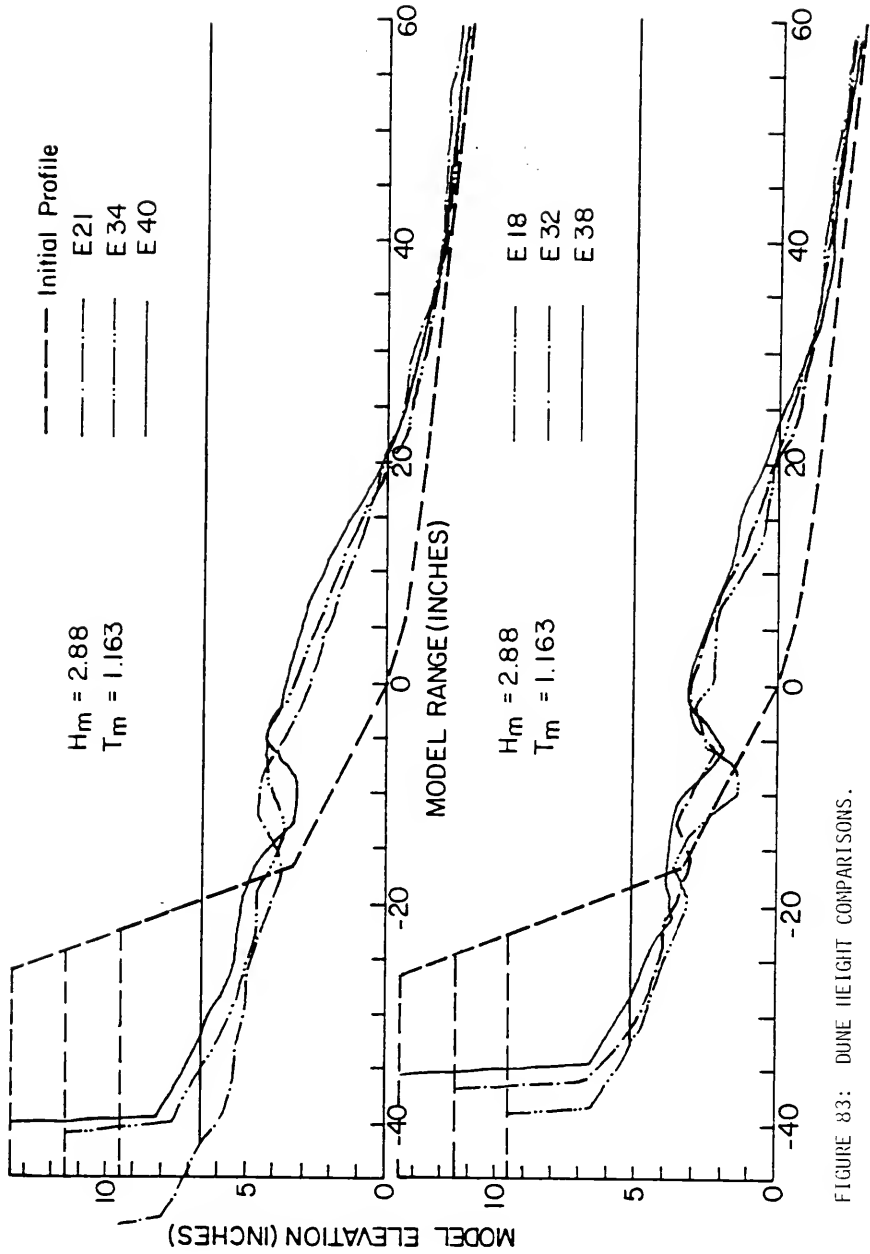


FIGURE 83: DUNE HEIGHT COMPARISONS.

APPENDIX D.2  
STORM SURGE COMPARISONS

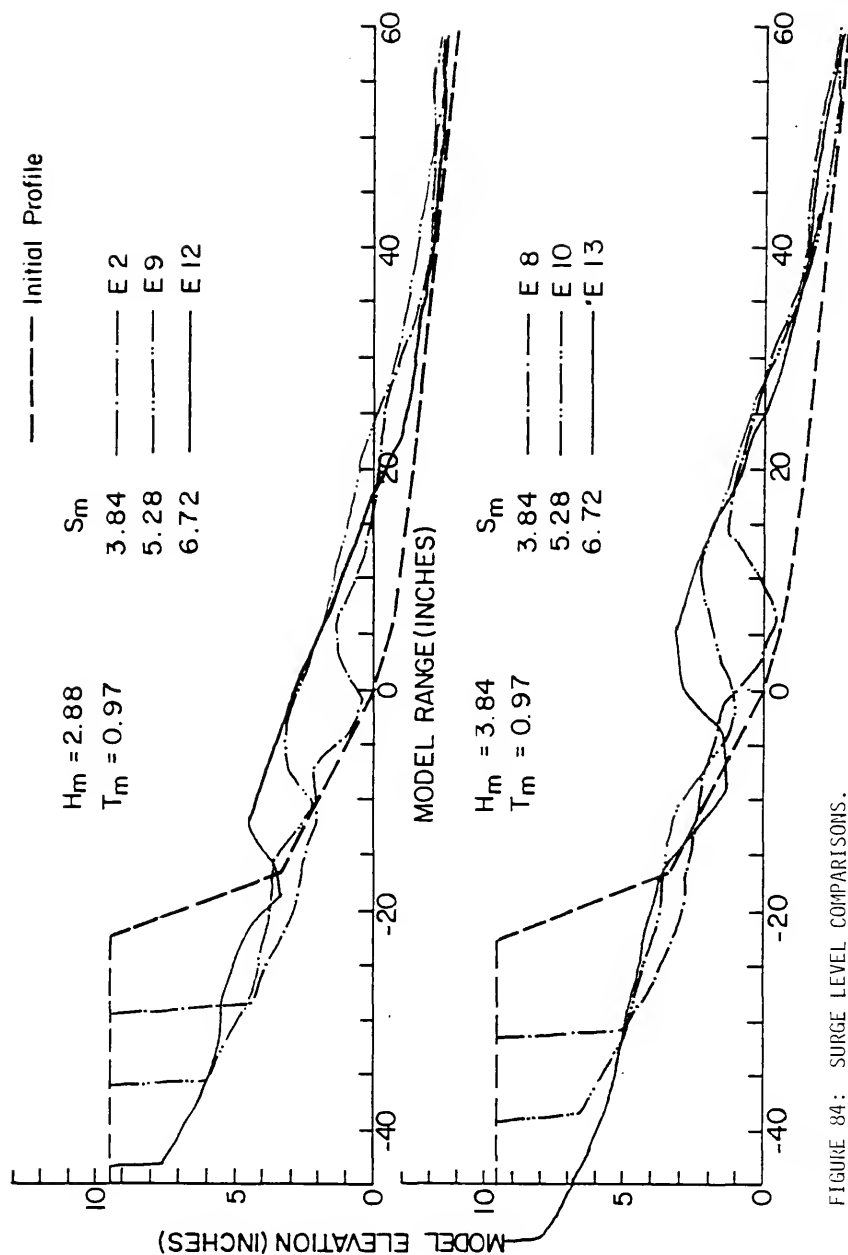


FIGURE 84: SURGE LEVEL COMPARISONS.

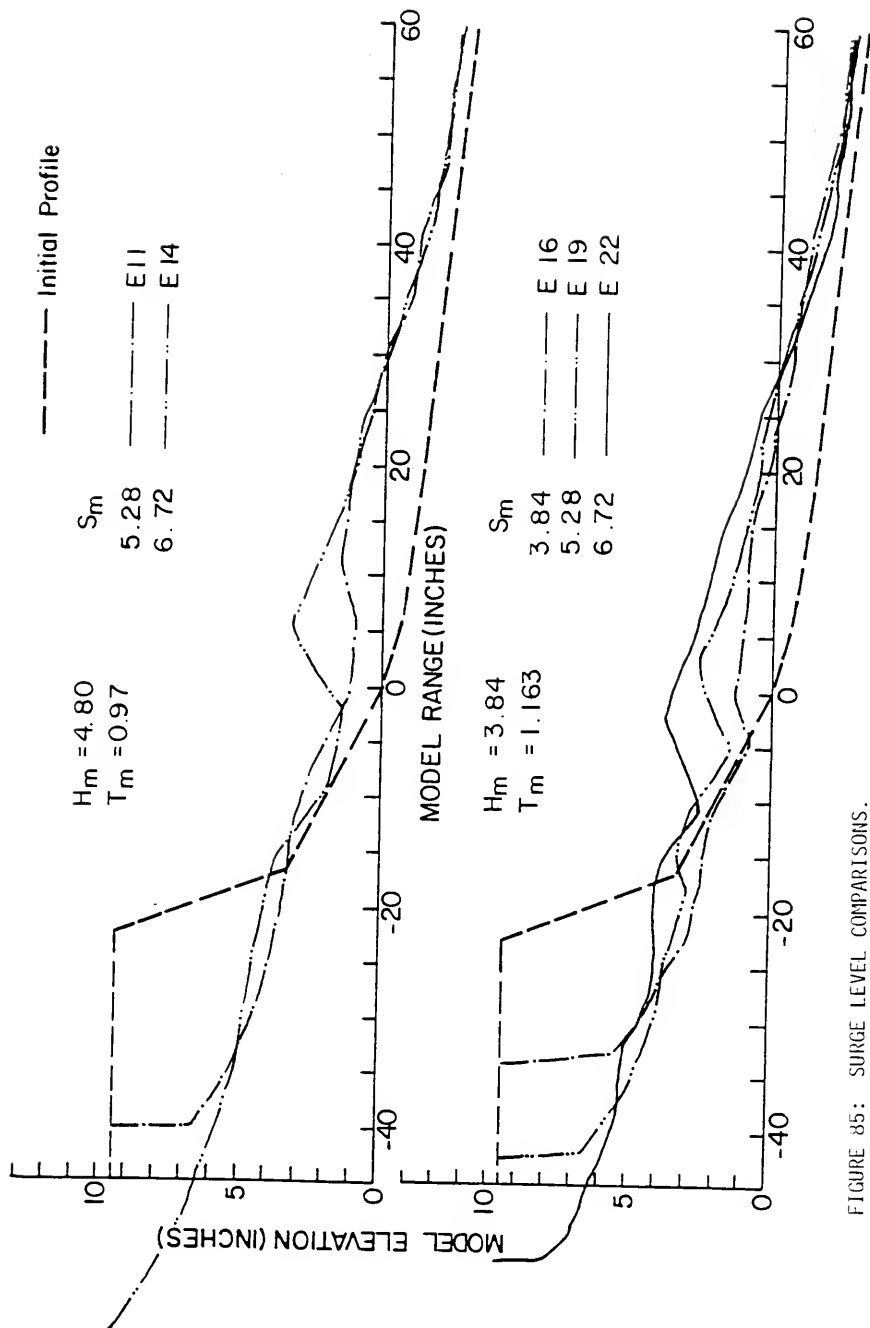


FIGURE 85: SURGE LEVEL COMPARISONS.

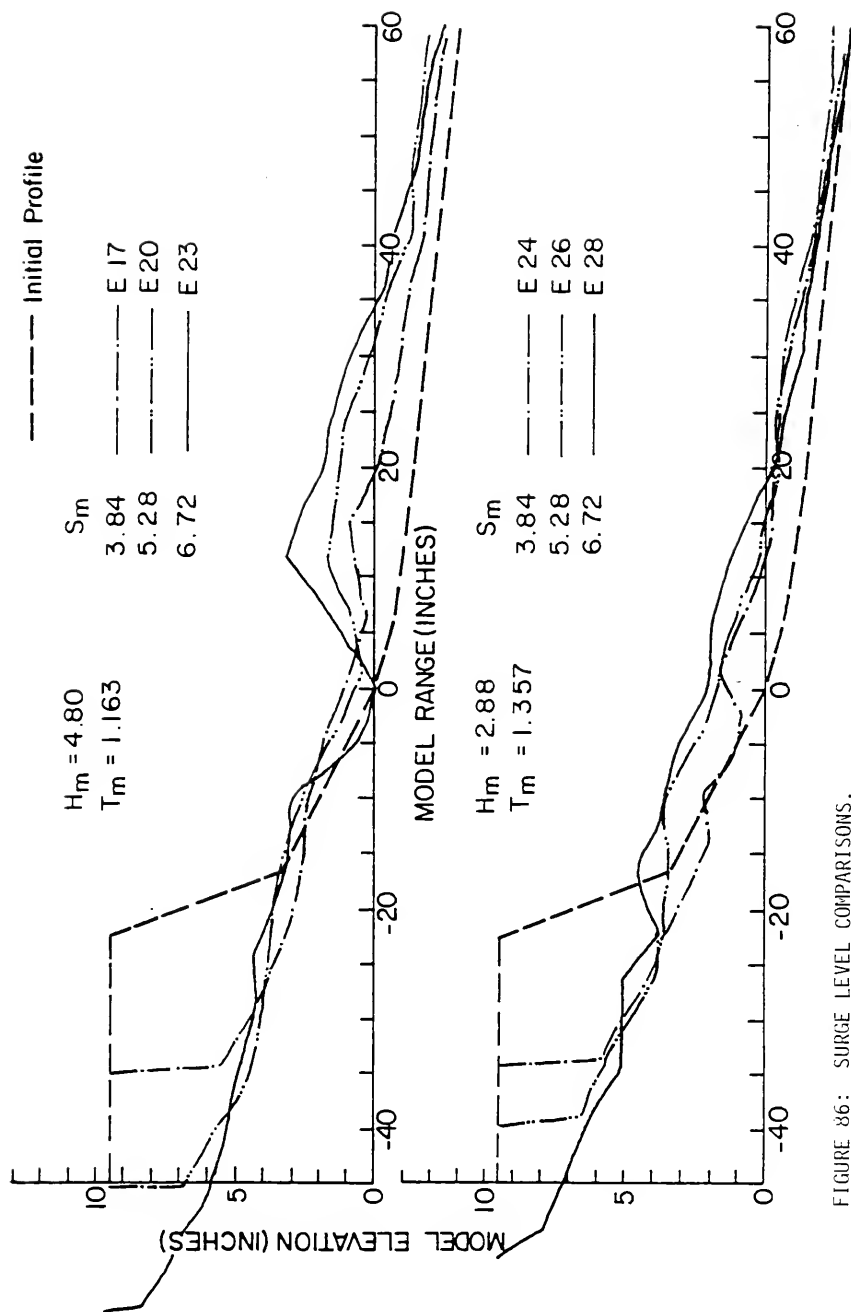


FIGURE 86: SURGE LEVEL COMPARISONS.



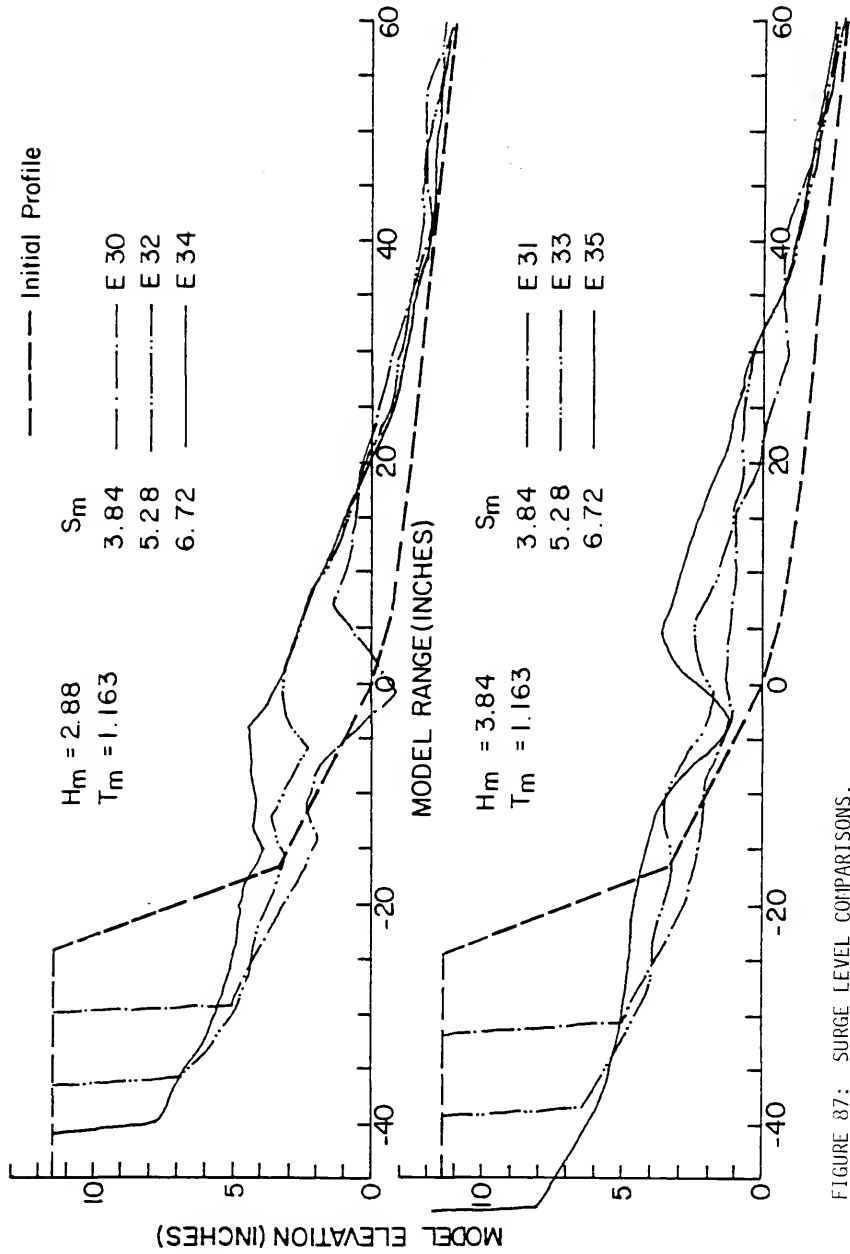
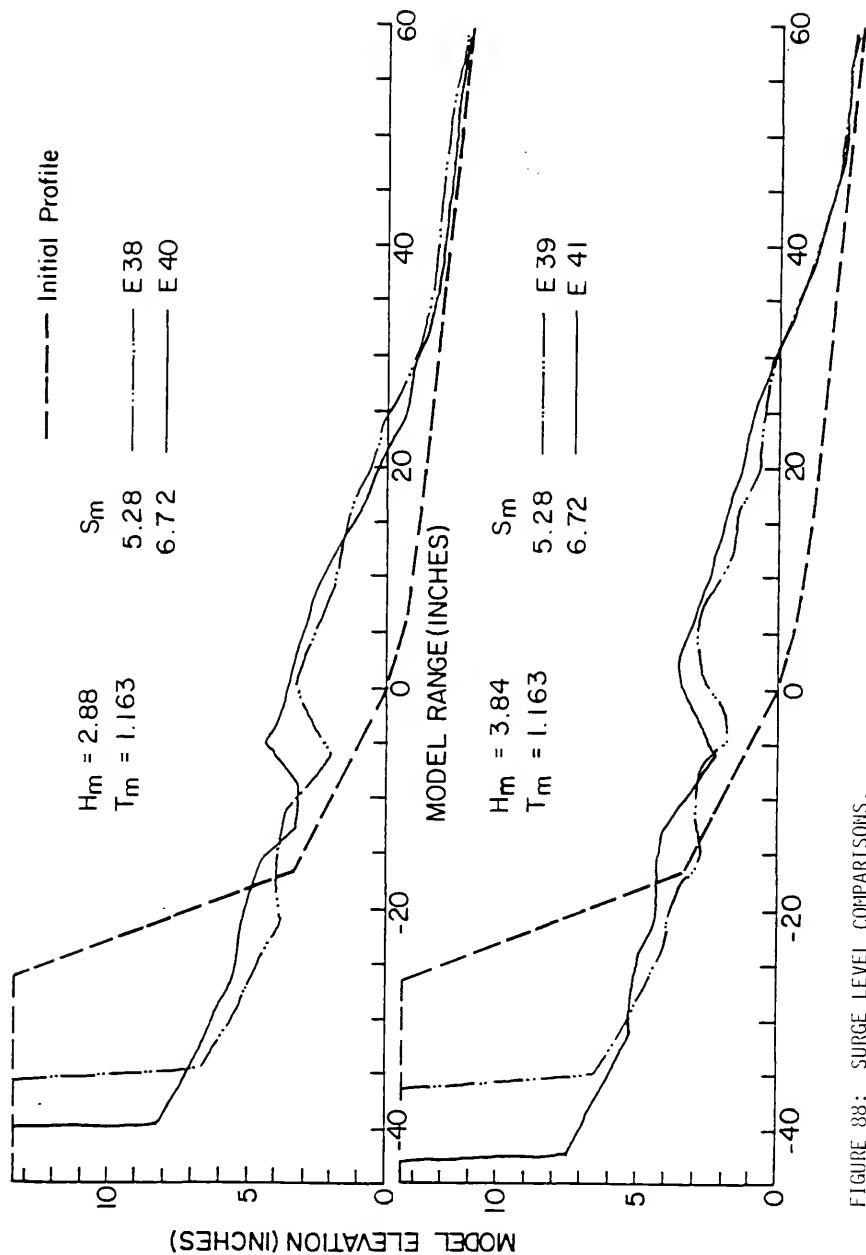


FIGURE 87: SURGE LEVEL COMPARISONS.



APPENDIX D.3

WAVE HEIGHT COMPARISONS

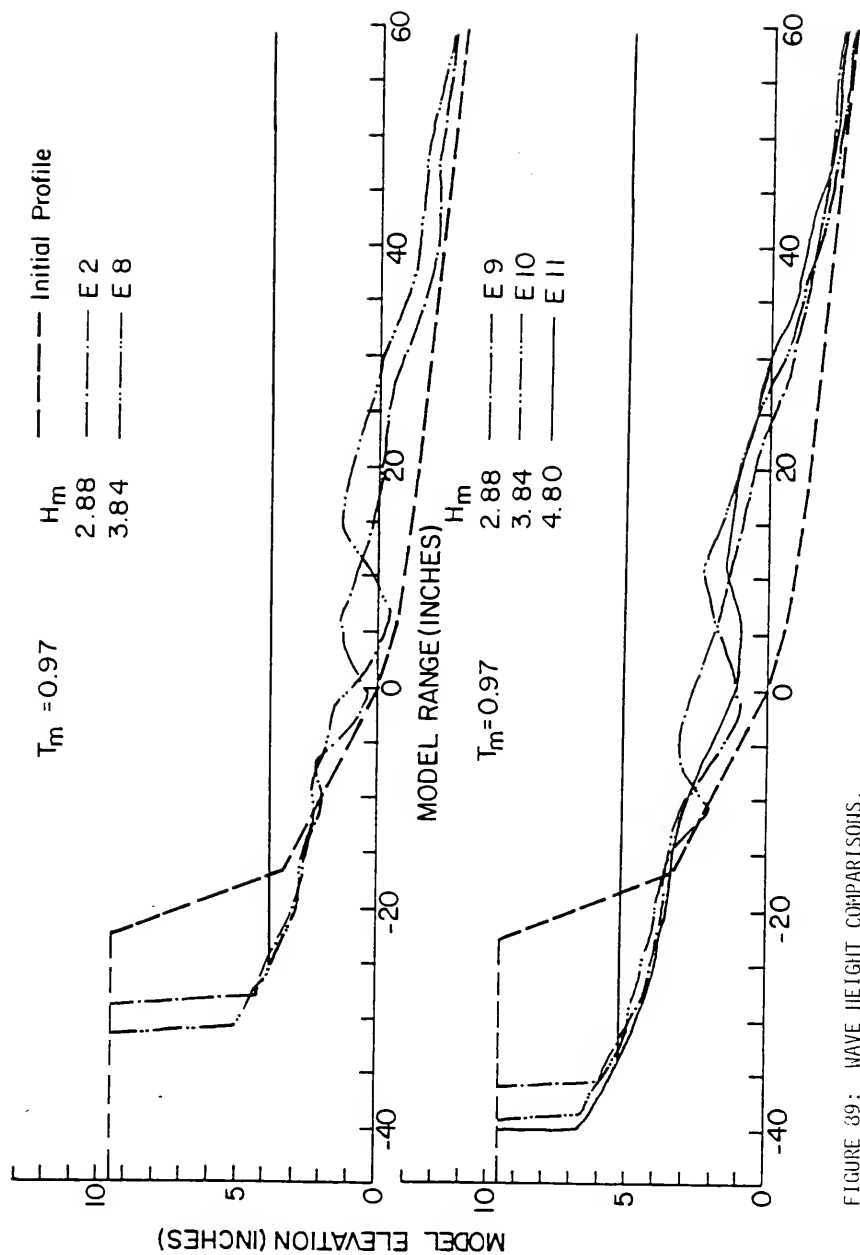


FIGURE 39: WAVE HEIGHT COMPARISONS.

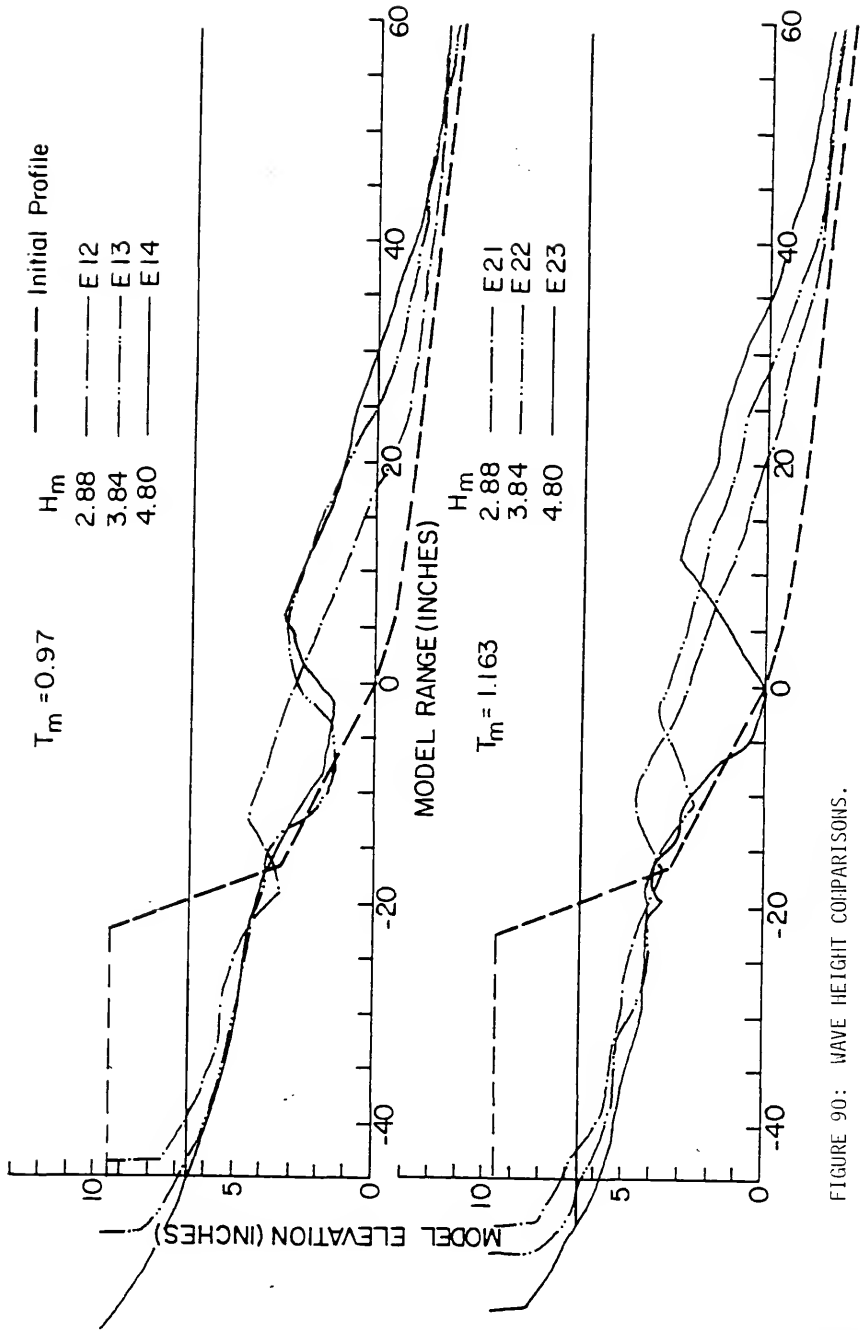


FIGURE 90: WAVE HEIGHT COMPARISONS.

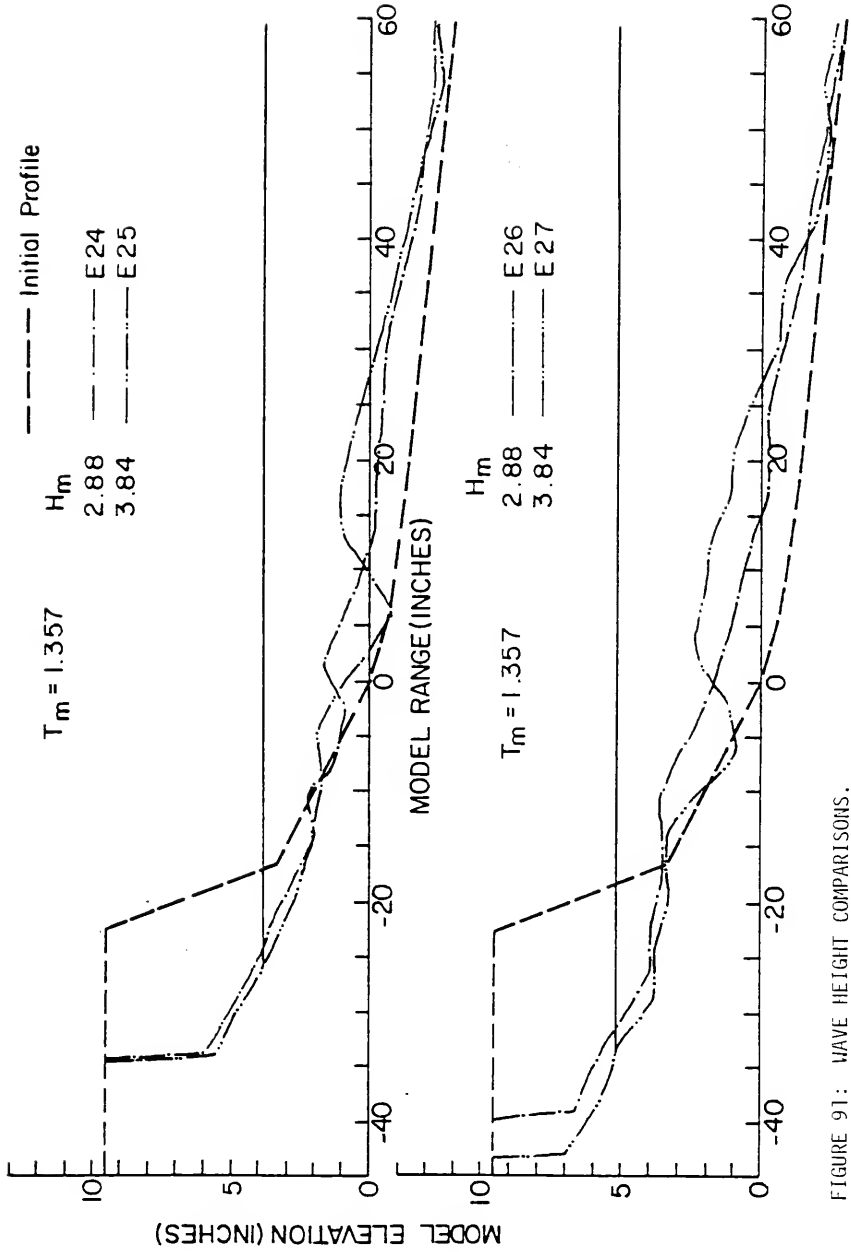


FIGURE 91: WAVE HEIGHT COMPARISONS.

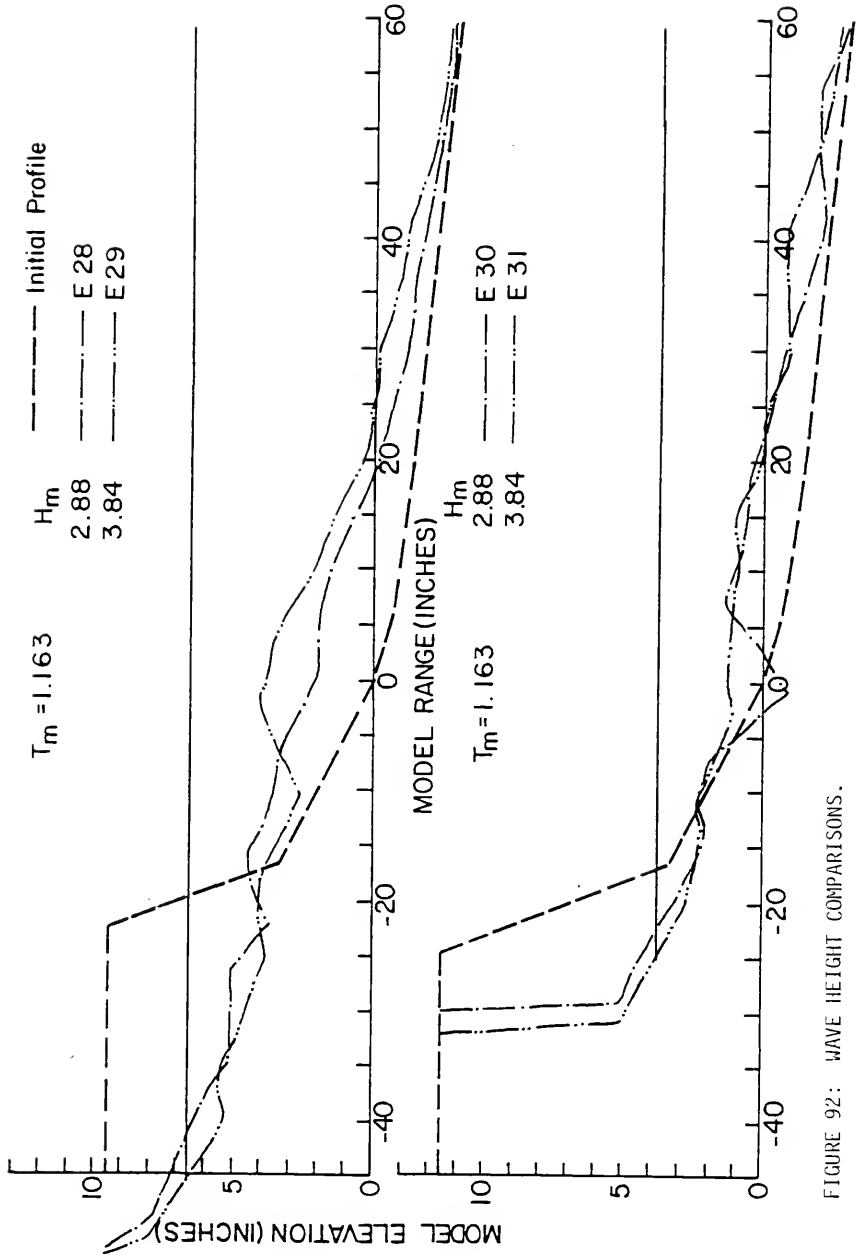


FIGURE 92: WAVE HEIGHT COMPARISONS.

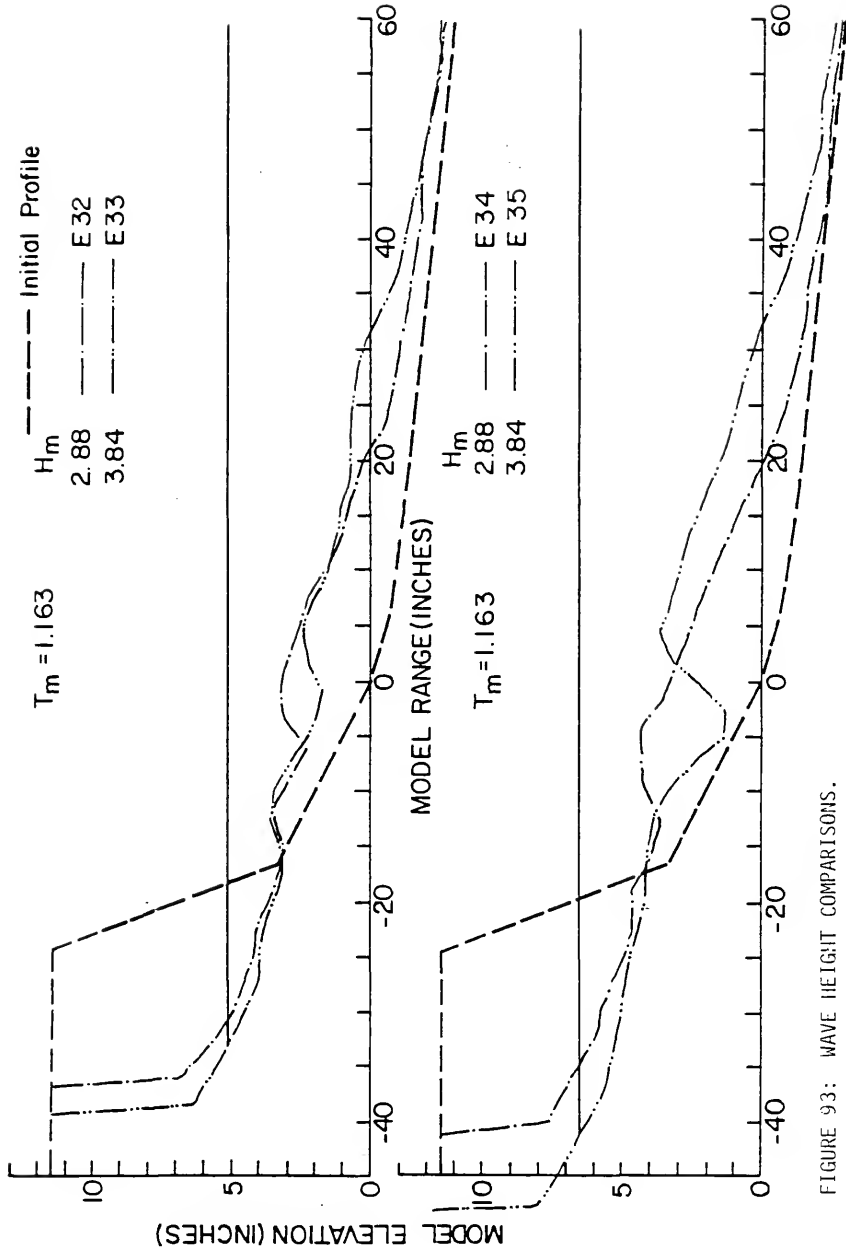


FIGURE 93: WAVE HEIGHT COMPARISONS.



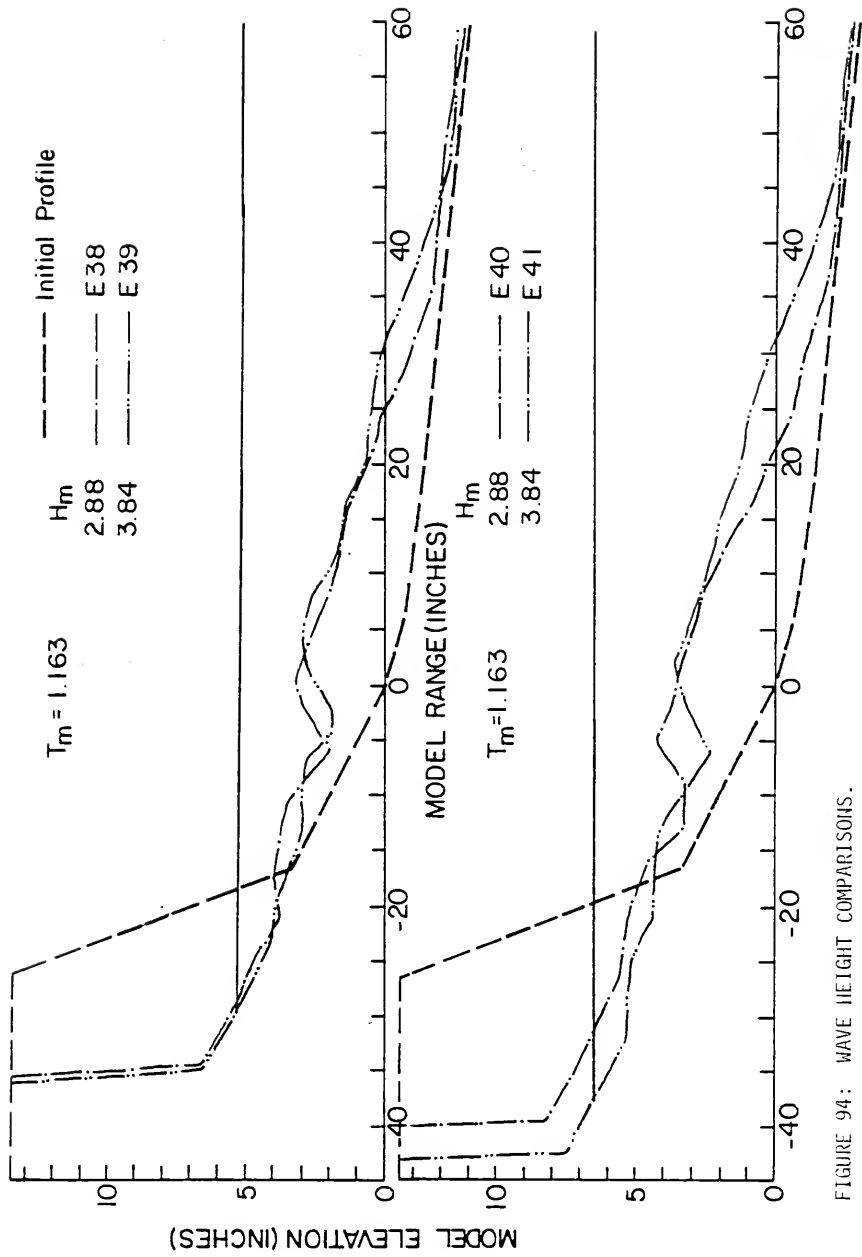


FIGURE 94: WAVE HEIGHT COMPARISONS.

#### APPENDIX D.4

#### WAVE PERIOD COMPARISONS

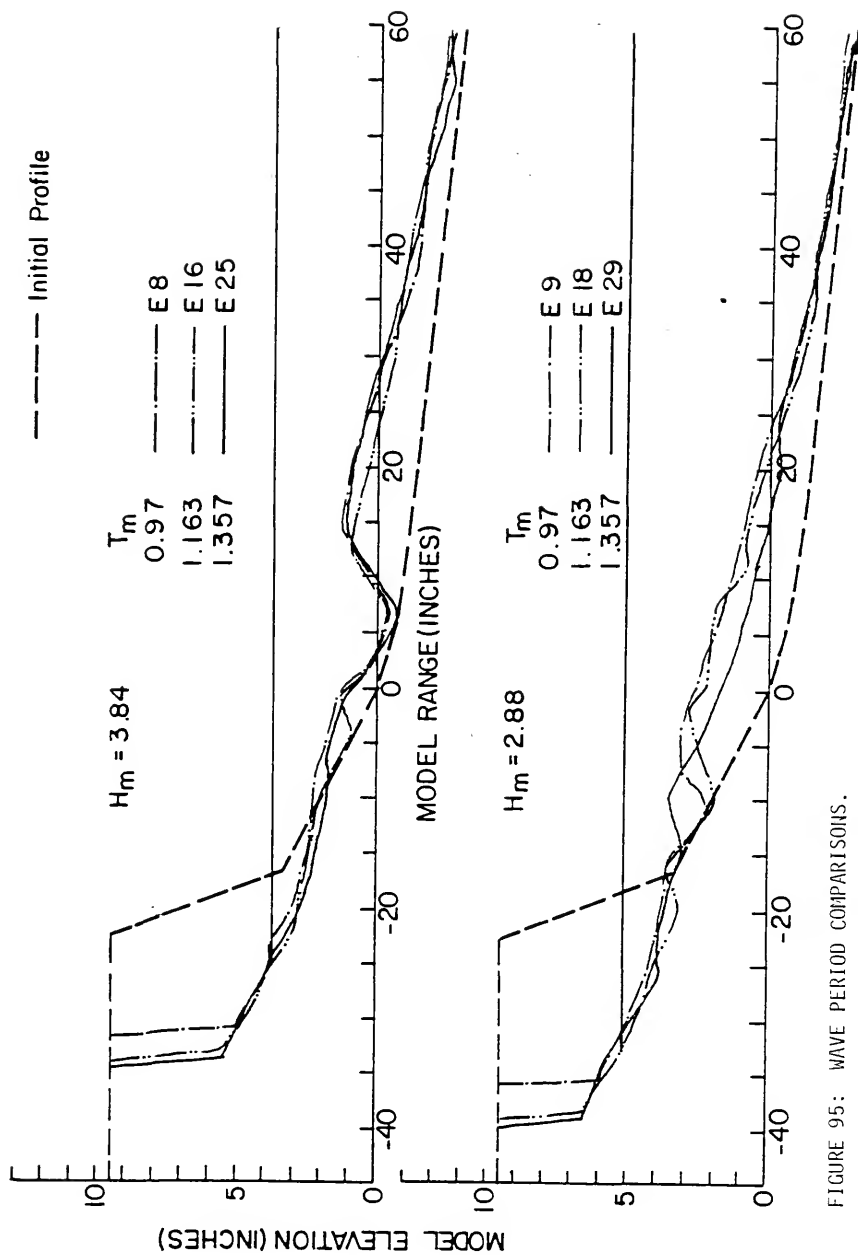


FIGURE 95: WAVE PERIOD COMPARISONS.

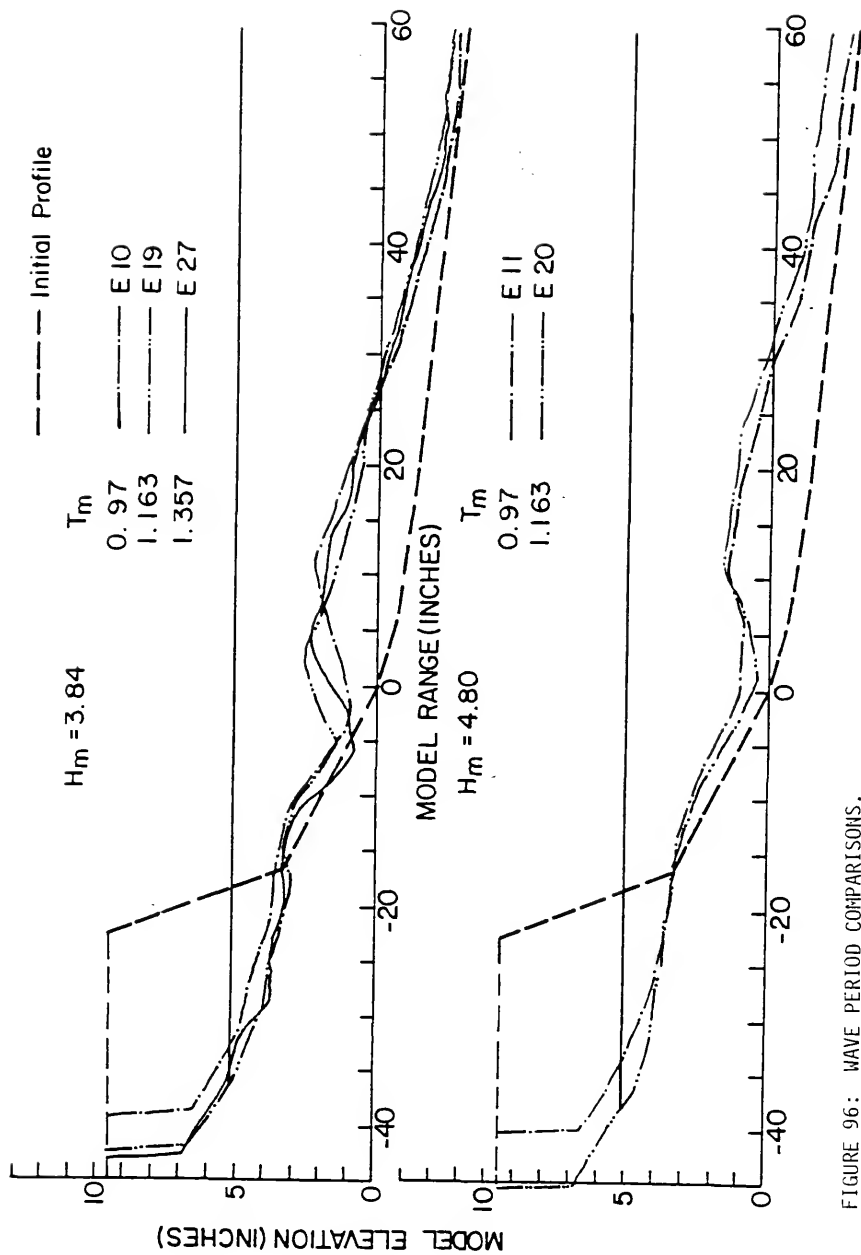


FIGURE 96: WAVE PERIOD COMPARISONS.

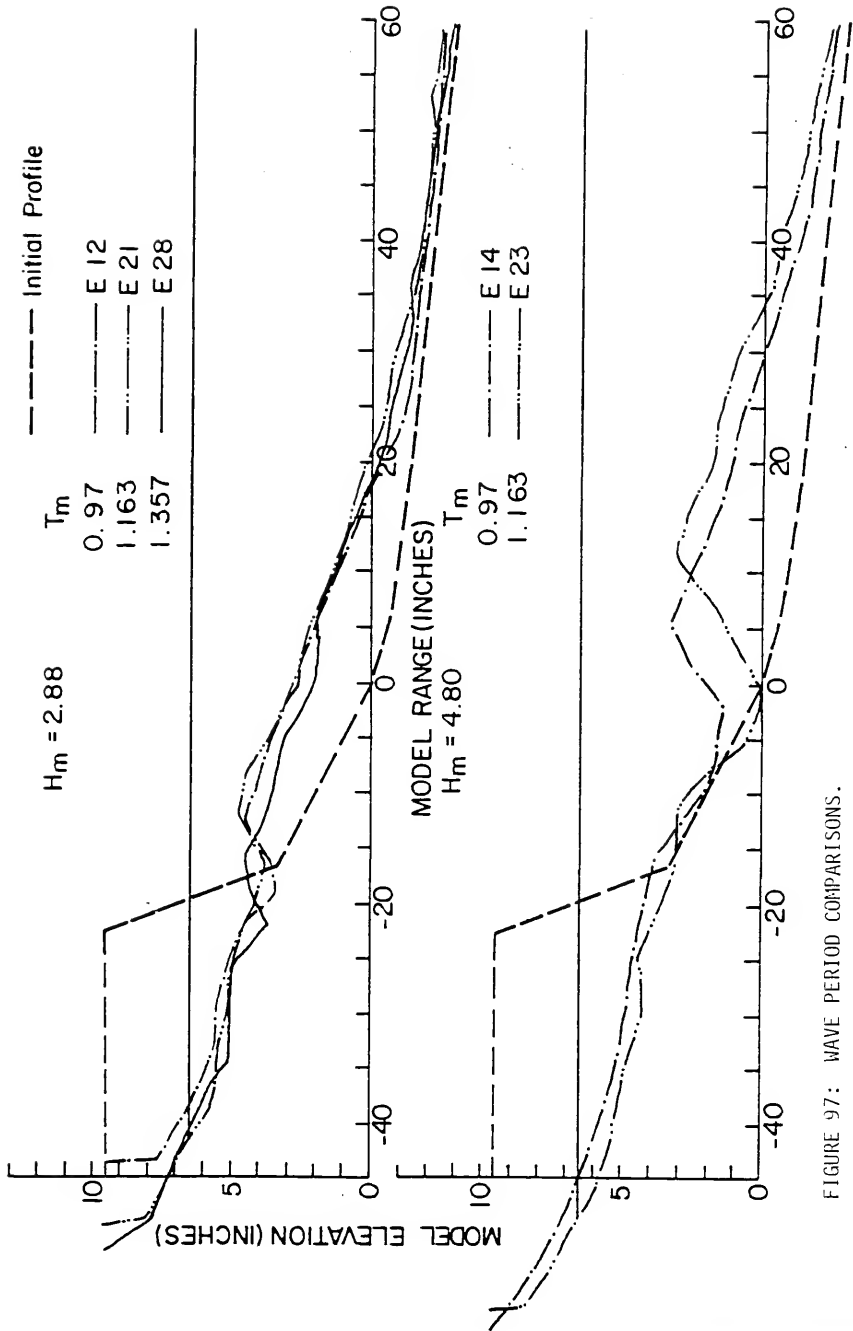


FIGURE 97: WAVE PERIOD COMPARISONS.

APPENDIX D.5

NEARSHORE BEACH PROFILE COMPARISONS

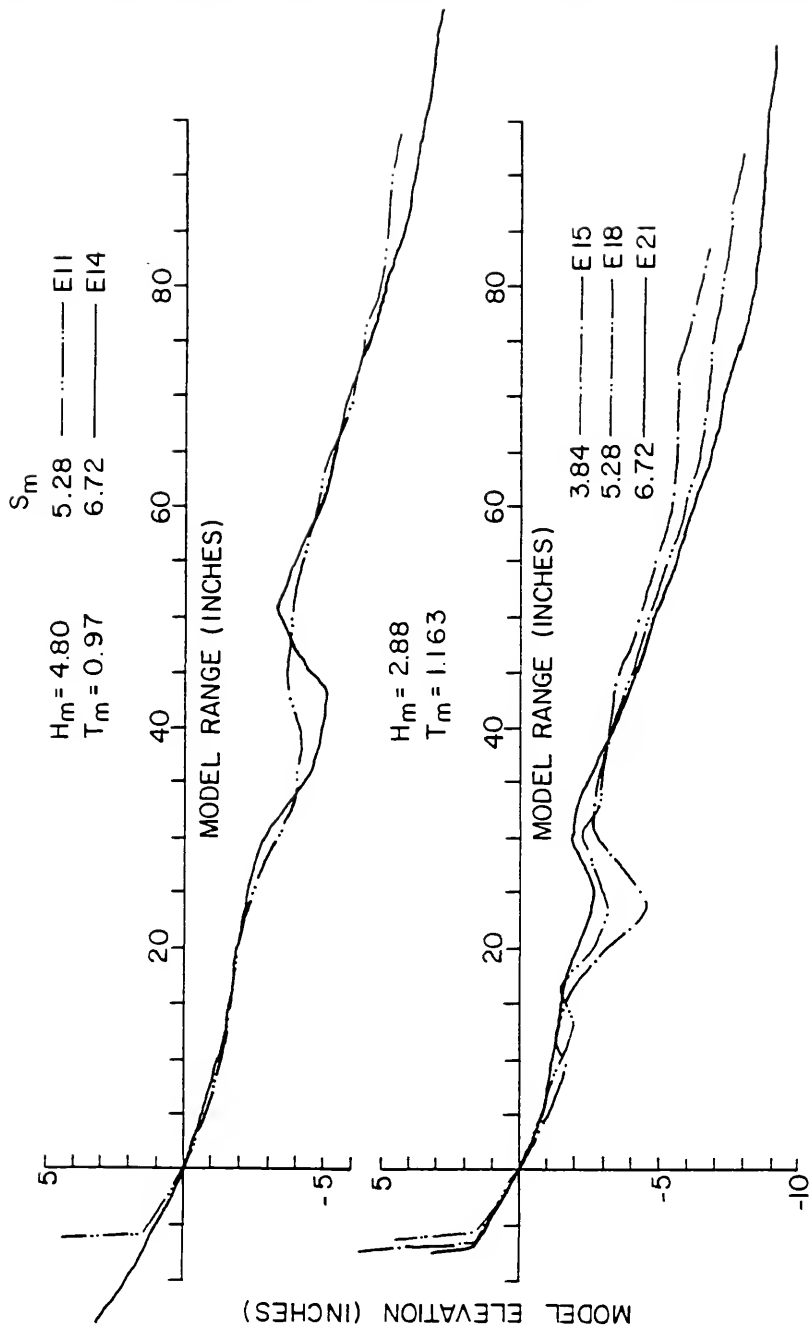


FIGURE 98: NEARSHORE PROFILE COMPARISONS.

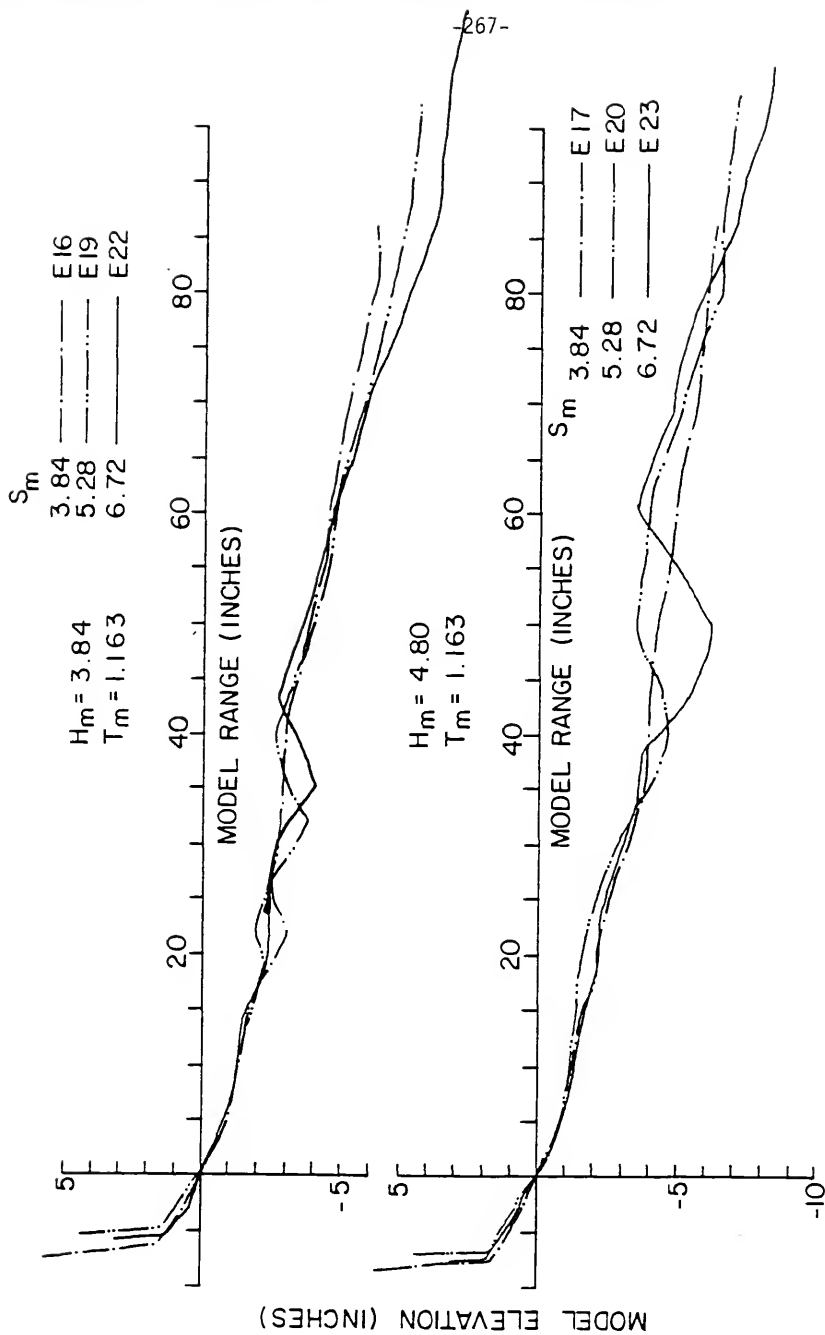


FIGURE 99: NEARSHORE PROFILE COMPARISONS.



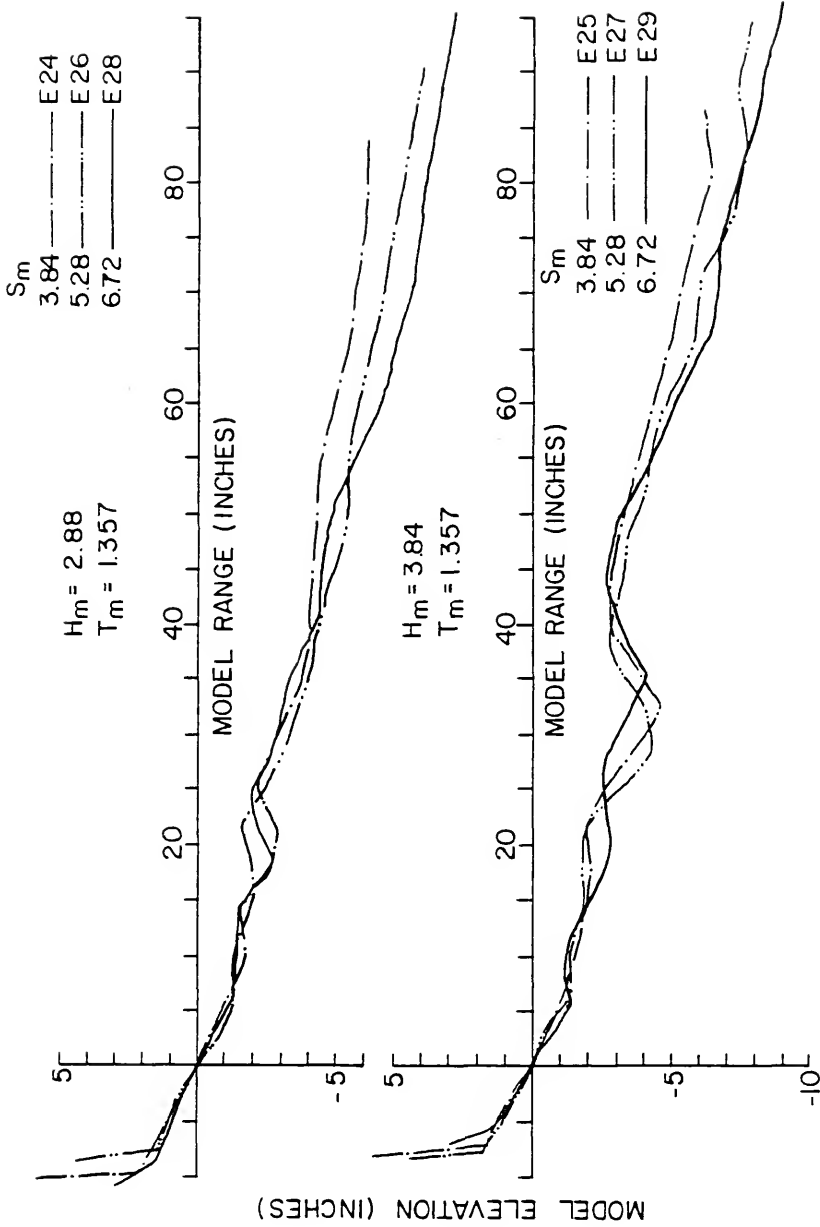


FIGURE 100: NEARSHORE PROFILE COMPARISONS.

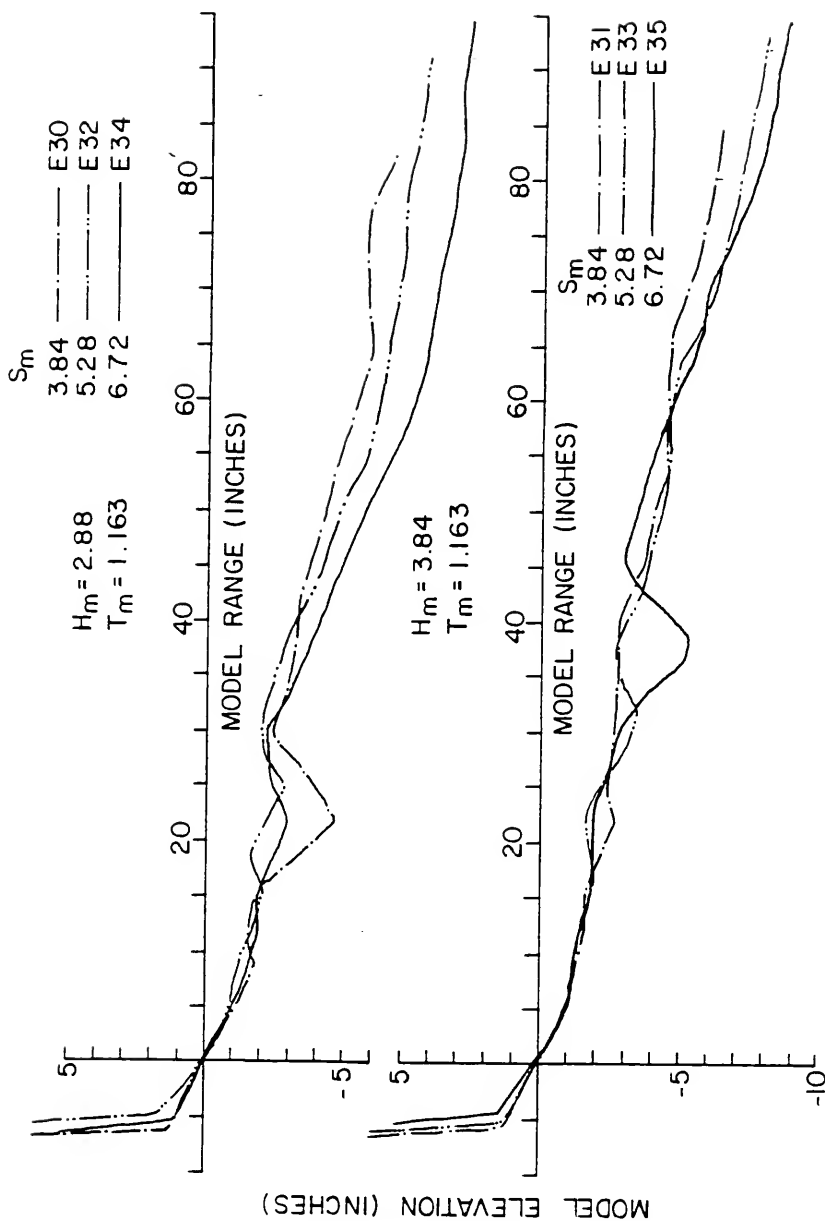


FIGURE 101: NEARSHORE PROFILE COMPARISONS.

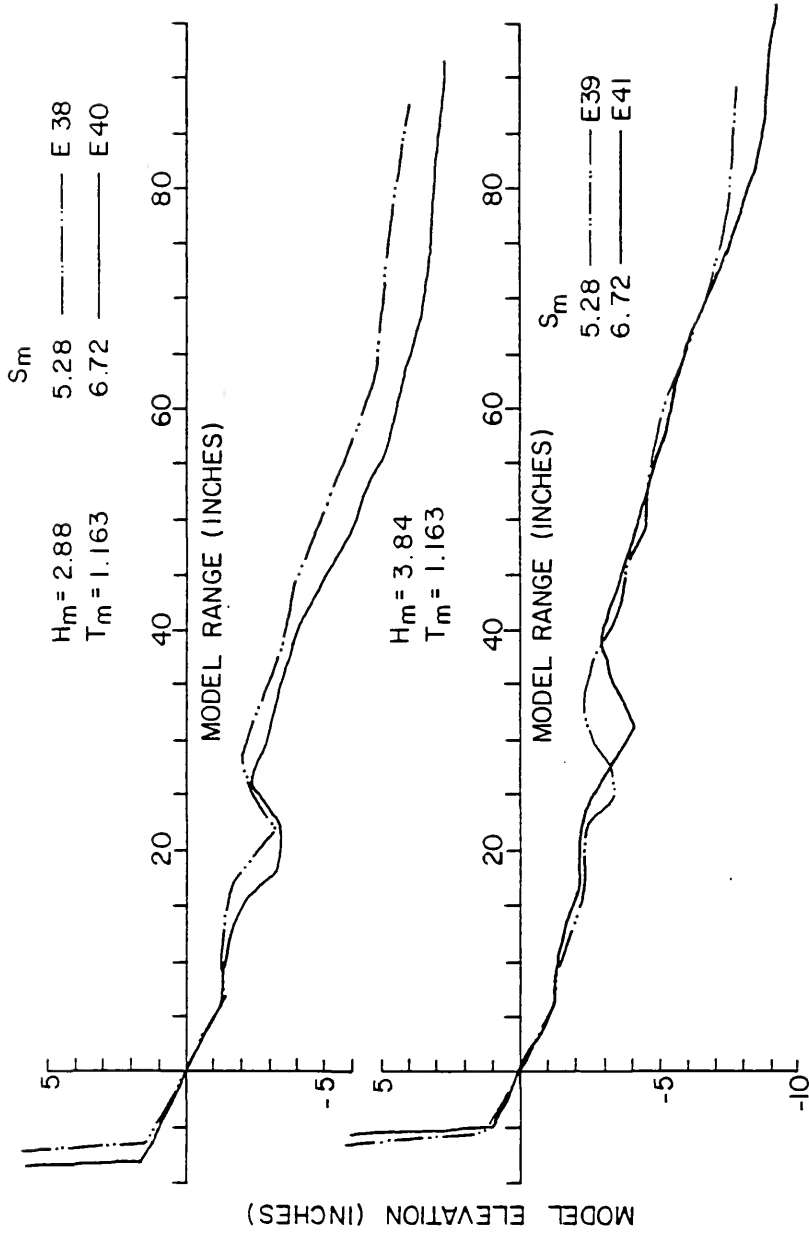


FIGURE 102: NEARSHORE PROFILE COMPARISONS.

APPENDIX E  
DERIVATIONS

# APPENDIX E.1

## DEAN'S DERIVATION FOR A BEACH PROFILE DUE TO UNIFORM ENERGY DISSIPATION PER UNIT VOLUME

The energy flux within the surf zone can be expressed as

$$\frac{\partial E}{\partial t} + \frac{\partial (EC_g)}{\partial x'} = -hD(d) , \quad (79)$$

where

$E$  = wave energy per unit width,

$C_g$  = wave group velocity,

$h$  = water depth,

$x'$  = coordinate directed shoreward from breaking point, and

$D(d)$  = rate of wave energy dissipation per unit volume as a function of grain size.

Equation (79) states that all of the incoming wave energy per unit width is completely dissipated uniformly, per unit volume, across the surf zone. In other words, it is assumed that a sediment particle can tolerate a certain level of wave energy dissipation per unit volume and still remain stable. In actual fact, the sediment is nearly always in motion, so stability in this case refers to net transport of sediment.

By considering steady conditions when averaging over a wave period, i.e.,

$$\frac{dE}{dt} = 0$$

and replacing  $dx'$  with  $-dx$ , which is a coordinate system directed seaward from the beach, equation (79) becomes

$$\frac{d(EC_g)}{dx} = hD(d) . \quad (80)$$

From linear wave theory,

$$E = \frac{\gamma H^2}{8} \quad \text{and} \quad C_g = (gh)^{1/2} ,$$

which can be used in equation (80). By further assuming that the bore is decreasing in height proportional to the depth, then

$$H = Kh .$$

Making these substitutions into equation (80) yields

$$\frac{\gamma K^2 g^{1/2}}{8} \frac{d(h^{5/2})}{dx} = hD(d) ,$$

which can be integrated to give

$$\frac{5\gamma K^2 g^{1/2}}{24} h^{3/2} = D(d)x .$$

Rearranging gives

$$h = Ax^{2/3} , \quad (81)$$

where

$$A = \left[ \frac{24D(d)}{5\gamma K^2 g^{1/2}} \right]^{2/3} . \quad (82)$$

Here it is seen that "A" is a function only of sediment size, and it is reasonable to believe that the grain fall velocity plays the predominant part in dissipating the turbulent energy.

As was pointed out in the chapter dealing with the model law, the form given by equation (81) is preserved by the model law when

$$N_{\omega} = N_A^{3/2},$$

which means "A" is proportional to  $\omega^{2/3}$ . This further aids in explaining why profile similarity exists when the parameter  $H/\omega T$  is scaled in the model.

## APPENDIX E.2

### DERIVATION OF THE OFFSHORE EQUILIBRIUM PROFILE EQUATION

Quite a few papers have been written on the subject of sediment transport rates and equilibrium beach conditions in the nearshore vicinity. While all papers have their merit, perhaps the most widely quoted on the subject of surf zone energetics are Bagnold (1963), Inman and Bagnold (1963), and more recently, Madsen (1976). All three papers deal with the mechanics of nearshore processes in a thorough physical manner.

Inman and Bagnold developed a model for the equilibrium beach slope given as

$$\tan\beta = \tan\phi \left( \frac{1 - c}{1 + c} \right), \quad (83)$$

where

$\tan\beta$  = equilibrium beach slope,

$\tan\phi$  = coefficient of intergranular friction, and

$$c = \frac{\text{energy dissipated during the seaward sediment flow}}{\text{energy dissipated during the shoreward sediment flow}}.$$

Essentially, equation (83) is a balance between gravity which tends to move sediment offshore, and the non-symmetrical bottom velocity distribution which moves sediment onshore. To illustrate this, consider a symmetrical velocity distribution in which  $c = 1$ . Equation (83) then gives  $\tan\beta = 0$ , or a horizontal bed. Thus, in order to have a beach



slope, it is necessary to have an oscillatory bottom velocity distribution which is skewed in the onshore direction.

In the nearshore region, seaward of the breaking point, beach slopes greater than 0.1 (1 in 10) would be highly unusual. For small slopes such as these,

$$\tan \beta \approx \beta \text{ in radians} = \frac{dh}{dx}.$$

Making this substitution into equation (83) and solving for "c" yields

$$c = \frac{1 - \frac{1}{\tan \phi} \frac{dh}{dx}}{1 + \frac{1}{\tan \phi} \frac{dh}{dx}}. \quad (84)$$

As an approximation for the ratio of energy dissipation, c, Inman and Frautschy (1965) proposed that

$$c = \left| \frac{U_{m-off}}{U_{m-on}} \right|^3, \quad (85)$$

where

$U_{m-off}$  = maximum offshore component of the orbital velocity and

$U_{m-on}$  = maximum onshore component of the orbital velocity.

More recently, Bailard and Inman (1981) demonstrated that equation (83) could be more accurately expressed as

$$\tan \beta = (\tan \phi)(S), \quad (86)$$

where

S = skewness of the oscillatory velocity distribution,  
defined as

$$S = \frac{\frac{1}{T} \int_t^{t+T} U^3(t) dt}{\frac{1}{T} \int_t^{t+T} |U(t)|^3 dt} .$$

Since they state that equation (83) can be shown to be approximately equal to equation (86), when "c" is given by equation (85), it is perhaps wise to use equation (83), in view of the almost total lack of knowledge regarding the time variation of the bottom oscillatory velocity field.

Equating equations (84) and (85) yields

$$\left| \frac{U_{m-off}}{U_{m-on}} \right| = \left( \frac{1 - \frac{1}{\tan \phi} \frac{dh}{dx}}{1 + \frac{1}{\tan \phi} \frac{dh}{dx}} \right)^{1/3} . \quad (87)$$

Since the beach slope must always be less than the angle of repose,  $\phi$ ,

$$0 < \frac{1}{\tan \phi} \frac{dh}{dx} < 1 ,$$

then the right-hand side of equation (87) can be expanded in terms of two binomial series, as shown below.

$$\left| \frac{U_{m-off}}{U_{m-on}} \right| = \frac{1 - \frac{1}{3 \tan \phi} \frac{dh}{dx} - \frac{1}{9 \tan^2 \phi} \left( \frac{dh}{dx} \right)^2 + \dots}{1 + \frac{1}{3 \tan \phi} \frac{dh}{dx} + \frac{1}{9 \tan^2 \phi} \left( \frac{dh}{dx} \right)^2 + \dots} .$$

Using just the first two terms of the expansions, it is seen that

$$\left| \frac{U_{m-off}}{U_{m-on}} \right| = \frac{1 - \frac{1}{3 \tan \phi} \frac{dh}{dx}}{1 + \frac{1}{3 \tan \phi} \frac{dh}{dx}} . \quad (88)$$

To test this approximation, the probable steepest beach slope of  $dh/dx = 0.1$  was chosen along with an angle of repose of  $29^\circ$ , taken from page 463 of Henderson (1966), which shows  $\phi \approx 29^\circ$  over the beach sediment range of .25 mm to 2.0 mm. Using these values in equation (88) produces

$$\left| \frac{U_{m-off}}{U_{m-on}} \right| = 0.8866 ,$$

while the exact equation (87) gives

$$\left| \frac{U_{m-off}}{U_{m-on}} \right| = 0.8855 .$$

Thus it can be concluded that equation (88) is an accurate approximation of equation (87).

Experimental measurements of the maximum bottom velocity asymmetry carried out by Hamada (1951) indicated that  $U_{m-off}/U_{m-on}$  varied between 0.78 and 0.86, which is in good agreement with the above values.

It is now desirable to find an expression for the near-bottom maximum velocity asymmetry.

Using the horizontal particle velocity under the wave crests as the single most important feature, LeMehaute et al. (1968) compared 12 shallow water wave theories. Among their conclusion was the surprising fact that simple 1st order linear (Airy) theory provides a reasonable approximation of the bottom velocity which the higher order Stokes theories never approach. Wave theories providing better approximations than linear theory include Solitary and Cnoidal wave theory. Since it is desirable to express the bottom maximum velocities

as a function of the depth,  $h$ , an analytical form, such as linear theory, is preferred over the numerical Cnoidal theory or Solitary theory, which give only onshore horizontal bottom velocity.

Goda (1964) observed that maximum horizontal velocities under the wave crest for nearshore, unbroken waves were slightly larger than predicted by linear theory.

By superimposing a small onshore-directed current,  $\bar{u}$ , on the oscillatory wave bottom-velocity from linear theory, given as

$$U(t) = U_m \cos \omega t ,$$

where

$$U_m = \frac{\pi H}{T \sinh(kh)} ,$$

the onshore maximum velocity magnitude can be expressed as  $U_m + \bar{u}$ ;

the maximum offshore velocity magnitude becomes  $U_m - \bar{u}$ , which gives

$$\left| \frac{U_{m-off}}{U_{m-on}} \right| = \frac{U_m - \bar{u}}{U_m + \bar{u}} = \frac{1 - \frac{\bar{u}}{U_m}}{1 + \frac{\bar{u}}{U_m}} , \quad (89)$$

where  $\bar{u} \ll U_m$ .

Equating equation (88) and equation (89) gives

$$\frac{1 - \frac{1}{3 \tan \phi} \frac{dh}{dx}}{1 + \frac{1}{3 \tan \phi} \frac{dh}{dx}} = \frac{1 - \frac{\bar{u}}{U_m}}{1 + \frac{\bar{u}}{U_m}} ,$$

from which it is immediately seen that

$$\frac{\bar{u}}{U_m} = \frac{1}{3 \tan \phi} \frac{dh}{dx} . \quad (90)$$

Assuming that  $\bar{u}/U_m$  can be written as a function of depth,  $h$ , only, equation (90) becomes

$$\frac{U_m}{u} dh = 3 \tan \phi \, dx \quad (91)$$

With the assumption that only small amounts of total wave energy are lost by movement of sediment to and fro, the local wave height may be expressed, approximately, by the linear shoaling relationship

$$H = H_o \left[ \frac{2 \cosh^2 kh}{\sinh 2kh + 2kh} \right]^{1/2} \quad (92)$$

for waves propagating normal to the beach.

As pointed out by Eagleson and Dean (1966), experiments indicate that equation (92) predicts smaller wave heights than measured on sloping bottoms in wave tank experiments. However, Guza and Thornton (1980) measured wave spectra on a line extending from a 10 meter depth to inside the surf zone at Torrey Pines Beach, California, and compared shallow water spectra with those calculated using linear shoaling theory applied to the 10 meter depth spectrum. Comparisons were very favorable, particularly in the dominant frequency band, which indicates that equation (92) is perhaps a reasonable assumption to make.

Substitution of equation (92) into equation (91), making use of the relationships

$$U_m = \frac{\pi H}{T \sinh kh} \quad \text{and} \quad L = \frac{g T^2}{2\pi} \tanh kh \quad ,$$

yields

$$U_m = \frac{g H_o T}{2L} \left[ \frac{2}{\sinh 2kh + 2kh} \right]^{1/2} \quad (93)$$

For shallow water waves,  $\sinh 2kh \approx 2kh$ . Noting that  $k = 2\pi/L$ , equation (93) becomes

$$U_m = \frac{gH_o T}{(16\pi Lh)^{1/2}} \quad (94)$$

Eagleson and Dean (1966) also point out that wave celerity is adequately predicted by linear theory for shoaling waves up to breaking. Thus for shallow water,

$$C = (gh)^{1/2} = \frac{L}{T} \quad \text{or} \quad L = (gh)^{1/2} T,$$

and equation (94) then becomes

$$U_m = \frac{g^{3/4} H_o T^{1/2}}{4\pi^{1/2} h^{3/4}} \quad (95)$$

Placing equation (95) into equation (91) yields

$$\frac{g^{3/4} H_o T^{1/2}}{4\pi^{1/2} \bar{u}} \frac{dh}{h^{3/4}} = 3 \tan \phi \, dx \quad (96)$$

It is now necessary to determine a form for  $\bar{u}$  as a function of  $h$ ,  $H_o$ , and  $T$ . For the wave velocity asymmetry to increase as depth decreases, it is necessary for the ratio  $\bar{u}/U_m$  to increase. Since  $U_m \sim 1/h^{3/4}$ , it can be stated in general that  $\bar{u} \sim 1/h^n$  where  $n > 3/4$ . Thus,

$$\frac{\bar{u}}{U_m} \sim \frac{h^{3/4}}{h^n} \sim \frac{1}{h^{n-3/4}}.$$

By this logic, it can be said that

$$\bar{u} = \frac{\alpha(H_0, T)}{h^n},$$

where  $\alpha$  is an arbitrary function and  $n > 3/4$ . Equation (96) can now be written and integrated as

$$\frac{g^{3/4} H_0 T^{1/2}}{4\pi^{1/2} \alpha(H_0, T)} \int_0^h h^{n-3/4} dh = 3 \tan \phi \int_{x_i}^x dx,$$

where  $x_i$  is a reference location, yielding a power equation for the equilibrium beach profile seaward of the breaking point given as

$$h = \left[ \frac{(12n + 3)\pi^{1/2} \tan \phi}{g^{3/4} H_0 T^{1/2}} \cdot \alpha(H_0, T) \right]^{\frac{4}{4n+1}} (x - x_i)^{\frac{4}{4n+1}}. \quad (97)$$

To find an upper limit for the exponent,  $n$ , assume  $\bar{u}$  is equal to the mass transport velocity obtained from 2nd order Stokes theory, given by Eagleson and Dean (1966) at the bottom as

$$\bar{u} = \left( \frac{\pi H}{L} \right)^2 \frac{C}{2 \sinh^2 kh}. \quad (98)$$

Applying the linear wave shoaling equation (92) and the shallow water wave length expression given before, this expression becomes

$$\bar{u} = \frac{g T H_0^2}{32 \pi h^2} = \frac{\alpha(T, H_0)}{h^2}. \quad (99)$$

Unfortunately, 2nd order Stokes theory gives very poor bottom velocity results in shallow water, as stated before, with maximum velocities being substantially larger than actual measurements indicate. For this

reason, as depth decreases, the theoretical mass transport velocity at the bottom increases too rapidly; as a consequence, the exponent  $n = 2$  in equation (99) represents an upper limit.

Writing equation (97) in shorter notation as

$$h = A(x')^m, \text{ where } m = \frac{4}{4n + 1} \text{ and } 3/4 < n < 2 ,$$

it can be seen that  $m$  varies between  $4/9$  and  $1$ .

It has been decided to choose  $m = 2/3$ , which lies almost exactly between  $4/9$  and  $1$  and corresponds to  $n = 5/4$  for the following reasons:

- 1) This gives the uniform onshore drift current as

$$\bar{u} = \frac{\alpha}{h^{5/4}} ,$$

which seems very reasonable in view of the analysis done using 2nd order Stokes theory.

- 2) When Hughes (1978) applied the curve  $h = Ax^m$  to 464 actual beach profiles from the east coast of Florida extending to depths of about 20 feet, he found that  $m = 2/3$  provided the "best fit" in a majority of the cases. Greater error was found when the curve was fitted to depths of about 32 feet.
- 3) Dean (1977) was able to derive an equation of the form  $h = Ax^{2/3}$  for the beach profile inside the surf zone based on the concept of uniform dissipation, per unit water volume, of incoming wave energy. He also employed linear wave theory in his derivation. It is reasonable to believe that there exists a type of "profile similarity" between the immediate nearshore region and the surf zone, since many of the surf zone



characteristics can be expressed in terms of Battjes' (1974) surf similarity parameter.

- 4) As pointed out in Chapter IV, the equilibrium profile given by  $h = Ax^{2/3}$  is preserved in the model law derived for these experiments.
- 5) Bruun (1954) also proposed an equation of the form  $h = Ax^{2/3}$  for the region just seaward of the breaker line and found good correspondence when applied to actual beach profiles.

So finally, the proposed equation for the bottom profile just seaward of the breaker line is given as

$$h = \left[ \frac{11\pi^{1/2} \tan \phi}{3^{3/4} H_o T^{1/2}} \cdot \alpha(H_o, T) \right]^{2/3} (x - x_i)^{2/3} . \quad (100)$$

At this point, little can be done about determining the function for  $\alpha(H_o, T)$ . Dimensionally,  $\alpha$  has the units of

$$\alpha [=] \frac{L^{9/4}}{T} ,$$

but dimensional analysis cannot be employed because  $\alpha$  may also contain the constants of gravity, fluid density, etc.

## BIBLIOGRAPHY

- Bagnold, R.A., "Mechanics of Marine Sedimentation," in The Sea, Vol. 3, edited by M.N. Hill, Interscience, New York, 1963, pp. 507-528.
- Bailard, J.A. and Inman, D.L., "An Energetics Bedload Model for a Plane Sloping Beach, Part I: Local Transport," Journal of Geophysical Research, Vol. 86, No. C-3, March 1981, pp. 2035-2043.
- Battjes, J.A., "Surf Similarity," Proceedings of the 14th Conference on Coastal Engineering, Copenhagen, Vol. 1, June 1974, pp. 466-480.
- Bruun, P., "Coast Erosion and the Development of Beach Profiles," Tech. Memo. No. 44, U.S. Army, Corps of Engineers, Beach Erosion Board, June 1954, 79p.
- Chiu, T.Y., "Beach and Dune Response to Hurricane Eloise of September 1975," Proceedings of the 5th Symposium of the Waterway, Port, Coastal and Ocean Division of the ASCE--Coastal Sediments '77, Charleston, South Carolina, Nov. 1977, pp. 116-134.
- Christensen, B.A., "Effective Grain-Size in Sediment Transport," Proceedings of the 15th Congress of the International Association for Hydraulic Research, Vol. 3, 1969, pp. 223-231.
- Christensen, B.A. and Snyder, R.M., "Physical Modeling of Scour Initiation and Sediment Transport in Distorted Tidal Models," Symposium on Modeling Techniques, San Francisco, Vol. 2, Sept. 1975, pp. 927-935.
- Coastal and Oceanographic Engineering Laboratory, "Recommended Coastal Setback Line for Walton County, Florida," UF/COEL 74/007, University of Florida, Gainesville, Florida, May 1974, 31p.
- Coastal Engineering Research Center, "Shore Protection Manual," 2nd Edition, U.S. Army, Corps of Engineers, Fort Belvoir, Virginia, 1975.
- Dalrymple, R.A. and Thompson, W.W., "Study of Equilibrium Beach Profiles," Proceedings of the 15th Conference on Coastal Engineering, Honolulu, Vol. 2, July 1976, pp. 1277-1296.
- Dean, R.G., "Heuristic Models of Sand Transport in the Surf Zone," Proceedings of the Conference on Engineering Dynamics in the Surf Zone, Sydney, May 1973, pp. 208-214.

- Dean, R.G., "Beach Erosion: Causes, Processes, and Remedial Measures," CRC Critical Reviews in Environmental Control, Vol. 6, Issue 3, Sept. 1976, pp. 259-296.
- Dean, R.G., "Equilibrium Beach Profiles: U.S. Atlantic and Gulf Coasts," Ocean Engineering Report No. 12, Dept. of Civil Engineering, University of Delaware, Newark, Delaware, Jan. 1977, 45p.
- Eagleson, P.S. and Dean, R.G., "Small Amplitude Wave Theory," in Estuary and Coastline Hydrodynamics, edited by A.T. Ippen, McGraw-Hill Book Company, Inc., New York, 1966, pp. 1-92.
- Edelman, T., "Dune Erosion During Storm Conditions," Proceedings of the 11th Conference on Coastal Engineering, London, Vol. 1, Sept. 1968, pp. 719-722.
- Edelman, T., "Dune Erosion During Storm Conditions," Proceedings of the 13th Conference on Coastal Engineering, Vancouver, Vol. 2, July 1972, pp. 1305-1311.
- Fan, L.N. and LeMehaute, B., "Coastal Movable Bed Scale Model Technology," Tetra Tech Report TC-131, Tetra Tech, Inc., Pasadena, California, June 1969, 122p.
- Frank, N.L., "Lessons from Hurricane Eloise," Weatherwise, Vol. 29, No. 5, Oct. 1976, pp. 220-227.
- Galvin, C.J., "Breaker Travel and Choice of Design Wave Heights," Proceedings of the American Society of Civil Engineers, Journal of the Waterways and Harbors Division, Vol. 95, No. WW2, May 1969, pp. 175-200.
- Galvin, C.J., "Wave Breaking in Shallow Water," in Waves on Beaches and Resulting Sediment Transport, edited by R.E. Meyer, Academic Press, New York, 1972, pp. 413-456.
- Goda, Y., "Wave Forces on a Vertical Circular Cylinder," Report of the Port and Harbor Technical Research Institute, Yokosuka, Japan, Report No. 8, Aug. 1964, 74p.
- Goda, Y., "A Synthesis of Breaker Indices," Transactions of the Japan Society of Civil Engineers, Vol. 2, Part 2, 1970, pp. 227-230.
- Guza, R.T. and Thornton, E.B., "Local and Shoaled Comparisons of Sea Surface Elevations, Pressures, and Velocities," Journal of Geophysical Research, Vol. 85, No. C3, March 1980, pp. 1524-1530.
- Hamada, T., "Breakers and Beach Erosions," Report of the Transportation Technical Research Institute, Tokyo, Japan, Report No. 1, Dec. 1951.
- Hansen, N.O. and Hebsgaard, M., "Parasitic Long Waves in Model Testing," Progress Report No. 47, Institute of Hydrodynamics and Hydraulic Engineering, Technical University of Denmark, Lyngby, Denmark, Dec. 1978, pp. 31-35.

- Hansen, N.O., Sorensen, T., Gravensen, H., Lundgren, H., and Sand, S., "Correct Reproduction of Long Waves in Physical Models," Abstracts of the 17th Conference on Coastal Engineering, Sydney, 1980, pp. 307-308.
- Harris, D.L., "Characteristics of the Hurricane Storm Surge," Tech. Paper No. 48, U.S. Dept. of Commerce, Weather Bureau, U.S. Government Printing Office, Washington, D.C., 1963, 139p.
- Henderson, F.M., Open Channel Flow, Macmillan Publishing Co., Inc., New York, 1966, 522p.
- Herbich, J.B., "Comparison of Model and Beach Scour Patterns," Proceedings of the 12th Conference on Coastal Engineering, Washington, Vol. 2, Sept. 1970, pp. 1281-1300.
- Hsiao, V., "On the Transformation Mechanisms and the Prediction of Finite-Depth Water Waves," UF/COEL 78/010, Coastal and Oceanographic Engineering Laboratory, University of Florida, Gainesville, Florida, 1978, 124p.
- Hudson, R., Herrmann, F., Sager, R., Whalin, R., Keulegan, G., Chatham, C., and Hales, L., "Coastal Hydraulic Models," SR-5, U.S. Army, Corps of Engineers, Coastal Engineering Research Center, Fort Belvoir, Virginia, May 1979, 539p.
- Hudspeth, R.T., Jones, D.F., and Nath, J.H., "Analyses of Hinged Wave-makers for Random Waves," Proceedings of the 16th Conference on Coastal Engineering, Hamburg, Vol. 1, Sept. 1978, pp. 372-387.
- Hughes, S.A., "The Variations in Beach Profiles When Approximated by a Theoretical Curve," UFL/COEL/TR-039, Coastal and Oceanographic Engineering Laboratory, University of Florida, Gainesville, Florida, 1978, 136p.
- Hunt, I.A., "Design of Seawalls and Breakwaters," Proceedings of the American Society of Civil Engineers, Journal of the Waterways and Harbors Division, Vol. 85, No. WW3, Sept. 1959, pp. 123-152.
- Inman, D.L. and Bagnold, R.A., "Littoral Processes," in The Sea, Vol. 3, edited by M.N. Hill, Interscience, New York, 1963, pp. 529-553.
- Inman, D.L. and Frautschy, J.D., "Littoral Processes and the Development of Shorelines," Coastal Engineering Specialty Conference, Santa Barbara, Oct. 1965, pp. 511-536.
- Iversen, H.W., "Laboratory Study of Breakers," Gravity Waves, Circ. No. 521, National Bureau of Standards, Washington, D.C., 1952a.
- Iversen, H.W., "Waves and Breakers in Shoaling Water," Proceedings of the 3rd Conference on Coastal Engineering, Cambridge, Oct. 1952b, pp. 1-12.

- Jain, S.C. and Kennedy, J.F., "An Evaluation of Movable-Bed Tidal Inlet Models," GIIT Report 17, U.S. Army, Corps of Engineers, Coastal Engineering Research Center, Fort Belvoir, Virginia, Feb. 1979, 82p.
- Johnson, J.W., "Scale Effects in Hydraulic Models Involving Wave Motion," Transactions of the American Geophysical Union, Vol. 30, 1949, pp. 517-525.
- Johnson, R.R., Mansard, E., and Ploeg, J., "Effects of Wave Grouping on Breakwater Stability," Proceedings of the 16th Conference on Coastal Engineering, Hamburg, Vol. 3, Sept. 1978, pp. 2228-2243.
- Kemp, P.H., "The Relationship Between Wave Action and Beach Profile Characteristics," Proceedings of the 7th Conference on Coastal Engineering, The Hague, Vol. 1, Aug. 1960, pp. 262-277.
- Kemp, P.H. and Plinston, D.T., "Beaches Produced by Waves of Low Phase Difference," Proceedings of the American Society of Civil Engineers, Journal of the Hydraulics Division, Vol. 94, No. HY5, Sept. 1968, pp. 1183-1195.
- Keulegan, G.H., "An Experimental Study of Submarine Sand Bars," Tech. Report No. 3, U.S. Army, Corps of Engineers, Beach Erosion Board, Aug. 1948, 40p.
- LeMehaute, B., Divoky, D., and Lin, A., "Shallow Water Waves: A Comparison of Theories and Experiments," Proceedings of the 11th Conference on Coastal Engineering, London, Vol. 1, Sept. 1968, pp. 86-96.
- Ma, Y., "Dune Erosion Model Study," UFL/COEL-79/009, Coastal and Oceanographic Engineering Laboratory, University of Florida, Gainesville, Florida, 1979, 72p.
- Madsen, O.S. and Grant, W.D., "Sediment Transport in the Coastal Environment," M.I.T. Report No. 209, Ralph M. Parsons Laboratory, Dept. of Civil Engineering, Massachusetts Institute of Technology Cambridge, Mass., Jan. 1976, 105p.
- Munk, W.H., "The Solitary Wave Theory and Its Application to Surf Problems," Annals of the New York Academy of Sciences, Vol. 51, 1949, pp. 376-462.
- Neumann, C.J., Cry, G.W., Caso, E.L., and Jarvinen, B.R., "Tropical Cyclones of the North Atlantic Ocean, 1871-1977," U.S. Dept. of Commerce, National Oceanic and Atmospheric Administration, U.S. Government Printing Office, Washington, D.C., June 1978, 170p.
- Noda, E.K., "Coastal Movable-Bed Scale-Model Relationship," Tetra Tech Report TC 191, Tetra Tech, Inc., Pasadena, California, March 1971, 88p.

- Noda, H., "Scale Relations for Equilibrium Beach Profiles," Proceedings of the 16th Conference on Coastal Engineering, Hamburg, Vol. 2, Sept. 1978, pp. 1531-1541.
- Pidgeon, V.W. and Pidgeon, N.A., "Severe Storm Effects in a Coastal Environment," FR-VIII-1, Dynex Consulting Co., Lynn Haven, Florida, May 1977, 152p.
- Purpura, J.A., "Establishment of a Coastal Setback Line in Florida," Proceedings of the 13th Conference on Coastal Engineering, Vancouver, Vol. 2, July 1972, pp. 1599-1615.
- Rector, R.L., "Laboratory Study of Equilibrium Profiles of Beaches," Tech. Memo. No. 41, U.S. Army, Corps of Engineers, Beach Erosion Board, Aug. 1954, 38p.
- Rouse, H., editor, Engineering Hydraulics, John Wiley and Sons, Inc., New York, 1950, 1039p.
- Saville, T., Jr., "Scale Effects in Two-Dimensional Beach Studies," Proceedings of the 7th Congress of the International Association for Hydraulic Research, Vol. 1, 1957a, pp. A3-1--A3-8.
- Saville, T., Jr., "Wave Run-Up on Composite Slopes," Proceedings of the 6th Conference on Coastal Engineering, Gainesville, Dec. 1957b, pp. 691-699.
- Saville, T., Jr., "Comparison of Scaled Beach Deformation Tests Using Sand and Coal," Abstracts of the 17th Conference on Coastal Engineering, Sydney, 1980, p. 439.
- Sensabaugh, W.M., Balsillie, J.H., and Bean, H.N., "A Program of Coastal Data Acquisition," Proceedings of the 5th Symposium of the Waterway, Port, Coastal and Ocean Division of the ASCE--Coastal Sediments '77, Charleston, South Carolina, Nov. 1977, pp. 1073-1085.
- Shemdin, O.H., "Air-Sea Interaction Laboratory Facility," TR-003, Coastal and Oceanographic Engineering Laboratory, University of Florida, Gainesville, Florida, Aug. 1969, 45p.
- Shepard, F.P., "Longshore-Bars and Longshore-Troughs," Tech. Memo. No. 15, U.S. Army, Corps of Engineers, Beach Erosion Board, Jan. 1950, 32p.
- Sunamura, T. and Horikawa, K., "Two-Dimensional Beach Transformation Due to Waves," Proceedings of the 14th Conference on Coastal Engineering, Copenhagen, Vol. 2, June 1974, pp. 920-937.
- Swart, D.H., "A Schematization of Onshore-Offshore Transport," Proceedings of the 14th Conference on Coastal Engineering, Copenhagen, Vol. 2, June 1974a, pp. 884-900.

- Swart, D.H., "Offshore Sediment Transport and Equilibrium Beach Profiles," Publication No. 131, Delft Hydraulics Laboratory, The Netherlands, Dec. 1974b, 302p.
- Swart, D.H., "Predictive Equations Regarding Coastal Transports," Proceedings of the 15th Conference on Coastal Engineering, Honolulu, Vol. 2, July 1976, pp. 1113-1132.
- Vallianos, L., "Beach Fill Planning--Brunswick County, North Carolina," Proceedings of the 14th Conference on Coastal Engineering, Copenhagen, Vol. 2, June 1974, pp. 1350-1369.
- Van de Graaff, J., "Dune Erosion During a Storm Surge," Coastal Engineering, Vol. 1, 1977, pp. 99-134.
- Van der Meulen, T. and Gourlay, M.R., "Beach and Dune Erosion Tests," Proceedings of the 11th Conference on Coastal Engineering, London, Vol. 1, Sept. 1968, pp. 701-707.
- Van Dorn, W.G., "Breaking Invariants in Shoaling Waves," Journal of Geophysical Research, Vol. 83, No. C6, June 1978, pp. 2981-2988.
- Vellinga, P., "Movable Bed Model Tests on Dune Erosion," Proceedings of the 16th Conference on Coastal Engineering, Hamburg, Vol. 2, Sept. 1978, pp. 2020-2039.
- Watts, G.M., "Laboratory Study of Effect of Varying Wave Periods on Beach Profiles," Tech. Memo. No. 53, U.S. Army, Corps of Engineers, Beach Erosion Board, Sept. 1954, 19p.
- Withee, G.W. and Johnson, A., Jr., "Data Report: Buoy Observations During Hurricane Eloise," U.S. Dept. of Commerce, National Oceanic and Atmospheric Administration, Environmental Sciences Division, U.S. Government Printing Office, Washington, D.C., Nov. 1975, 78p.

## BIOGRAPHICAL SKETCH

Steven Allen Hughes was born in Des Moines, Iowa, on the morning of August 9, 1949. When he was five, his family moved to a small town in northwest Iowa called Mallard, where he attended grade school and later high school. He was graduated from Mallard Community High School in May of 1967 and enrolled at the Iowa State University of Science and Technology in Ames, Iowa, three months later. While at Iowa State, he studied engineering and received his Bachelor of Science degree in February, 1972, in the field of aerospace engineering.

The following four years he spent in Brisbane, Australia, where he was employed as a structural design engineer with a local engineering consultant firm.

In 1976, he returned to the United States to pursue further study at the University of Florida's Department of Coastal and Oceanographic Engineering, from which he received his Master of Science degree in June, 1978.

In August of 1981 he was granted the degree of Doctor of Philosophy from the Department of Civil Engineering at the University of Florida.

Steve was married to Patricia Bowman on St. Patrick's Day, 1979; he witnessed the birth of his daughter, Kelsey, in October of 1980.

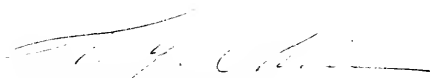


I certify that I have read this study and that in my opinion it conforms to acceptable standards of scholarly presentation and is fully adequate, in scope and quality, as a dissertation for the degree of Doctor of Philosophy.



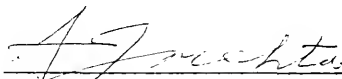
B.A. Christensen, Chairman  
Professor of Civil Engineering

I certify that I have read this study and that in my opinion it conforms to acceptable standards of scholarly presentation and is fully adequate, in scope and quality, as a dissertation for the degree of Doctor of Philosophy.



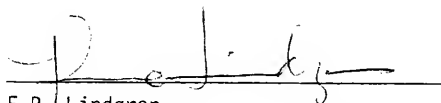
T.Y. Chiu, Co-Chairman  
Professor of Coastal Engineering

I certify that I have read this study and that in my opinion it conforms to acceptable standards of scholarly presentation and is fully adequate, in scope and quality, as a dissertation for the degree of Doctor of Philosophy.



A.J. Menta  
Associate Professor of Coastal  
Engineering

I certify that I have read this study and that in my opinion it conforms to acceptable standards of scholarly presentation and is fully adequate, in scope and quality, as a dissertation for the degree of Doctor of Philosophy.



E.R. Lindgren  
Professor of Engineering Sciences

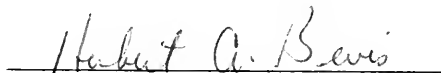
I certify that I have read this study and that in my opinion it conforms to acceptable standards of scholarly presentation and is fully adequate, in scope and quality, as a dissertation for the degree of Doctor of Philosophy.



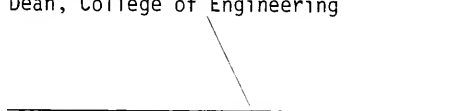
D.P. Spangler  
Associate Professor of Geology

This dissertation was submitted to the Graduate Faculty of the College of Engineering and to the Graduate Council, and was accepted as partial fulfillment of the requirements for the degree of Doctor of Philosophy.

August 1981



Dean, College of Engineering



Dean for Graduate Studies and Research

UNIVERSITY OF FLORIDA



3 1262 08666 299 5